ELSEVIER

JOURNAL OF CHROMATOGRAPHY

CONTENTS

Contents (continued)

High-Performance Liquid Chromatography of Biopolymers and Biooligomers

Part A: Principles, Materials and Techniques

by O. Mikeš, *Institute of Organic Chemistry and Biochemistry, Czechoslovak Academy of Sciences, Prague, Czechoslovakia*

The book describes modern methods for the rapid column liquid chromatography of high- and medium-molecular-weight compounds of biological origin, as well as some other compounds such as immunomodulators. The work comprises two volumes: Part A dealing with general chromatographic theory, principles, materials and techniques; and Part B which will deal with the separation of individual compound classes.

Not only is this a specialized, detailed treatise on chromatographic techniques, it also gives a broad, balanced review of rapid separation of all known important biopolymers and biooligomers, both simple and complex, and also of some synthetically prepared and pharmaceutically important biooligomers. It also provides an introduction to the application of HPLC to the study of the structure of these substances. In many cases, the description of the many examples of separation processes contain all the details necessary to enable the experienced experimenter to reproduce the separation methods without the need to consult the original literature. This feature, coupled with the description of some auxiliary chemical modification procedures, make this a particularly suitable laboratory handbook.

Parts A and B together contain *almost 3,000 citations*, the most important of which are listed alphabetically in Part B in a full-title bibliography which also serves as a reference for the voluminous register of chromatographed substances.

The book is of interest to chemists studying natural compounds, biochemists, biologists, physicians, pharmacologists, those working in clinical diagnostics, research and scientific institutes, research, control and testing institutions and laboratories in agricultural sciences and the food industry sector, as well as those involved in development, production and testing of chromatographic equipment and column packings.

Contents: 1. Introduction. 2. Theoretical Approach to Liquid Column Chromatography and Fundamental Terminology. 3. Principles of the Rapid Separation of Biopolymers and Biooligomers. 4. Column Packings for HPLC and MPLC of Biopolymers and Biooligomers. 5. Instrumentation for HPLC and MPLC. 6. Laboratory Techniques and Working Methods. Subject Index.

JOURNAL

of

CHROMATOGRAPHY

INTERNATIONAL JOURNAL ON CHROMATOGRAPHY

ELECTROPHORESIS AND RELATED METHODS

CHROMATOGRAPHIC DETECTION LIMITS IN PHARMACEUTICAL METHOD DEVELOPMENT

EUGENE L. INMAN* and EUGENE C. RICKARD

Lilly Research Laboratories, Eli Lilly & Co., Indianapolis, IN 46285 (U.S.A.)

(First received October 26th, 1987; revised manuscript received February 29th, 1988)

SUMMARY

A procedure for the determination of chromatographic method detection limits that incorporates the variabilities associated with sample preparation, measurement, and calculations is described. Theoretical considerations lead to an equation for the calculation of a method detection limit that evaluates the precision of the method near the detection limit and incorporates the number of sample and standard replicates used for a determination. Guidelines for the experimental determination of the method detection limit and for subsequent method procedure limitations were developed from the assumptions employed. This procedure is general and can be applied to chromatographic and non-chromatographic techniques. Several examples which demonstrate the effectiveness of this procedure for chromatographic methods are given. Method detection limits determined in this way should provide consistency for methods developed for pharmaceutical applications.

INTRODUCTION

The method detection limit is often used to characterize a method's effectiveness in the determination of a desired analyte. In general, the concept of a detection limit is one that is familiar to most analytical chemists. However, a diversity of views related to its significance and to the correct procedure for its determination have been discussed[1–3]. Its evaluation is especially important when the analyte is a minor or trace component in the sample matrix[4–6]. This presentation will focus on the definition and determination of the detection limit for analytical methods developed to evaluate pharmaceutical products, where detection limits take on real, rather than theoretical, significance.

Generally, the detection limit is defined as the lowest concentration or amount of an analyte in a given matrix whose response can be distinguished from the response of a blank[7]. The ability to distinguish between two response levels suggests a statistical basis for the definition of the detection limit. Historically, the precise statistical definition of the detection limit has been thoroughly debated. Furthermore, translation of the theoretical principles to practical application has led to confusion in experimental implementation. This paper outlines the experimental design considerations needed for the determination of the detection limit during method validation.

The importance of the detection limit is dependent upon the biological significance of the analyte itself. Analytes, often present as trace impurities that demonstrate significant toxicity, such as a carcinogen or mutagen, frequently require a decision as to their presence or absence at very low levels. The maximum sensitivity of these methods will define the control specification, *i.e.,* the control specification will be set at the method detection limit. Thus, the experimentally estimated detection limit will determine the level which will be reported as "none detected" in a regulatory sense. An evaluation of previously described approaches will provide a perspective for the design of an acceptable procedure for pharmaceutical products.

REVIEW OF APPROACHES TO DETECTION LIMIT DETERMINATION

A common experimental approach for estimating the detection limit is the measurement of serial dilutions of a stock analyte solution. An estimate of the detection limit is obtained by noting the concentration where the responses from the analyte solution and solvent blank are indistinguishable. However, this approach neglects the effects of many sources of variance, such as sample matrix. Thus, this approach produces estimates of the detection limit which are generally lower than those actually observed.

A second common experimental approach includes the effect of variance in the measured response. The detection limit is defined as a specific signal-to-noise ratio, usually a value of two or three depending on the desired confidence level. The limit of quantitation (LOQ) provides for a greater degree of confidence with the signal-to-noise ratio frequently set equal to ten[5]. When the signal-to-noise approach is selected, one must determine an appropriate procedure to measure the noise level. The noise level can be determined from measurements on a number of blanks or from peak-to-peak noise. For chromatographic determinations, the noise can be determined from a region of the chromatogram where no components elute[8,9]. Details of these approaches are described in the literature[10].

Long and Winefordner[7] reviewed the statistical basis for the IUPAC definition of detection limits, which recommends a signal-to-noise ratio of three and the noise is determined from the blank signal. The IUPAC model was evaluated and compared to alternate approaches, including graphical and propagation of errors models. These models allowed for errors in the calibration curve slope or slope and intercept, respectively in addition to errors in measurement of the blank signal. Application of these approaches to a number of spectroscopic examples demonstrated that the calculated detection limit can vary significantly. They concluded that the IUPAC approach is appropriate only when the major source of error is in the blank measurement and, in most cases, it yields artificially low detection limits.

A review of the concept of the detection limit applied to chromatographic techniques was presented by Foley and Dorsey[11]. A number of inconsistencies in common usage were pointed out and a set of definitions and models were proposed to provide standardized evaluation and reporting of detection limits. The detection limit calculations were based on the IUPAC and error propagation models, with special emphasis placed on the determination of baseline noise, analogous to the determination of the blank signal. They recommended a peak-to-peak noise measurement over a region of the chromatogram that is free of analyte peaks. This

standardization of chromatographic and statistical parameters for the detection limit determination allows direct comparisons of differing chromatographic methods.

All of the statistical models described above are based on the assumption that the sample preparation variability is negligible so that the detection limit is determined by the measurement process. In this way, an instrument detection limit (IDL) is described rather than a method detection limit (MDL). That is, the variances introduced by the separation, detection, and measurement processes are included in the IDL detection limit calculation, but not variances associated with the preparation of samples and standards. For most methods used to determine analytes near the detection limit, these other variances are significant and the IDL approach will yield a lower estimate for the detection limit than that which is actually observed. The method detection limit should include these additional sources of variability associated with processing the samples and standards through all of the steps in the analytical method. Furthermore, the assay design (e.g.,levels of replication) affects the method detection limit but cannot be accommodated by the IDL approach.

METHOD DETECTION LIMIT

The approach used in this paper will assume that the analyte must be quantitated. That is, that the level of the analyte (usually *versus* some regulatory limit) is important, rather than just a qualitative ability to detect the analyte. This definition has sometimes been referred to as a "limit of determination" in the literature, but an IDL approach is frequently used for its evaluation. The quantitative approach described below defines the MDL to incorporate all the variances associated with the assay. It also accounts for the increase in precision due to replication of samples and standards, i.e., assay design.

The evaluation of the MDL must incorporate variability from the sample preparation, separation, detection, and measurement processes. It also should allow for day-to-day variability in the method performance. That is, one should be confident that an analyte present at the MDL level can be reliably detected and quantitated any time an assay is performed. Finally, the variability associated with a background correction or comparison to a blank sample must be incorporated.

One procedure for the determination of a MDL for trace analyses of wastewaters has been described[6]. The entire analytical procedure was included in the evaluation of precision and the MDL for a single sample replicate was calculated from:

$$MDL = t(n-1, 1-\alpha=0.99)S_m \tag{1}$$

where $t(n-1, 1-\alpha=0.99)$ is the Student's t value for a one-tailed test at the 99% confidence level with $n-1$ degrees of freedom, and S_m is the standard deviation obtained from a number of replicate measurements (n). The value for t accounts for the limited number of measurements used to determine S_m. A minimum of seven replicates on a single sample with a concentration of one to five times the estimated MDL was proposed for the initial estimate of S_m. An iterative procedure with seven additional replicates on a solution with the concentration at the MDL estimated from the initial seven replicates is suggested to prevent overestimates of the MDL. Estimates of the MDL from measurements at high concentrations are frequently

incorrect. Glaser *et al.*[6] also estimate confidence limits on the MDL using the chi-square distribution. This concept has been adapted to the procedure proposed below for the evaluation of pharmaceutical methods.

MDL DERIVATION

MDL equation

The calculated method detection limit for a routine assay includes two separate contributions: the inherent method precision (which can be estimated) and the design of the routine assay procedure. That is, the experimental design of the validation procedure can have a dramatic effect on the accuracy of the estimated method precision, while the number of sample replicates and the number of standards used to define the calibration curve affect the expected precision of routine assay results. An effective expression for the MDL must provide for these terms.

The most general expression for the method detection limit can be written as:

$$MDL = kS_m \tag{2}$$

where k is a constant of proportionality and S_m is the method standard deviation. The determination of S_m must incorporate any background correction needed. Note that eqn. 1 fits this general form with the Student's t value introduced for k, accounting for the limited measurements used to estimate S_m. As a historical database is generated, S_m becomes more accurately determined and k can be set equal to 2, 3 or any other value corresponding to the z value of the normal distribution for the desired confidence level. The determination of S_m, however, is critical and errors in its experimental determination can become significant.

Eqn. 2 can be expanded by considering the contributions to S_m. For example, sample responses are generally compared to a calibration curve generated from one or more standard measurements. During the routine implementation of a method, one generally assays multiple sample replicates and a mean result is reported. The standard deviation of the mean of n independent measurements is inversely proportional to the square root of the replicate number. Introducing these relationships into eqn. 2 yields:

$$MDL = k(S_{std}^2/n_{std} + S_{sam}^2/n_{sam})^{1/2} \tag{3}$$

where S_{std} is the standard deviation of the standard measurement, S_{sam} is the standard deviation of the sample measurement, n_{std} is the number of standards used to generate a calibration curve, and n_{sam} is the number of sample replicates. As described, k is defined by the t-distribution value when the number of replicates used is small and the z statistic is appropriate when the number of replications used in the validation process is increased so that S_m becomes reasonably well known. Eqn. 3 may be appropriately modified to incorporate additional sources of variances. However, experimental errors and/or inappropriate assumptions greatly influence the reliability of the estimate for S_m.

Assumptions

The first assumption in eqn. 3 is that the method standard deviation is concentration independent near the detection limit. This is in contrast to the assumption of a constant relative precision observed at higher concentrations and implies a constant rather than a proportional error. The key to the validity of this assumption is that the standard concentration is approximately equal to the sample concentration. The second assumption is that the random error associated with a measurement is approximated by a Gaussian distribution. These assumptions are routinely met over small concentration ranges for many analytical techniques.

EXPERIMENTAL CONSIDERATIONS

The accuracy of the estimated method detection limit is most critically influenced by the experimental determination of S_m. From the definition of S_m and the assumptions given above, three general guidelines can be provided. First, the experimental determination of S_m must incorporate all contributions to the method variability, and therefore should include complete replication of sample preparation, measurement, and calculations. One must not limit the evaluation to the separation and detection steps only. Secondly, the analyte should be present in the sample matrix. Finally, variance contributions such as those due to multiple samples, instruments, analysts, days, or labs may need to be included. These variance components are typically evaluated using analysis of variance approaches from multiple levels of each variable[12,13].

Although these techniques are well known and will yield experimental designs which minimize variance, in some cases it may be sufficient to design the evaluation of S_m so that all relevant variables are included, *e.g.,* multiple samples on multiple days using available people and equipment. Thus, the specific experimental design to determine S_m will be unique for each method.

The experimental design used to determine S_m is dependent upon the major sources of method variability. If the sample and standard preparation and measurement procedures are identical, then S_{std} and S_{sam} are approximately equal, and eqn. 3 can be simplified to:

$$MDL = kS_{sam}(1/n_{sam} + 1/n_{std})^{1/2} \qquad (4)$$

When standards are prepared as solutions of analyte spiked into the sample matrix, this assumption is generally valid. If, however, the standard and sample preparation procedures differ significantly, then S_{std} and S_{sam} must be determined separately. For example, standard solutions that are prepared in the absence of sample matrix often yield conditions where $S_{std} < S_{sam}$.

Further examination of eqn. 4 offers another guideline for method design. If S_{std} and S_{sam} are equal, one can not lower the detection limit significantly by increasing the number of sample replicates without increasing the number of standards. The most efficient approach includes an equivalent number of standard and sample replicates. Using this condition, eqn. 4 can be reduced to:

$$MDL = k \sqrt{2} \, S_{sam} / \sqrt{n_{sam}} \qquad (5)$$

While the conditions required for use of this equation seem restrictive, they are routinely met if standards are prepared by spiking analyte into the blank sample matrix. In trace analysis, standards are often prepared in this way. Note that k in eqns. 4 and 5 can be chosen specifically for each method according to the confidence level required.

With these guidelines, the following procedure is outlined for the determination of S_m: (i) obtain a sample with little or no analyte present; (ii) spike in a quantity of analyte estimated to be near the detection limit; (iii) confirm that this amount of analyte is detectable; (iv) spike two to five times this level into multiple lots of sample, multiple replicates each; (v) if a background correction is needed, samples should be run as sample-blank pairs; (vi) for multiple data sets, pool the variance obtained for each lot, using the following equation:

$$S_p = \left\{ \sum_{i=1}^{j} [n_{(i)} - 1] \, S_{\mathrm{sam}(i)}^2 \middle/ \sum_{i=1}^{j} [n_{(i)} - 1] \right\}^{1/2} \tag{6}$$

The pooled standard deviation, S_p, is calculated from the variances, $S_{\mathrm{sam}(i)}$, obtained from $n_{(i)}$ measurements on j lots. S_p is then used in place of S_m in eqn. 2 and S_{sam} in eqn. 5.

The guidelines require that several limitations be placed on the method procedure. These recommendations should be incorporated into the method and followed each time the method is run. First, the number of replicate samples should be considered in conjunction with the number of standard replicates depending on the values of S_{sam} and S_{std}. Secondly, the concentration range of the standards should be small, probably within a factor of 10 of the estimated detection limit. Finally, the lowest standard concentration should be at or just above the MDL calculated for a single replicate. This standard provides a system suitability check.

An examination of these guidelines and the detection limit equation results in several observations and conclusions. The determination of S_m is critical for the derivation of the MDL and careful experimental design is required. The number of measurements used to determine S_m should be as large as practical. With the inclusion of the term for n, the detection limit is dependent upon the number of replicate determinations made on a sample. With sufficient replication of a single sample, it is possible for the MDL to be lower than the IDL. However, this generally has only theoretical significance since the required number of sample replicates is likely to be quite large. Also note that under many circumstances, increasing the sample replication number has little effect on the MDL if the standard replication number is not increased as well.

This procedure for the determination of the limit of detection is general and can be applied to chromatographic and non-chromatographic techniques. Foley and Dorsey[11] recommend that chromatographic detection limits (IDL) be reported as analyte amounts. However, the amount of analyte is related back to an original sample amount. Thus, the MDL can be reported in terms of concentration for a specific procedure. Since the MDL is dependent upon the initial sample size, sample size must be specified in the method procedure.

EXAMPLES

To demonstrate the effectiveness of the outlined procedure, several examples were selected in high-performance liquid chromatography (HPLC), gas chromatography (GC) and thin-layer chromatography (TLC). The details of these methods will not be presented, rather, the validation results will be reviewed. Three examples are representative of methods used to monitor process-related impurities in bulk drug characterizations, and one example focuses on degradation products and impurities in the dosage form. In each case, the development of experimental conditions for sample preparation, analyte separation, and measurement was completed and defined before the method was validated. Final MDL calculations were based on the use of eqn. 4 and the number of standard and sample replicates are the same for each method. For pooled data, eqns. 5 and 6 were used.

The first example represents a method developed for the detection of a fluorescent component in a bulk drug. The analyte is separated from the main component by TLC and is detected with a scanning densitometer operated in the fluorescence mode. Sample preparation includes dissolution of the drug substance in an appropriate solvent and spotting the solution on the TLC plate. During the development of the method, it appeared that a major source of variability was due to differences in the TLC plates. The MDL evaluation included sixteen lots of bulk drug run on five different plates. It was estimated that the variability of the standard measurement was approximately equivalent to the variability of the sample measurement. The IDL was estimated at a concentration equivalent to 5 ppm in the bulk drug, so a quantity of analyte equivalent to 10 ppm was spiked into each sample. A standard deviation was calculated for each plate and pooled to yield a method standard deviation of 2.7 ppm. Using a value of 2 for k, the results shown in Table I were generated, assuming that the number of standard and sample replicates are the same. A replicate number of three was selected with a detection limit of 5 ppm. The method procedure was written to include a standard curve for each TLC plate with standard concentrations of 5, 20 and 50 ppm. Detection of the 5-ppm standard is used as a system suitability check.

The basic assumption of concentration independence for the standard devia-

TABLE I

EXAMPLE 1 RESULTS FOR TLC–FLUORESCENCE DETECTION METHOD

$S_{sam} = S_{std} = 2.7$ ppm.

n	MDL (ppm)
1	8
2	6
3	5
4	4
7	3
15	2
59	1

TABLE II

EXAMPLE 2 RESULTS FOR GC–NITROGEN-SELECTIVE DETECTION METHOD

$S_{sam} = S_{std} = 1.6$ ppm.

n	MDL (ppm)
1	5.7
2	4.0
3	3.3
4	2.8
8	2.0
32	1.0

tion is true only over a limited concentration range. That is, the analyte level has a great effect on the estimated MDL. To illustrate this point, the MDL of the first example (actual MDL = 5 ppm) was estimated from a sample which contained 500 ppm of analyte. It yielded a method detection limit of about 50 ppm. This poor estimate confirms that detection limit measurements should be made near the detection limit.

The second method was developed for the detection of an impurity in a bulk drug, where chemical derivatization is needed for separation and detection. After derivatization, the analyte is separated from the main component by GC and detected with a nitrogen-selective detector. Variability includes major contributions from the derivatization step and changes in detector sensitivity from day-to-day. A method standard deviation of 1.6 ppm was determined from a pooled set of 31 determinations of several lots of bulk drug, with each determination including three sample and three standard preparations. Assuming S_{sam} and S_{std} are equal, S_{sam} was calculated to be equal to 2.0 ppm. Using a value of 2 for k, the results shown in Table II were generated. A replicate number of three was selected with a MDL of 3.3 ppm. The use of analyte standards is significant in this determination since the derivatization is not selective for the analyte, but also includes the bulk drug substance. Therefore, standards are prepared by spiking analyte into an acceptable lot of bulk drug. This procedure accounts for incomplete reaction and matrix effects. In this method, standard preparation variability is significant.

Another method was developed for the detection of sodium bicarbonate in a vial of formulated antibiotic. The method procedure includes the injection of a volume of hydrochloric acid into a vial, with the headspace above the solution assayed for carbon dioxide by GC with a thermal conductivity detector. Measurement of the bicarbonate detection limit was important to evaluate the acceptability of this simple assay scheme. A typical chromatogram is shown in Fig. 1. Note that an atmospheric level of carbon dioxide is found in the blank. For this method, one is not interested in the absolute detection limit of the chromatographic procedure, but the ability to distinguish between sample and blank. The IDL was estimated to be about 0.01 to 0.02%. Therefore, a spiked concentration of 0.1% was selected for the determination of S_{sam}. The results are shown in Table III. Five separate lots were assayed with ten replicates each to determine an S_p of 0.018%. Note that S_{sam} for the individual lots ranges from 0.011% to 0.026% demonstrating that a sufficient number of samples
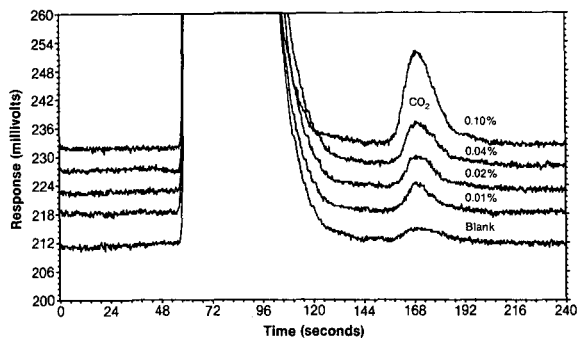
Fig. 1. Example 3, determination of sodium bicarbonate in a vial of formulated antibiotic by GC.

should be used for this evaluation and that the determination of S_{sam} is critical to the final method detection limit assignment. The corresponding MDL table is shown in Table IV.

The fourth example illustrates a common problem, detection of an isomeric impurity. This example involves the detection by HPLC of small levels of the S isomer in the R isomer. Since the activity of the compound resides in the R isomer, but the toxicity may be increased by the presence of the S isomer, a 0.1 to 1% detection limit goal was established. The compound was first derivatized to the corresponding mono-ester diastereomers with (S,S)-O,O-dibenzoyltartaric acid anhydride, dried down, and reconstituted with sample solvent. Analyte quantitation was estimated by an external standard approach where the response of the impurity peak in a concentrated sample solution was compared to the response of the main peak of a diluted sample solution, with a 1 to 10 dilution factor.

This example is described more extensively to demonstrate the actual steps involved in the evaluation of the MDL. Numerous data were collected for unspiked samples and additional data were obtained by spiking four levels of the S isomer into the sample (Table V). Since the R isomer was used as the standard, no standard curve

TABLE III

EXAMPLE 3 SUMMARY

Estimated IDL = 0.02%; spiked concentration = 0.1%.

Sample lot	S_{sam}
1 $(n = 10)$	0.020%
2 $(n = 10)$	0.026
3 $(n = 10)$	0.016
4 $(n = 10)$	0.011
5 $(n = 10)$	0.012
	S_p = 0.018%

TABLE IV

EXAMPLE 3 MDL TABLE

n	MDL (%)
1	0.05
2	0.04
3	0.03
7	0.02
26	0.01

TABLE V

EXAMPLE 4 DATA

S Isomer spike level	Day	S Isomer found (%)	Within day	
			Average	S_{sam}
0	1	0.19	0.19	—
0	2	0.21, 0.24, 0.23, 0.28, 0.27	0.25	0.03
0	3	0.10, 0.09, 0.14	0.11	0.03
0	5	0.10	0.10	—
0	6	0.16, 0.06, 0.10	0.11	0.05
0.3%	5	0.19, 0.23, 0.37	0.26	0.09
0.5%	4	0.31, 0.23, 0.26	0.27	0.04
0.5%	5	0.48, 0.37, 0.44	0.43	0.06
1.0%	3	1.02, 0.64, 1.12	0.93	0.25

was needed and the data are reported directly in percentage S isomer. Although the diastereomer peaks were well resolved, there were other trace contaminants present in the sample which contributed to the difficulty in establishing baselines and integrating peaks (Fig. 2). Thus, differences were observed between days and sometimes within the same day (e.g., 1% spike level in Table V). The data at each spike level were combined to give the averages and standard deviations shown in Table VI.
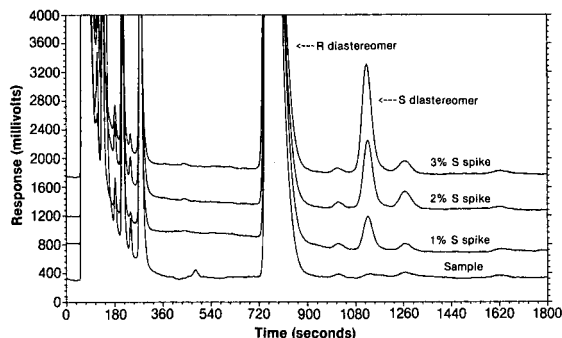
Fig. 2. Example 4, determination of S diastereomer in R diastereomer by HPLC.

TABLE VI

EXAMPLE 4 SUMMARY

S Isomer spike level	Days	n	Average	S_{sam}
0	5	13	0.17	0.08
0.3%	1	3	0.26	0.10
0.5%	2	6	0.35	0.10
1.0%	1	3	0.93	0.25
				$S_P = 0.11$

n	MDL (%)*
1	0.3
2	0.2
5	0.1

* $MDL = 0.30/\sqrt{n}$.

Then, the pooled (across spike levels) standard deviation, S_P, and the MDLs were calculated using a value of 2 for k.

   Several observations can be made regarding the results for the fourth example. First, the calculated method detection limit is higher than the instrument detection limit, estimated at less than 0.1%, even though the external standard approach acts as an internal control for the completeness of the derivatization reaction. Secondly, the standard deviations for all data at one dose level are higher than the standard deviation for data obtained within a single day. This indicates a difficulty in reproducing the derivatization reaction, chromatography, and/or the peak integration between days. Thirdly, the standard deviations are relatively independent of spike level except for the one anomalous data point at the 1.0% spike level. Finally, although the average percentage S found increases with spike level, there seems to be a bias which affects samples at low percentage S isomer. Spikes at higher levels were necessary to demonstrate complete recovery and linearity (Table VII), but were not used in calculation of the MDL.

TABLE VII

EXAMPLE 4, HIGH LEVELS

Regression line: slope = 1.03, y-intercept = 0.13, correlation coefficient = 0.989

S Isomer spike level (%)	S Isomer found (%)
0	0.2
1	1.2
2	1.9
3	3.4

CONCLUSIONS

The determination of a method detection limit is included in the validation of that method. This determination is greatly influenced by the experimental design used for its evaluation. The equation used to calculate the MDL includes the sample and standard replicate numbers and the standard deviation of each, determined by assaying a sufficient number of samples near the estimated detection limit. All sources of variability should be included, allowing for the complete sample preparation scheme and daily sensitivity differences in the instrumentation used for analyte measurement. A number of guidelines have been presented to aid in this determination. MDLs determined in this way should prove to be acceptable for the long-term application of the method for the analysis of pharmaceutical samples.

ACKNOWLEDGEMENTS

REFERENCES

1 B. L. Karger, M. Martin and G. Guiochon, *Anal. Chem.*, 46 (1974) 1640.
2 L A. Currie, *Anal. Chem.*, 40 (1968) 586.
3 H. Kaiser, *Pure Appl. Chem.*, 34 (1973) 35.
4 S. M. Ficarro and K. A. Shah, *Pharm. Manuf.*, 3 (Sept.) (1984) 25.
5 *Principles of Environmental Analysis*, ACS Committee on Environmental Improvement, L. H. Keith, Chairman, *Anal. Chem.*, 55 (1983) 2210.
6 J. A. Glaser, D. L. Foerst, G. D. McKee, S. A. Quave and W. L. Budde, *Environ. Sci. Technol.*, 15 (1981) 1426.
7 G. L. Long and J. D. Winefordner, *Anal. Chem.*, 55 (1983) 712A.
8 J. E. Knoll, *J. Chromatogr. Sci.*, 23 (1985) 422.
9 R. E. Synovec and E. S. Yeung, *Anal. Chem.*, 57 (1985) 2162.
10 H. C. Smit and H. L. Walg, *Chromatographia*, 8 (1975) 311.
11 J. P. Foley and J. G. Dorsey, *Chromatographia*, 18 (1984) 503.
12 J. C. Miller and J. N. Miller, *Statistics for Analytical Chemistry*, Wiley, New York, NY, 1984, Ch. 3 and 4.
13 G. T. Wernimont and W. Spendley, *Use of Statistics to Develop and Evaluate Analytical Methods*, Association of Official Analytical Chemists, Arlington, VA, 1985, Ch. 3 and 4.

CHROM. 20 554

RETENTION RELATIONSHIPS FOR AROMATIC HYDROCARBONS ELUTED FROM CAPPED AND UNCAPPED OCTADECYL SILICA GELS

JOHN H. KNOX*

Wolfson Liquid Chromatography Unit, Department of Chemistry, University of Edinburgh, West Mains Road, Edinburgh EH9 3JJ (U.K.)

and

JOSEF KŘÍŽ and EVA ADAMCOVÁ

Laboratory of Synthetic Fuels, Institute of Chemical Technology, Suchbatarova 5, Prague 6 (Czechoslovakia)

(First received February 15th, 1988; revised manuscript received April 18th, 1988)

SUMMARY

Retention characteristics of 54 aromatic hydrocarbons have been measured on three reversed-phase packing materials, ODS Hypersil (a fully capped octadecyl bonded reversed-phase silica gel), uncapped ODS Hypersil (an intermediate in the production of ODS Hypersil), and LiChrosorb RP-18, using three different eluent compositions, 90:10, 80:20, and 70:30 methanol–water (by weight).

For all nine combinations of packing material and eluent log k' shows a linear dependence on carbon number for the *n*-alkylbenzenes and for those polymethylbenzenes in which all methyl groups are *ortho* to each other. The gradients of the plots are essentially identical for ODS Hypersil and LiChrosorb RP-18, but are slightly lower for uncapped ODS Hypersil. For compounds with the same carbon number, those with higher hydrogen numbers are more retained. Examination of the correlation of log k' for all 54 solutes with carbon number, hydrogen number and connectivity index shows that none of these parameters provides a satisfactory universal correlation.

For isomeric alkylbenzenes, retention is significantly affected by the number of alkyl groups, by the structure of the alkyl groups and by the arrangement of the groups on the benzene ring. It is noted specifically that *ortho*-substituted alkylbenzenes have lower retention than isomers where the groups are not adjacent. This is termed the "reverse *ortho* effect". Branching of alkyl substituents reduces retention.

While the chromatographic behaviour of the 54 solutes on capped and uncapped ODS Hypersil is broadly similar, the retention of the alkylbenzenes is slightly increased by capping while the retention of polynuclear aromatics is slightly reduced by capping. LiChrosorb behaves similarly to uncapped ODS Hypersil except that its retention is much greater.

INTRODUCTION

A detailed understanding of the relationship between retention and molecular structure in liquid chromatography (LC) enables us to interpolate the chromatographic behaviour of homologues and related solutes, to estimate the chromatographic behaviour of structurally similar compounds, and to optimise the chromatographic conditions for the separation of complex mixtures in analytical and preparative separations.

In the case of aromatic hydrocarbons, relationships between retention and molecular structure have been extensively studied for both adsorption (normal-phase LC) and reversed-phase LC.

Relationships for alumina were early established by Snyder[1,2] and later in more detail by Popl and co-workers[3-5]. More precise data was obtained by Kříž et al. in their studies of alkylbenzenes[6] and alkylbiphenyls[7], using a moisture control system (MCS) which provided a constant water content on the adsorbent surface.

Relationships for silica gel were established by Popl et al.[5,8,9] for mono- and diaromatic hydrocarbons, and by Kříž and co-workers for alkylbenzenes[10], alkylnaphthalenes[11] and alkylbiphenyls[12], again using MCS.

Retention measurements for *n*-alkylbenzenes as a function of mobile phase composition and temperature for reversed-phase systems have been made by Melander and co-workers[13-15], by Grushka et al.[16], by Colin and co-workers[17-20] and by Berendsen and De Galan[21]. The relation of retention to molecular structure has been extensively considered[16,17,22-26]

Jandera[27] used *n*-alkylbenzenes as reference compounds to predict retention on the basis of interaction indices. Sleight[28] studied alkylbenzenes with different substitution patterns, and correlated log k' with the total number of carbon atoms. He also established the strictly linear relationship between log k' and carbon number for the *n*-alkylbenzenes.

Shabron et al.[29] compared the retentive behaviour on μBondapak C_{18} of alkyl substituted aromatic and hydroaromatic compounds having different parent groups, and obtained empirical correlation factors for different structural features He pointed out, for example, that when the parent compound contained a non-aromatic double bond, as with indene and acenaphthalene, the two double bonded C-atoms had the same effect on retention as a single aliphatic C-atom. Koopmans and Rekker[30] studied the relationship of retention to hydrophobicity and connectivity indices for polymethylbenzenes and basic polyaromatics using methanol–water (70:30, v/v) as eluent and μBondapak C_{18} as stationary phase. Karger et al.[31] studied hydrophobic effects using basic phases. Kiselev et al.[25] compared retention of polymethylbenzenes and of *n*-alkylbenzenes on silanized silica gel using 2-propanol–water (40:60, v/v) as eluent with their retention on underivatized silica with hexane as eluent. In the latter system the polymethylbenzenes were less retained than the *n*-alkylbenzenes of the same carbon number.

Smith[32] carried out a comprehensive study of the retentive behaviour of C_1–C_4 substituted alkylbenzenes on three different reversed-phase silica gels using methanol–water (70:30, v/v) as eluent. He confirmed the well established linear relationship between log k' and carbon number for the *n*-alkylbenzenes and established a similar relationship for polymethylbenzenes with adjacent methyl groups.

The lower slope of the latter was explained on the basis of the increased electron density on the benzene ring caused by the increased methyl substitution. Smith found that the two bicyclic aromatics, biphenyl and naphthalene, eluted much earlier than would be expected from their carbon numbers. Log k' correlated well with the connectivity index for the n-alkylbenzenes and polymethylbenzenes but poorly for other isomeric alkylbenzenes.

The present study aimes at finding relationships between molecular structure and retention for an extended series of 54 aromatic hydrocarbons including, alkylaromatics, cycloaromatics, hydroaromatics, and polynuclear aromatics, using three different ODS bonded silica gels, and three different methanol–water eluents. The three bonded silica gels were: ODS Hypersil, which is a fully capped octadecyl bonded silica gel manufactured by Shandon Southern Products (Runcorn, U.K.), uncapped ODS Hypersil, which is the intermediate in the production of ODS Hypersil just prior to capping, and LiChrosorb RP-18 manufactured by Merck (Darmstadt, F.R.G.). Comparison of the results from capped and uncapped ODS Hypersil was expected to reveal the effects of underivatized silanol groups, while comparison of ODS Hypersil and LiChrosorb RP-18 was expected to indicate any significant differences between two materials both claiming the same bonding functionality.

EXPERIMENTAL

Equipment and chemicals

The HPLC equipment comprised a Waters Model M6000 pump (Waters Assoc., Croydon, U.K.), a Rheodyne injection valve (Shandon Southern Products), a Cecil Model 212 UV spectrophotometer (Cecil Instruments, Cambridge, U.K.). Columns were of the Shandon design, 160 mm × 5 mm I.D. They were packed by the slurry method using 2-propanol as slurry medium with methanol and finally hexane as follower liquids. For chromatography a flow-rate of 1 ml/min was used throughout. ODS Hypersil and uncapped ODS Hypersil were kindly gifted by Shandon Southern Products. LiChrosorb RP-18 was obtained from BDH, Poole, U.K. Eluents were water–methanol mixtures. The methanol was HPLC grade from Rathburn Chemicals, Walkerburn, U.K.; water was doubly distilled and stored in glass. Methanol–water mixtures were made up by weight, not volume, to avoid uncertainties arising from volume changes on mixing. Most of the hydrocarbons were kindly provided by the Institute of Chemical Technology, Prague, Checkoslovakia; the remainder were purchased from U.K. chemical suppliers.

Retention data were analysed and processed on an HP-85 personal computer (Hewlett-Packard, Avondale, PA, U.S.A.) equipped with an 82905B impact printer, an 8901 disk drive and a Servigor Model 281 plotter. Visicalc software was used to prepare, compute and print tables.

Procedure

On the basis of preliminary chromatographic runs, mixtures containing from two to five completely resolved hydrocarbons were prepared in methanol. Injections of between 0.5 and 5 μl of each such mixture were made in triplicate. Column capacity ratios, k', were calculated from the recorder traces using direct measurement of retention distances according to

$$k' = (t_R - t_0)/t_0 \qquad (1)$$

TABLE I

RETENTION DATA

C = No. of carbon atoms in molecule, H = No. of hydrogen atoms in molecule, Con. = connectivity index. C_1 = column with LiChrosorb RP-18, C_2 = column with Hypersil ODS, C_3 = column with Hypersil ODS-uncapped.

Compound	C	H	Con.	Capacity factor 70:30*			80:20			90:10		
				C_1	C_2	C_3	C_1	C_2	C_3	C_1	C_2	C_3
1 Benzene	6	6	2.0000	1.41	0.89	0.79	0.74	0.46	0.43	0.41	0.25	0.24
2 Toluene	7	8	2.4107	2.38	1.47	1.28	1.16	0.71	0.68	0.59	0.37	0.35
3 Ethylbenzene	8	10	2.9713	3.54	2.23	1.85	1.58	0.99	0.90	0.74	0.47	0.43
4 n-Propylbenzene	9	12	3.4713	5.66	3.61	2.81	2.30	1.44	1.24	0.98	0.62	0.55
5 n-Butylbenzene	10	14	3.9713	9.20	5.87	4.37	3.36	2.12	1.72	1.32	0.84	0.71
6 n-Amylbenzene	11	16	4.4713	15.35	9.75	6.85	4.99	3.09	2.41	1.75	1.12	0.92
7 n-Hexylbenzene	12	18	4.9713	25.41	16.03	10.79	7.40	4.55	3.39	2.37	1.49	1.18
8 n-Heptylbenzene	13	20	5.4713	42.85	26.67	17.22	11.14	6.73	4.83	3.23	1.98	1.54
9 n-Octylbenzene	14	22	5.9713	—	44.36	27.54	16.60	10.12	6.87	4.37	2.62	1.99
10 n-Nonylbenzene	15	24	6.4713	—	—	—	24.21	14.72	9.75	6.00	3.47	2.62
11 n-Decylbenzene	16	26	6.9713	—	—	—	36.22	21.28	13.96	8.18	4.61	3.40
12 n-Tridecylbenzene	19	32	8.4713	—	—	—	—	—	—	20.32	10.74	7.21
13 o-Xylene	8	10	2.8274	3.72	2.30	1.92	1.82	1,04	0.94	0.84	0.50	0.47
14 m-Xylene	8	10	2.8214	4.03	2.52	2.07	1.81	1.09	1.00	0.87	0.55	0.48
15 p-Xylene	8	10	2.8214	4.12	2.68	2.09	1.80	1.15	0.95	0.87	0.54	0.48
16 Isopropylbenzene	9	12	3.3541	5.89	3.35	2.92	2.16	1.36	1.17	0.88	0.57	0.51
17 o-Ethyltoluene	9	12	3.3880	5.46	3.43	2.57	2.28	1.36	1.16	1.04	0.64	0.57
18 m-Ethyltoluene	9	12	3.3820	5.70	3.77	2.86	2.34	1.50	1.28	1.05	0.67	0.58
19 p-Ethyltoluene	9	12	3.3820	6.01	3.86	2.99	2.43	1.53	1.32	1.08	0.68	0.59
20 1,2,3-Trimethylbenzene	9	12	3.2440	5.79	3.72	2.94	2.51	1.53	1.34	1.17	0.71	0.64
21 1,2,4-Trimethylbenzene	9	12	3.2380	6.37	4.47	3.18	2.67	1.62	1.40	1.21	0.72	0.66
22 1,3,5-Trimethylbenzene	9	12	3.2321	6.82	4.29	3.33	2.84	1.74	1.47	1.23	0.77	0.69

Compound												
23 Isobutylbenzene	10	14	3.8272	8.20	5.56	3.95	3.01	1.98	1.59	1.22	0.79	0.67
24 sec.-Butylbenzene	10	14	3.8921	7.50	4.67	3.55	2.81	1.84	1.46	1.16	0.76	0.62
25 tert.-Butylbenzene	10	14	3.6607	6.62	3.84	3.13	2.45	1.50	1.28	1.02	0.69	0.58
26 p-Cymene	10	14	3.7647	8.87	5.55	4.00	3.13	2.02	1.64	1.28	0.82	0.69
27 o-Diethylbenzene	10	14	3.9487	7.62	5.12	3.71	2.92	1.91	1.55	1.24	0.82	0.68
28 m-Diethylbenzene	10	14	3.9427	8.43	5.21	3.96	3.08	1.99	1.61	1.26	0.82	0.69
29 p-Diethylbenzene	10	14	3.9427	8.95	5.60	4.15	3.30	2.10	1.70	1.34	0.85	0.72
30 1,2,3,4-Tetramethylbenzene	10	14	3.6607	9.33	5.97	4.55	3.78	2.26	1.92	1.66	0.99	0.86
31 1,2,3,5-Tetramethylbenzene	10	14	3.6547	10.07	6.22	4.75	3.99	2.39	2.00	1.67	1.02	0.89
32 1,2,4,5-Tetramethylbenzene	10	14	3.6547	10.19	6.59	4.82	3.96	2.40	1.99	1.69	1.00	0.89
33 Pentamethylbenzene	11	16	4.0774	15.35	9.66	7.10	5.62	3.37	2.71	2.32	1.36	1.17
34 4-tert.-Butyltoluene	11	16	4.0714	12.16	7.55	5.40	3.94	2.57	1.98	1.52	0.99	0.80
35 m-Diisopropylbenzene	12	18	4.7081	14.76	10.23	6.70	4.60	3.18	2.32	1.64	1.11	0.90
36 p-Diisopropylbenzene	12	18	4.7081	16.71	11.35	7.59	5.32	3.53	2.55	1.80	1.22	0.94
37 Hexamethylbenzene	12	18	4.5000	23.01	14.29	10.33	8.07	4.76	3.69	3.21	1.86	1.56
38 Cyclohexylbenzene	12	16	5.0159	16.22	10.23	7.29	5.30	3.24	2.57	2.00	1.21	1.02
39 p-Di-tert.-butylbenzene	14	22	5.3214	31.62	21.93	13.06	8.20	5.71	3.81	2.53	1.74	1.25
40 1,2,3-Triisopropylbenzene	15	24	5.9848	38.90	28.18	15.85	9.33	6.79	4.26	2.65	1.91	1.31
41 p-Dicyclohexylbenzene	18	26	8.0317	—	—	—	37.50	21.93	12.88	8.36	5.09	3.63
42 Hexaethylbenzene	18	30	7.8640	—	—	—	19.72	12.02	6.55	4.11	2.99	1.91
43 Indane	9	10	3.5345	5.07	2.89	2.39	2.14	1.29	1.15	1.02	0.62	0.57
44 Indene	9	8	3.2112	2.96	1.69	1.60	1.42	0.83	0.81	0.71	0.42	0.43
45 Tetrahydronaphthalene	10	12	4.0345	7.38	4.40	3.61	3.06	1.82	1.58	1.38	0.82	0.73
46 Naphthalene	10	8	3.4047	3.65	1.97	1.88	1.64	0.90	0.92	0.79	0.44	0.46
47 Phenanthrene	14	10	4.8154	12.30	5.22	5.71	4.51	1.95	2.25	1.87	0.83	0.98
48 Anthracene	14	10	4.8094	12.02	5.31	5.71	4.51	1.95	2.25	1.85	0.84	0.98
49 Biphenyl	12	10	4.0714	5.97	3.21	2.90	2.35	1.29	1.25	1.01	0.57	0.57
50 Fluorene	13	10	4.6118	8.75	4.49	4.22	3.49	1.70	1.79	1.50	0.74	0.81
51 Acenaphthene	12	10	4.4451	8.09	4.33	3.90	3.38	1.77	1.74	1.51	0.82	0.81
52 o-Terphenyl	18	14	6.1487	13.49	8.43	6.00	4.30	2.59	2.12	1.45	0.90	0.80
53 m-Terphenyl	18	14	6.1427	24.04	12.79	10.26	7.13	3.69	3.35	2.28	1.22	1.21
54 p-Terphenyl	18	14	6.1427	33.19	13.96	13.06	9.53	3.97	3.98	2.92	1.28	1.39

* Composition of methanol–water (w/w) mobile phase.

where t_R is the retention time (or distance on chart) for a solute peak, and t_0 is the retention time (or distance on chart) of the unretained solute peak. The retention time of the unretained solute peak was taken as the time interval from the moment of injection to the time when the trace for the solvent disturbance crossed the baseline. The solvent disturbance peak was generated by the methanol in which the samples were dissolved. Retention data were reproducible to better than 2% from run to run provided that an entire set of data were obtained over a period of 10–18 h. Column activity was checked several times during any such experiment by injecting a standard mixture of n-alkylbenzenes.

RESULTS AND DISCUSSION

Table I lists the values of the capacity factors for the 54 hydrocarbons on the three stationary phases and with the three eluent compositions. Each value represents the average of at least three measurements. The majority of compounds examined were alkylbenzenes and had the empirical formula C_nH_{2n-6}, but compounds with the following empirical formulae were also characterised: C_nH_{2n-8} (indane, tetralin, cyclohexylbenzene), C_nH_{2n-10} (indene), C_nH_{2n-12} (naphthalene), C_nH_{2n-14} (biphenyl and acenaphthene) and so on up to C_nH_{2n-22} (terphenyls).

We have examined the following aspects of the structure–retention relationship for the 54 solutes. (i) Correlations between log k' and (a) the number of carbon atoms in each molecule, (b) the number of hydrogen atoms in each molecule, and (c) the connectivity index of each molecule[33]. (ii) The effects of the following structural features: (a) the length of the alkyl chain, (b) the number of alkyl groups, (c) the arrangement of the alkyl groups (the *ortho* effect), and (d) the shape of the alkyl groups. (iii) The effect of capping an ODS silica gel.
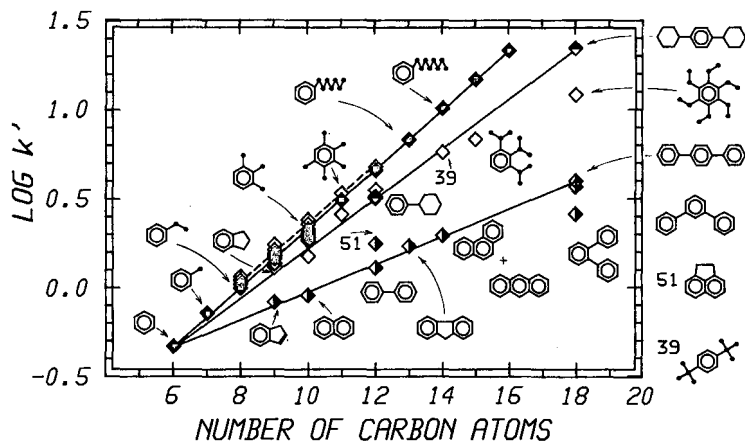
Fig. 1. Dependence of log k' for 54 aromatic hydrocarbons on carbon number. Packing material, ODS Hypersil; eluent, methanol–water (80:20, w/w). Solutes identified by number are listed in Table I. Symbol representation: (◆) n-alkylbenzenes, (◇) polymethylbenzenes and other alkylbenzenes, (◆) cyclohexyl benzenes, (◆) polycyclic aromatics. Broken line is drawn through points for the all-*ortho* polymethylbenzenes; full lines are drawn (in order from the top) through points for n-alkylbenzenes, cyclohexylbenzenes, and polycyclic aromatics.

Correlations of log k' with structural features

   Correlation with carbon number. In reversed-phase LC, k' invariably increases with carbon number for any series of compounds, although with adsorbents in normal-phase LC[6,7] k' may hardly change (alumina) or may even decrease (silica gel) with increase in n..

   Fig. 1 shows the dependence of log k' upon carbon number with ODS Hypersil as packing and methanol–water (80:20) as eluent. Similar results were obtained for the other packing materials and other mobile phases. More or less linear dependences were observed for *n*-alkylbenzenes, polymethylbenzenes, cyclohexylbenzenes, and polynuclear aromatics. The dependence for *n*-alkylbenzenes is strictly linear for all members except benzene (slighly low k') and toluene (slightly high k'), and is shown by the uppermost full line. The dependence for the polymethylbenzenes is also linear when all the methyl groups are adjacent (broken line above the full line for the *n*-alkylbenzenes) as found by Smith[32]. The other polymethylbenzenes show slightly higher retention than the all-*ortho* isomers: By contrast, the points for branched chain alkylbenzenes and cyclohexylbenzenes are significantly below those for the *n*-alkylbenzenes. The points for the cyclohexylbenzenes mark more or less the lower limit of this group (hexaethylbenzene being the exception). In general the points for all the alkyl- and cycloalkylbenzenes fall within a relatively narrow band marked out by the two full lines in Fig. 1. Log k' values for the polynuclear aromatics (PNAs) fall well below those for the other aromatics and show considerable variance from a straight line. *o*-Terphenyl shows particularly low retention, and acenaphthene (compound 51) particularly high retention relative to the general body of the PNAs. In addition the general gradient of the log k' *versus n* plot for the PNAs is about half that for the *n*-alkylbenzenes, confirming the earlier results of Shabron *et al.*[29].

   Correlations with hydrogen number. The H-atoms in the sample molecules had a remarkably large effect on their retention in the reversed-phase systems studied. This is seen clearly by comparing Figs. 2 and 3. Fig.. 2 shows chromatograms where the number of C-atoms was kept constant while the number of hydrogen atoms was changed. Fig. 3 shows chromatograms where the number of hydrogen atoms was kept constant while the number of carbon atoms was changed. The effect of adding
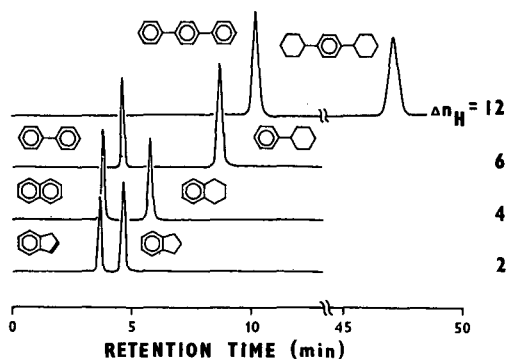
Fig. 2. Chromatogram of selected mixtures showing the effect of addition of hydrogen atoms when the carbon number is fixed. Column packing, ODS Hypersil; eluent, methanol–water (80:20). Δn_H gives the difference in the hydrogen number for the solutes in each chromatogram.
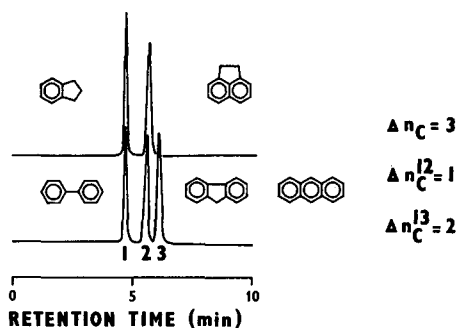
Fig. 3. Chromatograms of selected mixtures showing the effect of addition of carbon atoms when the hydrogen number is fixed. Conditions as for Fig. 2. Δn_c gives the difference in the carbon number for the solutes in each chromatogram.

another hydrogen atom is only slightly less than that of adding another carbon atom. Addition of hydrogen atoms invariably increases retention: thus indane is more retained than indene, cyclohexylbenzene is more retained than biphenyl, and tetrahydronaphthalene is more retained than naphthalene.

Fig. 4 plots the dependence of log k' upon hydrogen number using the same data as for Fig. 1. Necessarily a strict linear dependence is still observed for the n-alkylbenzenes and for the all-*ortho* polymethylbenzenes. However the cyclohexylbenzenes now fall on the same line as the n-alkylbenzenes, while the points for the PNAs now lie above those for the n-alkylbenzenes, and the best straight line through them has a much higher slope.

Correlations with connectivity indices. The connectivity index has been found to give a useful correlation with retention in reversed-phase systems[34]. For example
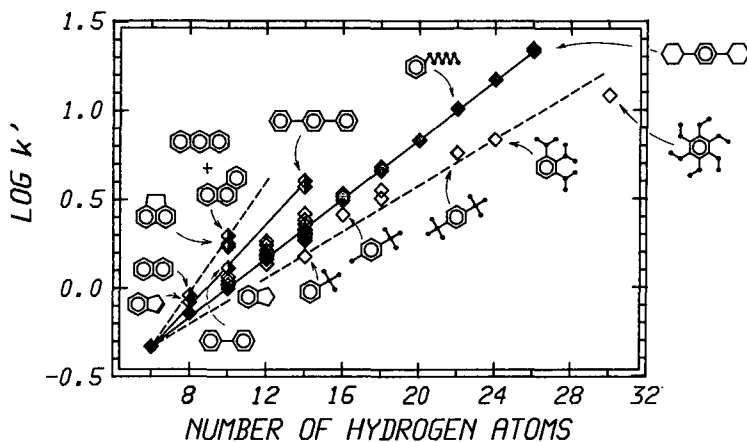
Fig. 4. Dependence of log k' upon hydrogen number. Conditions and data as for Fig. 1. Symbol identification: (♦) n-alkylbenzenes, (◇) polymethylbenzenes and other alkylbenzenes, (◆) polycyclic aromatics. Lines in order from the top are drawn through points for: condensed ring polynuclear aromatics (broken line), polyphenyls (full line), n-alkylbenzenes (full line), and propylbenzenes (broken line).
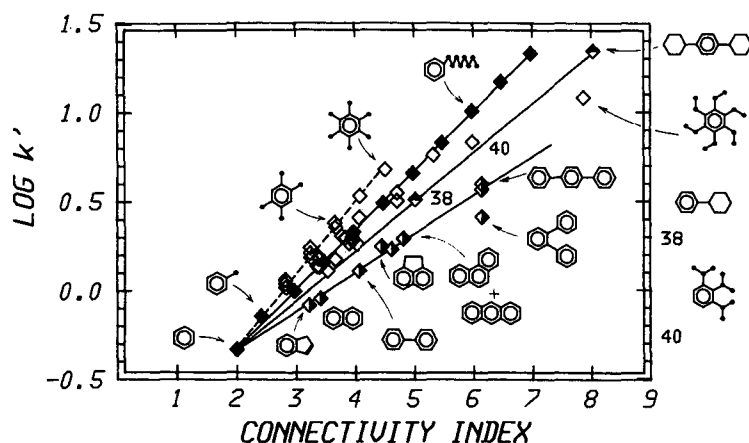
Fig. 5. Dependence of log k' upon connectivity index. Conditions, data, symbols and lines as for Fig. 1.

the log k' values of a large set of C_5–C_{11} alkanes with different degrees of branching were found to lie within a much narrower band when plotted against the connectivity index than when plotted against the carbon number.

Fig. 5, again using the same data as Fig. 1, plots log k' against the connectivity index, and is rather similar to Fig. 1. Evidently the connectivity index mainly reflects the number of carbon atoms in the group under study. The four more or less linear dependences are again shown. The polymethylbenzenes now show a considerably higher slope than the n-alkylbenzenes, while the slope for the PNAs is only a little less than that for the cyclohexylbenzenes. Amongst the PNAs only o-terphenyl is now exceptional; the point for acenaphthene falls on the line of the other PNAs, and the spread of points about the line is generally less than in Fig. 1 and 4. While the

TABLE II

PARAMETERS OF LINEAR REGRESSION FOR ALKYLBENZENES

log $k' = bn + a$; where k' = capacity factor, n = carbon number, a and b are regression coefficients, r^2 = coefficient of determination.

Column	Mobile phase ratio	b	a	r^2
LiChrosorb RP-18	70:30	0.210	−1.118	0.99894
	80:20	0.168	−1.142	0.99955
	90:10	0.129	−1.166	0.99931
Hypersil ODS	70:30	0.212	−1.335	0.99947
	80:20	0.166	−1.328	0.99976
	90:10	0.124	−1.321	0.99970
Hypersil uncapped	70:30	0.191	−1.259	0.99921
	80:20	0.148	−1.237	0.99921
	90:10	0.112	−1.268	0.99947

correlation in specific areas may be better than when using carbon and hydrogen numbers it is not significantly better overall.

We conclude that none of the simple structural parameters examined can provide a unique correspondence with retention for the range of aromatic compounds covered.

Effect of structural changes on retention

Alkyl chain length. Numerous studies have established that the retention of *n*-alkylbenzenes increases exponentially with chain length according to

$$\log k' = a + bn \tag{2}$$

where *n* is the number of carbon atoms in the molecule. The data obtained in this work and listed in Table I, provide the regression coefficients for the three stationary phases and the three eluents listed in Table II. Only *k'* values of benzene and toluene show deviations from eqn. 2. If, for example, toluene and benzene are omitted from the data for ODS Hypersil with methanol–water (70:30) as eluent, the correlation coefficient is increased from 0.99947 to 0.99989.

The regression coefficients giving the values of *b* in eqn. 2 are essentially the same for ODS Hypersil and LiChrosorb RP-18, but are slightly lower for uncapped ODS Hypersil. This is what might be expected in view of the presence of accessible silanol groups in the uncapped material. Of course, in this work, the eluents contained a considerable proportion of water which would undoubtedly reduce the adsorptive effects of the silanol groups drastically. Nevertheless they still have some of the repulsive effect on alkyl chains which they show when the *n*-alkylbenzenes are chromatographed in non-polar eluents on bare silica gel[6,7].

Number of alkyl groups. Retention increases with increasing number of alkyl groups when the total carbon number is fixed, and of, course, whenever the carbon

TABLE III

PARAMETERS OF LINEAR REGRESSION FOR *ORTHO*-SUBSTITUTED METHYLBENZENES

Benzene, toluene, *o*-xylene, 1,2,3-trimethylbenzene, 1,2,3,4-tetramethylbenzene, pentamethylbenzene and hexamethylbenzene. $\log k' = bn + a$; where k' = capacity factor, n = carbon number, a and b are regression coefficients, r^2 = coefficient of determiniation.

Column	Mobile phase	b	a	r^2
LiChrosorb RP-18	70:30	0.202	−1.050	0.99937
	80:20	0.172	−1.140	0.99849
	90:10	0.149	−1.272	0.99967
Hypersil ODS	70:30	0.203	−1.256	0.99933
	80:20	0.168	−1.333	0.99956
	90:10	0.144	−1.453	0.99944
Hypersil uncapped	70:30	0.186	−1.210	0.99936
	80:20	0.154	−1.262	0.99787
	90:10	0.134	−1.404	0.99916
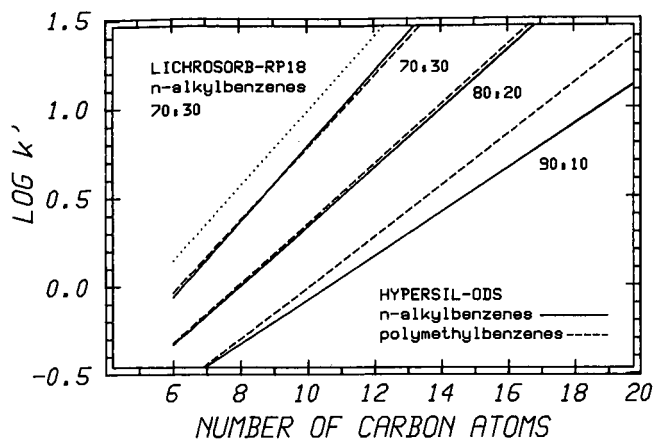
Fig. 6. Effect of eluent composition on selectivity of ODS Hypersil for *n*-alkylbenzenes (full lines) and all-*ortho* polymethylbenzenes (broken lines). The dotted line for LiChrosorb RP-18 is for *n*-alkylbenzenes using methanol–water (70:30) as eluent.
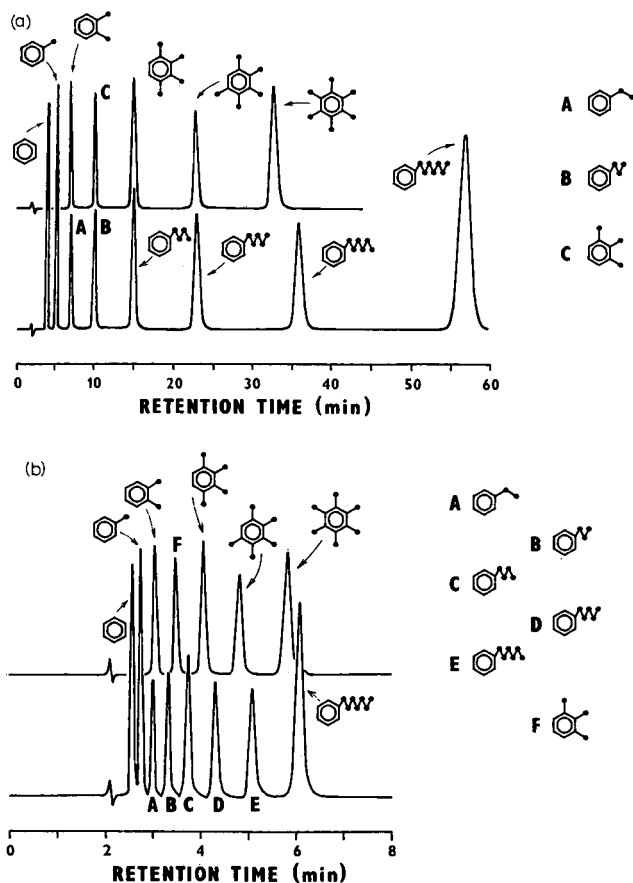
Fig. 7. (a) Chromatogram showing the close correspondance of retention times for the all-*ortho* polyme-thylbenzenes and *n*-alkylbenzenes having the same carbon numbers when using methanol–water (70:30) as eluent. (b) Chromatogram showing the selectivity for the same group when using methanol–water (90:10) as eluent. Packing material, ODS Hypersil.

RETENTION TIME (min)
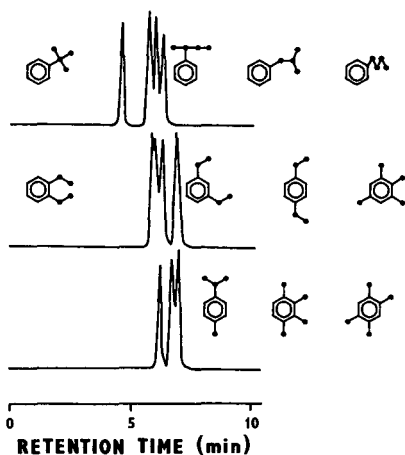
Fig. 8. Chromatograms of selected isomeric alkylbenzenes showing selectivity effects. Packing, ODS Hypersil; eluent, methanol–water (80:20).

number is increased. When all groups are *ortho* to each other there is a linear relationship between Log k' and n. The linear regression coefficients are given in Table III. Fig. 6 shows the plots with ODS Hypersil as packing for the three eluents used, and for both n-alkylbenzenes and polymethylbenzenes. The dotted line gives the plot for n-alkylbenzenes on LiChrosorb RP-18 for comparison using one of the eluents.

    With the same eluent, the retention of the n-alkylbenzenes relative to that of the polymethylbenzenes having the same carbon number is roughly equivalent for the three stationary phases, but selectivity increases as the water content is lowered, being greatest for methanol–water (90:10). This is illustrated in Fig. 7a and b. Fig. 7a shows the near equivalence of the retention times of solutes of the same carbon number when using 70:30 eluent, while Fig. 7b shows the increased retention of the polymethylbenzenes over the n-alkylbenzenes in the 90:10 mixture.
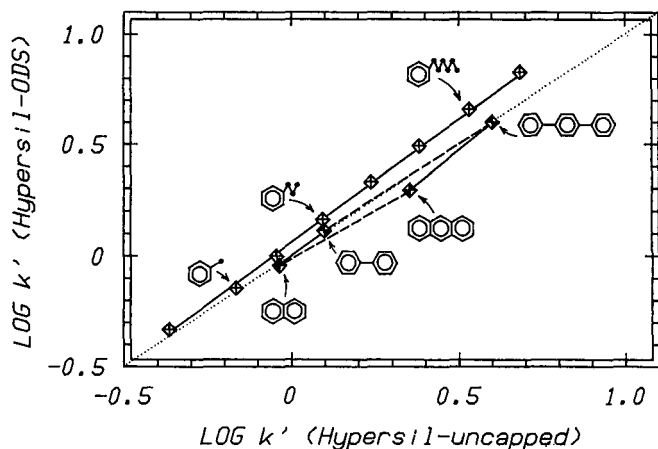
Fig. 9. Correlation of log k' on ODS Hypersil with log k' on uncapped ODS Hypersil. Eluent, methanol–water (80:20). Dotted line is locus for equal k' on the two packing materials.

The reversed ortho effect. The "*ortho* effect" is an effect observed with alumina and silica gel whereby the retention of substances with substituents in the *ortho* position is greater than that of isomers with substituents in other positions. With the ODS silica gels studied here the opposite effect is observed and the *ortho*-substituted isomers show the least retention. This is seen in the retention parameters for the xylenes, ethyltoluenes, diethylbenzenes, trimethylbenzenes and tetramethylbenzenes (see Table I). The inverse ortho-effect is particularly strong when large substituents are in ortho positions.

The inversion of the *ortho* effect on transferring from adsorption to reversed-phase chromatography is evidently just what one would expect.

Shape of alkyl groups. Branching of the alkyl group generally reduces retention as in other modes of chromatography. This is illustrated in Fig. 8 which shows chromatograms of the butylbenzenes and of other isomeric alkylbenzenes. The order of elution of the butylbenzenes, namely *tert.-, sec.-, iso-* and *n*-butylbenzene is in agreement with Smith[32] and is the same as found in gas chromatography. This order does not follow the connectivity index (see Table I).

Comparison of capped and uncapped ODS silica gels

Fig. 9 plots log k' on ODS Hypersil against log k' on uncapped ODS Hypersil. Points are shown for the *n*-alkylbenzenes, the polyphenyls, and the condensed ring aromatics. Points for the other alkylbenzenes lie on or close to the line for the *n*-alkylbenzenes. The dotted line (1:1 line) represents equal k' values on the two phases. For the alkylbenzenes the points lie above the 1:1 line so the process of capping ODS Hypersil slightly increases retention. This is no doubt due to a slight increase in carbon content produced by capping. Points for the polynuclear aromatics lie either on or below the 1:1 line. Accordingly capping either leaves their retention unchanged or decreases it. Apparently with the uncapped ODS Hypersil there still remains some small interaction between the residual silanol groups of the uncapped material and the aromatic rings. The effect of capping which removes these interactions is not
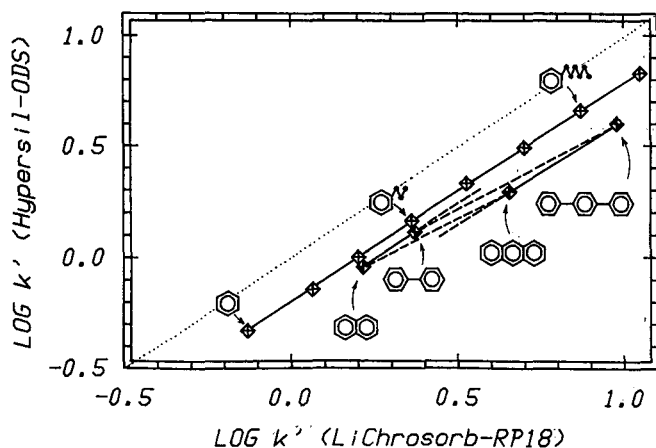
Fig. 10. Correlation of log k' on ODS Hypersil with log k' on LiChrosorb RP-18. Conditions as for Fig. 9.

quite compensated by the increased hydrophobic interaction resulting from the extra carbon content. Thus as shown earlier even with a high water content in the eluent the silanol groups still appear to have some adsorptive capacity.

Fig. 10 shows a similar plot comparing LiChrosorb RP-18 with ODS Hypersil. The retention on LiChrosorb RP-18 is substantially greater than that on ODS Hypersil as seen by the position of the points relative to the 1:1 line. This is no doubt due to the greater carbon content of LiChrosorb RP-18. Otherwise the relative positions of the points are very similar in Figs. 9 and 10, indicating that LiChrosorb RP-18 is closer to uncapped ODS Hypersil than to the standard capped ODS Hy-
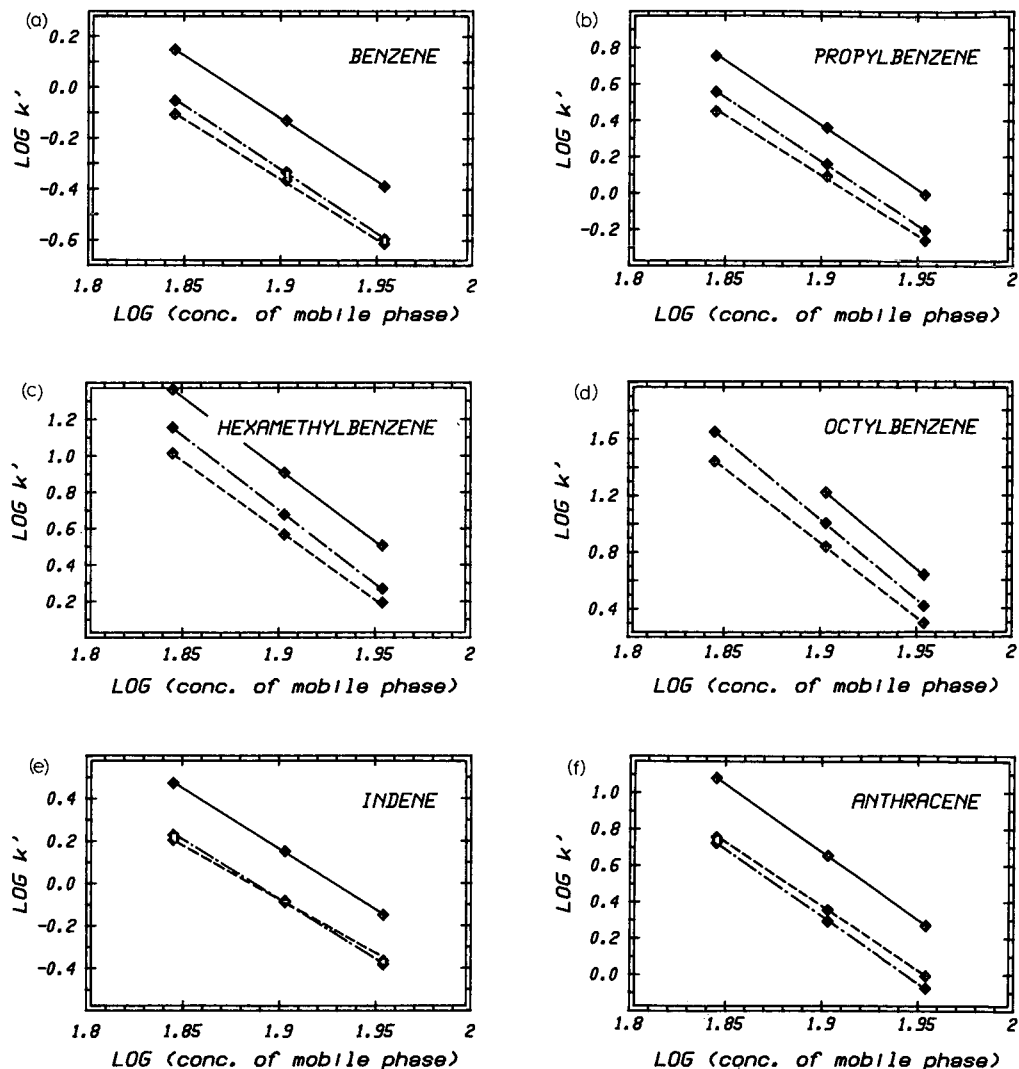
Fig. 11. Dependence of log k' upon eluent composition for the three packing materials. (———) LiChrosorb RP-18; (– · –) ODS Hypersil; (– – –) uncapped ODS Hypersil.

persil in its selectivity for different types of aromatic hydrocarbon. However the gradient of the line through the points for the *n*-alkylbenzenes is very close to unity in Fig. 10 whereas it is significantly above unity in Fig. 9. This similarity between LiChrosorb RP-18 and ODS Hypersil is also shown in Fig. 11a–f which give examples of the linear relationships between log k' and log (% methanol). The gradients for ODS Hypersil and LiChrosorb RP-18 are virtually identical while those for uncapped ODS Hypersil are significantly lower.

We note the danger in making judgements as to whether a material such as LiChrosorb RP-18 is capped or uncapped on the basis of retention measurements made only with hydrocarbons.

ACKNOWLEDGEMENT

REFERENCES

1 L R. Snyder, *Principles of Adsorption Chromatography*, Marcel Dekker, New York, 1968.
2 L. R. Snyder, *J. Chromatogr.*, 6 (1961) 22.
3 M. Popl, V. Dolanský and J. Mostecký, *J. Chromatogr.*, 59 (1971) 329.
4 M. Popl, J. Mostecký, V. Dolanský and M. Kuraš, *Anal. Chem.*, 43 (1971) 518.
5 M. Popl, V. Dolanský and J. Mostecký, *J. Chromatogr.*, 91 (1974) 649.
6 J. Kříž, J. Punčochářová, L. Vodička and J. Vařeka, *J. Chromatogr.*, 437 (1988) 177.
7 J. Kříž, J. Punčochářová, L. Vodička and J. Vařeka, Poster presented at the *11th Symposium on Column Liquid Chromatography, Amsterdam, 1987*, Abstract No. Mo-P-84.
8 M. Popl and V. Dolanský *Coll. Czech. Chem. Commun.*, 39 (1974) 1836.
9 M. Popl, V. Dolanský and J. Mostecký, *J. Chromatogr.*, 117 (1976) 117.
10 J. Kříž, L. Vodička, J. Punčochářová and M. Kuraš, *J. Chromatogr.*, 219 (1981) 53.
11 J. Punčochářová, L. Vodička and J. Kříž, *J. Chromatogr.*, 267 (1983) 222.
12 J. Kříž, J. Punčochářová and L. Vodička, *J. Chromatogr.*, 354 (1986) 145.
13 W. R. Melander, B.-K. Chen and Cs. Horváth, *J. Chromatogr.*, 185 (1979) 99.
14 W. R. Melander, C. A. Mannan and Cs. Horváth, *Chromatographia*, 15 (1982) 611.
15 W. R. Melander and Cs. Horváth, *Chromatographia*, 15 (1982) 86.
16 E. Grushka, H. Colin and G. Guiochon, *J. Chromatogr.*, 248 (1982) 325.
17 H. Colin and G. Guiochon, *J. Chromatogr. Sci.*, 18 (1980) 54.
18 H. Colin, G. Guiochon and J. C. Diez-Masa, *Anal. Chem.*, 53 (1981) 146.
19 A. M. Krstulovic, H. Colin, A. Tchalpa and G. Guiochon, *Chromatographia*, 17 (1983) 228.
20 H. Colin, G. Guiochon, Z. Yun, J C. Diez-Masa and P. Jandera, *J. Chromatogr. Sci.*, 21 (1983) 179.
21 G. E. Berendsen and L. de Galan, *J. Chromatogr.*, 196 (1980) 21.
22 K. Jinno and K. Kawasaki, *Chromatographia*, 17 (1983) 337.
23 K. Jinno and K. Kawasaki, *Chromatographia*, 18 (1984) 211.
24 A. N. Ageev, A. V. Kiselev and Ya. I. Yashin, *Chromatographia*, 14 (1981) 638.
25 A. V. Kiselev, L. V. Tarasova and Ya. I. Yashin, *Chromatographia*, 13 (1980) 599.
26 H. Hemetsberger, P. Behrensmeyer, J. Henning and H. Ricken, *Chromatographia*, 12 (1979) 71.
27 P. Jandera, *J. Chromatogr.*, 314 (1984) 13.
28 R. B. Sleight, *J. Chromatogr.*, 83 (1973) 31.
29 J. F. Shabron, R. J. Hurtubise and H. F. Silver, *Anal. Chem.*, 49 (1977) 2253.
30 R. E. Koopmans and R. F. Rekker, *J. Chromatogr.*, 285 (1984) 267.
31 B. L. Karger, J. R. Gant, A. Hartkopf and P. H. Weiner, *J. Chromatogr.*, 128 (1976) 65.
32 R. M. Smith, *J. Chromatogr.*, 209 (1981) 1.
33 M. Randic, *J. Am. Chem. Soc.*, 97 (1975) 6609.
34 J. Burda, M. Kuraš, J. Kříž and L. Vodička, *Fresenius' Z. Anal. Chem.*, 321 (1985) 548.

CHROM. 20 537

CAPILLARY COLUMN GAS CHROMATOGRAPHIC METHOD FOR THE STUDY OF DYNAMIC INTRAMOLECULAR INTERCONVERSION BEHAVIOUR

PHILIP J. MARRIOTT*,* and YEE-HING LAI

Department of Chemistry, National University of Singapore, 10 Kent Ridge Crescent, Singapore 0511 (Singapore)

(First received November 11th, 1987; revised manuscript received March 7th, 1988)

SUMMARY

Reversible reactions which proceed unimolecularly and are mediated by temperature may be suited to gas chromatographic (GC) study. This paper describes the study of a series of intramolecular sterically-hindered isomerisations of some novel aromatics in which the isomers possess different capacity factors on the column, and where by appropriate selection of operating temperature and gas flow-rate, the extent of interconversion can be altered. Restricted rotation about the $C=N$ bond in oximes can also be readily observed and quantified as it occurs on the GC column, leading to derivation of rate and activation parameters (for forward and reverse processes). Capillary columns enhance the resolution of isomers and interpretation of data. Some equations are presented to describe the on-column phenomenon in a simplified way. The route to activation parameters afforded by GC, especially at high temperatures, is a possible adjunct to the use of variable-temperature NMR studies. Activation energies in the order of 100–140 kJ mol^{-1} were obtained for the sterically-hindered aromatics, and the oximes gave energies of about 70 kJ mol^{-1} by the GC method, but coalescence of NMR signals was not observed even up to 150°C.

INTRODUCTION

The variable-temperature nuclear magnetic resonance (VTNMR) method is well established as a means of estimating the free energy of the transition state (ΔG^*) for conformational interconversion using the coalescence temperature (T_c) and the frequency difference (∂v) of the particular resonances of the two conformers whose coalescence is to be monitored. Studies have shown that chromatographic techniques may be applied to study various processes, such as decomposition reactions[1,2] and interconversions of molecules[3]. Evidence for dynamic behaviour in thin-layer

---

* Present address: Department of Applied Chemistry, Royal Melbourne Institute of Technology, G.P.O. Box 2476V, Melbourne 3001, Australia.

chromatography was presented as early as 1960[4], however it was some time before column chromatographic methods were employed in this respect.

In a series of papers dealing with kinetic studies of fast equilibrium using high-performance liquid chromatography (HPLC), Moriyasu and co-workers investigated a number of isomer interconversions including acetanilides[5,6], rotamers of palladium dialkyldithiocarbamates[7], sugar anomers[8], and the classical keto–enol tautomerism phenomenon[9,10]. In some of these reports, VTNMR data are compared with those obtained using the dynamic HPLC method. The temperature regime of HPLC is encompassed within that of VTNMR, and so application of HPLC to fluxional processes will be, to a large extent, also possible by VTNMR. Melander *et al.*[11] have reported the *cis–trans* isomerisation of proline-containing dipeptides during chromatography, illustrating the effect of flow-rate, temperature and pH upon the elution profile.

The observation of peak broadening and multiple peaks in HPLC and electrophoresis of proteins has been attributed to conformational equilibria and interconversion between native and unfolded or denatured forms of the protein[12] where the separation takes place on a similar time scale to that of the equilibration phenomenon. No thermodynamic parameters have been reported for the HPLC data however, although the NMR studies of proteins, with particular reference to conformational behaviour, have received attention[13].

Temperature limits for VTNMR (*ca.* 150–180°C) impose restriction on the range of barrier energies which may be conveniently studied. In order to obtain information on sterically hindered molecular motions with energy barriers which require higher temperatures, complementary methods must be found such as time dependent techniques involving an iterative routine of heating followed by measurement of a physical property which differentiates the isomers. This was found to be necessary in a study of barriers to enantiomerisation in helical phenanthrenes[14]. For high rotational barriers the use of gas chromatography (GC) may provide a means whereby dynamic interconversion can be followed, as we have recently reported for 9,10-bis(2,3-dimethylphenyl)phenanthrene[15]. We have also recently investigated two examples of fluxional processes involving lability of coordination to chromium, one in *cis–trans* isomerization of a tris-chelate and another in structural isomerisation accompanying a shift in complexation of $Cr(CO)_3$ from one ring to another is substituted naphthalene[16]. On-column inversion of labile enantiomeric nitrogen invertomers has been followed by complexation GC[17].

In this paper we wish to highlight further applications of GC to conformational analysis which are out of the scope of VTNMR, and to propose the potential use of the technique as an adjunct to dynamic NMR to obtain activation parameters.

EXPERIMENTAL

Reagents

9,10-Bis(2-methylphenyl)anthracene (1a, 1b) was synthesised following the procedure of Grein *et al.*[18]. Instead of using the aryl lithium reagent, the corresponding Grignard reagent was used. 9,10-Bis(2,3-dimethylphenyl)phenanthrene (2a, 2b) and 9,10-bis(3-chloro-2-methylphenyl)phenanthrene (4a, 4b) were synthesised as recently has been reported by one of us[19]. 9,10-Bis(2-methylphenyl)phenanthrene

$$2a, 2b;\ R=R'=CH_3$$
$$3a, 3b;\ R=CH_3,\ R'=H$$
$$4a, 4b;\ R=CH_3,\ R'=Cl$$
$$5a, 5b;\ R=H,\ R'=CH_3$$

$$6a,\ 6b;\ R = -CH_3$$
$$7a,\ 7b;\ R = -CH(CH_3)_2$$
$$8a,\ 8b;\ R = -CH_2CH_2CH_3$$
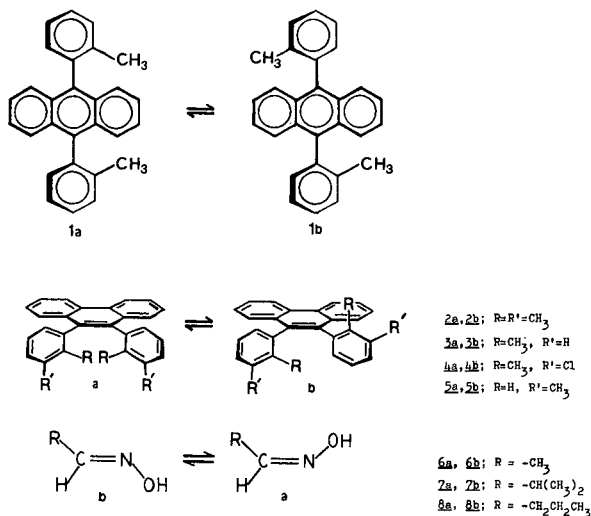
(3a, 3b) and 9,10-bis(3-methylphenyl)phenanthrene (5a, 5b) were synthesised as reported in a recent paper[20]. Acetaldoxime (6a, 6b) was purchased from Tokyo Kasei and used as received. The *anti*:*syn* isomer ratio was *ca.* 55:45. Isobutanaldoxime (7a, 7b) and butanaldoxime (8a, 8b) were prepared based upon standard procedures[21] by adding sodium hydroxide followed by hydroxylamine hydrochloride to the appropriate aldehyde. Carbon dioxide was passed through the mixture until a surface emulsion formed. The solution was extracted with diethyl ether, the diethyl ether was dried and the excess solvent removed. The oxime was then distilled over and collected under reduced pressure. *Anti*:*syn* ratios were approximately: 7a:7b, 80:20 and 8a:8b, 60:40.

Capillary GC was performed on a Hewlett-Packard Model 5790A GC using nitrogen or hydrogen carrier gas, flame ionisation detection and split injection with a Hewlett-Packard Model 3390A computing integrator. Capillary columns used in this work were a Chrompack free fatty acid phase (FFAP)-coated fused-silica capillary (6 m × 0.23 mm I.D.) for the oxime samples, and a Scientific Glass Engineering dimethylsiloxane-coated fused-silica capillary column (25 m × 0.023 mm I.D.) for the anthracene and phenanthrene compounds. Internal standards were benzaldehyde or amylalcohol for the oximes and *n*-octacosane for the aromatics.

GC protocol

The requisite data were obtained according to the procedure outlined briefly elsewhere[15]. The method involves estimation of the extent of "reaction" or "interconversion" that each of the isomers undergoes for each of a number of carrier gas flow-rates and column temperatures. The data are then analysed using an Arrhenius type procedure in order to obtain activation parameters, which entailed calculation of the rates of conversion, k, of the isomer at a number of different temperatures, T, followed by plotting $\ln k$ against $1/T$ which produces a line whose slope is equated to $-E_a/R$, where E_a is the activation energy and R is the universal gas constant.

To quantify the interconversion involves monitoring the disappearance of the

peak corresponding to the unconverted isomer and normalising this against an inert internal standard. This is done at each carrier gas flow setting as the flow-rate of carrier gas is altered which has the effect of changing the residence time of the compound on the column; as the time increases the extent of "reaction" that takes place will likewise increase. The most important determination is that of the amount of isomer that has not undergone isomerisation during passage along the column. Looking forward to Fig. 2 we can discern the three regions corresponding to elution of the two isomers; the peak for unconverted compound 6a, the peak for unconverted compound 6b, and the broad intra-peak zone which arises from isomers 6a and 6b which have undergone isomerisation. Since there will necessarily be some overlap of the regions for unconverted and converted peaks, baseline correction must be taken into account[22]. Manual area calculation with baseline correction for product/reactant overlap poses some problems with narrow capillary GC peaks, although using fast chart speeds overcomes some of the errors involved. For greater accuracy, computerised data acquisition and handling would be preferred. Component separation commences immediately upon conversion of reactant into product.

For the process A → B, if an isomerisation event occurs at time t, the product B molecules will commence to be chromatographically resolved from A according to their relative capacity ratios, k' (A) and k' (B). Clearly those product B molecules will elute with a retention time neither the same as unconverted A molecules [for which $t_R(A) = t_M k'(A)$, where t_M is the column dead time] nor the same as any molecules of B originally injected and passing through the column unchanged [for which $t_R(B) = t_M k'(B)$]. Rather, the molecules of B formed from A at time t, hereinafter denoted B′, will have retention times of

$$t_R(B') = t + [t_R(A) - t] [t_R(B)/t_R(A)] \qquad (1)$$

This equation can be rationalised thus: after time t, the compound B′ travels under the capacity ratio conditions of B. The compounds A and B have a relative retention time ratio of $t_R(B)/t_R(A)$, so the additional retention time of B′ after time t when the isomerisation occurs will be the differences in the retention time of A and t, multiplied by the relative retention time ratio of B and A.

Similarly for the process B → A,

$$t_R(A') = t + [t_R(B) - t] [t_R(A)/t_R(B)] \qquad (2)$$

Since all values of t are possible from 0 to $t_R(A)$ (for A → B), product B′ molecules will potentially have values of $t_R(B')$ from $t_R(A)$ to $t_R(B)$, with the distribution of B′ molecules related to the relative rate of conversion A → B. This will of course be superimposed on the A′ distribution.

For eqn. 1, if $t = 0$, i.e. the interconversion event occurs at the time of injection, then

$$t_R(B') = 0 + t_R(A) t_R(B)/t_R(A) = t_R(B)$$

and B′ will elute with the same retention as original molecules of B injected.

Similarly

if $t = t_R(A)$, then $t_R(B') = t_R(A)$

if $t = t_R(A)/2$, then $t_R(B') = [t_R(A) + t_R(B)]/2$ (3)

with B′ eluting midway between A and B.

Likewise for eqn. 2,

if $t = 0$, $t_R(A') = t_R(A)$

if $t = t_R(B)$, $t_R(A') = t_R(B)$

if $t = t_R(B)/2$, $t_R(A') = [t_R(B) + t_R(A)]/2$ (4)

The similarity of results in eqns. 3 and 4 can be readily appreciated.

The efficacy of resolution is reflected in the equation

$$R_S = (\sqrt{N}/4)\,[(\alpha - 1)/\alpha]$$

thus either high-resolution columns (high N values) and/or increased phase selectivity (higher α values) is required. Both of these advantages were exploited by Bürkle et al.[17] in his invertomer work. In our experience, not only do capillary columns provide the necessary resolution for the appropriate choice of liquid phase, they also exhibit the interconversion phenomenon most nicely, and this enhances the accuracy of the analysis of the resulting chromatogram and would aid computer fitting of data to a model describing the process.

The rate processes pertaining to intramolecular interconversion and chromato-graphic resolution in this work, with a simple two-component system, are presented in Fig. 1. Reversible conversion occurs both in the gas and liquid phases according to the rate constants governing each phase. For simplification of our approach, the rates in both phases are considered to be equivalent and only a function of temperature. For thermally labile rotamers with reasonably non-polar phases and a transition state not affected by stabilization through interactions with polar solvents, this assumption seems reasonable. We believe that on the liquid-phase coated silica columns any potential surface catalytic effects play a negligible role in the interconversion process we are investigating.
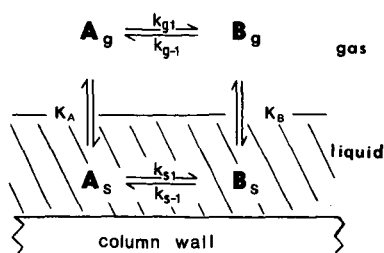
Fig. 1. Partitioning and interconversion process for the reaction A $\rightleftharpoons$ B within the gas–liquid chromatography column. k = rate constants for interconversion; K = partition coefficient for the compounds subscript g and s refer to gas phase and stationary phase species and rates respectively.
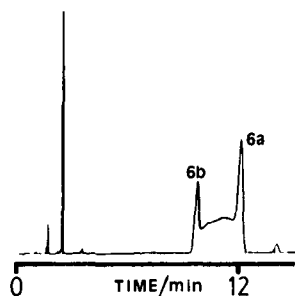
Fig. 2. Chromatogram of *anti* (6b) and *syn* (6a) acetaldoxime on a free fatty acid phase-coated capillary column at 50°C. The early-eluting peak(s) in this and other chromatograms is due to the solvent.

Fig. 2 exhibits a classic dynamic GC trace, in this case for acetaldoxime. The terminal peaks are sharp and well resolved from each other. The inter-peak zone illustrates the baseline shift which corresponds to the interconversion between isomers. In comparison to the packed column work of Langer *et al.*[23], the advantages accruing from capillary column methodology can be appreciated.

RESULTS AND DISCUSSION

Phenanthrene/anthracene compounds 1–5

We have previously reported a study on one member of this group of compounds[15], 2a, 2b. We were interested in the sterically hindered rotation about the C–C single bond for the 2-methyl substituted aromatics, where steric interaction between the methyl group and the planar fused aromatic parent ring results in a barrier to the free rotation. During rotation, the benzene substituent will be coplanar with the aromatic parent. For 1a, 1b, the substituent methyl group will interact with the C-1 proton of the parent ring (Scheme 1). This same scheme may be invoked for one possible intermediate for substituent rotation in (2–4)a, (2–4)b. The other main interaction possible for steric hindrance in this series of compounds is represented in Scheme 2, where the *o*-methyl group approaches the neighbouring aryl ring substituent. We discount any interaction between *ortho* protons on the phenyl substituent and the C-1 proton, analogous to that represented in Scheme 1, since compounds 5a, 5b have considerably lower barrier to interconversion (see later).

The preparative procedures produce isomers a and b in different proportions,
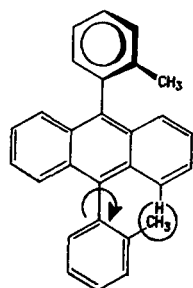
SCHEME 1
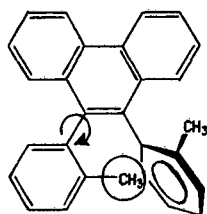
SCHEME 2

according to the conditions employed. However for the anthracene 1a and 1b, both isomers are of essentially equal abundance and they apparently interconvert with almost equal facility as evidenced in the GC study (Fig. 3). The overall GC distribution maintains good symmetry as isomerization progresses. The *trans*, or *anti*, isomer is presumed to elute as the later GC peak in accordance with usually observed relative GC retentions for positional isomers of such compounds as alkylbenzenes, where *trans* isomers elute after those in which the substituents are not trans. The free energy difference between the ground states of the anthracene isomers is small, as is shown by their approximately equal abundance at equilibrium. Thus in order to carry out a conventional time-dependent study of isomerization it would be necessary to separate the isomers. However, for the GC reactor study prior separation is not required since isomer separation is inherent in the column-based method.

For the phenanthrene compounds 2–4, one isomer is usually produced in far greater proportion. For 2a, 2b the minor isomer abundance was about half that of the major isomer[15]. In 3a, 3b, the major isomer was considerably more abundant (Fig. 4), with the minor one about 5%. Thus there is considerable preference energetically for one isomer. In this series of compounds, the two phenyl substituents at the 9,10 positions on the phenanthrene will be expected to experience interaction through the delocalized electron density and some ring tilting may result, thereby leading to the

TIME (s)
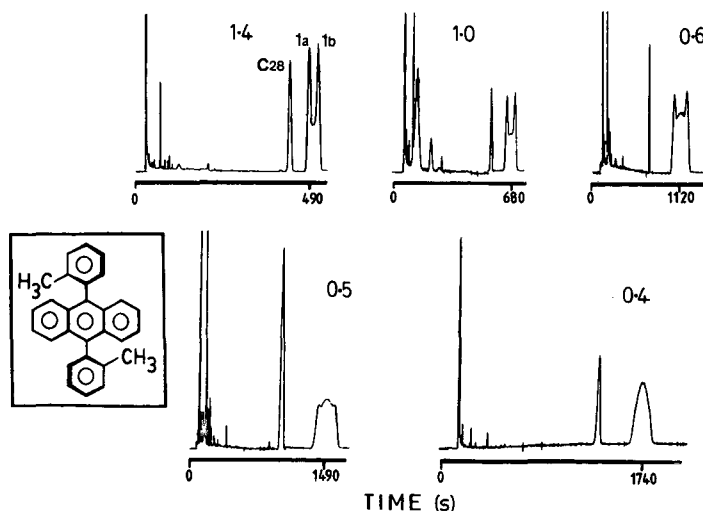
Fig. 3. GC study of interconversion of anthracene isomers 1a and 1b at 240°C and using different hydrogen carrier gas flow-rates. The flow-rates are set by the capillary pressure, given in dyne · cm^{-2} × 10^{-6} indicated on each individual chromatogram. 1a is believed to elute first. C28 = internal standard; *n*-octacosane.
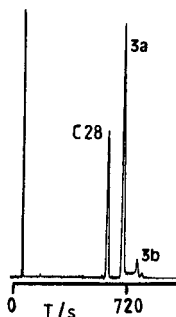
Fig. 4. Gas chromatogram of 3a and 3b at 240°C. The later eluting lesser abundant conformer, 3b, is about 5% abundance. Some evidence of a plateau and hence interconversion between 3a and 3b can be discerned. C28 designated as in Fig. 3.

observed preference for one isomer. The early eluting isomer is in most cases also the one of greater abundance, and by similar reasoning to the above, we might conclude this to be the *cis* isomer. In those instances where the second isomer was of very low abundance, no estimation of its barrier to interconversion could be made.

Fig. 5 shows a series of chromatograms for 3a, 3b at different temperatures from 280 to 320°C. At the lower temperatures, the shoulder extending to longer time is typical behaviour observed for the interconversion process where the later isomer has essentially completely undergone an isomerization event into the earlier eluting isomer. No unconverted later-isomer peak can be identified. At 300°C the first isomer can no longer be seen as a separate peak and the recorded profile becomes broad and squat with slightly distorted downslope. At 320°C the peak has sharpened and becomes more symmetric. We interpret this to be indicative of rapid interconversion between the two isomers.
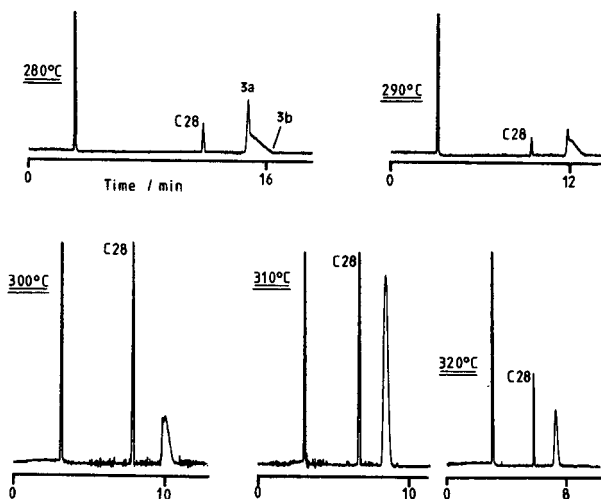
Fig. 5. Chromatograms illustrating progression in dynamic interchange between 3a and 3b with increasing column temperature. C28 designated as in Fig. 3.
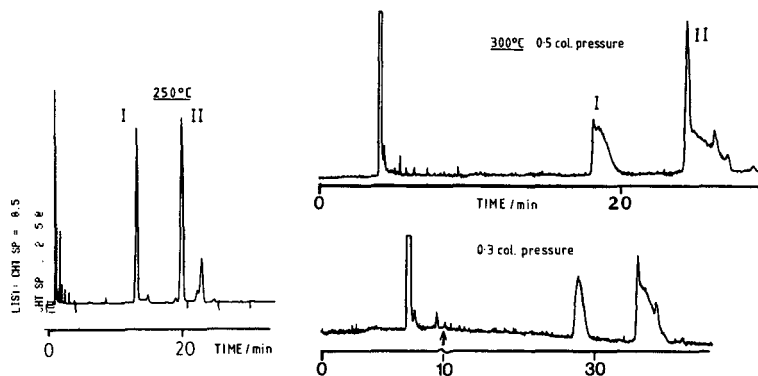
Fig. 6. Chromatograms of 4. At 250°C two groups of peaks are seen, I and II, each with one large (earlier) and one small (later) peak. At 300°C and 0.5 dyne · cm^{-2} × 10^{-6} pressure, I almost fully isomerises but II has appreciable unconverted isomer still present. Peak II corresponds to 4, whereas peak I appears to be a mono-chloro analogue of 4.

Compounds 4a, 4b behaved much like their analogues 2a, 2b reported earlier[15]. Chromatograms are given in Fig. 6. The minor isomer occurs in much less abundance, however the chromatogram illustrates two groups of peaks, labelled I and II. Peaks II correspond to 4a and 4b and from GC–mass spectrometry peaks at I contain only one chlorine. Whilst the chromatogram suggests I undergoes isomerisation more readily than II, the occurrence of I in the sample has not yet been explained. The analogue without a methyl group in the *ortho* position of the phenyl substituents, 5a, 5b, were then prepared for comparison purposes. Even though VTNMR studies[20] indicated both isomers to be present, no resolution of two peaks could be achieved on the GC even at temperatures as low as 200°C (the lowest temperature at which it could be chromatographed). We believe this to be indicative of rapid interchange such that only the averaged retention is seen. The alternative possibility, that the two isomers are not resolved, is rejected since if the conformers were stereochemically rigid at the temperatures used isomer separation would be expected on the basis of the ready

TABLE I

CALCULATED BARRIERS TO INTERCONVERSION USING THE GC METHOD

Compound	E_a (kJ mol^{-1})*
1	123, 104
2	145, 115
3	132, NA**
4	***
5	85§
6	52, 48
7	64, 69
8	70, 66

    * The first entry is for the major isomer of the compound.
    ** The minor isomer is in too small abundance to allow for reliable measurement of the energy.
    *** The values for this compound were not estimated.
    § This value was obtained by VTNMR (refer to text) and so it is ΔG^*.
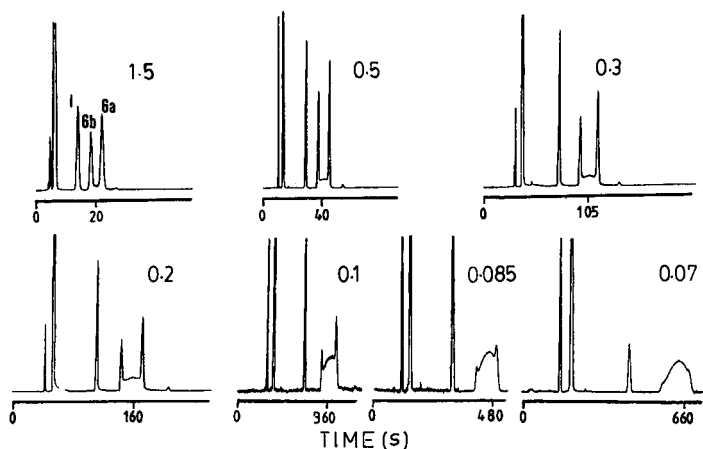
Fig. 7. Chromatograms of oximes 6a and 6b at 65°C for varying carrier flow-rates. I = internal standard = benzaldehyde.

resolution of the isomers of the other compounds of this series. Clearly, the steric interactions illustrated in Schemes 1 and 2 cannot play a role in this molecule.

Calculations of some example energy barriers give the results in Table I. VTNMR has not been successful in estimating ΔG^* for the compounds (1–4)a, (1–4)b. With high energy barriers in excess of 100 kJ mol^{-1}, no coalescence phenomena of ^{1}H NMR signals could be seen up to 150°C. However for 5a, 5b, $T_c = 98$°C with $\Delta G_c^* = 85$ kJ mol^{-1} (ref. 20). This supports the conclusion above that rapid isomerisation precludes the resolution of the isomers of 5.
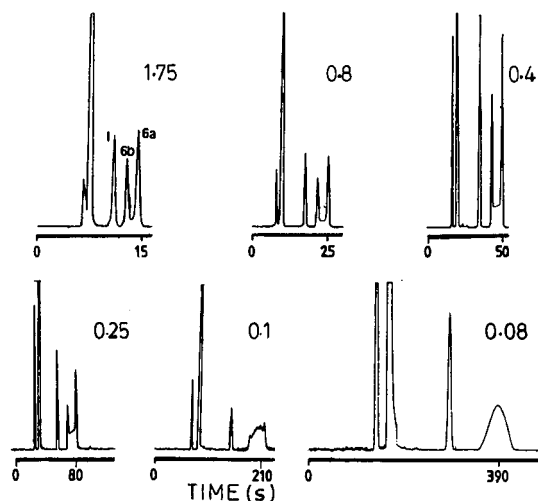
Fig. 8. Same compounds as Fig. 7 but at 80°C. Note that after 390 s a smooth-peaked distribution is obtained, whereas at 65°C the distribution still shows traces of unconverted starting isomer even after 660 s.
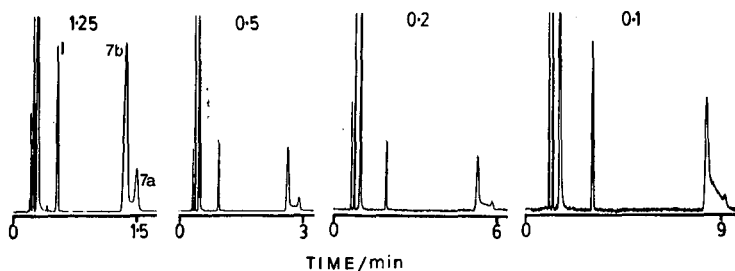
Fig. 9. Chromatograms of 7a and 7b at 70°C. I = benzaldehyde.

Oxime compounds 6–8

The example of Langer *et al.*[24] of on-column interconversion of acetaldoxime, widely quoted in treatments on physicochemical GC work, was reinvestigated in this study in order to attempt to evaluate the GC data for activation energy (not done in the earlier work) and at the same time to try to correlate the GC study with a VTNMR study on the same molecular system. Oximes 6–8 were chromatographed over the temperature regimes of 50, 65 and 80°C, 70, 85 and 100°C and 75, 90 and 105°C, respectively. The higher temperatures for 7 and 8 reflect their slightly longer retention and lower volatility compared with 6. If rates of interconversion are similar at these different temperatures, then we might conclude that 7 and 8 would have higher activation energies by virtue of the higher temperatures. The data do appear to support this. However even with E_a in the region of 50–70 kJ mol^{-1}, VTNMR did not exhibit coalescence up to 150°C for any of the compounds.

Representative GC traces are illustrated in Figs. 7–10. The chromatographic data are reproduced reasonably fully in order to faithfully represent and illustrate how the process of interconversion proceeds at different temperatures, and under varying conditions of carrier flow-rates. In some cases coalescence of peaks is included, with a resultant smooth and broad peak observed. The different forward and reverse activation energies (Table I) indicate the different ground state energies of the two isomers.
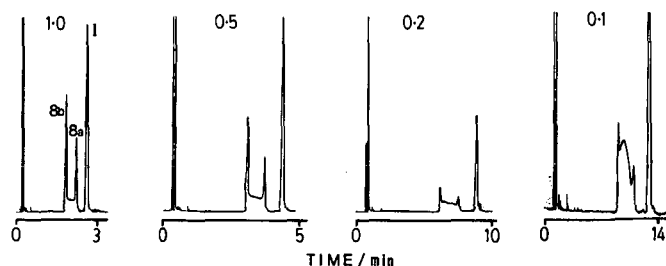
Fig. 10. Chromatograms of 8a and 8b at 75°C. I = amylalcohol.

CONCLUSION

The primary limitation on GC, and indeed HPLC also, for dynamic chromatographic study is the need for chromatographically distinguishable antipodes or isomers in the exchange process. Whilst "symmetrical" compounds such as dimethylformamide or N,N-dimethylcarbamates[25] are eminently suited to dynamic NMR, they would not be suited to dynamic chromatography. Dynamic chromatography can be applied to some systems with high activation barriers, it can be used in situations where the isomers are not of similar abundance, and does not require prior separation of equilibrium mixtures (which is necessary for time-dependent studies such as continuous heating/analysis methods). It is applicable to the resolution and interconversion of thermally labile optical isomers on optically active columns —an application not suited to solution NMR work. Having received attention only relatively recently, and with the limited range of applications studied to date, it is to be expected that an increasing number of molecular motions will be subjected to chromatographic scrutiny in the future.

Whether any special information is derivable from the conditions of coalescence of chromatographic peaks, much as is employed to derive ΔG^* from T_c in VTNMR, will await further detailed analysis of the theory of the dynamic chromatography method and interpretation of the data.

ACKNOWLEDGEMENTS

REFERENCES

1 C. S. G. Phillips, in R. Stock (Editor), *Gas Chromatography 1970*, Institute of Petroleum, London, 1971, p. 1.
2 N. C. Saha and D. S. Mathur, *J. Chromatogr.*, 81 (1973) 207.
3 J. Coca and S. H. Langer, *CHEMTECH.*, November (1983) 682.
4 R. A. Keller and J. C. Giddings, *J. Chromatogr.*, 3 (1960) 205.
5 M. Moriyasu, K. Kawanishi, A. Kato, Y. Hashimoto and M. Sugiura, *Bull. Chem. Soc. Jpn.*, 58 (1985) 2581.
6 M. Moriyasu, K. Kawanishi, A. Kato, Y. Hashimoto, M. Sugiura and T. Sai, *Bull. Chem. Soc. Jpn.*, 58 (1985) 3351.
7 M. Moriyasu, Y. Hashimoto and M. Endo, *Bull. Chem. Soc. Jpn.*, 56 (1983) 1972.
8 M. Moriyasu, A. Kato, M. Okada and Y. Hashimoto, *Anal. Lett.*, 17 (1984) 689.
9 M. Moriyasu, A. Kato and Y. Hashimoto, *Chem. Lett.*, 17 (1984) 1181.
10 M. Moriyasu, A. Kato and Y. Hashimoto, *J. Chem. Soc., Perkin Trans. 2*, (1986) 515.
11 W. R. Melander, J. Jacobson and Cs. Horváth, *J. Chromatogr.*, 234 (1982) 269.
12 M. T. W. Hearn, A. N. Hodder and M.-I. Aguilar, *J. Chromatogr.*, 327 (1985) 47.
13 V. F. Bystrov, *J. Mol. Struct.*, 126 (1985) 529.
14 H. Scherubl, U. Fritzsche and A. Mannschreck, *Chem. Ber.*, 117 (1985) 336.
15 Y.-H. Lai, P. J. Marriott and B. C. Tan, *Aust. J. Chem.*, 38 (1985) 307.
16 P. J. Marriott and Y.-H. Lai, *Inorg. Chem.*, 25 (1986) 3680.
17 W. Bürkle, H. Karfunkel and V. Schurig, *J. Chromatogr.*, 288 (1984) 1.
18 K. Grein, B. Kirste and H. Kurreck, *Chem. Ber.*, 114 (1981) 254.
19 Y.-H. Lai, *J. Am. Chem. Soc.*, 107 (1985) 6678.

20 Y.-H. Lai, *J. Chem. Soc., Perkin Trans. 2*, (1986) 1667.
21 J. B. Cohen, *Practical Organic Chemistry*, MacMillan, London, 1924, p. 239.
22 S. H. Langer and J. E. Patton, *J. Phys. Chem.*, 76 (1972) 2159.
23 S. H. Langer, J. Y. Yurchak and J. E. Patton, *Ind. Eng. Chem.*, 61 (1969) 10.
24 J. R. Condor and C. L. Young, *Physicochemical Measurement by Gas Chromatography*, Wiley Interscience, Chichester, 1979, Ch. 13.
25 J. Sandstrom, *Dynamic NMR Spectroscopy*, Academic Press, London, 1982.

CHROM. 20 558

EFFECT OF OVERLOAD OF CAPILLARY GAS–LIQUID CHROMATOGRAPHIC COLUMNS ON THE EQUIVALENT CHAIN LENGTHS OF C18 UNSATURATED FATTY ACID METHYL ESTERS

CECIL D. BANNON, JOHN D. CRASKE* and LYNNETTE M. NORMAN

Central Research Department, Unilever Australia Limited, P.O. Box 9, Balmain, N.S.W. 2041 (Australia)

(First received January 29th, 1988; revised manuscript received April 8th, 1988)

SUMMARY

Column overload causes errors in the estimation of equivalent chain lengths (ECLs) of fatty acid methyl esters (FAMEs), and the extent of these errors on fused-silica open tubular columns has been investigated. Load limits for several common FAMEs were accurately determined utilizing a synchronized, rapid automatic liquid sampler. The findings were applied to obtain estimates of ECLs of a range of C_{18} unsaturated FAMEs to a precision (repeatability) of about $\pm$ 0.001 ECL units. Three stationary phases, DEGS, SP-2330 and Supelcowax 10, were studied, each at three temperatures.

INTRODUCTION

The equivalent chain length (ECL), a concept first developed by Woodford and Van Gent[1] and by Miwa *et al.*[2], conveniently expresses the retention properties of a fatty acid methyl ester (FAME) in a form which allows its position in a chromatogram to be readily visualized in relationship to nearby saturated, straight-chain FAMEs or, conversely, for an unknown FAME in a chromatogram to be tentatively identified. While ECL is defined according to eqn. 1, its determination in practice presents a number of well-debated problems.

$$ECL = n + \frac{\log t'_{R,x} - \log t'_{R,n}}{\log t'_{R,n+1} - \log t'_{R,n}} \qquad (1)$$

where $t'_{R,x}$ = corrected retention time of unknown FAME x; $t'_{R,n}$ = corrected retention time of nearest saturated, straight chain FAME eluting ahead of x; $t'_{R,n+1}$ corrected retention time of next higher homologue of n; and $t'_R = t_R - t_M$, where t_R = uncorrected retention time; and t_M = column dead time. Errors in the determination of ECL may result from two sources. First, there are errors resulting from purely chromatographic phenomena which include errors in the determination of the column dead time, t_M[3-5], errors resulting from the retention time relationship for members of an homologous series shown in eqn. 2 which, according to some work-

ers[6,7], may not be strictly linear, and errors resulting from peak overlap or column overload[8-12].

$$\log t'_R = aN + b \tag{2}$$

where a and b are constants and N is the number of carbon atoms in the major chain of the molecule. Errors in the determination of ECL may also result from external physical variables such as type, variability and stability of the stationary phase[13,14] column oven temperature and its stability[13,15,16] and interaction with the solid support in the case of packed columns, or with the wall material in the case of capillary columns[17].

The problem of column overload has not been extensively discussed, probably because much of the earlier work was carried out on packed columns where overload is not a significant problem. However, wall-coated open tubular columns, especially those with thin stationary phase films, are highly vulnerable to overload, which results in error due to retardation of retention times. Ackman and Castell[8] showed that, in the case of monenoic FAME, a large amount of an earlier eluting isomer displaced other isomers of longer retention times from their normal positions, provided that the isomers were of similar structure. In a later paper, Ackman and Hooper[9] showed that structurally dissimilar materials, such as *trans* acids in a mixture of *cis* isomers, did not exhibit this "load effect" and proposed that the displacement was due to mutual exclusion of structurally very similar materials through saturation effects in the partitioning between liquid and gas planes. This phenomenon was further discussed by Ackman[10] and by Ackman and Eaton[11]. Gillan[12] recognized column overload as problem and developed a mathematical model to reduce the retention time of overloaded peaks in capillary columns to a "standard retention time" and also a polynomial equation to correct ECL estimates. In the present work we have further investigated the problem of overload to improve the accuracy of ECL estimation. An important tool in this work has been the use of a synchronized, rapid automatic liquid sampler for the very accurate estimation of retention times, and we report ECLs of improved precision for a wide range of unsaturated C_{18} FAMEs determined on three fused-silica open tubular (FSOT) columns, each at three temperatures.

EXPERIMENTAL

Isooctane (2,2,4-trimethylpentane) was Pronalys analytical reagent grade (May and Baker, West Footscray, Australia). Reference saturated esters were methyl palmitate, methyl stearate and methyl arachidate (Sigma, St. Louis, MO, U.S.A.). Reference octadecenoic acid methyl esters had the double bond configurations *cis*-4, -5, -6, -7, -8, -9, -10, -11, -12, -13, -14, -15, -16, *trans*-5, -6, -7, -8, -9, -10, -11, -12, -13, -14, -15, -16, and -17 [Hormel Institute, Austin, MN, U.S.A., except *cis*-9 (Sigma) and *cis*-6; *trans*-6 and *trans*-9 (Alltech, Deerfield, IL, U.S.A.)]. Reference octadecadienoic acid methyl esters had the double bond configurations *cis*-9, *cis*-12 (Sigma); *trans*-8, *trans*-12; *cis*-9, *trans*-12; *trans*-9, *cis*-12; *trans*-9, *trans*-12; *trans*-9, *trans*-13; *trans*-9, *trans*-15 (Unilever Research Laboratory, Vlaardingen, The Netherlands). The octadecatrienoic acid ester was methyl linolenate (Sigma). For simplicity we use 18:1 to mean methyl oleate (*cis*-9), 18:2 to mean methyl linoleate (*cis*-9, *cis*-12) and 18:3 to mean methyl linolenate (*cis*-9, *cis*-12, *cis*-15).

Apparatus

Gas–liquid chromatography (GLC) was carried out on a Hewlett-Packard Model 5880A gas chromatograph fitted with a flame ionization detector, a split/-splitless capillary inlet system and a Model 7673A rapid automatic liquid sampler. The sampler was synchronized with a Hewlett-Packard Model 3350A laboratory automation system which was used to measure retention times and peak areas. The injection volume was 1 μl. The columns were 22 m $\times$ 0.22 mm I.D. FSOT coated with 0.2 μm film thickness of DEGS (Chrompack, Middelburg, The Netherlands), 60 m $\times$ 0.25 mm I.D. FSOT coated with 0.2 μm of SP-2330 (Supelco, Bellefonte, PA, U.S.A.) and 50 m $\times$ 0.35 mm I.D. FSOT coated with 0.25 μm of Supelcowax 10 (Supelco).

The inlet system was used in the split mode and was fitted with a standard Hewlett-Packard glass liner of the type described by Jennings[18]. The injector temperature was 375°C for DEGS and 300°C for SP-2330 and Supelcowax 10. The carrier gas was hydrogen (99.995%) with the inlet pressure adjusted for the various columns to give a carrier gas linear velocity of 35–45 cm/s. The pressures were 10 p.s.i. for DEGS, 22 p.s.i. for SP-2330 and 12 p.s.i. for Supelcowax 10. The septum purge flow-rate was *ca.* 3 ml/min. The split vent flow-rate was varied to give a split ratio of approximately 140:1 for each column in order to provide comparable peak masses in the column overload experiments described below. The split vent flow-rates were 160 ml/min for DEGS, 150 ml/min for SP-2330 and 250 ml/min for Supelcowax 10. Three oven temperatures were used for each phase and were 150, 160 and 170°C for DEGS, 180, 200 and 220°C for SP-2330 and 200, 220 and 240°C for Supelcowax 10. Supplementary hydrogen was supplied to the detector to give a total flow-rate of 30 ml/min, the make-up gas was nitrogen (99.995%) and had a flow-rate of 24 ml/min, and oil-free, compressed air was supplied at a flow-rate of 240 ml/min. The detector temperature was 250°C.

Calculation of ECLs

ECLs were determined by co-injecting a mixture of the FAMEs 16:0, 18:0 and 20:0 with the unsaturated ester. The mathematical dead time of the column was first calculated by the method of Peterson and Hirsch[19] as modified by Hafferkamp[20] and Hansen and Andresen[21] using the uncorrected retention times of 16:0, 18:0 and 20:0 according to eqn. 3.

$$t_{\mathrm{M}} = \frac{t_{18}^2 - (t_{16}t_{20})}{2t_{18} - t_{16} - t_{20}} \tag{3}$$

where t_{M} = mathematical dead time; t_{16} = uncorrected retention time of 16:0; t_{18} = uncorrected retention time of 18:0; t_{20} = uncorrected retention time of 20:0. The ECL of the unsaturated ester x was then calculated according to eqn. 4 which is a modification of eqn. 1 to suit the present investigation, using the retention times of 16:0, 20:0 and of the unsaturated ester, all corrected with respect to the mathematical dead time.

$$\mathrm{ECL}_x = 16 + \frac{4(\log t'_x - \log t'_{16})}{\log t'_{20} - \log t'_{16}} \tag{4}$$

where t'_x = corrected retention time of the unsaturated ester = $t_x - t_M$; t'_{16} = corrected retention time of 16:0 = $t_{16} - t_M$; t'_{20} = corrected retention time of 20:0 = $t_{20} - t_M$. The precision (repeatability) of ECL determinations was estimated by carrying out ten consecutive injections and calculating the standard deviation and coefficient of variation.

Estimation of column load limits

In order to investigate the effect of column overload on ECL, the load limits for the esters 16:0, 18:0, 18:1, 18:2, 18:3 and 20:0, which are referred to herein as the reference esters, were established by preparing mixtures such that, in a given mixture, each of these esters had the same concentration, with this concentration being progressively increased for each of the mixtures. The concentrations of each component in the individual mixtures were 0.005, 0.01, 0.025, 0.05, 0.1, 0.2, 0.5 and 1.0%. For a given set of chromatographic conditions on a column, 1-μl injections of each mixture were made consecutively in increasing order of concentration, with the 0.005% mixture being injected again at the end to determine if systematic changes in any of the retention times had occurred since the initial injection. Peak retention times were observed as a function of peak area, and the column load limit for each peak was specified in terms of a maximum peak area at which no significant retardation of retention time was observed, *i.e.* the peak had not started to develop the skewed leading edge characteristic of overloaded peaks. These areas were also converted to absolute mass loads using the split ratio. It was assumed that the various mono- and dienoic FAMEs which were later studied had load limits similar to those of 18:1 and 18:2 respectively.

Determination of ECLs of unsaturated FAMEs

Having established load limits for the various reference FAMEs, each of the unsaturated FAMEs were in turn co-injected with a mixture of the esters 16:0, 18:0 and 20:0 under conditions which did not exceed these limits and the ECL calculated according to eqns. 3 and 4. In order to monitor the validity of the ECL determinations, a mixture of the reference FAME 16:0, 18:0, 18:1, 18:2, 18:3 and 20:0 was injected ten times initially to establish the status of the system and thereafter at frequent intervals while the unsaturated esters were being investigated. The ECLs of 18:1, 18:2 and 18:3 thus determined were used to detect fluctuations in the effective polarity of the column being examined. Minor fluctuations were in fact observed for all three columns, and corrections, which were rarely greater than 0.001 ECL units, were made to estimates of the ECLs of the various unsaturated FAMEs according to the method of Scholfield[22], the principle of which is shown in eqn. 5 for a monoenoic FAME.

$$\text{ECL}_x(\text{corrected}) = \text{ECL}_x(\text{observed}) + \text{ECL}_{18:1}(\text{average}) +$$

$$- \text{ECL}_{18:1}(\text{observed}) \qquad (5)$$

where $\text{ECL}_{18:1}(\text{average})$ = average ECL of 18:1 over the duration of the experiment; $\text{ECL}_{18:1}(\text{observed})$ = ECL of 18:1 determined as near as possible in time to the estimate of ECL_x. A similar correction was applied to dienoic FAMEs using corresponding ECLs for 18:2.

RESULTS AND DISCUSSION

Calculation of ECLs

The method used to calculate an ECL can itself affect the accuracy and pre-cision of the estimate obtained. The first source of error lies in the determination of the column dead time, t_M, which itself may be estimated experimentally by measuring the retention time of methane or mathematically from the retention properties of selected reference FAMEs. Dorris *et al.*[13] have discussed these problems pointing out that although some workers[3] believe that the retention time of methane is a good approximation of t_M' others[4,5] maintain that methane is significantly retained on most stationary phases. They demonstrated that the use of the mathematical dead time did in fact produce more accurate ECL values than those using the retention time of methane, the major drawback of the use of the mathematical dead time being the assumption that the relationship shown in eqn. 2 is linear. Wainwright and Haken[23] have reviewed methods for the calculation of the mathematical dead time and have also severely questioned the use of methane to estimate column dead time.

The second source of error in calculating ECL is the assumption, already point-ed out above, that eqn. 2 may not be strictly linear. While there is evidence to support this non-linearity[6,7] the effect can be minimized by the choice of a suitable technique. In order to minimize both the above sources of error we have used the mathematical dead time defined by eqn. 3 for our own determinations. This equation necessarily gives an exact determination of ECL for 18:0 in eqn. 4 and, accordingly, would be expected to give very accurate estimates for other peaks in this vicinity, which is our main areas of interest.

Estimation of peak load limits

In order to carry out the column load limit experiments it was essential that the columns gave highly reproducible retention times under a given set of conditions, as the criterion for detecting the point of overload was that the retention time of the ester was significantly retarded when this point was reached. Accurate determination of the retention times required, first, that the timing device be started in a very re-producible manner and, second, that systematic drift of retention times was not sig-nificant. The first problem was overcome by the use of the synchronized rapid au-tomatic liquid sampler. The second was overcome by allowing the column to stabilize over a long period of time, say, overnight. To verify that the column was stable, it was required that a reproducible retention time was obtained when the sample which introduced the lowest load (0.005% solution) was injected at the start and at the end of an experimental run.

The results of the column load limit experiment which was carried out on the SP-2330 column at 200°C are given in Table I. Similar experiments were carried out on the DEGS and Supelcowax 10 columns, but are not reported here because of the essentially similar findings and conclusions. Several conclusions were drawn from the results in Table I. First, the stability of the system and, in turn, the validity of the experiment was indicated by the close similarity of the values obtained respectively for retention times, peak areas and ECLs when the 0.005% solution was analysed at the beginning and end of the series. Second, the synchronized rapid injector/computer system gave high accuracy of determination of retention times. this conclusion also

TABLE I

RETENTION TIMES, RAW PEAK AREAS AND ECL VALUES OF SELECTED FAMEs AS A FUNCTION OF SAMPLE SIZE INJECTED

Concentration of each ester in sample (%) 1 µl injection	Approximate peak mass (ng)	Retention time (min)						Raw peak area						ECL		
		16:0	18:0	20:0	18:1	18:2	18:3	16:0	18:0	20:0	18:1	18:2	18:3	18:1	18:2	18:3
0.005	0.04	4.291	5.163	6.593	5.569	6.237	7.184	449	472	441	464	530	497	18.675	19.587	20.605
0.01	0.07	4.291	5.163	6.591	5.569	6.236	7.182	704	752	683	735	802	800	18.675	19.587	20.606
0.025	0.18	4.292	5.164	6.594	5.570	6.237	7.184	1588	1672	1620	1648	1720	1806	18.675	19.586	20.604
0.05	0.4	4.294	5.168	6.601	5.575	6.242	7.190	3383	3515	3430	3475	3634	3783	18.674	19.584	20.601
0.1	0.7	4.293	5.168	6.603	5.574	6.242	7.190	6185	6429	6297	6358	6564	7047	18.673	19.582	20.599
0.2	1.5	4.295	5.173	6.613	5.579	6.247	7.196	12 617	13 320	12 869	13 176	12 615	11 570	18.671	19.578	20.593
0.5	4	4.298	5.182	6.635	5.588	6.258	7.208	32 037	33 810	32 541	33 305	31 999	29 384	18.660	19.568	20.578
1.0	7	4.304	5.196	6.661	5.602	6.273	7.226	66 366	69 764	67 237	68 801	65 696	69 677	18.660	19.558	20.566
0.005	0.04	4.293	5.167	6.598	5.573	6.241	7.189	442	467	446	465	527	497	18.675	19.586	20.605

being supported by the results given later in Table II. Third, because of the high accuracy of retention time determinations, it was easy to detect even the smallest retardation of retention time, indicative of peak skewing due to column overload. Fourth, sensitivity to overload increased with increasing chain length, which is, of course, only a manifestation of the well known phenomenon that any compound will elute as a skewed (leading) peak as the temperature is reduced. These limits corresponded to absolute loads of approximately 15 ng (0.2% solution) for 16:0 and approximately 2 ng (0.025% solution) for 20:0. Fifth, under conditions of overload, the ECLs of unsaturated esters were underestimated, first, because the 20:0 peak was retarded to a greater extent than the 16:0 peak and, second, because the unsaturated esters were retarded less than the corresponding saturated ester, *viz.* 18:0. This is consistent with Ackman's comment[10] that, as the unsaturation of the FAME increases, its susceptibility to overload decreases. It may be further noted that the conclusions that we have drawn from this work carried out on thin film FSOT columns are in general agreement with those variously made by earlier workers who used steel columns that were frequently more heavily coated. It would be of interest to determine whether the generality of the phenomena is such as to extend also to the "megabore" columns now in common use.

The above results enabled a load specification to be selected for the valid determination of ECLs in terms of a maximum raw peak area which was set empirically at 1000 counts for the system being used.

Accuracy of retention time and ECL determinations

It has already been indicated above that systematic drift in retention times normally occurred unless the columns were well stabilized. As it was impractical to achieve such stability all of the time, the reproducibility of ECL determinations was examined under realistic conditions *viz.,* after baselines were allowed to stabilize, but

TABLE II

RETENTION TIMES, ECLs AND STATISTICAL RESULTS FOR 10 CONSECUTIVE DETERMINATIONS FOR 18:3 ON SP-2330 AT 180°C

Retention time (min)	ECL
11.737	20.3879
11.762	20.3881
11.779	20.3880
11.802	20.3873
11.836	20.3869
11.847	20.3876
11.853	20.3872
11.861	20.3863
11.864	20.3860
11.859	20.3870
Mean	20.3872
Standard deviation	0.00069
Coefficient of variation	0.0034

no other precautions against systematic drift taken. Results illustrating a typical rate of drift and the repeatability of the ECL of 18:3 under these conditions are given in Table II. The column was the SP-2330 at 180°C, and the load limit was not exceeded. Similar studies were carried out for all of the unsaturated reference esters for each of the columns and oven temperatures, but are too extensive and the results too similar to report here. The results given in Table II illustrate typical rates of drift of retention times encountered under normal operating conditions during the experiments. More importantly, this drift had little effect on the calculated ECL value of 18:3, as the estimates of the retention times of the reference saturated esters and of t_M also drifted and this resulted in potential errors being largely cancelled out. As a result it was found possible to estimate ECLs with a precision of about ±0.001 compared with errors reported in the literature which are most commonly in the range ±0.01 to ±0.04[13,22,24]. It was concluded that the technique used in the experiments, especially the precautions taken to avoid column overload, had been effective in significantly improving both the accuracy and the precision of ECL estimation.

ECLs of unsaturated FAMEs

The results of the ECL determinations for the various unsaturated FAMEs are given in Table III. These results provide a database which is more comprehensive and more precise than those which have appeared in the literature to date[16,25-33]. It may accordingly be used for the more reliable identification of unknown FAMEs or for selecting improved conditions for the separation of particular FAMEs, providing certain inherent problems are dealt with. The first difficulty lies in dealing with column overload, which must be avoided, if accurate comparisons of ECLs are to be made. Because of the widely differing concentrations of fatty acids in most practical mixtures, it may be necessary to run the sample at a number of different sample sizes or, alternatively, it may be possible to apply corrections using mathematical techniques such as those of Gillan[12]. Similar techniques could also possibly be used to deal with peak overlap.

A more serious difficulty lies in relating data such as those given in Table III to those obtained on nominally similar columns. This problem arises out of stationary phase variability and instability which, of all the parameters relevant to the estimation of ECLs, are the two that are likely to present the most intractable problems. Thus, the vast majority of useful phases available at the present time are mixtures which vary in composition, albeit slightly, from batch to batch and which may be subject to change by way of bleeding and reactions such as further polymerization, oxidation, reaction with analytes and the like. While the results given in Table III were very reproducible over a time frame of several weeks, small, but significant changes were sometimes found after a time frame of several months, which we ascribe to marginal polarity changes in the phase. This behaviour does not detract from the significance of the results given above which represent very accurate estimates of the relative locations of the various unsaturated esters under conditions which remained very stable for each of the various sets of parameters. It should be possible to correlate such data accurately to those obtained on similar, if not absolutely identical phases at the stated temperatures by determining ECLs for one or more of the commonly available unsaturated esters and applying corrections accordingly.

TABLE III

ECLs OF UNSATURATED C_{18} FAMEs

FAME	ECL DEGS			SP-2330			Supelcowax 10		
	Column temperature (°C)			Column temperature (°C)			Column temperature (°C)		
	150	160	170	180	200	220	200	220	240
18:1:-									
cis-4	18.318	18.348	18.376	18.394	18.453	18.511	18.225	18.245	18.264
cis-5	18.217	18.254	18.290	18.393	18.473	18.551	18.147	18.178	18.208
cis-6	18.325	18.363	18.399	18.534	18.616	18.695	18.217	18.245	18.271
cis-7	18.294	18.333	18.372	18.524	18.612	18.698	18.192	18.222	18.252
cis-8	18.305	18.348	18.387	18.548	18.639	18.729	18.202	18.233	18.264
cis-9	18.334	18.377	18.416	18.584	18.675	18.765	18.223	18.254	18.283
cis-10	18.365	18.407	18.446	18.619	18.710	18.801	18.250	18.281	18.309
cis-11	18.412	18.453	18.492	18.667	18.757	18.845	18.291	18.320	18.347
cis-12	18.479	18.521	18.557	18.731	18.819	18.906	18.350	18.377	18.403
cis-13	18.551	18.591	18.629	18.801	18.887	18.973	18.417	18.442	18.466
cis-14	18.633	18.673	18.712	18.875	18.959	19.043	18.497	18.519	18.542
cis-15	18.728	18.768	18.805	18.937	19.016	19.095	18.579	18.588	18.618
cis-16	19.053	19.102	19.147	19.286	19.383	19.479	18.896	18.919	18.942
trans-5	18.301	18.329	18.352	18.333	18.379	18.415	18.231	18.248	18.261
trans-6	18.321	18.350	18.372	18.383	18.428	18.467	18.236	18.250	18.262
trans-7	18.302	18.332	18.359	18.390	18.441	18.485	18.221	18.239	18.254
trans-8	18.308	18.339	18.366	18.396	18.450	18.501	18.226	18.244	18.259
trans-9	18.317	18.348	18.375	18.423	18.475	18.522	18.228	18.248	18.263
trans-10	18.345	18.377	18.403	18.448	18.501	18.549	18.252	18.268	18.284
trans-11	18.373	18.403	18.430	18.471	18.523	18.573	18.274	18.291	18.304
trans-12	18.414	18.442	18.467	18.517	18.566	18.613	18.306	18.319	18.331
trans-13	18.461	18.490	18.513	18.548	18.592	18.635	18.346	18.358	18.366
trans-14	18.478	18.505	18.526	18.555	18.595	18.629	18.357	18.366	18.371
trans-15	18.574	18.596	18.618	18.618	18.651	18.680	18.433	18.436	18.435
trans-16	18.824	18.857	18.886	18.862	18.905	18.949	18.661	18.666	18.667
Δ-17	18.7345	18.771	18.805	18.910	18.981	19.052	18.561	18.573	18.586
18:2:-									
trans-8,*trans*-12	18.718	18.770	18.816	18.866	18.959	19.048	18.509	18.534	18.560
cis-9,*cis*-12	18.995	19.069	19.131	19.429	19.586	19.748	18.688	18.733	18.777
cis-9,*trans*-12	19.003	19.067	19.123	19.266	19.390	19.511	18.730	18.763	18.793
trans-9,*cis*-12	18.957	19.007	19.050	19.087	19.166	19.244	18.701	18.716	18.730
trans-9,*trans*-12	18.959	19.008	19.050	19.087	19.169	19.245	18.700	18.717	18.730
trans-9,*trans*-13	18.773	18.824	18.869	18.921	19.012	19.100	18.554	18.578	18.600
trans-9,*trans*-15	18.926	18.975	19.019	19.059	19.142	19.221	18.674	18.689	18.703
trans-10,*trans*-12	20.529	20.619	20.699	21.062	21.228	21.391	20.140	20.170	20.199
18:3	19.848	19.948	20.039	20.387	20.606	20.834	19.326	19.385	19.441

CONCLUSIONS

The effect of column overload on the accuracy of estimating the ECLs of FAMEs has not been extensively studied to date. This effect is very significant in the case of capillary columns and probably accounts in part for many of the discrepancies

seen in the literature. If due precautions are taken, estimates of ECL may be made with a precision of about ± 0.001 ECL units.

ACKNOWLEDGEMENTS

REFERENCES

1 F. P. Woodford and C. M. van Gent, *J. Lipid Res.*, 1 (1960) 188.
2 T. K. Miwa, K. L. Mikolajczak, F. R. Earle and I. A. Wolf, *Anal. Chem.*, 32 (1960) 1739.
3 W. E. Sharples and F. Vernon, *J. Chromatogr.*, 161 (1978) 83.
4 M. S. Wainwright, J. K. Haken and D. Srisukh, *J. Chromatogr.*, 179 (1979) 160.
5 J. F. Parcher and D. M. Johnson, *J. Chromatogr. Sci.*, 18 (1980) 267.
6 G. J. Nelson, *Lipids*, 9 (1974) 254.
7 F. J. Heeg, R. Zinburg, M. J. Neu and K. Ballschimiter, *Chromatographia*, 12 (1979) 451.
8 R. G. Ackman and J D. Castell, *J. Gas Chromatogr.*, 5 (1967) 489.
9 R. G. Ackman and S. N. Hooper, *J. Chromatogr. Sci.*, 7 (1969) 549.
10 R. G. Ackman, *Prog. Chem. Fats Other Lipids*, 12 (1972) 211–213.
11 R. G. Ackman and C. A. Eaton, *Fette, Seifen, Angstrichm.*, 80 (1978) 21.
12 F. T. Gillan, *J. Chromatogr. Sci.*, 21 (1983) 293.
13 G. M. Dorris, M Douek and L. H. Allen, *J. Am. Oil Chem. Soc.*, 59 (1982) 494.
14 R. G. Ackman, *Chem. Ind. (London)*, (1981) 715.
15 J. Hrivnak, L. Sojak, J. Krupcik and Y. P. Duchesne, *J. Am. Oil Chem. Soc.*, 50 (1973) 68.
16 S. H. Ojanpera, *J. Am. Oil Chem. Soc.*, 55 (1978) 290.
17 J. Krupcik, J. Hrivnak and J. Janak, *J. Chromatogr. Sci.*, 14 (1976) 4.
18 W. G. Jennings, *J. Chromatogr. Sci.*, 13 (1975) 185.
19 M. L. Peterson and J. Hirch, *J. Lipids Res.*, 1 (1959) 132.
20 M. Hafferkamp, in R. Kaiser (Editor), *Chromatographie in der Gasphase Teil II*, Bibliographisches Institut, Mannheim, 1966, p. 93.
21 H. L. Hansen and K. Andresen, *J. Chromatogr.*, 34 (1968) 246.
22 C. R. Scholfield, *J. Am. Oil Chem. Soc.*, 58 (1981) 663.
23 M. S. Wainwright and J. K. Haken, *J. Chromatogr.*, 184 (1980) 1.
24 R. G. Ackman, *J. Chromatogr.*, 42 (1969) 170.
25 F. D. Gunstone, I A. Ismail and M. Lie Ken Jie, *Chem. Phys. Lipids*, 1 (1967) 376.
26 W. W. Christie, *J. Chromatogr.*, 37 (1968) 27.
27 C. R. Scholfield and H. J. Dutton, *J. Am. Oil Chem. Soc.*, 47 (1970) 1.
28 C. R. Scholfield and H. J. Dutton, *J. Am. Oil Chem. Soc.*, 48 (1971) 228.
29 R. G. Ackman and S. N. Hooper, *J. Chromatogr. Sci.*, 12 (1974) 131.
30 R. G. Ackman and S. N. Hooper, *J. Am. Oil Chem. Soc.*, 51 (1974) 42.
31 J. Flanzy, M. Boudon, C. Leger and J. Pihet, *J. Chromatogr. Sci.*, 14 (1976) 17.
32 H. Heckers, K. Dittmar, F. W. Melcher and H. O. Kalinowski, *J. Chromatogr.*, 135 (1977) 93.
33 H. B. S. Conacher and J R. Iyengar, *J. Assoc. Off. Anal. Chem.*, 61 (1978) 702.

CHROM. 20 542

INCREASING EXTRACTION EFFICIENCY IN SUPERCRITICAL FLUID EXTRACTION FROM COMPLEX MATRICES

PREDICTING EXTRACTION EFFICIENCY OF DIURON AND LINURON IN SUPERCRITICAL FLUID EXTRACTION USING SUPERCRITICAL FLUID CHROMATOGRAPHIC RETENTION

MARY ELLEN P. McNALLY* and JULIA R. WHEELER

E. I. du Pont de Nemours & Co., Inc., Agricultural Products Department, Experimental Station, Wilmington, DE 19898 (U.S.A.)

(First received January 14th, 1988; revised manuscript received March 25th, 1988)

SUMMARY

Supercritical fluid extraction (SFE) conditions have been investigated in terms of mobile phase modifier, pressure, temperature and flow-rate to improve extraction efficiency. Extraction efficiencies of up to 100% in less than 2 h have been obtained. These extraction efficiencies resulted from our extensive parameter optimization experiments.

Packed column supercritical fluid chromatography (SFC) has been used to examine the effect of these parameters on retention behavior. A relationship between chromatographic retention and extraction efficiency was sought. By determining trends of the chromatographic capacity factors using SFC conditions corresponding to SFE parameters, a prediction of extraction efficiency can be made. These predictions have shortened method development time in SFE.

INTRODUCTION

Supercritical fluid extraction (SFE) has eliminated some of the disadvantages of current extraction procedures for analysis of complex mixtures[1,2]. Packed column supercritical fluid chromatography (SFC) has been used as a technique for chromatographic elution of thermally labile agricultural compounds and their metabolites[3]. The adapted instrumentation needed to achieve the union of these two techniques has previously been demonstrated[1]. In this study, extraction conditions have been explored in terms of mobile phase modifier, pressure, temperature and flow-rate. Improved extraction efficiency in less extraction time was the goal of these optimization experiments.

Changing the mobile phase modifier, pressure, temperature and flow-rate can effect the packed column SFC capacity factor and/or limit of detection. Relationships between extraction efficiency and chromatographic retention have been proposed.

The goal of these studies was to determine the best functional conditions which would yield high efficiencies for extracting thermally labile herbicides from soils and animal materials. Results of these studies will be discussed.

EXPERIMENTAL

Instrumentation

The Hewlett-Packard 1082 liquid chromatograph used in these studies was modified for SFC and extraction. The modifications have previously been described[1,4]. The flow-rate range for this instrument is from 0 to 10 ml/min. The collection device, previously described, is simply a glass vessel after the back pressure regulator[1].

In addition, a Varian 8500 syringe pump (250-ml syringe volume) has been coupled with a Fiatron TC-50 column oven to conduct additional extraction work. The Varian 8500 flow-rate range is from 0 to 16.5 ml/min.

A limitation to the syringe pump is the reservoir size, 250 ml. As opposed to the continuous flow from the diaphragm pumps of the HP1082B, the syringe pump must be refilled approximately every 15 min when pumping at maximum flow-rate. However, the larger flow-rates obtainable with this instrument increase the range over which the extraction efficiency as a function of flow-rate can be explored.

Species of interest

The target compounds of interest for these studies were diuron and linuron and their principle metabolite, 3,4-dichloroaniline. Structures and molecular weights can be found in Table I. The melting points of diuron and linuron are 158 and 93°C, respectively. ^{14}C-labeled diuron and linuron were used for these studies in order to easily monitor extraction efficiency.

Our studies have concentrated on the extraction of these compounds from a sandy loam soil. Soil parameters can be found in Table II.

TABLE I

COMPOUNDS OF INTEREST
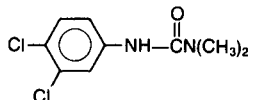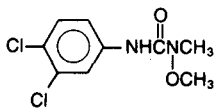
Name	Structure	Mol. wt.
Diuron		233.1
Linuron		249.1

TABLE II

CHARACTERISTICS OF SASSAFRAS SOIL

Texture	Sandy loam
pH (water)	6.1
P, K, Mg, Ca	150, 70, 85, 80 ppm in soil on a volume basis
Organic matter (%)	0.74

Parameters investigated

Temperature, flow-rate, pressure and mobile phase modifier type and concentration were examined for their effect on the extraction efficiency of the species of interest from the sample matrix.

Pressure and temperature were investigated because of their intrinsic influence on the behavior of supercritical fluids. Flow-rate was examined because the extraction system used is a dynamic not a static equilibrium system. Mobile phase modifier was varied based on experimental evidence of the influence of different modifiers on extraction efficiencies. It is expected that modifier effects would vary depending upon the solute and matrix of interest.

Conditions

The starting points for our SFE were determined from classical extraction conditions and SFC retention times.

Classical extraction procedures for diuron and linuron from soil used predominantly one solvent, methanol, to achieve greater than 80% recovery for both diuron and linuron[5]. This liquid–liquid classical extraction procedure is outlined in Table III. The procedure is more labor intensive and time consuming than our simple SFE scheme where the soil sample is pulverized, then packed into an empty 25 cm × 4.6 mm I.D. stainless-steel tube. The total sample handling time for this procedure is 1 h or less.

TABLE III
CLASSIC EXTRACTION METHOD OF DIURON AND LINURON FROM SASSAFRAS SOIL

(1) Pulverize soil.
(2) Extract at room temperature with three portions of methanol–water (9:1), wrist action shaker, centrifuge
(3) Extract at room temperature with three portions of 100% methanol, wrist action shaker, centrifuge

Yield room temperature extractions: 92% diuron, 78–79% linuron
Time: 1 day

(4) Soxhlet extraction with 100% methanol at 65°C

Yield: 3–4% diuron and linuron
Time: 1 day

(5) Soxhlet extraction with 100% hexane at 69°C

Yield: 1% diuron and linuron
Time: 1 day

Chromatographic experiments utilizing different mobile phase modifiers while varying temperatures and pressures showed the ability to vary the capacity factor, k', of these parent compounds. Tables IV–VI illustrate the chromatographic trends for diuron and linuron with methanol, ethanol and acetonitrile modified carbon dioxide mobile phase. The low chromatographic capacity factors and the minimal solvent variety in the classical extraction procedure suggested that diuron and linuron in soil would be ideal candidates for the evaluation of SFE parameters.

The SFE sample handling procedure is simple and requires minimal operator time[1]. Instrument time varies according to the difficulty of the extraction. Generally, the extraction efficiency was measured on a predetermined time basis. Samples were measured at 3- and 15-min intervals in preliminary extraction experiments. Larger samples or more complex matrices required longer extraction times. Extractions of 1–2 h were usually sufficient. Overnight extractions were utilized if necessary.

Efficiency evaluation

After collection of the extracted ^{14}C-labeled diuron and linuron, liquid scintillation counting permitted the extraction efficiency to be monitored during the experiments. Periodic evaluation of the extraction effluent with SFC and liquid chromatography (LC) confirmed the presence of the diuron or linuron parent compound and not the most common hydrolysis on breakdown product, dichloroaniline.

RESULTS

Diuron from Sassafras soil

Effects of temperature. Several studies were conducted to evaluate the effects of temperature. Extractions of 15 min of radiolabeled diuron from Sassafras soil using methanol-modified carbon dioxide were conducted at three different temper-

TABLE IV

CHROMATOGRAPHIC RESULTS USING ACETONITRILE-MODIFIED CARBON DIOXIDE AND VARYING PRESSURES AND TEMPERATURES

(a) Capillary SFC, 100% carbon dioxide, 20 m × 100 μm I.D. SB-cyanopropyl-25, 80°C, initial density = 0.25 g/ml for 5 min, ramp rate = 0.1 g/ml/min, final density = 0.65 g/ml. (b) Packed column SFC, acetonitrile–carbon dioxide (2:98), 4.0 ml/min, Whatman Partisil 5 ODS-3 column, 25 cm × 4.6 mm, I.D.

Conditions	Temperature (°C)	Pressure (bar)	k'	
			Diuron	Linuron
a	80	Programmed	8.7	5.7
b	55	220	4.4	0.6
b	55	330	3.0	0.3
b	75	220	3.9	0.8
b	75	330	2.2	0.4
b	100	220	4.2	2.9
b	100	290	2.4	0.8
b	100	330	2.3	0.7

TABLE V

CHROMATOGRAPHIC RESULTS USING METHANOL-MODIFIED CARBON DIOXIDE AND VARYING PRESSURES AND TEMPERATURES

Packed column SFC, methanol–carbon dioxide (4:96), 4.5 ml/min, Whatman Partisil 5 ODS-3 column, 25 cm × 4.6 mm I.D. DCA = Dichloroaniline.

Temperature (°C)	Pressure (bar)	k'		
		Diuron	DCA	Linuron
55	220	1.2	0.8	0.6
55	330	0.8	0.6	0.4
75	220	1.3	0.8	0.7
75	330	0.9	0.6	0.5
100	220	1.7	0.9	1.0
100	330	0.9	0.6	0.6

TABLE VI

CHROMTOGRAPHIC RESULTS USING ETHANOL-MODIFIED CARBON DIOXIDE AND VARYING PRESSURES AND TEMPERATURES

Packed column SFC ethanol–carbon dioxide (4:96), 4.5 ml/min, Whatman Partisil 5 ODS-3 column, 25 cm × 4.6 mm I.D.

Temperature (°C)	Pressure (bar)	k'		
		Diuron	DCA	Linuron
55	220	1.7	0.9	0.7
55	330	1.2	0.6	0.4
75	220	2.5	1.2	1.1
75	330	1.1	0.7	0.6
100	220	3.2	1.6	1.0
100	330	1.3	0.6	0.6

atures, 55, 75 and 100°C, at a constant pressure. The highest recovery was obtained at 100°C, the lowest at 55°C. A longer study was conducted at the two higher temperatures. Again the higher temperature yielded the greatest recovery: 100°C yielded 81%, 75°C yielded 48% (Fig. 1).

The first 15 min of each extraction yielded the highest recovery, 61% and 47% for the 100 and 75°C temperatures respectively. A leveling of the amount extracted was observed in less than 1 h in both cases; after this hour, the amount which continued to be extracted was reduced to less than 0.5% every 15 min.

Effects of pressure. Increasing the pressure increased the extraction efficiency of diuron from soil during the early extraction times (Fig. 2). Eventually, even though the rate of extraction was slower, the total amount extracted was statistically the same for the three pressure levels investigated, 110, 235 and 338 bar. Recoveries for these 100°C extractions averaged approximately 70%.

Effects of temperature and pressure. To see if the effects which has been exhibited in the previous experiments were additive, the pressure was increased at two
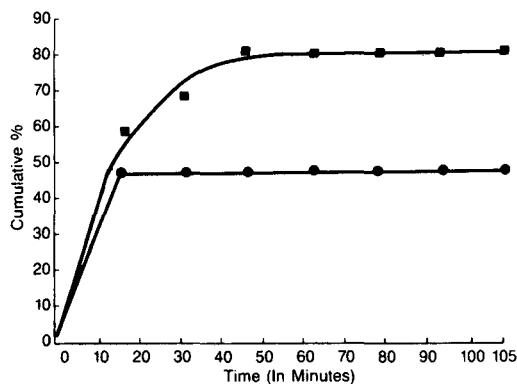
Fig. 1. Effects of increasing temperature on the extraction of diuron from Sassafras soil at constant pressure (340 bar). Flow-rate, 5 ml/min; modifier, methanol (10%). Key: (●) 75°C; (■) 100°C.

different temperatures. Increasing the pressure at 75°C increased the extraction efficiency more than at 100°C. This is not unexpected since the mobile phase density at a constant pressure is greater with lower temperature. Once again, the final extracted yield for the two pressure levels was equivalent at both temperatures.

Effects of mobile phase modifier. When experiments were conducted with no modifier in the supercritical carbon dioxide, no significant quantities of solute were extracted. Increasing the percent modifier increased the extraction efficiency. For 1.25% and 10.0% methanol, the cumulative percents extracted were 4% and 81% respectively (Fig. 3).

Methanol concentrations up to 20% were investigated at lower pressures; the
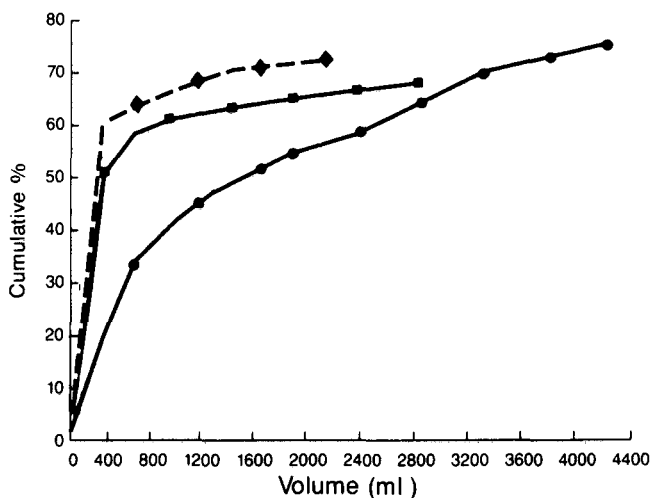
Fig. 2. Effects of increasing pressure on the extraction of diuron from Sassafras soil at constant temperature (100°C). Flow-rate, 16.5 ml/min; modifier, acetonitrile (10%). Key: (●) 110 bar; (■) 235 bar; (◆) 338 bar.
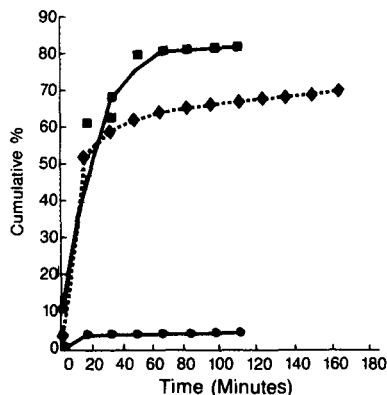
Fig. 3. Effects of modifier on the extraction of diuron from Sassafras soil at constant pressure (340 bar) and temperature (100°C). Flow-rate, 5 ml/min. Key: (●) 1.25% methanol; (■) 10% methanol; (◆) 10% acetonitrile.

general trend of greater extraction efficiency with higher mobile phase modifier concentration was obtained (Fig. 4). Irreproducibility in the amount of methanol delivered from the tank was noted with concentrations in the carbon dioxide above 10%. This was attributed to the solubility of methanol in liquid carbon dioxide as a function of temperature; homogeneity of the mixture as it leaves the tank over a period of time is suspect.

Acetonitrile was examined in addition to methanol modifier because of its slightly higher polarity. The dielectric constant of acetonitrile is 38.8 *versus* 33.6 for methanol. The extraction recoveries for acetonitrile were lower, 69% *versus* 81% for methanol (Fig. 3). The solubility of diuron in methanol is not significantly different than in acetonitrile, indicating that solubilities of solute in the liquid modifier can not necessarily predict extraction efficiency.

An investigation of solute solubility in the supercritical mobile phase was conducted where six pesticides were extracted from activated carbon using supercritical
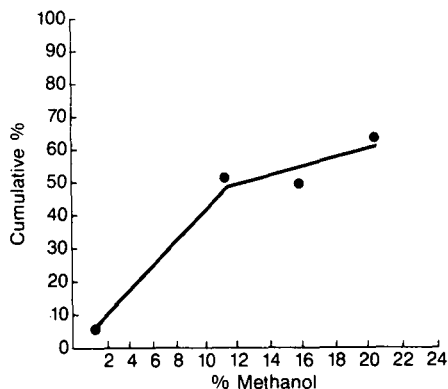
Fig. 4. Effects of increasing mobile phase modifier strength on the extraction of diuron from Sassafras soil at constant pressure (340 bar) and temperature (100°C). Flow-rate, 5 ml/min.
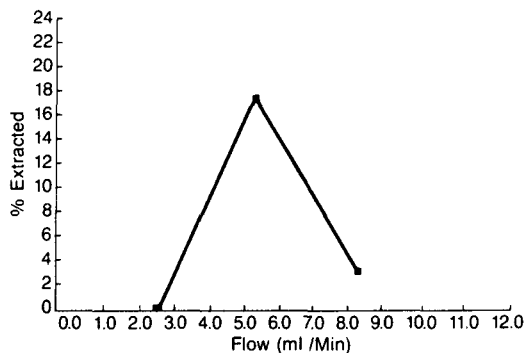
Fig. 5. Effects of increasing flow-rate on the extraction of diuron from Sassafras soil. Modifier, 10% methanol; inlet pressure, 350 bar; temperature, 75°C.

carbon dioxide[6]. In essence, their conclusions were that some sites of activated carbon were easier to regenerate than others. This was attributed to inconsistent strength of sorption forces in some positions. Higher solubilities in carbon dioxide did not yield easier removal. In addition to adsorption effects, surface chemical reactions can vary depending on the available site. These same matrix effects could be influencing our extraction experiments.

Effects of flow-rate. Experiments investigating the effects of flow variations were conducted at three rates. The percent extracted increased with a change in flow from 2.5 to 5.0 ml/min. When the flow-rate was increased from 5.0 to 7.5 ml/min, the extraction efficiency dropped dramatically (Fig. 5). Examining the pressure drop across the extraction column explained these results (Fig. 6). The pressure drop at 2.5 ml/min was 100 p.s.i., 400 p.s.i. at 5.0 ml/min, and greater than 1000 p.s.i. at 7.5 ml/min. Better control of the pressure drop across an extraction tube yields higher extraction efficiencies at higher flow-rates than 5 ml/min.

Higher pressures and temperatures were also examined at the low flow-rate of 2.5 ml/min. Recovery increases were negligible (< 1%).
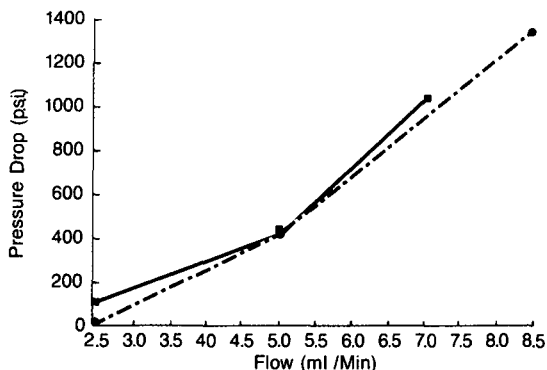
Fig. 6. Variation in pressure drop across the extraction tube with change in flow-rate. Modifier, 10% methanol. Temperature: (■) 75°C, (●) 100°C.
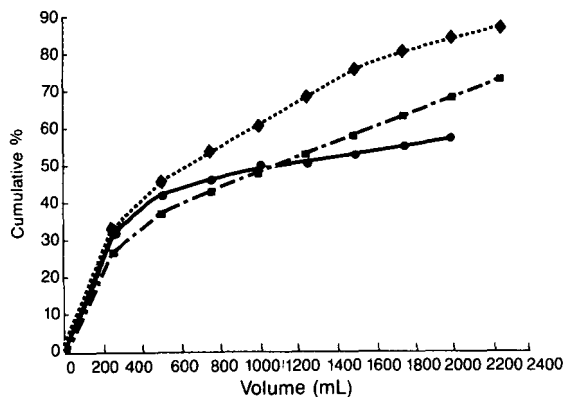
Fig. 7. Effects of increasing temperature on the extraction efficiency of linuron from Sassafras soil. Modifier, 10% acetonitrile; pressure, 290 bar; flow-rate, 16.5 ml/min. Temperature: (●) 80°C; (■) 100°C; (♦) 120°C.

Linuron from Sassafras soil

Effects of temperature and pressure. As was exhibited for diuron, increases in temperature and pressure increased the extraction efficiency of linuron from soil. Temperatures were varied up to 120°C, which significantly increased the recovery over the 100°C result from 74% to 90%. Extraction recoveries were not shown to level off with time at the lower pressures (Fig. 7 and 8).

Effects of mobile phase modifier. A drastic increase in extraction efficiency was exhibited when 10% ethanol was used as the polar modifier as opposed to methanol. The dielectric constant for ethanol is 25.0 compared to 33.6 for methanol. This seemed to suggest that lower polarity modifiers would be more conducive for these extractions; however, extractions involving more non-polar solvents as modifiers such as methylene chloride and chloroform yielded negligible recoveries. Our current hypothesis is that the polarity of the mobile phase mixture must be optimized to match the polarity of the solute.
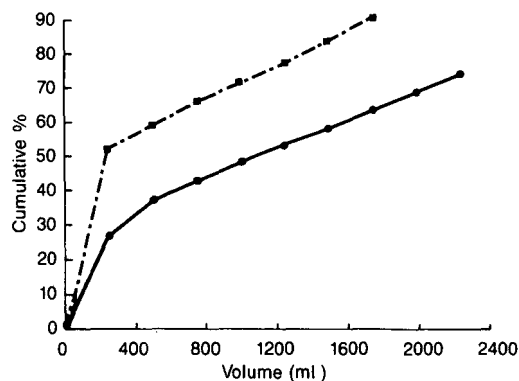
Fig. 8. Effects of increasing pressure on the extraction efficiency of linuron from Sassafras soil. Flow-rate, 16.5 ml/min; modifier, 10% acetonitrile; temperature, 100°C. Pressure: (●) 290 bar; (■) 310 bar.

Effects of flow-rate. At 75 and 100°C, the change in extraction efficiency with increasing flow followed the same trends as seen in the diuron extractions. Pressure drops across the extraction tubes were not as great; this is a function of how the individual extraction tubes were packed and is an error intrinsic to our system. Correspondingly, the percent extracted did not decrease as dramatically at the higher flow-rates.

Chromatographic correlations

The k' values (see Tables IV–VI) decreased with an increase in pressure for diuron and linuron. This supports the increased extraction efficiencies noted at higher pressures. In general, throughout all the parameters investigated linuron had lower capacity factors than diuron. Equal or higher extraction efficiencies were achieved for linuron over diuron, suggesting elution order or capacity factor can be used as an aid in predicting extraction efficiency.

Mobile phase modifier concentration is well known as a major influence in chromatographic retention. Increases in modifier concentration decreased k' values[2]. This supports the increase in extraction efficiency obtained with increased modifier in the carbon dioxide mobile phase.

Temperature trends vary both in our extraction experiments and in our chromatographic retention studies. An influence of an alternate mechanism is possible with these trends. Linuron has a lower melting point than diuron, 93°C and 158°C respectively, and a higher vapor pressure. During the extraction experiments, the volatility of the major metabolite of both linuron and diuron, dichloroanaline, could also have an influence. Further investigations are required.

CONCLUSIONS

Increasing temperature yields increased extraction efficiencies of diuron, linuron and their metabolite dichloroaniline from soil. As pressure is increased higher extraction efficiencies over shorter time periods result. Longer extraction times at lower pressures yield equivalent recoveries to those obtained with the higher pressures.

Increasing flow-rates result in higher extraction efficiencies; these effects start to diminish when larger pressure drops are obtained over the length of the sample extraction tube. An optimum flow-rate of 5.0 ml/min for our extraction experiments has been determined.

Increased concentration of polar modifier supplies higher extraction efficiencies; extraction efficiencies vary with the mobile phase modifier as shown with acetonitrile *versus* methanol and methanol *versus* ethanol. This relationship changes with solute of interest and sample matrix.

SFC retention characteristics enable some prediction of extraction efficiency. Our studies assume that the chromatographic column is behaving as a soil matrix; a more suitable stationary phase might yield more parallel results.

REFERENCES

1 M. E. P. McNally and J R. Wheeler, *J. Chromatogr.*, 435 (1988) 63–71.
2 M. A. Schneiderman, A. K. Sharma and D C. Locke, *J. Chromatogr.*, 409 (1987) 343–353.
3 J. R. Wheeler and M. E. P. McNally, *J. Chromatogr.*, 410 (1987) 343–353.
4 D. R. Gere, R. Board and D. McManigill, *Anal. Chem.,* 259 (1982) 736.
5 I. E. Stevenson and A. M. Brown, personal communication, 1987.
6 R. P. de Fillipi, V. J. Krukonis, R. J. Ruby and M. Modell, *Report EPA-600/2-80-054,* Industrial Environmental Research Lab., Research Triangle Park, NC, March, 1980.

HIGH-PERFORMANCE LIQUID CHROMATOGRAPHIC SEPARATION OF SUBCOMPONENTS OF ANTIMYCIN A

S. L. ABIDI

U.S. Fish & Wildlife Service, National Fishery Research Center, P.O. Box 818, La Crosse, WI 54602-0818 (U.S.A.)

(First received January 7th, 1988; revised manuscript received April 7th, 1988)

SUMMARY

Using a reversed-phase high-performance liquid chromatographic (HPLC) technique, a mixture of antimycins A was separated into eight hitherto unreported subcomponents, A_{1a}, A_{1b}, A_{2a}, A_{2b}, A_{3a}, A_{3b}, A_{4a}, and A_{4b}. Although a base-line resolution of the known four major antimycins A_1, A_2, A_3, and A_4 was readily achieved with mobile phases containing acetate buffers, the separation of the new antibiotic subcomponents was highly sensitive to variation in mobile phase conditions. The type and composition of organic modifiers, the nature of buffer salts, and the concentration of added electrolytes had profound effects on capacity factors, separation factors, and peak resolution values. Of the numerous chromatographic systems examined, a mobile phase consisting of methanol–water (70:30) and 0.005 M tetrabutylammonium phosphate at pH 3.0 yielded the most satisfactory results for the separation of the subcomponents. Reversed-phase gradient HPLC separation of the dansylated or methylated antibiotic compounds produced superior chromatographic characteristics and the presence of added electrolytes was not a critical factor for achieving separation. Differences in the chromatographic outcome between homologous and structural isomers were interpreted based on a differential solvophobic interaction rationale. Preparative reversed-phase HPLC under optimal conditions enabled isolation of pure samples of the methylated antimycin subcomponents for use in structural studies.

INTRODUCTION

A few years ago, we reported the high-performance liquid chromatographic (HPLC) resolution of a mixture of dilactonic antibiotics (antimycin A complex)[1]. Since then, because of the reported ready decomposition of these substances in alkaline media[2–6], we have been interested in pursuing studies on structural modifications and on the chemical reactivity of individual antimycin A_1, A_2, A_3, and A_4 components. After a number of unsuccessful attempts at conducting product analyses by spectroscopic methods, it was necessary to examine the reactant antimycin A by nuclear magnetic resonance (NMR) spectroscopy. Results of a subsequent intensive

NMR study[7] revealed that each of the known major components (A_1, A_2, A_3, and A_4) of the antimycin A complex appeared to comprise two subcomponents isomeric at the 8-acyloxy side chain (Fig. 1). Prompted by the spectroscopic findings, HPLC experiments were performed on the individual antimycins A_1, A_2, A_3, and A_4 with a high-efficiency octadecylsilica (ODS) column (80 000 plates/m). A preliminary study showed that each of the four major components of antimycin A was, in fact, a

$$R^1 = -CH_2 \overset{CH_2}{\diagdown} CH_2 \overset{CH_2}{\diagup} CH_2 \diagup CH_3$$

(I)

$$R^1 = -CH_2 \overset{CH_2}{\diagdown} CH_2 \diagup CH_3$$

(II)

$$R^2 = -\overset{CH_3}{\underset{|}{CH}} \overset{CH_2}{\diagdown} \diagup CH_3$$

(III)

$$R^2 = -CH \overset{CH_3}{\underset{CH_3}{\diagup}}$$

(IV)

$$R^3 = -CH_2-CH \overset{CH_3}{\underset{CH_3}{\diagup}}$$

(V)

$$R^3 = -CH_2-CH_2-CH_3$$

(VI)
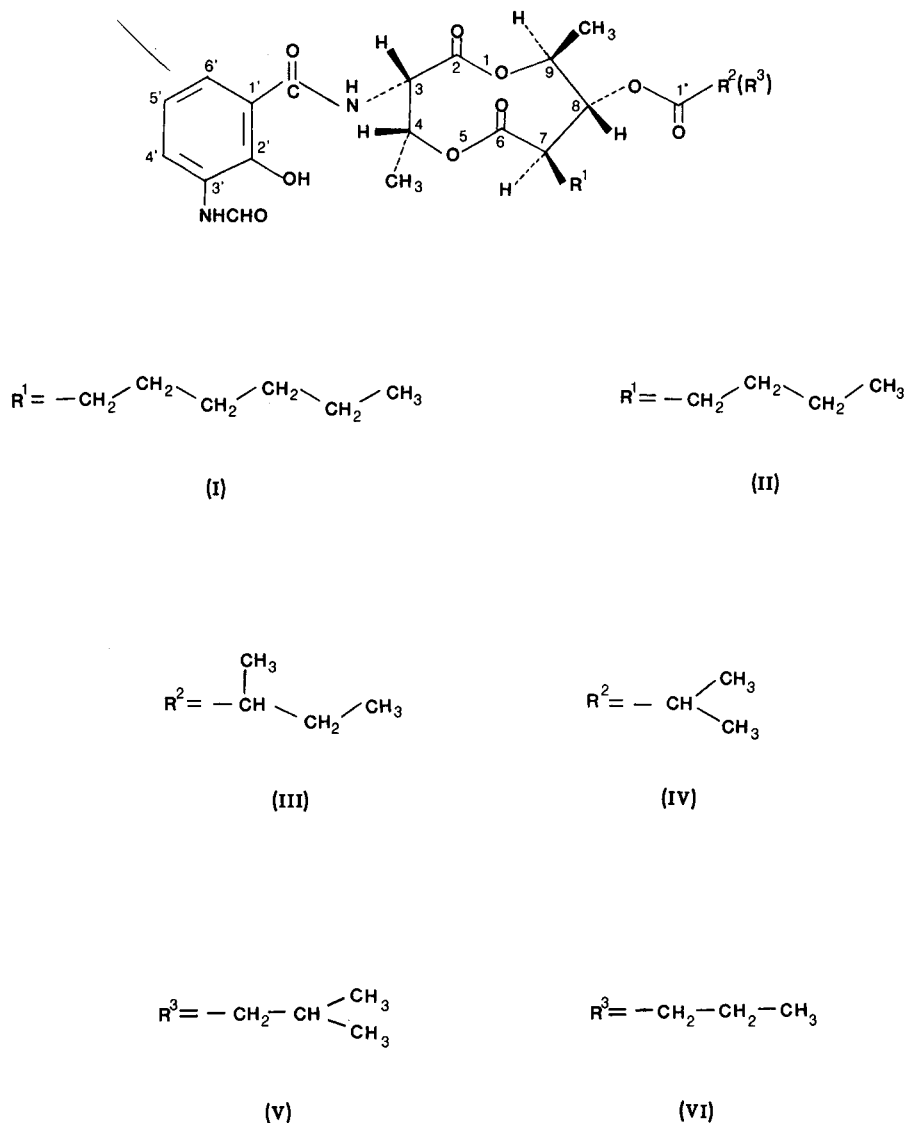
Fig. 1. Structures of subcomponents of antimycin A complex. A_{1a}, $R^1 = I$, $R^2 = III$; A_{1b}, $R^1 = I$, $R^3 = V$; A_{2a}, $R^1 = I$, $R^2 = IV$; A_{2b}, $R^1 = I$, $R^3 = VI$; A_{3a}, $R^1 = II$, $R^2 = III$; A_{3b}, $R^1 = II$, $R^3 = V$; A_{4a}, $R^1 = II$, $R^2 = IV$; A_{4b}, $R^1 = II$, $R^3 = VI$.

two-component mixture as disclosed by the splitting of individual HPLC peaks. Further elaborate experiments on optimization of the HPLC conditions led to the adequate separation of the antimycin subcomponents. The results are presented in this paper.

EXPERIMENTAL

Chemicals and reagents

Samples of antimycin A complex and individual antimycins A_1, A_2, A_3, and A_4 were purchased from Sigma (St. Louis, MO, U.S.A.) or prepared from the crude antibiotics (Aquabiotics Corp., North Brook, IL, U.S.A.) at the National Fishery Research Center (La Crosse, WI, U.S.A.) according to the published procedure[1]. HPLC-grade sodium acetate, 1-dimethylaminonaphthalene-5-sulfonyl chloride (dansyl chloride), pyridine, and "Diazald" (diazomethane precursor) were obtained from Aldrich (Milwaukee, WI, U.S.A.). Diazomethane was generated from Diazald following instructions supplied with the chemical by the manufacturer. Antimycins were dansylated as described previously[1]. Methylated derivatives of antimycins were prepared by treating a solution of antimycins in diethyl ether with an ethereal solution of diazomethane (25% in excess of the theoretical amount) followed by stirring the resultant solution at room temperature overnight. Pure methylated antibiotics were obtained from the crude materials by thin-layer chromatography (TLC). This TLC purification experiment was performed on a preparative silica gel plate (20 × 20 cm taper plate, Analtech, Newark, DE, U.S.A.) using a mixed solvent [benzene–chloroform–methanol–acetic acid (15:5:1:1)] for development of the chromatogram. A *ca.* 50-mg sample was streaked onto the TLC plate (impregnated with a fluorescence indicator by Analtech) and, after development, visualized with a mineralight lamp (Model UVSL-58 multiband UV-254/366 nm, Ultraviolet Products, San Gabriel, CA, U.S.A.). The dark purple band as seen under the short-wavelength UV light (or the fluorescence band as observed under the long-wavelength UV light) was scraped off, extracted three times with 10 ml methanol–methylene chloride (1:1), and evaporated at a reduced pressure to give pure methylated antimycins. Tetrabutylammonium salts were products of Eastman Kodak (Rochester, NY, U.S.A.) and were used as received. All HPLC solvents and other buffer salts were of chromatography-quality and purchased from J. T. Baker (Phillipsburg, NJ, U.S.A.).

High-performance liquid chromatography

A Varian Model LC-5020 liquid chromatograph was used in all HPLC experiments. The chromatograph was equipped with a multiple-wavelength UV–VIS detector (Varian Model 100), a Varian Model 9176 strip chart recorder, and a high-efficiency reversed-phase column [Ultrasphere ODS column, 5 μm, 25 cm × 4.6 mm I.D. (Altex, Berkeley, CA, U.S.A.)]. The analytical column was connected to a Valco (Houston, TX, U.S.A.) CV-6-UHPa-N60 injector. In a typical analysis, samples (20–50 ppm) were injected via a Valco 10-μl loop and a mobile phase eluent was pumped through the column at a flow-rate of 2 ml/min. For analyses of underivatized antimycin A complex, it was necessary in all cases to use mobile phases that consisted of methanol and water containing different concentrations of various buffer salts (or counter ion electrolytes). On the other hand, HPLC separations of both methylated

and dansylated antimycins were carried out with mobile phases of methanol–water in various proportions. No electrolyte was required in the mobile phase for analyses of either type of derivatives.

The detector output signals were fed into the strip chart recorder and the chromatographic data [peak areas, retention times, isomeric ratios, retention (k'), selectivity (α), and resolution (R)] were automatically processed by a Varian Model 1427 integrator.

Subcomponents of methylated antimycin A complex were simultaneously resolved by gradient elution with an initial mobile phase composition of methanol–water (60:40) to a final composition of 70:30 in the same solvent system over a period of 3 h at a flow-rate of 1.5 ml/min. The analytical procedure was applied to the isolation of individual subcomponents by preparative HPLC. An Altex reversed-phase column (Ultrasphere ODS, 5 μm, 25 cm × 10 mm I.D.) was used for this purpose. In a routine preparative HPLC experiment, a 50–100 mg sample was chromatographed and the column effluents, while monitored with a Varian refractive index detector, were collected in 0.5-ml fractions using a Buchler linear automatic fraction collector. Fractions containing pure subcomponents as revealed by analytical HPLC–UV detection were combined and evaporated under reduced pressure. The aqueous residue was extracted three times with methylene chloride. The combined organic extract was dried over anhydrous sodium sulfate and evaporated to yield pure subcomponents. The structures of these materials were determined by ^{1}H and ^{13}C NMR[7] and confirmed by fast atom bombardment mass spectrometry.

In an alternative method for the isolation of subcomponents, HPLC experiments were performed individually with samples of methylated antimycin components A_1, A_2, A_3, and A_4 obtained by our published preparative HPLC method[1]. Thus, under isocratic conditions with a mobile phase of methanol–water (70:30), pure subcomponents of antimycins A_{1a}, A_{1b}, A_{2a}, and A_{2b} were obtained in milligram quantities. Likewise, preparative HPLC under isocratic conditions using a mobile phase consisting of methanol–water (60:40) afforded pure subcomponents of antimycins A_{3a}, A_{3b}, A_{4a}, and A_{4b}.

RESULTS AND DISCUSSION

As demonstrated in our earlier publication[1], a homologous mixture of antimycin A complex can be efficiently resolved into its four major component homologues A_1, A_2, A_3, and A_4 by reversed-phase HPLC with a chemically bonded hydrocarbonaceous silica column. The only structural differences among the component antibiotics are in the alkyl substituents at the 7 and 8 side-chains that differ by at least one methylene (CH$_2$) unit (Fig. 1). Considering the homologous structures of the antimycin A complex in the context of the basic principles of reversed-phase HPLC on an alkyl-bonded silica, optimization of reversed-phase HPLC conditions for achieving an excellent separation of the homologous mixture should be straightforward. This has been experimentally corroborated[1]. However, the situation in reversed-phase HPLC of subcomponents of this antibiotic complex would be more complicated because the structural isomers of these subcomponents are no longer homologously interrelated. As depicted in Fig. 1, the 8-acyloxy ester moieties of the eight subcomponents are described as follows: A_{1a} vs. A_{1b}, isopentanoyl vs. isovaleryl; A_{2a} vs. A_{2b}, isobutyryl vs. n-butyryl; A_{3a} vs. A_{3b}, isopentanoyl vs. isovaleryl; A_{4a} vs. A_{4b},

isobutyryl *vs. n*-butyryl. The differential solvophobic interactions of the a–b sub-components with a given straight-chain alkyl bonded silica stationary phase during separation processes would be more specific and more susceptible to changes in mobile phase conditions than those would be expected in the separation of homologous components A_1, A_2, A_3, and A_4. Ideally, HPLC on a branched-chain alkylsilica would facilitate resolution of the subcomponents because of increased degrees of specific hydrophobic interactions.

Fig. 2 presents two representative chromatograms showing separations of subcomponents of antimycin A complex with mobile phases of methanol–water (70:30) containing (Fig. 2A) 0.2 *M* sodium acetate at pH 5 and (Fig. 2B) 0.005 *M* tetrabutylammonium phosphate at pH 3.0. An eight-subcomponent constitution of antimycin A complex is immediately discernible from each of the chromatograms, even though, in both instances, only partially resolved peaks are seen for the earlier eluting antimycins that have shorter alkyl side-chains at the 7- and 8-alkyl substituents. In spite of the required longer retention times, incorporation of tetrabutylammonium phosphate into the mobile phase appeared to be more advantageous than that of sodium acetate for the separation of a–b subcomponents. In the light of the straight-chain nature of the alkyl bonded phase used throughout this study, the later-eluting components (the more strongly retained components) (Fig. 2) corre-sponded to the minor components (b-isomers) in which the α-carbons contain no methyl substituent (Fig. 1). We presume that hydrophobic interactions between the major components (a-isomers) and the stationary phase were weaker and less efficient than for the minor counterparts as a result of branching of the hydrocarbon chain at the α-carbons (a-isomer, Fig. 1).

Fig. 3 shows the effect of mobile phase composition on the separation of the eight antimycin constituents and their dansylated and methylated derivatives. Using a 0.2 *M* acetate buffer at pH 5, the a–b components were not at all resolved with a mobile phase of methanol–water (80:20), though the four antimycin homologues A_1, A_2, A_3, and A_4 were well resolved under these conditions (Fig. 3A). Similarly, with a mobile phase of methanol–water (80:20), HPLC of derivatized antimycin A complex yielded no separation of the subcomponents of the dansylated (Fig. 3B) and methylated (Fig. 3C) antimycin subcomponents, notwithstanding excellent resolution of the homol-ogous components. We found that the presence of buffer salts and other counter ion electrolytes in mobile phases was not necessary for separating either type of subconstituent derivatives. Variations in separation factors (α) of a homologous pair with mobile phase solvent compositions were much greater than those of an a–b subcomponent pair as predicted. Solvophobic interactions between homologous solutes and the reversed-phase bonded stationary phase would be much stronger than those derived from structural isomers of equal carbon contents. As seen in Fig. 3, resolution of the latter isomers (a–b pairs), as well as of homologous isomers, increases as the percent methanol in the mobile phase decreases. This compositional effect of the mobile phase seemed to follow conventional trends normally observed in reversed-phase HPLC of isomeric compounds[8]. A maximum methanol content of 70% was found for obtaining a quantifiable simultaneous resolution of all eight subcomponents of both parent and methylated antimycins (Fig. 3A and C). For the separation of dansylated subcomponents, a mobile phase of methanol–water (75:25) was required to be analytically useful in practical application.
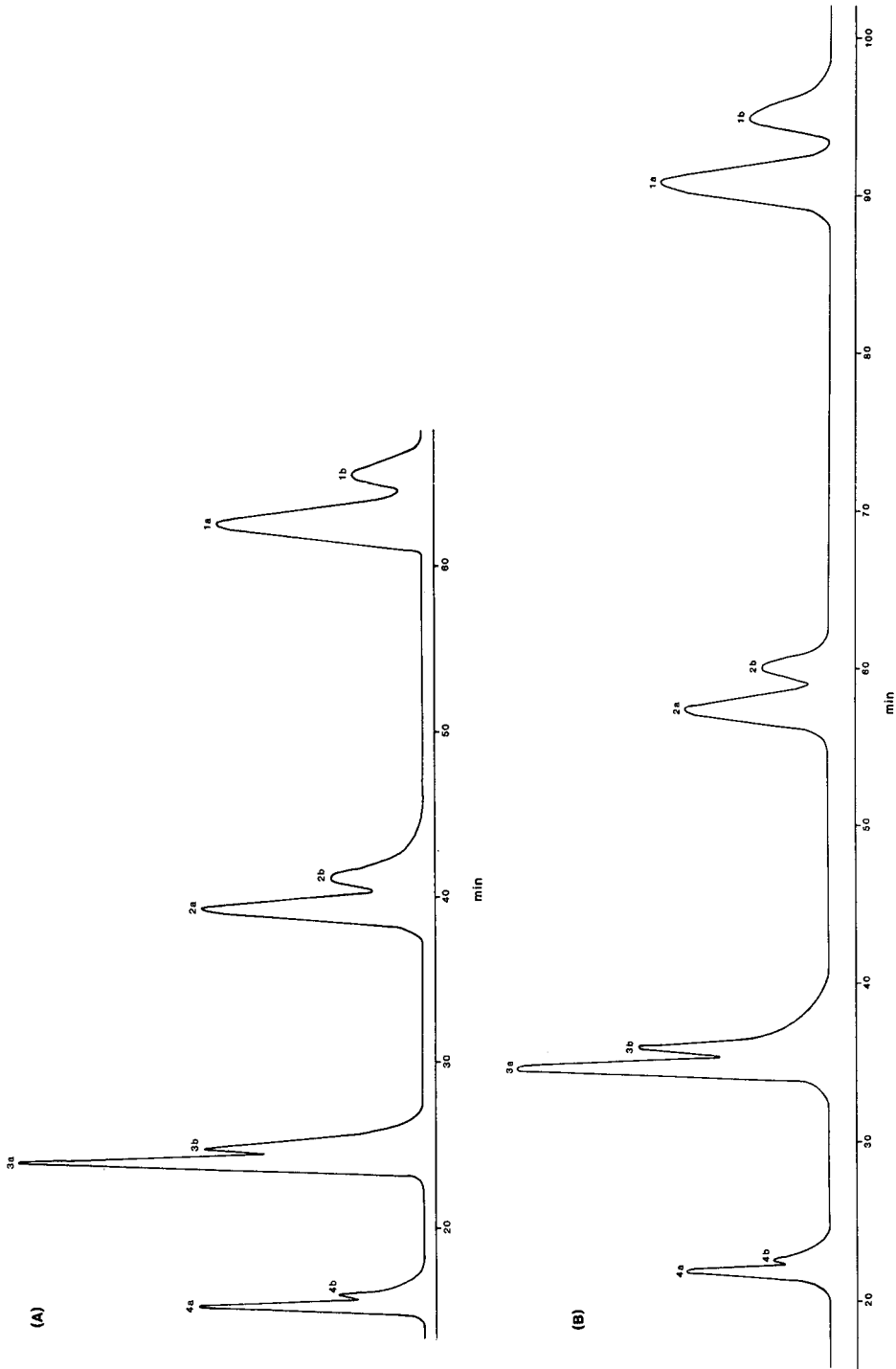
Fig. 2. Isocratic HPLC separation of antimycin A subcomponents. Peak designations same as in Fig. 1. (A) Mobile phase, methanol–water (70:30) containing 0.2 *M* sodium acetate at pH 5.0. (B) Mobile phase, methanol–water (70:30) containing 0.005 *M* tetrabutylammonium phosphate (TBAP) at pH 3.0.
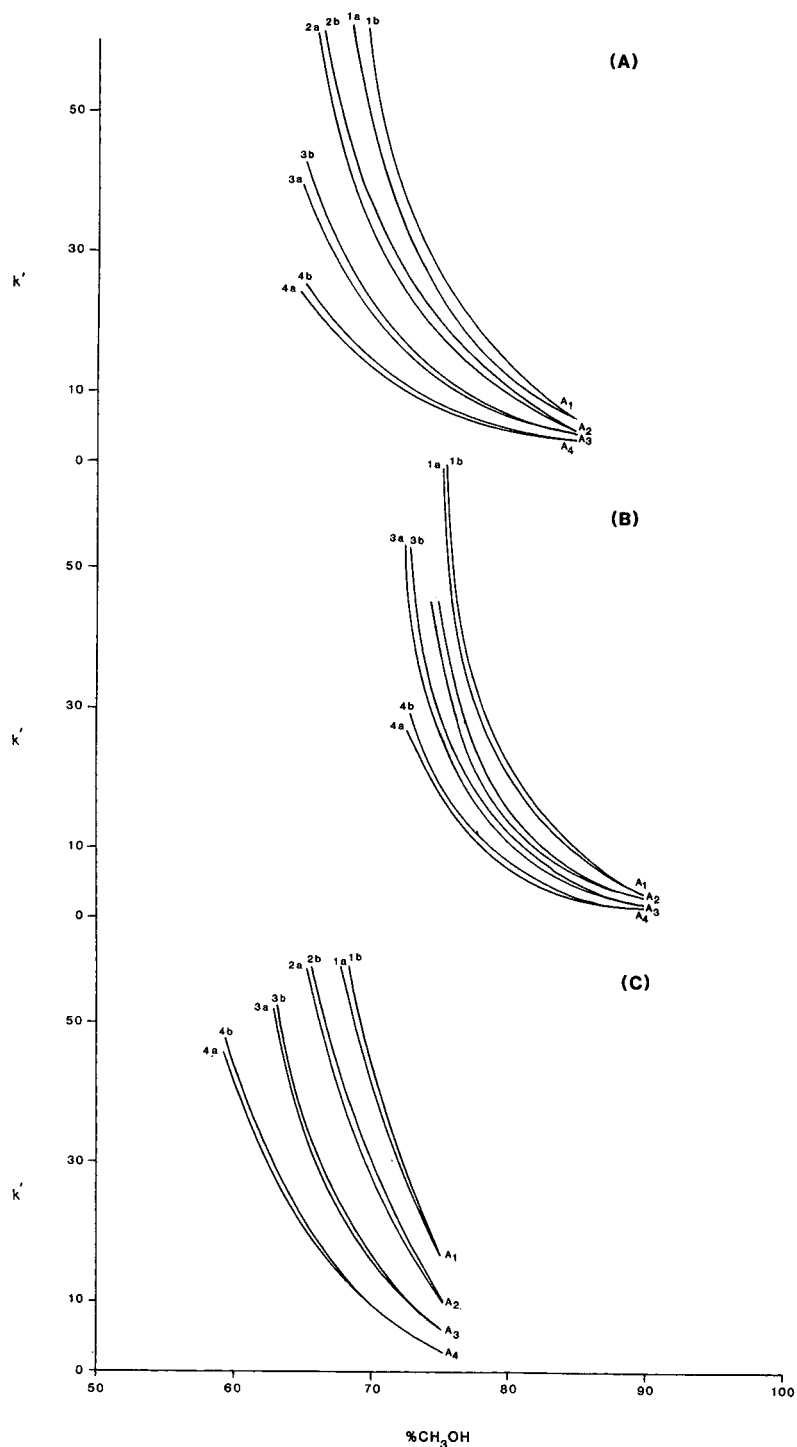
Fig. 3. Mobile phase (methanol–water) effects on the separation of subcomponents of (A) antimycin A, (B) dansylated derivatives and (C) methylated derivatives. Mobile phase in (A) contained 0.2 M sodium acetate at pH 5.

TABLE I

MOBILE PHASE EFFECTS ON CHROMATOGRAPHIC CHARACTERISTICS OF ANTIMYCIN A SUBCOMPONENTS (flow-rate = 2 ml/min)

Mobile phase pH*	A_{1a}		A_{1b}	A_{2a}		A_{2b}	A_{3a}		A_{3b}	A_{4a}		A_{4b}
	k'	(α)	k'	k'	(α)	k'	k'	(α)	k'	k'	(α)	k'
(I) Methanol–water (70:30)												
(A) 6.6	19.4	(1.06)	20.5	12.3	(1.04)	12.8	7.24	(1.00)	7.24	4.52	(1.00)	4.52
(B) 5.4	42.4	(1.06)	44.8	26.9	(1.04)	28.1	16.1	(1.04)	16.8	10.1	(1.00)	10.1
(C) 3.0	71.6	(1.05)	75.2	41.9	(1.06)	44.4	24.9	(1.06)	26.4	15.4	(1.05)	16.1
(D) 3.0	62.4	(1.04)	64.6	39.0	(1.03)	40.2	15.8	(1.04)	16.4	14.5	(1.02)	14.8
(E) 5.0	49.0	(1.05)	51.4	30.4	(1.05)	31.8	18.1	(1.04)	18.8	11.2	(1.05)	11.8
(F) 5.0	42.4	(1.03)	43.7	25.9	(1.03)	26.7	15.2	(1.02)	15.5	9.32	(1.00)	9.32
(II) Acetonitrile–water (60:40)												
(G) 3.0	28.7	(1.00)	28.7	18.8	(1.00)	18.8	12.0	(1.00)	12.0	7.80	(1.00)	7.80
(H) 6.6	8.28	(1.00)	8.28	5.64	(1.00)	5.64	3.72	(1.00)	3.72	2.44	(1.00)	2.44
(I) 4.5	20.6	(1.00)	20.6	13.5	(1.00)	13.5	9.24	(1.00)	9.24	6.20	(1.00)	6.20
(J) 4.5**	44.8	(1.00)	44.8	29.2	(1.00)	29.2	18.4	(1.00)	18.4	11.9	(1.00)	11.9

* Mobile phases contained 0.005 M tetrabutylammonium phosphate (A, B, C, G, H), 0.005 M tetrabutylammonium hydrogensulfate (D), 0.2 M sodium acetate (E, I, J), and 0.2 M ammonium acetate (F).
** Acetonitrile–water (55:45).

Results in Table I (all flow-rates were 2 ml/min) indicate that the chromatographic behavior of both homologous and structural isomers of antimycin A complex was heavily dependent on the mobile phase constituents (the nature of the organic modifiers, the type of added electrolytes, pH, and the solvent composition). In particular, the nature of the organic modifier in the mobile phase had a dramatic influence on the separation of antimycin subcomponents (the structural isomers). When methanol was used in the mobile phase [as in mobile phases A, B, C, D, E, and F (Table I)], most of the subcomponent a–b pairs [$(A_{1a}-A_{1b})$, $(A_{2a}-A_{2b})$, $(A_{3a}-A_{3b})$, and $(A_{4a}-A_{4b})$] were resolved with α values in the range 1.00–1.08. However, no separation ($\alpha = 1.00$) of any of these subcomponent pairs was observed in all cases where acetonitrile was used (as in mobile phases G, H, I, and J). It should be pointed out that, with all mobile phases listed in Table I, undoubtedly the homologous components A_1, A_2, A_3, and A_4 were all very well resolved. The slightly stronger solvent strength of acetonitrile (3.1) relative to methanol (3.0)[9,10] might be attributable to the apparent reduction in the hydrophobic interactions that are critical for the specific differentiation of the subcomponent isomers.

HPLC experiments with mobile phases containing 0.005 M tetrabutylammonium phosphate (TBAP) as in A, B, and C (Table I) showed remarkable pH effects on the retention and separation characteristics of antimycin subcomponents. The pK_a value of antimycin A in water has been estimated to be 5.1 (ref. 5). Of the three mobile phases, C (pH 3) provided the most satisfactory results yielding α values of 1.04–1.05 for the four a–b pairs. Experiments A and B, both conducted at higher pH values, afforded incomplete resolution of the structural isomers with α values of 1.00–1.06 and with some of the early-eluting pairs remained unresolved. The higher k' values obtained at lower pH values may presumably reflect the less ionic character of the 2'-OH group of the aromatic side-chain of antimycin A. Comparisons of the data (Table I) between C and D and between E and F indicate that the k' and α values of antimycin subcomponents were somewhat affected by changes in the nature of added ion species, including cations and anions of closely related electrolytes. TBAP and sodium acetate seemed to be somewhat better mobile phase additives than the respective tetrabutylammonium hydrogensulfate and ammonium acetate for effecting separation of antimycin subcomponents.

The chromatographic data in Table II were obtained under the same mobile phase conditions as in Table I except for the flow-rate which were at 1 ml/min in all cases. There was no appreciable improvement in selectivity values for the separation of subcomponents as the flow-rates of mobile phases were reduced from 2 ml/min (Table I) to 1 ml/min (Table II). In some cases at lower flow-rates, the retention times of the analytes became too long to be of analytical significance.

Table III shows the concentration effect of sodium acetate on the separation of subcomponents. It is clearly demonstrated that the presence of sodium acetate at higher concentrations (0.2–0.25 M) in the mobile phases consisting of methanol–water (70:30) tended to favor the separation of the isomers of interest. In these cases, the peak resolution (R) (0.51–1.01) and α (1.04–1.05) values were greater than those found at lower concentrations (0.05–0.10 M) ($R = 0.00$, $\alpha = 1.00$). At an intermediate concentration 0.15 M, the respective R and α values ranged from 0.00 to 0.67 and from 1.00 to 1.05. The only inseparable peak (A_4) at this concentration was for the $A_{4a}-A_{4b}$ pair that had a k' value of 12.6.

TABLE II

MOBILE PHASE EFFECTS ON CHROMATOGRAPHIC CHARACTERISTICS OF ANTIMYCIN A SUBCOMPONENTS (flow-rate = 1 ml/min)

Mobile phase pH*	A_{1a}		A_{1b}	A_{2a}		A_{2b}	A_{3a}		A_{3b}	A_{4a}		A_{4b}
	k'	(α)	k'	k'	(α)	k'	k'	(α)	k'	k'	(α)	k'
(I) Methanol–water (70:30)												
(A) 6.6	20.0	(1.06)	21.2	12.5	(1.05)	13.1	7.28	(1.04)	7.57	4.54	(1.00)	4.54
(B) 5.4	44.0	(1.06)	46.6	28.1	(1.05)	29.5	16.9	(1.04)	17.6	10.6	(1.00)	10.6
(C) 3.0	72.9	(1.06)	77.3	43.0	(1.06)	45.6	25.8	(1.06)	27.3	15.8	(1.05)	16.6
(D) 3.0	63.5	(1.04)	66.0	40.1	(1.03)	41.3	16.5	(1.04)	17.2	14.9	(1.02)	15.2
(E) 5.0	50.4	(1.05)	52.9	31.2	(1.05)	33.4	18.9	(1.04)	19.7	11.6	(1.05)	12.2
(F) 5.0	43.9	(1.04)	45.7	26.6	(1.03)	27.4	16.1	(1.02)	16.4	9.35	(1.00)	9.35
(II) Acetonitrile–water (60:40)												
(G) 3.0	28.9	(1.00)	28.9	19.0	(1.00)	19.0	12.2	(1.00)	12.2	7.84	(1.00)	7.84
(H) 6.6	8.40	(1.00)	8.40	5.69	(1.00)	5.69	3.75	(1.00)	3.75	2.46	(1.00)	2.46
(I) 4.5	20.8	(1.00)	20.8	13.7	(1.00)	13.7	9.40	(1.00)	9.40	6.25	(1.00)	6.25
(J) 4.5	45.1	(1.00)	45.1	29.4	(1.00)	29.4	18.5	(1.00)	18.5	12.0	(1.00)	12.0

* For mobile phase designations, see footnote to Table I.

Table IV shows the concentration effect of TBAP on the separation of antimycin subcomponents. The observed decrease in k' values with increasing concentrations of TBAP may be interpreted as a competition for adsorption sites by the neutral solutes and the mobile phase additives. In the concentration range studied (0.005–0.10 M), resolution of a–b pairs was achieved with various degrees of separations (R = 0.30–1.25, α = 1.02–1.06) despite the obvious failure in resolving the A_{4a}–A_{4b} pair (R = 0.00, α = 1.00) with 0.10 M TBAP. In general, the concentration effect on the R and α values seemed to be small, even though the R values declined gradually as the TBAP concentration increased. Evidently, the α values of the early-eluting pairs (A_{3a}–A_{3b} and A_{4a}–A_{4b}) were adversely affected by the higher TBAP concentrations of 0.05–0.10 M. In addition, some stationary phase effect was observed when R values obtained with two octadecylsilica (ODS) columns (Altex Ultrasphere ODS and Ultrasphere ODS-IP) were compared. Significantly higher R values were attained with the latter column (experiments B and C, Table IV) than with the former (experiment A, Table IV).

Since there are several polar groups in an antimycin structure (Fig. 1), the observed mobile phase effects, as well as stationary phase effects, on the separation of antimycin subcomponents are indicative of strong solute-silanol interactions in the HPLC systems.

As noted earlier from Fig. 3, substitution of 2'-phenolic proton with methyl and

TABLE III

EFFECT OF SODIUM ACETATE CONCENTRATIONS (pH 5) ON THE SEPARATION OF ANTIMYCIN A SUBCOMPONENTS

Mobile phase, methanol–water (70:30).

Subcomponent		Acetate concentration (M)				
		0.05	0.10	0.15	0.20	0.25
A_{1a}	k'	66.2	60.8	55.5	49.0	46.0
	(α)	(1.00)	(1.00)	(1.05)	(1.05)	(1.05)
	R	0.00	0.00	0.67	1.00	1.01
A_{1b}	k'	66.2	60.8	58.0	51.4	48.1
A_{2a}	k'	41.0	37.7	34.9	30.4	28.8
	(α)	(1.00)	(1.00)	(1.04)	(1.05)	(1.05)
	R	0.00	0.00	0.56	0.65	0.67
A_{2b}	k'	41.0	37.7	36.4	31.8	30.3
A_{3a}	k'	24.3	22.3	20.6	18.1	17.2
	(α)	(1.00)	(1.00)	(1.04)	(1.04)	(1.04)
	R	0.00	0.00	0.28	0.51	0.54
A_{3b}	k'	24.3	22.3	21.4	18.8	17.9
A_{4a}	k'	14.1	13.1	12.6	11.2	10.6
	(α)	(1.00)	(1.00)	(1.00)	(1.05)	(1.04)
	R	0.00	0.00	0.00	0.53	0.55
A_{4b}	k'	14.1	13.1	12.6	11.8	11.0

TABLE IV

EFFECT OF TBAP CONCENTRATIONS ON THE SEPARATION OF ANTIMYCIN A SUB-COMPONENTS

Mobile phases consisted of methanol–water (70:30) at pH values of 5.0 (A, B), and 5.2 (C). Stationary phases used in A, and B and C were Altex Ultrasphere-ODS and Ultrasphere-ODS-IP, respectively.

Subcomponent		Mobile phase TBAP concentration (M)						
		0.005	0.01		0.05		0.10	
		A	A	B	A	C	A	C
A_{1a}	k'	65.4	53.8	64.6	44.5	38.0	35.4	28.9
	(α)	(1.04)	(1.05)	(1.06)	(1.05)	(1.05)	(1.05)	(1.05)
	R	1.02	0.94	1.25	0.92	1.02	0.88	0.97
A_{1b}	k'	68.2	56.3	68.6	46.8	39.9	37.2	30.3
A_{2a}	k'	40.2	34.0	39.2	27.9	24.2	22.4	18.8
	(α)	(1.05)	(1.02)	(1.06)	(1.05)	(1.05)	(1.05)	(1.04)
	R	0.96	0.93	1.05	0.93	0.95	0.78	0.88
A_{2b}	k'	42.2	34.6	41.5	29.1	25.3	23.4	19.6
A_{3a}	k'	23.6	19.3	22.4	16.4	14.4	13.6	11.6
	(α)	(1.04)	(1.04)	(1.04)	(1.03)	(1.04)	(1.02)	(1.03)
	R	0.59	0.53	0.70	0.51	0.70	0.30	0.40
A_{3b}	k'	24.5	20.0	23.2	16.9	15.0	13.9	12.0
A_{4a}	k'	14.3	11.6	13.6	10.1	9.08	8.47	7.32
	(α)	(1.04)	(1.03)	(1.03)	(1.04)	(1.03)	(1.00)	(1.00)
	R	0.70	0.58	0.62	0.54	0.55	0.00	0.00
A_{4b}	k'	14.8	12.0	14.0	10.5	9.32	8.47	7.32
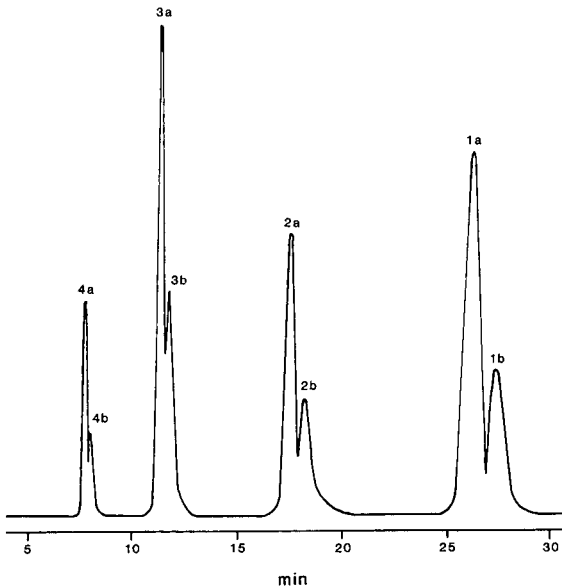
Fig. 4. Isocratic HPLC separation of methylated antimycin A subcomponents. Mobile phase: methanol–water (75:25).
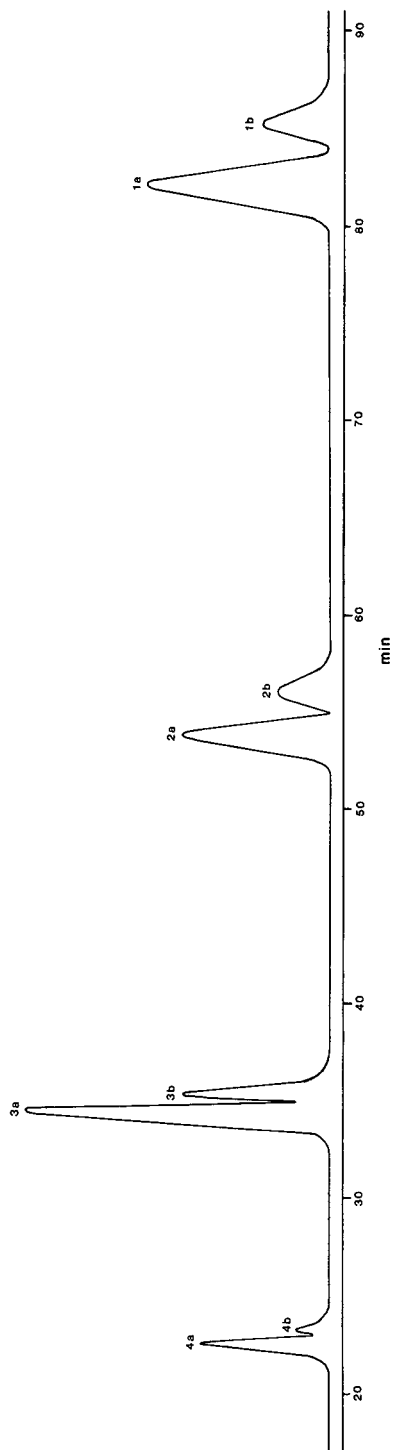
Fig. 5. Isocratic separation of dansylated antimycin A subcomponents. Mobile phase same as in Fig. 4.

TABLE V

EFFECT OF MOBILE PHASE ELUTION MODES (METHANOL–WATER) ON THE SEPARATION OF METHYLATED ANTIMYCIN A SUBCOMPONENTS

Mobile phases were under isocratic conditions, 2 ml/min (A) and gradient conditions (B) methanol–water (60:40) (15 min) → (70:30) for 2 h at 1.5 ml/min; (C) methanol–water (60:40) → (70:30) for 3 h at 2 ml/min; (D, E) methanol–water (60:40) → (70:30) for 3 h at 1.7 ml/min; (F) methanol–water (60:40) → (70:30) for 3 h at 1.5 ml/min. Stationary phases used in (A–D) and (E, F) were Altex Ultrasphere ODS-IP and Ultrasphere ODS, respectively.

Subcomponent		Mobile phase elution mode					
		A	B	C	D	E	F
A_{1a}	k'	20.0	123	122	125	125	144
	(α)	(1.04)	(1.03)	(1.02)	(1.03)	(1.03)	(1.03)
	R	0.83	1.09	1.25	1.47	1.29	1.60
A_{1b}	k'	20.8	127	125	129	129	148
A_{2a}	k'	13.1	97.0	93.2	97.0	95.3	111
	(α)	(1.04)	(1.02)	(1.03)	(1.03)	(1.03)	(1.03)
	R	0.71	0.87	1.05	1.24	1.15	1.44
A_{2b}	k'	13.6	99.0	96.0	99.8	98.0	114
A_{3a}	k'	8.12	71.3	59.8	65.4	62.6	77.4
	(α)	(1.03)	(1.03)	(1.05)	(1.04)	(1.04)	(1.04)
	R	0.40	0.97	1.17	1.31	1.24	1.79
A_{3b}	k'	8.36	73.6	62.6	68.3	65.3	80.5
A_{4a}	k'	5.24	50.0	34.5	43.2	37.7	51.2
	(α)	(1.01)	(1.04)	(1.04)	(1.05)	(1.06)	(1.05)
	R	0.33	0.98	1.06	1.24	1.14	1.50
A_{4b}	k'	5.32	52.1	36.0	45.2	39.8	53.6

dansyl groups gave rise to the corresponding antimycin derivatives whose subcomponents were separable with mobile phases devoid of added electrolytes. Adding either sodium acetate or TBAP to the mobile phases produced no appreciable change in the separation of subcomponent isomers. Typical chromatograms showing reasonable separations of the methylated and dansylated compounds are given in Figs. 4 and 5, respectively. Each of the HPLC profiles obtained under isocratic elution manifests a logarithmic relationship between the k' values and the number of carbons[11–14]. Examination of the isocratic HPLC chromatograms in Figs. 4 and 5 together with those in Fig. 2 indicates that the extent of peak resolution for each a–b pair diminishes with a shortening of the carbon chain length. To resolve the problem of uneven distribution of peak resolution among the four pairs of a–b isomers, gradient elution techniques were employed. Table V summarizes the results obtained with different elution modes of the mobile phases. When the method of elution was switched from isocratic (A, Table V) to gradient systems (B–F, Table V), there was a clear indication of improvement (higher R values) in peak resolution for the subcomponents of lower members of antimycin homologues (A_{3a}–A_{3b} and A_{4a}–A_{4b}). Further, HPLC at a lower flow-rate and a longer period of elution under gradient

conditions resulted in higher R values (D, E, and F, Table V). The gradient HPLC techniques were scaled up for the preparative isolation of subcomponents in sufficient amounts for use as substrates in chemical and spectroscopic studies.

For analytical application, the underivatized antimycin subcomponents can be simultaneously and sensitively determined by reversed-phase HPLC–electrochemical detection[1] using the optimized HPLC conditions developed in this study.

REFERENCES

1 S. L. Abidi, *J. Chromatogr.*, 234 (1982) 187.
2 B. R. Dunshee, C. Leben, G. W. Keitt and F. M. Strong, *J. Am. Chem. Soc.*, 71 (1949) 2436.
3 M. Reporter, *Biochemistry*, 5 (1966) 2416.
4 A. J. Birch, D. W. Cameron, Y. Harada and R. W. Rickard, *J. Chem. Soc.*, (1961) 889.
5 E. E. Van Tamelen, J. P. Dickie, M. L. Loomans, R. S. Dewey and F. M. Strong, *J. Am. Chem. Soc.*, 83 (1961) 1639.
6 K. Ahmad, H. G. Schneider and F. M. Strong, *Arch. Biochem.*, 28 (1950) 281.
7 S. L. Abidi and B. R. Adams, *Magnet. Reson. Chem.*, (1988) in press.
8 S. L. Abidi, *J. Chromatogr.*, 317 (1984) 383.
9 L. R. Snyder, *J. Chromatogr.*, 92 (1974) 223.
10 L. R. Snyder, *J. Chromatogr. Sci.*, 16 (1978) 223.
11 H. Hemetsberger, W. Maasfeld and H. Ricken, *Chromatographia*, 9 (1976) 303.
12 M. C. Hennion, C. Picard and M. Caude, *J. Chromatogr.*, 166 (1978) 21.
13 S. L. Abidi, *J. Chromatogr.*, 255 (1983) 101.
14 S. L. Abidi, *J. Chromatogr.*, 324 (1985) 209.

SEPARATION CHARACTERISTICS OF ALKYLATED GUANINES IN HIGH-PERFORMANCE LIQUID CHROMATOGRAPHY

WEILING XUE* and ROBERT M. CARLSON*

Department of Chemistry, University of Minnesota, Duluth, MN 55812 (U.S.A.)

(First received October 19th, 1987; revised manuscript received March 8th, 1988)

SUMMARY

The retention behavior of thirteen alkylated guanines on normal-phase silica gel and amino columns and on reversed-phase ODS and phenyl columns was studied. The larger the alkyl substituent at the same position of guanine the weaker was the retention in the normal-phase chromatographic system and the greater the retention during reversed-phase chromatography. O^6-Derivatives possess the lowest polarity in each set of isomers. An amino column was found to be of highest efficiency in terms of separation of the set of ethylguanine isomers and of benzylguanines studied. A phenyl column provided the best resolution of methylated guanines.

INTRODUCTION

The alkylation of DNA bases, especially guanine, has been considered to be of great significance in chemical carcinogenesis and mutagenesis[1-3]. A variety of chromatographic techniques have, therefore, been proposed for the reliable and rapid analysis of the modified nucleobases formed *in vitro* and *in vivo*. Ion-exchange chromatography[4-8] and reversed-phase chromatography (including ion-pair chromatography)[8-15] were commonly employed. In a reversed-phase chromatographic method, a phenyl column was shown to give a more satisfactory separation of common nucleobases and of methylated purines and pyrimidines[16,17]. Normal-phase unmodified silica was also found useful for the separation of polar compounds such as nucleobases and nucleosides[18-20]. These methods were limited to unmodified nucleobases and nucleosides and to methylated or ethylated nucleobases. This paper addresses the lack of comprehensive chromatographic data for alkylated guanines by evaluating the separation of a series of alkylated guanines under both normal-phase and reversed-phase chromatographic conditions. Emphasis was placed on the separation of the isomers having identical alkyl substituents at various nucleophilic sites on the guanine (*i.e.*, an isomer set) and, therefore, having direct application for site-specificity studies of DNA alkylation.

---

* Former spelling Weiling Hsueh, permanent address: The Research Center for Eco-Environmental Sciences, Academia Sinica, P.O. Box 934, Beijing, China. Current address: Department of Environmental Health, University of Cincinnati Medical Center, 3223 Eden Ave., Cincinnati, OH 45267-0056, U.S.A.

EXPERIMENTAL

Materials

Guanine (Gua), 6-chloroguanine(6-ClG), 1-methylguanine (1-MG), N^2-methylguanine (N^2-MG), 3-methylguanine (3-MG), and 7-methylguanine (7-MG) were purchased from Sigma. O^6-Methylguanine (O^6-MG)[21], O^6-ethylguanine (O^6-EG)[21], O^6-allylguanine (O^6-AG)[22], O^6-benzylguanine (O6-BG)[23,24], 7-ethylguanine (7-EG)[25], 7-allylguanine (7-AG)[22], 7-benzylguanine (7-BG)[26], N^2-ethylguanine (N^2-EG)[27], and N^2-benzylguanine (N^2-BG)[27] were synthesized in this laboratory following published methods and identified by ultraviolet and mass spectrometry. From commercial sources were obtained analytical grade chemicals and solvents.

Apparatus

The high-performance liquid chromatography (HPLC) measurements were carried out on a Perkin-Elmer Series 2 liquid chromatograph equipped with an LC-75 spectrophotometric detector at ambient temperature (usually 23°C). The wavelength selected for all measurements was 254 nm. Separations were examined using a Silica A column (Perkin-Elmer, 10 μm, 25 cm × 0.26 cm I.D.), a Chromasil NH$_2$ column (American Scientific Products, 10 μm, 25 cm × 0.46 cm I.D.), an ODS column (Alltech, 10 μm, 25 cm × 0.46 cm I.D.) and a μBondapak phenyl column (Waters Assoc., 10 μm, 30 cm × 0.39 cm I.D.). Data were taken with a Hewlett-Packard 3390A integrator. A Graphic Controls PHM 7900 pH meter with a Corning combination electrode was used to measure pH values.

Procedure

Each individual guanine derivative was dissolved in a solvent mixture consisting of 1 volume of 0.1 M hydrochloric acid and 5 volumes of methanol at a concentration of approximately 20–100 μg/ml. Mixtures were generated by combinations of individual standard solutions. These abbreviations were used for sets of alkylated guanine isomers: set 1 for a solution of 1-MG, N^2-MG, 3-MG, O^6-MG (containing a small amount of 6-ClG, a residue from the synthesis of O^6-MG), 7-MG, and Gua; set 2 for N^2-EG, O^6-EG, 7-EG and Gua; set 3 for N^2-BG, O^6-BG, 7-BG and Gua and set 4 for O^6-AG (containing 6-ClG), 7-AG and Gua. All solutions were stored in a freezer. For the measurement of the retention time (t_R), a 0.1–0.5 μg amount of each compound in about 5 μl was applied to the HPLC system. The solvent peak was measured as the time of non-retarded solute (t_0). The mobile phases were prepared daily and degassed by ultrasound prior to use. Buffers were prepared weekly and kept in refrigerated storage. The pH of the buffer was adjusted as follows to the desired value with the addition of an appropriate acid or base: 5% orthophosphoric acid or 5% ammonium hydroxide for ammonium phosphate buffer solutions; 97% formic acid for ammonium formate buffers and 5% sulfuric acid or 5% sodium hydroxide for sodium octanesulfonate solutions.

When changing the eluents, the silica gel and amino columns were washed with methylene chloride–methanol (2:1, v/v) and the ODS column and the phenyl column were eluted with water–methanol (1:1, v/v), then equilibrated for 1 h with the selected mobile phase. After each day's set of experiments, the columns were washed with the solvents indicated above.

RESULTS AND DISCUSSION

    The retention behavior of the alkylated guanines on four normal and reversed-phase columns was investigated. The capacity factors, k', were measured and calculated as a function of the mobile phase composition and pH. Optimum chromato-
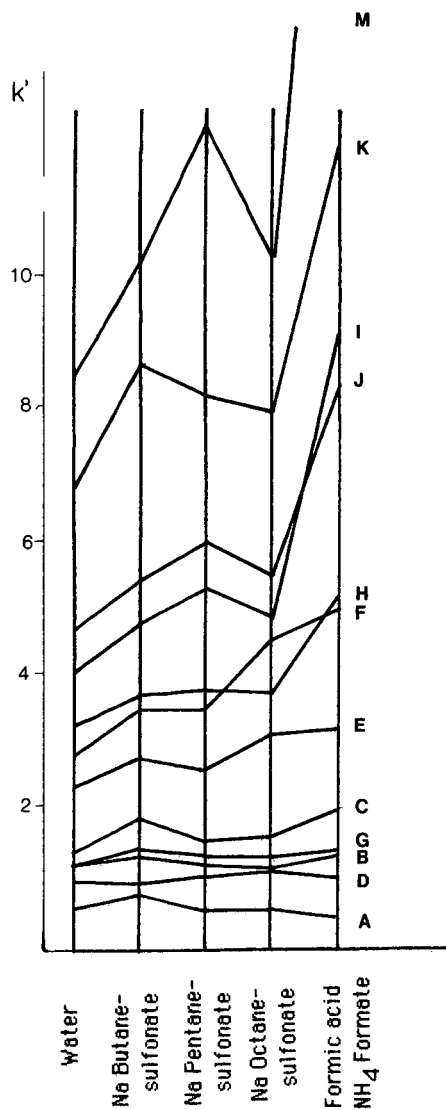
Fig. 1. Effect of the type of buffer solution on the capacity factor (k') of alkylated guanines on a silica gel column. Mobile phase: methylene chloride–methanol–water or buffer solution (90:9:1, v/v/v) containing 0.02 M of salt indicated (pH 3.1). A = O^6-BG; B = 7-BG; C = N^2-BG; D = O^6-EG; E = 7-EG; F = N^2-EG; G = O^6-MG; H = 7-MG; I = N^2-MG; J = 1-MG; K = 3-MG; L = 6-ClG; M = Gua; S = solvent.

graphic conditions were established for the separation of each set of alkylated gua-
nine isomers.

Normal-phase HPLC

Preliminary evaluation revealed that the addition of water (*ca.* 1%) to the
eluent of a suitable proportion of methanol and methylene chloride resulted in an
improvement in peak width but not in the reduction of peak tailing for the separation
of methylated guanines on silica gel and amino columns. Several ion-pairing agents
and buffer systems were tested and the peak symmetry and column efficiency were
improved. However, ion-pairing agents were not found to be advantageous in either
selectivity or efficiency over a formic acid–ammonium formate buffer. A represen-
tative selection of chromatographic data is shown in Fig. 1. For both silica gel and
amino columns, mixtures of methylene chloride, methanol and aqueous ammonium
formate were selected as the mobile phases.

Effect of methanol content. The influence of methanol was studied (Table I)
and k' was found to decrease with increasing methanol content in the mobile phase.
However, the dependence of log k' on the methanol content shows a non-linear
relationship. Brugman *et al.*[18], noticed similar phenomena with nucleobases on a
silica gel column and attributed it to the involvement of other distribution processes
than adsorption. As can be seen from Table I there was a minimal influence of
methanol content on the selectivity with the exception of the N^2-derivatives. The

TABLE I

EFFECT OF METHANOL CONTENT IN THE MOBILE PHASE ON THE CAPACITY FACTORS
OF ALKYLATED GUANINES

Mobile phase: methylene chloride–methanol–0.05 *M* solution of ammonium formate and formic acid, pH
3.2.

	Silica gel column			Amino column		
	93:6:0.66	*90:9:0.66*	*85:14:0.66*	*84:14:2*	*80:18:2*	*73:25:2*
O^6-BG	1.16	0.82	0.50	0.20	0.22	0.19
7-BG	3.15	1.97	1.01	0.54	0.51	0.42
N^2-BG	4.04	2.25	0.94	1.42	1.27	1.15
O^6-AG	1.73	1.08	0.66	0.37	0.36	0.21
7-AG	5.10	2.78	1.25	1.06	0.79	0.54
O^6-EG	1.97	1.25	0.73	0.45	0.39	0.28
7-EG	6.20	3.26	1.73	1.09	0.93	0.61
N^2-EG	8.55	4.08	1.46	2.74	2.29	1.63
O^6-MG	2.63	1.52	0.87	0.66	0.56	0.36
7-MG	9.34	4.51	2.38	1.77	1.32	0.85
N^2-MG	13.1	5.70	2.40	4.28	3.15	2.01
1-MG	13.6	6.70	3.08	3.07	2.00	1.00
3-MG	22.5	10.1	4.53	3.36	2.22	1.23
6-ClG	2.47	1.34	–	0.86	0.69	–
Gua	31.6	12.1	4.75	8:56	6.34	3.08

TABLE II

EFFECT OF WATER CONTENT IN THE MOBILE PHASE ON THE CAPACITY FACTORS OF ALKYLATED GUANINES

Mobile phase: methylene chloride–methanol–0.05 M solution of ammonium formate and formic acid, pH 3.2.

	Silica gel column			Amino column			
	90:9:0.33	90:9:0.66	90:9:1	80:18:0.6	80:18:1	80:18:1.5	80:18:2
O^6-BG	0.91	0.82	0.64	0.23	0.24	0.20	0.22
7-BG	1.98	1.97	1.45	0.74	0.71	0.62	0.49
N^2-BG	2.37	2.25	2.14	2.86	2.43	1.78	1.35
O^6-AG	1.20	1.08	0.92	0.36	0.35	0.33	0.35
7-AG	3.11	2.78	2.38	1.03	0.92	0.87	0.81
O^6-EG	1.36	1.25	1.08	0.39	0.39	0.34	0.40
7-EG	3.39	3.26	3.09	1.12	1.19	1.01	1.01
N^2-EG	4.33	4.08	5.14	4.17	3.16	2.65	2.25
O^6-MG	1.67	1.52	1.34	0.45	0.46	0.49	0.51
7-MG	5.57	4.51	4.24	1.42	1.38	1.30	1.24
N^2-MG	6.49	5.70	6.26	4.39	3.81	3.44	3.10
1-MG	7.73	6.70	6.72	2.05	1.94	1.88	1.85
3-MG	11.8	10.1	10.2	2.30	2.18	2.10	1.91
6-ClG	1.30	1.34	1.38	—	—	—	—
Gua	19.6	12.1	18.9	8.47	7.82	5.96	5.53

retention order of 7-BG/N^2-BG and 7-EG/N^2-EG on the silica gel column was re-versed when the proportion of methanol was increased to 14:85.

Influence of water content. Table II presents the effect of the proportion of aqueous buffer solution in the mobile phase on k'. When the amount of buffer so-lution was increased on the silica gel column, the k' values decreased for all com-pounds. When the aqueous buffer content was increased further, k' values increased again for N^2-EG, N^2-MG and Gua. A similar phenomenon was noticed earlier with nucleobases and nucleosides and was attributed to the transition from a distribution process (adsorption) to a liquid–liquid partition process when changing the water content[18]. For most compounds, k' steadily decreased on an amino column when aqueous buffer content increased. No inflection was seen. Due to the difficulty in measuring small changes in k', this tendency was not observable for a few compounds with low k' values.

Effect of pH. The effect of pH of the buffer in the mobile phase on k' was studied over the pH range 2.6–4.1 on both silica gel and amino columns. As expected for basic compounds such as amino purines and amino pyrimidines[20] in normal-phase chromatography, the k' increased with increasing pH for most of the guanine derivatives investigated. However, this effect was weak and on both columns reten-tion was not very sensitive to pH. An exception was the exocyclic amino alkylated N^2-isomers where the k' was more pH dependent (Fig. 2, minimum observed at pH 3.2) on a silica gel column.
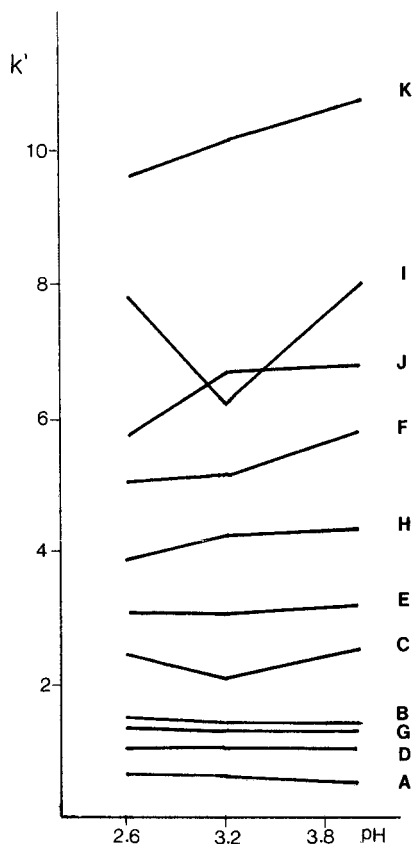
Fig. 2. Effect of pH values of the buffer solution in the mobile phase on the k' of alkylated guanines on a silica gel column. Mobile phase: methylene chloride–methanol–buffer solution (90:9:1, v/v/v) containing 0.05 M of sodium formate and formic acid. Key as in Fig. 1.

Using a normal-phase silica gel or amino column, all four sets of isomers were well separated under appropriate conditions. In terms of column efficiencies and peak shapes, an amino column showed improved performance. The height equivalent to a theoretical plate (HETP) was 0.026 mm at a flow-rate of 1.0 ml/min for an amino column (25 cm × 0.46 cm I.D.) while the HETP of the silica gel column was 0.06 mm at the same flow-rate. A typical chromatogram of a separation for set 3 on an amino column is shown in Fig. 3. As the alkyl chain length increased in alkylated guanine analogues of the same class (i.e. a different alkyl substituent at the same position of guanine) the capacity factor decreased. Within each set of guanine derivatives, O^6-isomers had the lowest retention.

Reversed-phase HPLC

On an ODS column, an ion-pairing technique was employed for better selectivity and column efficiency. An earlier report[17] using a phenyl column confirmed our preliminary experiments which showed that with a mixture of ammonium phos-
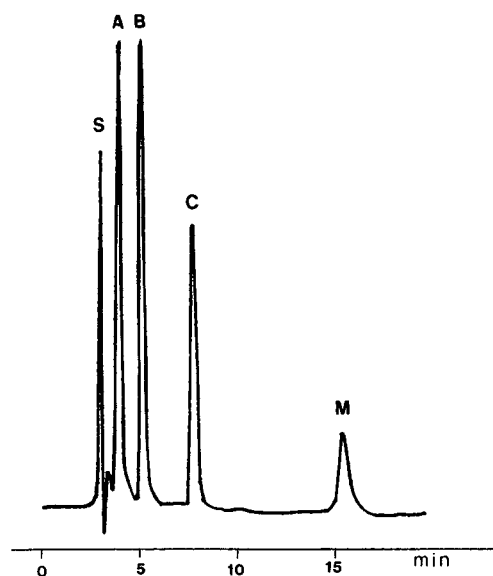
Fig. 3. Chromatogram of set 4 on an NH$_2$ column. Mobile phase: methylene chloride–methanol–0.05 M of ammonium formate + formic acid, pH 2.6 (80:18:1.5, v/v/v), flow-rate: 1 ml/min, after 6.5 min changed to 2 ml/min. Key as in Fig. 1.

TABLE III

EFFECT OF METHANOL CONTENT IN THE MOBILE PHASE ON THE CAPACITY FACTORS OF ALKYLATED GUANINES

	ODS column*				Phenyl column**			
	20:80	30:70	40:60	50:50	4:96	10:90	20:80	35:65
O⁶-BG	—	>15	14.2	4.01	>17	>17	16.7	5.51
7-BG	—	10.5	3.44	1.39	>17	>17	14.4	2.76
N²-BG	—	15.6	4.89	1.87	>17	16.6	7.84	2.67
O⁶-AG	—	10.6	3.72	1.19	7.97	5.10	2.81	1.04
7-AG	—	2.39	0.99	0.36	5.13	3.40	1.51	0.54
O⁶-EG	—	8.15	2.87	1.16	5.06	3.07	1.69	0.76
7-EG	—	4.84	1.65	0.85	1.46	0.86	0.39	0.11
N²-EG	7.94	2.31	0.99	0.44	2.39	1.90	1.01	0.44
O⁶-MG	5.57	3.69	1.39	0.48	2.40	1.60	0.91	—
7-MG	2.88	1.31	0.55	—	1.38	0.99	0.51	—
N²-MG	2.29	0.99	0.43	—	1.37	0.88	0.51	—
1-MG	2.69	1.14	0.53	—	1.03	0.67	0.38	—
3-MG	4.99	2.33	1.02	—	0.75	0.37	0.18	—
6-ClG	—	1.07	0.57	0.26	3.29	2.20	1.34	0.44
Gua	—	—	—	—	0.46	0.30	0.18	—

* Mobile phase: methanol–0.01 M solution of ammonium phosphate + 0.005 M solution of sodium octanesulfonate, pH 4.0.

** Mobile phase: methanol–0.01 M solution of ammonium phosphate, pH 3.3.

phate buffer and methanol as the mobile phase, adequate separation of methylated guanines could be achieved. Further improvements were not obtained with the use of ion-pairing agents.

Influence of methanol content. The effect of methanol content on k' was investigated and the results shown in Table III. As expected, all alkylated guanines studied exhibited a significant decrease in k' with an increase in the proportion of methanol. Except for few compounds (*e.g.* N^2-MG, 7-EG and 7-BG), the selectivity was maintained with varying methanol content on an ODS or a phenyl column. However, due to apparently different separation mechanisms involved, for the compounds in the same set, the retention on ODS or phenyl columns were not in the same order.

Effect of pH. The retention behavior of the alkylated guanines with varying pH of the mobile phase was studied (Tables IV and V). In accordance with the prediction of retention behavior of organic bases in reversed-phase ion-pairing chromatography, the capacity factor values on an ODS column for all guanine derivatives decreased markedly with increasing pH. On a phenyl column without ion-pairing agent, k' values increased with increasing pH of the mobile phase (in the pH range 3.0–4.8). The dependence of selectivity on pH was observed to be significant. As was reported earlier for guanine in reversed-phase LC[28], for several alkylated guanines, k' values were also observed to have inflection points at an intermediate pH value.

Effect of buffer concentration. The effect on k' resulting from changes in phosphate buffer concentrations in the phenyl column system and the effect of sodium octanesulfonate concentration on the ODS column was found to be minimal. A

TABLE IV

EFFECT OF pH VALUES OF THE MOBILE PHASE ON THE CAPACITY FACTORS OF ALKYLATED GUANINES ON AN ODS COLUMN

Mobile phase: methanol–0.01 M solution of ammonium phosphate +0.005 M sodium octanesulfonate. A, 3:7; B, 4:6.

	pH (mobile phase A)			pH (mobile phase B)		
	4.0	5.2	6.2	3.1	4.0	5.3
O^6-BG	>15	>15	>15	19.8	14.2	9.6
7-BG	10.5	7.61	6.42	6.23	3.44	2.92
N^2-BG	15.6	9.91	9.77	9.73	4.89	3.74
O^6-AG	10.6	4.83	4.81	6.20	3.72	2.00
7-AG	2.39	1.44	1.36	1.81	0.99	0.56
O^6-EG	8.15	3.50	2.82	4.75	2.87	1.51
7-EG	4.84	–	–	–	1.65	–
N^2-EG	2.31	1.31	1.24	1.91	0.99	0.48
O^6-MG	3.69	1.54	1.97	2.50	1.39	0.73
7-MG	1.31	0.53	0.51	1.06	0.55	0.26
N^2-MG	0.99	0.51	0.52	0.71	0.43	0.18
1-MG	1.14	0.54	0.38	1.03	0.53	0.15
3-MG	2.33	0.64	0.38	1.50	1.02	0.17
6-ClG	1.07	1.04	1.08	0.63	0.57	0.49
Gua	–	–	–	0.36	0.18	0

TABLE V

EFFECT OF pH VALUES OF THE MOBILE PHASE ON THE CAPACITY FACTORS OF AL-KYLATED GUANINES ON A PHENYL COLUMN

Mobile phase: methanol–0.01 M solution of ammonium phosphate. A, 10:90; B, 35:65.

	pH (mobile phase A)			pH (mobile phase B)		
	3.3	4.1	4.8	3.0	3.3	3.8
O^6-BG	–	–	–	3.81	5.51	5.57
7-BG	–	–	–	2.42	2.76	2.95
N^2-BG	–	–	–	2.40	2.67	2.95
O^6-AG	5.10	7.81	9.21	0.85	1.04	1.28
7-AG	3.40	4.21	3.99	0.46	0.54	0.60
O^6-EG	3.07	6.24	6.21	0.61	0.76	0.99
7-EG	0.86	1.25	1.10	0.06	0.11	0.12
N^2-EG	1.90	2.83	2.50	0.32	0.44	0.49
O^6-MG	1.60	2.88	2.88	–	–	–
7-MG	0.99	1.55	1.43	–	–	–
N^2-MG	0.88	1.27	1.12	–	–	–
1-MG	0.67	1.02	0.91	–	–	–
3-MG	0.37	0.71	0.76	–	–	–
6-ClG	2.20	2.35	2.16	0.45	0.44	0.42
Gua	0.30	0.43	0.37	–	–	–
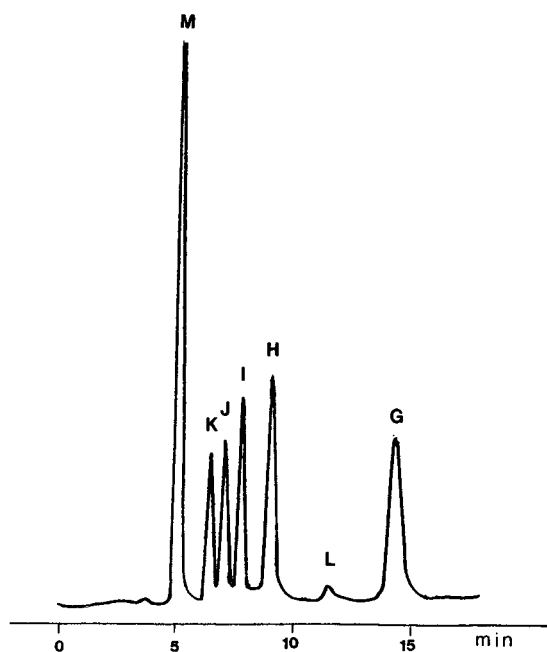
Fig. 4. Chromatogram of set 1 on a phenyl column. Mobile phase: methanol–0.01 M solution of ammonium phosphate (10:90, v/v), pH 4.8, flow-rate: 1 ml/min. Key as in Fig. 1.

similar result was reported in the HPLC study of 5-alkyluracils, where these compounds apparently did not form ion pairs in the pH range studied[12]. The peak widths of O^6-BG, N^2-BG, O^6-AG, O^6-EG and N^2-EG were narrowed slightly when the concentration of buffer or ion-pairing agent increased to 0.003 M.

Using an ODS column with ion-pairing techniques, set 2 and set 3 were adequately separated. However, in set 1, N^2-MG, 7-MG and (or) 1-MG were poorly resolved. The best separation for set 1 was achieved using a phenyl column. For example, the resolution (R) between 1-MG and N^2-MG is 2.22 and between N^2-MG and 7-MG is 2.95 (Fig. 4). 6-ClG, which was always overlapped with O^6-MG, was observed under these chromatographic conditions. In contrast with normal-phase chromatography described above, analogues with a longer alkyl substituent at the same position had stronger retention in a reversed-phase system. O^6-Derivatives always possessed the highest k' value in each set of alkylated guanine isomers.

ACKNOWLEDGEMENTS

REFERENCES

1 B. Singer and D. Grunberger, *Molecular Biology of Mutagens and Carcinogens*, Plenum Press, New York, 1983, p. 69, p. 169.
2 A. E. Pegg, *Cancer Investigat.*, 2 (1984) 223.
3 B. Singer, *Cancer Res.*, 46 (1986) 487.
4 B. Shaikh, S.-K. S. Huang, N. J. Pontzer and W. L. Zielinski Jr., *J. Liq. Chromatogr.*, 1 (1978) 75.
5 H. Yuki, H. Kawasaki, A. Imayuki and T. Yajima, *J. Chromatogr.*, 168 (1979) 489.
6 D. C. Herron and R. Shank, *Anal. Biochem.*, 100 (1979) 58.
7 E. M. Faustman and J. I. Goodman, *J. Pharm. Methods*, 4 (1980) 305.
8 T. Tanabe, K. Yamauchi and M. Kinoshita, *Bull. Chem. Soc. Jpn.*, 54 (1981) 1415.
9 C. E. Salas and O. Z. Sellinger, *J. Chromatogr.*, 133 (1977) 231.
10 P. R. Brown, R. A. Hartwick and A. M. Krstulovic, *Adv. Chromatogr.*, 18 (1980) 101.
11 M. Zakaria and P. R. Brown, *J. Chromatogr.*, 226 (1981) 267.
12 Á. H. Csárnyi, M. Vajda and J. Sági, *J. Chromatogr.*, 204 (1981) 213.
13 D. T. Bernek, C. C. Weis and D. H. Swenson, *Carcinogenesis (N.Y.)*, 1 (1981) 595.
14 L. Citti, P. G. Gervasi, G. Turchi, L. Mariani and M. Durante, *J. Chromatogr.*, 261 (1983) 315.
15 J. Da Silva Gomes and C.-J. Chang, *Anal. Biochem.*, 129 (1983) 387.
16 H. W. Thielman, *Cancer Lett. (Shannon, Irel.)*, 6 (1979) 311; *C.A.*, 91 (1979) 84395x.
17 R. Valencia, H. N. Cong and O. Bertaux, *J. Chromatogr.*, 325 (1985) 207.
18 W. J. Th. Brugman, S. Heemstra and J. C. Kraak, *Chromatographia*, 15 (1982) 282.
19 J. E. Evans, H. Thieckelmann, E. W. Naylor and R. Guthrie, *J. Chromatogr.*, 163 (1979) 29.
20 M. Ryba and J. Beránek, *J. Chromatogr.*, 211 (1981) 337.
21 R. W. Balsiger and J. A. Montgomery, *J. Org. Chem.*, 25 (1960) 1573.
22 N. J. Leonard and C. R. Frihart, *J. Am. Chem. Soc.*, 96 (1974) 5894.
23 A. J. Kiburis and J. H. Lister, *J. Chem. Soc., Perkin Trans. 1*, (1971) 3942.
24 M. MacCoss, A. Chen and R. C. Telman, *Tetrahedron Lett.*, 26 (1985) 1815.
25 J. W. Jones and R. K. Robins, *J. Am. Chem. Soc.*, 85 (1963) 193.
26 P. Brookes, A. Dipple and P. D. Lawley, *J. Chem. Soc., Perkin Trans.*, 1 (1968) 2026.
27 R. Shapiro, B. I. Cohen, S-J. Shiuey and H. Maurer, *Biochemistry*, 8 (1969) 238.
28 M. Zakaria, P. R. Brown and E. Grushka, *Anal. Chem.*, 55 (1983) 457.

CHROM. 20 534

LIQUID CHROMATOGRAPHIC STUDY OF THE HYDROLYSIS REACTIONS OF CYCLIC AND LINEAR POLYPHOSPHATES IN AQUEOUS SOLUTION

GENICHIRO KURA

Department of Chemistry, Fukuoka University of Education, Akama, Munakata, Fukuoka 811-41 (Japan)
(Received April 5th, 1988)

SUMMARY

Hydrolysis reactions of inorganic cyclic and linear tri-, tetra-, hexa- and octaphosphates were studied by liquid chromatography. The rate constants in 0.1 M hydrochloric acid and 0.5 M lithium hydroxide solutions at various temperatures were determined. The reaction mechanism is discussed on the basis of the rate constants and the activation energies.

INTRODUCTION

Condensed polyphosphates produced by the condensation of an orthophosphate are important and interesting materials as inorganic multivalent electrolytes and their chemistry has been studied from various viewpoints[1]. In particular, the chemical properties of di- and triphosphates have been extensively investigated in connection with ADP and ATP, which are biochemically important.

However, the investigation of higher linear and cyclic polyphosphates has been hindered by the difficulty involved in their preparation and isolation. We have been studying the various properties and structures of higher cyclic polyphosphates for many years[2–16]. Cyclic polyphosphates with degrees of polymerization of 3, 4, 6 and 8 have been prepared relatively easily and are very interesting materials[17,18].

In this study, the hydrolysis reactions of above four cyclic polyphosphates and the corresponding linear polyphosphates were investigated. The hydrolysis products containing linear hexa- or octaphosphate were prepared by the mild hydrolysis of cyclohexa- or cyclooctaphosphate, respectively.

To determine the hydrolysis rate accurately, it is necessary to separate and determine quantitatively each component of the hydrolysis samples and we have used anion-exchange liquid chromatography for this purpose. To analyse the hydrolysis products of cyclic polyphosphates, an isocratic elution method was successfully employed to separate the parent cyclic polymer from the other hydrolysis products.

For the determination of the hydrolysis rates of linear polymers, the linear polymer, the cyclic polymer (source material) and lower linear polymer hydrolysis products must be separated. For this purpose, a gradient elution method[19] was satisfactorily employed.

We have previously reported that the hydrolysis rates of cyclic polyphosphates are significantly affected by the presence of cations[16]. In alkaline solutions, Li^+ ion accelerates most strongly the hydrolysis rates of the cyclic polymers. This can be related to the formation of an inner-sphere complex (or ion pair) between Li^+ and the cyclic polyphosphate anion. Of both series of polyphosphates used in this study, cyclotriphosphate, $P_3O_9^{3-}$ was the least stable in both acidic and alkaline solutions. We presume that this instability results from strain in the six-membered ring in aqueous solution.

In acidic solution (0.1 M hydrochloric acid), the hydrolysis rates of the linear polyphosphates were higher than those of the corresponding cyclic polyphosphates. For both series, highly polymerized species were degraded faster. In alkaline solution, the linear polymers were more stable than the cyclic polymers. For the linear series the hydrolysis rates for the higher polymers are higher, but for the cyclic polymers even the large ring polymers were stable.

In this paper, linear and cyclic polyphosphates are abbreviated to P_n and P_{nm}, respectively, where n is the degree of polymerization.

EXPERIMENTAL

Materials

Sodium salts of cyclic polyphosphates were prepared by the usual methods[17,18] Sodium triphosphate was obtained commercially and ammonium tetraphosphate was prepared by the method of Griffith[20]. All other chemicals used were of reagent grade.

Hydrolysis procedure

The initial concentration of each phosphate to be hydrolysed was adjusted to about $1.25 \cdot 10^{-3}$ M and the hydrolysis was performed in a water-bath, the temperature of which was maintained to within $\pm 0.1°C$. The hydrolysis reactions were stopped by rapid neutralization and cooling, and the hydrolysis products were analysed.

Chromatographic system

The anion exchanger TSK Gel SAX 10 μm was packed into a 250 mm $\times$ 4 mm I.D. column. A Hitachi 655-11 elution pump was used, and a Hitachi 655A-13 reaction pump was connected to mix the Mo^V–Mo^{VI} reagent with the column effluents for the spectrophotometric determination of the phosphates. A Hitachi 228A spectrophotometer with a micro flow cell was used as a detector. The flow system was similar to that shown previously[12].

Elution procedure

For the determination of the hydrolysis rates of the cyclic polyphosphates, isocratic elution with 0.4 M potassium chloride (+ 0.1% EDTA) buffered at pH 10.2 was applied and the separation of the parent cyclic polymer and the hydrolysis products was complete. On the other hand, for the analysis of the linear polymer hydrolysis reaction, elution with a gradient of potassium chloride concentration (pH 10.2) as shown in Fig. 1 was used and the cyclic polymer and all linear polymers were well separated from each other.
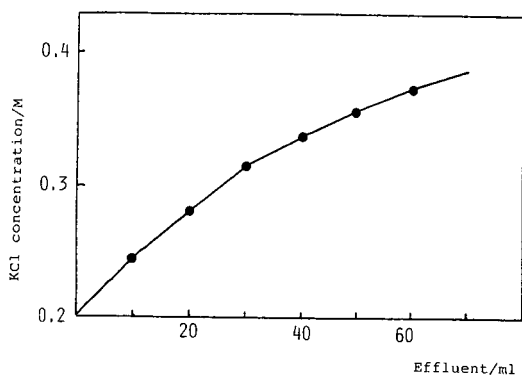
Fig. 1. Gradient elution conditions for the separation of cyclic and linear polyphosphates.

RESULTS AND DISCUSSION

The cation present significantly affect the hydrolysis rates of the cyclic polyphosphates. Complex or ion-pair formation of cyclic polyphosphate anions and the cations renders the phosphorus atom more susceptible to nucleophilic attack by OH^- or H_2O. In this study, the effect of Li^+ on the hydrolysis rates of cyclic polyphosphates in alkaline solutions was further investigated. The hydrolysis rates at various Li^+ concentrations were determined, the OH^- concentration being maintained constant. As an example, chromatograms of the hydrolysis products of cyclooctaphosphate in 0.5 M lithium hydroxide at 50°C are shown in Fig. 2. The separation of the cyclic polymer and its hydrolysis products by isocratic elution with 0.4 M potassium chloride (pH 10.2) was satisfactory. Under these conditions, the linear polymer hydrolysis products from the cyclic polymer were eluted together at an early stage of elution.

The first-order rate constants for the overall disappearance of a cyclic polymer, k_m, obtained from the analysis of the chromatograms as shown in Fig. 2 are given in Table I. The hydrolysis rates increase appreciably with increase in the Li^+ concentration. The k_m value for cyclohexaphosphate hydrolysis is plotted against Li^+ concentration in Fig. 3 and a parabola was obtained. With Na^+, the graph showed a linear relationship and the slope of the line was much lower. In alkaline solutions where M^+ was used as a counter ion of OH^-, the first-order rate equation for the overall disappearance of a phosphate can be expressed as follows:

$$-\frac{dc}{dt} = k_0[OH^-][P_nO_{3n}^-] + k_1[OH^-][MP_nO_{3n}^{(n-1)-}] +$$

$$+ k_2[OH^-][M_2P_nO_{3n}^{(n-2)-}] \quad (1)$$

where the formation of a 1:1 and 2:1 ($M^+:P_nO_{3n}^-$) complex (or ion pair) was assumed and k_0, k_1 and k_2 are the rate constants for the three species. If the stability constants for the 1:1 and 2:1 complexes are denoted β_1 and β_2, respectively, eqn. 1 can be written as
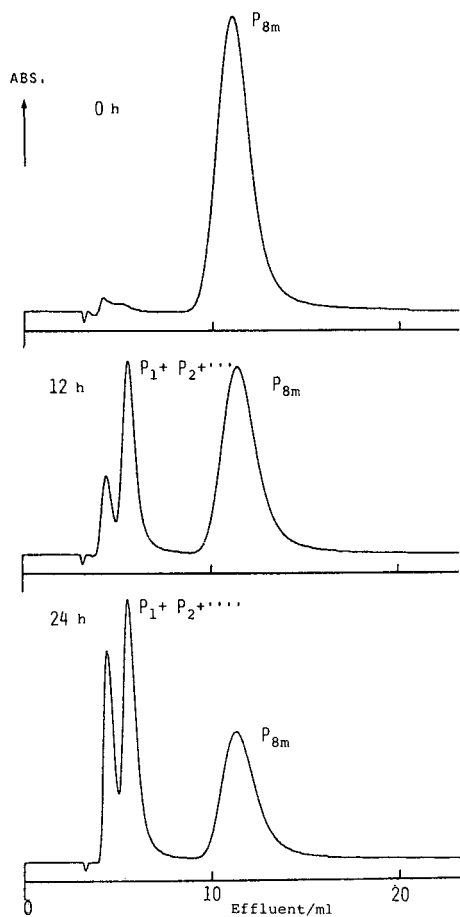
Fig. 2. Chromatograms of the hydrolysis products of cyclooctaphosphate in 0.5 M lithium hydroxide at 40°C.

TABLE I

RATE CONSTANTS FOR HYDROLYSIS OF CYCLIC POLYPHOSPHATES AT VARIOUS Li^+ CONCENTRATIONS

$[OH^-] = 0.5\ M$; 50°C.

$[Li^+]\ (M)$	$k_m\ (h^{-1})$			
	P_{3m}	P_{4m}	P_{6m}	P_{8m}
0.50	3.69	0.372	0.0913	0.106
0.75	5.73	0.683	0.148	0.177
1.00	7.21	1.00	0.228	0.258
1.25	10.8	1.36	0.315	0.354
1.50	14.3	1.79	0.423	0.457
1.75		2.14	0.529	0.601
2.00		2.61	0.697	0.752
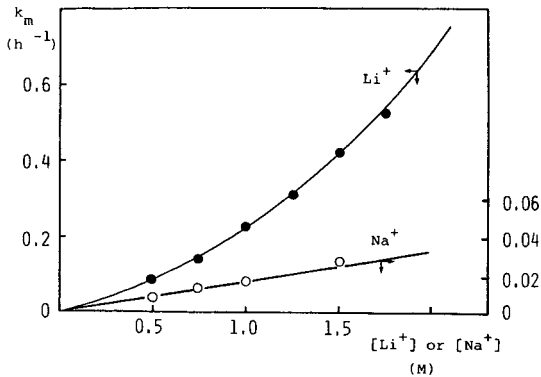
Fig. 3. The effect of lithium and sodium ions on the rate constant of cyclohexaphosphate in alkaline solution ([OH$^-$] = 0.5 M) at 50°C.

$$-\frac{dc}{dt} = k_0[OH^-]\,[P_nO_{3n}^{n-}] + k_1[OH^-]\,\beta_1[M^+]\,[P_nO_{3n}^{n-}] +$$
$$+ k_2[OH^-]\,\beta_2[M^+]^2\,[P_nO_{3n}^{n-}] \qquad (2)$$

The molar fraction of the free ion, $P_nO_{3n}^{n-}$, X_0, is

$$X_0 = \frac{1}{1 + \beta_1[M^+] + \beta_2[M^+]^2}$$

and $[P_nO_{3n}^{n-}] = X_0 c$. Hence eqn. 2 is rewritten as

$$-\frac{dc}{dt} = (k_0 + k_1\beta_1[M^+] + k_2\beta_2[M^+]^2)\,[OH^-]\,X_0 c \qquad (3)$$

$$k_m = (k_0 + k_1\beta_1[M^+] + k_2\beta_2[M^+]^2)\,[OH^-]\,X_0 \qquad (4)$$

The apparent rate constant as a function of $[M^+]$ shows a quadratic relationship. For larger cyclic polymers such as P_{6m} and P_{8m}, the value of k_0 is very low and the graph of k_m *versus* $[M^+]$ is a parabola passing through the origin. The above analysis explains qualitatively the results shown in Fig. 3. The reason why Li$^+$ accelerates the hydrolysis rate more strongly than Na$^+$ is speculated as follows. As the crystal radius of Li$^+$ is very small compared with that of Na$^+$, an inner-sphere complex (or a contact ion pair) forms more easily and promotes the nucleophilic attack of OH$^-$ on P atoms. We believe that the formation of an inner-sphere complex or contact ion pair is necessary for the acceleration of the hydrolysis rates.

As shown in the chromatograms of the hydrolysis products of P_{8m} during the half-life period, the concentration of the linear octaphosphate, which is the first hydrolysis product of cyclooctaphosphate, is relatively high. The hydrolysis reaction of cyclooctaphosphate might be utilized for the preparation of octaphosphate. We

have determined the hydrolysis rates of hexa- and octaphosphate using the product obtained by the mild hydrolysis of cyclohexa- and cyclooctaphosphate, respectively. To determine the hydrolysis rates of the above linear polymers, gradient elution must be applied, the separation using a potassium chloride concentration gradient as in Fig. 1 was satisfactory.

The hydrolysis reaction of a linear phosphate may proceed by any one of at least three routes[21], the end group breaking off the chain to form orthophosphate and a phosphate that is one phosphorus atom shorter; breaking of the chain somewhere in the middle of the chain to yield two chains; or a cyclotriphosphate abstraction. In this work, the first-order rate constants for the overall disappearance of a phosphate species, k_m or k_n, were determined. For example, linear hexaphosphate degrades to linear polymers with degrees of polymerization less than 5 and cyclotriphosphate; however, new hexaphosphate is generated from cyclohexaphosphate.

The hydrolysis scheme is written as

$$P_{nm} \xrightarrow{k_m} P_n \xrightarrow{k_n} P_{n-1}, P_{n-2}, \ldots, P_{3m}$$
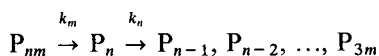
where k_m and k_n are the first-order rate constants for the cyclic and linear polymers, respectively. If the concentrations of cyclic and linear polyphosphates at time t are defined as x and y, respectively, the following equations can be derived:

$$-\frac{dx}{dt} = k_m x \tag{5}$$

$$-\frac{dy}{dt} = -k_m x + k_n y \tag{6}$$

These differential equations are solved by assuming that the values of x and y at time zero are a and b, respectively:

$$x = a \exp(-k_m t) \tag{7}$$

$$y = \frac{k_m a}{k_n - k_m} \exp(-k_m t) + \left(b - \frac{k_m a}{k_n - k_m}\right) \exp(-k_n t) \tag{8}$$

The values of k_m are determined by separate experiments and k_n can be calculated from the data obtained from the chromatograms shown in Fig. 4. A least-squares approximation was applied to calculate k_n and the time dependence of the octaphosphate concentration is shown in Fig. 5. The coincidence of the experimental values and those calculated from k_m and k_n by the least-squares method is satisfactory, as shown in Fig. 5.

Similarly, the rate constants in 0.1 M hydrochloric acid were determined. The chromatograms of the hydrolysis product in 0.1 M hydrochloric acid are shown in Fig. 6. All results obtained are summarized in Table II. The following conclusions might be drawn. Cyclotriphosphate with a six-membered ring structure is most rapidly
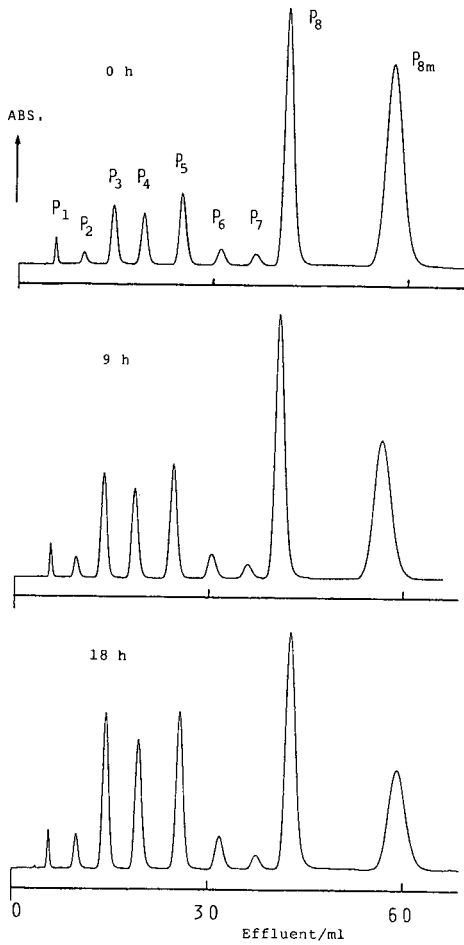
Fig. 4. Chromatograms of the hydrolysis products of octaphosphate in 0.5 M lithium hydroxide at 40°C.
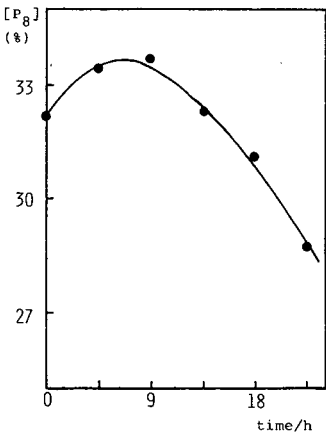
Fig. 5. Octaphosphate hydrolysis in 0.5 M lithium hydroxide at 40°C. Points, experimental values; solid line, calculated.
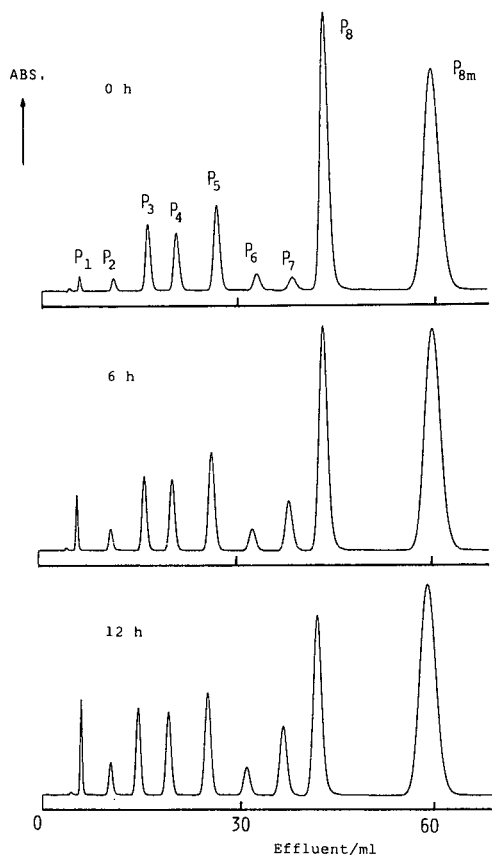
Fig. 6. Chromatograms of the hydrolysis products of octaphosphate in 0.1 M hydrochloric acid at 20°C.

hydrolysed in both acidic and alkaline conditions. In aqueous solutions, a six-membered ring structure is thought to be unfavourable owing to the high strain[1].

In acidic solution, linear polymers degrade rapidly compared with the cyclic polymer with same degree of polymerization. For both the cyclic and linear series, the polymers with a higher degree of polymerization degrade more rapidly under these conditions. For cyclic polyphosphates, the reason why the hydrolysis rates of larger ring compounds are higher was discussed in a previous paper[12]. Faster hydrolysis rate for longer linear polymers might be explained by the abstraction of metaphosphate resulting from the formation of a coiled structure, which is possible by neutralization of the charges on PO[-] by H^{+} in the acidic solution. Cleavage of the end group also occurs.

In alkaline solution, linear polyphosphates are more stable. Tri- and tetra-phosphate are especially stable and for their preparation alkaline hydrolysis of cyclotri- and cyclotetraphosphate has been used[22-25]. For linear polymers, the stabilities decrease as the chain length increases. For of cyclic polymers, highly

TABLE II

THE RATE CONSTANTS OF CYCLIC AND LINEAR POLYPHOSPHATES IN 0.5 M LiOH AND 0.1 M HCl

Medium	k_m or k_n (h^{-1})							
0.5 M LiOH (50°C)	P_{3m}	4.62,	P_{4m}	0.373,	P_{6m}	0.0912,	P_{8m}	0.104
	P_3	$6.93 \cdot 10^{-4}$,	P_4	$6.19 \cdot 10^{-3}$,	P_6	0.0592,	P_8	0.135
0.1 M HCl (40°C)	P_{3m}	0.371,	P_{4m}	0.0430,	P_{6m}	0.0608,	P_{8m}	0.150
	P_3	0.132,	P_4	0.164,	P_6	0.348,	P_8	0.624

polymerized cyclohexa- and cyclooctaphosphate are degraded less rapidly. This tendency is marked in tetramethylammonium hydroxide solution[16].

Arrhenius plots for the hydrolysis of linear phosphates in 0.5 M lithium hydroxide are shown in Fig. 7. Good straight lines were obtained. The activation energies for the hydrolysis of both cyclic and linear polymers in 0.1 M hydrochloric acid and 0.5 M lithium hydroxide are shown in Table III. In 0.1 M hydrochloric acid, about E_a values of 20 kcal/mol for both the cyclic and linear series were obtained and they did not depend on the degree of polymerization. A similar reaction mechanism for P–O–P bond cleavage in condensed phosphates under acidic conditions can be proposed.

In 0.5 M lithium hydroxide solution, the activation energies of cyclic polyphosphates increase with increase in the ring size. In particular, that for cyclotriphosphate is lower than those for the other cyclic polyphosphates. This is due to the ease of nucleophilic attack on the P atom at PO_4 tetrahedra by nucleophilic reagents such as NH_3, OH^- and H_2O. A planar six-membered ring structure in aqueous
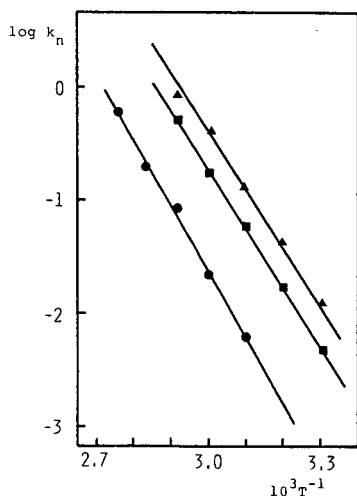
Fig. 7. Arrhenius plots for the hydrolysis reactions of tetra-, hexa- and octaphosphate in 0.5 M lithium hydroxide. ▲, P_8; ■, P_6; ●, P_4.

TABLE III

ACTIVATION ENERGIES OF CYCLIC AND LINEAR POLYPHOSPHATES IN 0.5 M LiOH AND 0.1 M HCl

Medium	E_a (kcal mol^{-1})							
0.5 M LiOH	P_{3m}	15.3,	P_{4m}	18.6,	P_{6m}	21.6,	P_{8m}	22.2
	P_3	–,	P_4	26.3,	P_6	24.2,	P_8	23.5
0.1 M HCl	P_{3m}	21.3,	P_{4m}	24.0,	P_{6m}	21.9,	P_{8m}	23.2
	P_5	20.4,	P_4	20.3,	P_6	20.9,	P_8	21.3

solution has been proposed[26]. This ring structure is unfavourable owing to the high strain. In a transition state where the P atom in the ring combines with the nucleophilic reagent, the P atom forms a trigonal bipyramidal structure using sp^{3}d hybrid orbitals. The stability of the intermediate and the reactivity of the phosphate with nucleophilic reagents can be explained by the above assumption.

On the other hand, for linear polymers the activation energies are generally higher than those for cyclic polymers. The values decrease with increasing chain length and seem to approach the same value for larger ring phosphates as the chain length increases. Such higher activation energies may be due to the P atom in the chain polymers being unfavourably attacked by nucleophilic reagents such as OH$^-$.

We can treat such complex systems easily and rapidly as many compounds are produced by the degradation of the parent compounds. This is the result of the development of high-performance liquid chromatography as an analytical tool for the condensed phosphates.

REFERENCES

1 J. R. Van Wazer, *Phosphorus and Its Compounds*, Interscience, New York, 1958.
2 S. Ohashi, G. Kura and M. Kamo, *Mem. Fac. Sci. Kyushu Univ. Ser. C*, 7 (1970) 43.
3 G. Kura and S. Ohashi, *J. Chromatogr.*, 56 (1971) 111.
4 G. Kura and S. Ohashi, *J. Inorg. Nucl. Chem.*, 34 (1972) 3899.
5 G. Kura, S. Kura and S. Ohashi, *J. Inorg. Nucl. Chem.*, 36 (1974) 1605.
6 G. Kura and S. Ohashi, *J. Inorg. Nucl. Chem.*, 38 (1976) 1151.
7 S. Ohashi, G. Kura, Y. Shimada and M. Hara, *J. Inorg. Nucl. Chem.*, 39 (1977) 1513.
8 M. Koganemaru, H. Waki, S. Ohashi and G. Kura, *J. Inorg. Nucl. Chem.*, 41 (1979) 1457.
9 G. Kura, *J. Chromatogr.*, 211 (1981) 87.
10 G. Kura, T. Nakashima and F. Oshima, *J. Chromatogr.*, 219 (1981) 385.
11 G. Kura, *J. Chromatogr.*, 246 (1982) 73.
12 G. Kura, *Bull. Chem. Soc. Jpn.*, 56 (1983) 3769.
13 G. Kura, *Polyhedron*, 5 (1986) 2097.
14 G. Kura, *Polyhedron*, 6 (1987) 531.
15 G. Kura, *Bull. Chem. Soc. Jpn.*, 60 (1987) 2857.
16 G. Kura, *Polyhedron*, 6 (1987) 1863.
17 E. J. Griffith and R. L. Buxton, *Inorg. Chem.*, 4 (1965) 549.
18 U. Schülke, *Z. Anorg. Allg. Chem.*, 360 (1968) 231.
19 Y. Baba, N. Yoza and S. Ohashi, *J. Chromatogr.*, 350 (1985) 461.
20 E. J. Griffith, *J. Inorg. Nucl. Chem.*, 26 (1964) 1381.

21 R. K. Osterheld, in E. J. Griffith and M. Grayson (Editors), *Topics in Phosphorus Chemistry*, Wiley, New York, 1972, p. 146.
22 E. Thilo and R. Rätz, *Z. Anorg. Allg. Chem.*, 260 (1949) 255.
23 A. E. R. Westman and A. E. Scott, *Nature (London)*, 168 (1951) 740.
24 O. T. Quimby, *J. Phys. Chem.*, 58 (1954) 603.
25 J. I. Watters, P. E. Sturrock and R. E. Simonaitis, *Inorg. Chem.*, 2 (1963) 765.
26 W. P. Griffith and K. J. Rutt, *J. Chem. Soc.*, 1968 (1968) 2331.

GEOMETRIC STRUCTURAL PROPERTIES OF BONDED LAYERS OF CHEMICALLY MODIFIED SILICAS

A. Yu. FADEEV and S. M. STAROVEROV*

Laboratory of Petrochemical Synthesis, Department of Chemistry, Lomonosov State University, Leninskye Gory, 119899 Moscow (U.S.S.R.)

(First received December 23rd, 1987; revised manuscript received April 5th, 1988)

SUMMARY

The effects of the support structure and the modifier structure on the characteristics of chemically modified stationary phases (bonding density, thickness of the bonded layer) were studied and the principle of geometric structural conformity was formulated. It has been demonstrated that reversed phases can be divided into "rigid", "flexible" and intermediate structures of a bonded layer. Only structurally uniform stationary phases have been found to possess similar properties.

INTRODUCTION

Silicas chemically modified with organic compounds are the main type of stationary phases used in liquid chromatography. Reversed phases containing groups with long hydrocarbon chains bonded to silica are important as stationary phases and more than half of all analyses by high-performance liquid chromatography (HPLC) use reversed phases. A comparison of reversed phases with similar compositions shows that their characteristics may be very different, and this is not easily explained[1,2].

The complexity of these materials can be illustrated with the simplest models of the arrangement of bonded hydrocarbon chains[3]. The number of bonded modifier groups per unit surface area (bonding density) depends on the pore structure of the support. For instance, when the diameter of a pore does not exceed 11 nm, the bonding density of C_{18} stationary phases decreases as the diameter becomes smaller[4]. A decrease in bonding density leads to alterations in the bonded layer thickness and to an increase in the amount of residual unreacted silanol groups of silica. In most instances uncontrolled bonding density and bonded layer thickness are the main reason for the variations in the adsorptive and chromatographic properties of silicas that have similar chemical compositions, *e.g.*, C_{18} stationary phases.

This paper presents an analysis of the effects of the pore structure of support on the characteristics of chemically modified stationary phases (bonding density, thickness of bonded layer). The principle of geometric structural conformity is formulated. It has been demonstrated that reversed phases can be divided into "rigid",

"flexible" and intermediate structures of the bonded layer. Only structurally uniform stationary phases have been found to possess similar properties.

MODEL OF MODIFIED SURFACE

The adsorptive and chromatographic characteristics of silicas modified with organic compounds depend to a great extent on the bonding density of the modifier and the bonded layer thickness. The bonding density, p, is the number of modifier molecules per unit surface area, usually per 1 nm^2, and it reaches its maximum value, p_{max}, on flat or permanent surfaces and depends on the dimensions of the modifier. The maximum value of the bonding density is determined by the minimum permitted distance between points of fixation of the modifier molecules, L_{min}. A decrease in bonding density causes an increase in the number of unreacted silanol groups, which can change the adsorptive and chromatographic characteristics of modified silicas.

In most instances organosilicon compounds are employed as surface modifiers and therfore the sizes of "anchor groups" responsible for fixing modifier molecules on the silica surface [e.g., $-Si(CH_3)_2Cl$ or $-SiCl_3$] determine the minimum distance between two points of fixation on a flat surface, which depends to a minor extent on the residue of the modifier molecule[3,4]. In practice, the value of p can be calculated from carbon analysis data and the specific surface area of silica[5]. On the other hand, the surface concentration of bonded molecules can be expressed by another parameter, L, the mean distance between two points of fixation of bonded molecules. The relationship between these two parameters is[3]

$$p = 1.15/L^2 \tag{1}$$

or

$$L = 1.075/p^{0.5}$$

If $p = p_{max}$, $L = L_{min}$. For alkylsilanes[3,5] $p_{max} = 2.3$ groups per nm^2 and $L_{min} = 0.75$ nm.

The bonded layer thickness, h, is the mean distance between the fixation point of the bonded molecule and its top. The bonded layer thickness is directly connected with the conformation of bonded chains. Straight bonded molecules may extend perpendicular to the support surface to form the so-called "brush" structure of the bonded layer (Fig. 1). Conformational changes of bonded hydrocarbon chains may lead to the formation of the so-called "liquid-like" structure of the bonded layer (Fig. 1). When proceeding from one extreme case to the other the bonded layer thickness

Fig. 1. "Brush" and "liquid-like" structures of bonded layer of silica modified with n-alkylsilanes.

almost doubles. The differences in bonded layer thickness may lead to distinctions in the retention mechanism of a sample on chemically modified stationary phases. Hence the bonded layer thickness is an important parameter of bonded phases.

On passing from a flat to a concave surface the bonding density does not depend on the anchor group size but is determined by steric hindrance that occurs when the upper parts of the bonded molecules come into contact (Fig. 2). The experimental data show[4] that the bonding density is lower in small pores, which means that the mean distance between fixation points of bonded molecules is longer than that obtained with a surface that is close to flat. These changes affect the conformational transitions of bonded molecules and therefore the thickness of the bonded layer also alters.

To calculate p and h for chemically modified porous silica stationary phases we choose the following model: the support contains cylindrical pores (this is the most generally accepted view of the porous silica structure); the mean distance between fixation points of bonded molecules in pores of equal diameter is constant; and bonded hydrocarbon chains have a conformation that provides the maximum bonding density, as follows from the irreversibility of the reaction of organosilicon compounds with a silica surface carried out with an excess of a modifier during the time required to complete the reaction.

Within the framework of the suggested model, it is easy to evaluate the pore diameter D^* at which steric hindrance of attached chains will appear. Indeed, for a bonded molecule of length l a similarity correlation will give

$$\frac{L_{min}}{d} = \frac{D^*}{D^* - 2l}$$

Hence

$$D^* = \frac{2l}{L_{min} - d} \tag{2}$$

where L_{min} is the minimum distance between two anchor groups on a flat surface, d is twice the Van der Waals radius of a methyl group and l is the length of the molecule
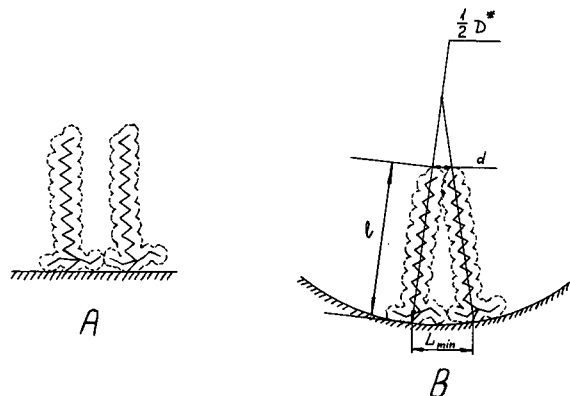
Fig. 2. Steric hindrance arising on passing from (A) a flat to (B) a concave surface of a cylindrical pore of diameter D^*.

TABLE I
VALUE OF D^* FOR DIFFERENT BONDED MODIFIER MOLECULES

Modifier	D^* (nm)
$-C_8H_{17}$	4.9
$-C_{16}H_{33}$	9.8
$-C_{18}H_{37}$	10.8
$-(CH_2)_{10}CN$	6.1

as the sum of the bond lengths, and taking into account the angles between them (Fig. 2). For example, for octadecyldimethylchlorosilane[3] l = 2.45 nm, L_{min} = 0.75 nm, d = 0.4 nm and D^* will be 10.8 nm. This means that if the pore diameter is less than D^* the bonded molecules are exposed to mutual steric hindrance. The data calculated from eqn. 2 for different bonded molecules are given in Table I.

Let us consider in detail the state of bonded hydrocarbon chains in small pores (pores with diameter D less than D^*). In conformity with the principle of maximum bonding density, long-chain n-alkyl chains have a conformation that provides the most compact packing of bonded molecules on a surface, as is possible, for instance, when the n-alkyl chains are "folded" (Fig. 3).

Further, we consider the bonded n-alkyl chain as a cylinder standing perpendicular to the surface, its height and diameter being h and q, respectively. Then the conformational transitions of bonded chains will be determined as changes in h and q. It should be noted that the height of the cylinder is the thickness of the bonded layer. There is an evident connection between h and q; thus, considering the molecule volume constant, $V_{mol} = \pi h q^2 / 4$, we have

$$q = \sqrt{\frac{4V}{h\pi}}$$

Then geometric consideration of the pore diameter D ($D < D^*$) gives (Fig. 3)
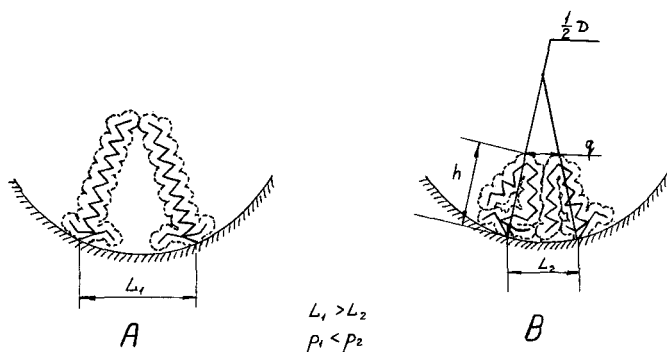
Fig. 3. Model of collision of bonded chains. (A) Alkyl chains as straight as possible; (B) alkyl chains with a conformation providing a denser attachment.

$$L = \frac{Dq}{D-2h} \tag{3}$$

and therefore the bonding density, assuming $q = \sqrt{4V/h\pi}$, is expressed by

$$p = \frac{1.15}{L^2} = \frac{1.15h(D-2h)^2\pi}{4VD^2} \tag{4}$$

The analysis of the first derivative of $p(h)$ shows that it has the only extreme value (for h from 0 to $D/2$) at $h = D/6$ (Fig. 4) and the value of the bonding density at $h = D/6$ is

$$p\left(h = \frac{D}{6}\right) = \frac{1.15D\pi}{54V} \tag{5}$$

Therefore, for a pore diameter D, the greatest bonding density is obtained when the conformation of the bonded molecules provides a bonded layer thickness equal to $D/6$. For silicas with bonded octadecyl groups with pore diameters less than 10.8 nm we have

$$p = 0.217D \tag{6}$$

$$h = \frac{D}{6} \tag{7}$$

The p and h data calculated from eqns. 6 and 7 for C_{18} bonded phases are given in Table II.

Hence within the framework of the suggested model the bonding density decreases linearly with decrease in pore diameter when D is less than D^*. If the pore diameter is 6 nm, the bonding density reaches only 55% of the maximum possible value, p_{max}, obtained on a flat surface or in pores with D greater than D^* (Table II). A decrease in the bonding density causes an increase in the number of unmodified silanol groups and, hence, changes in the adsorption characteristics of stationary phases. As the diameter decreases, bonded molecules must fold more densely to pro-
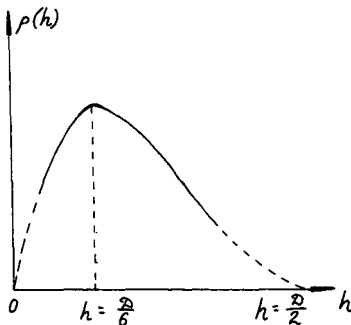
Fig. 4. Dependence of bonding density on conformation of alkyl chains (bonded layer thickness).

TABLE II

BONDING DENSITIES AND BONDED LAYER THICKNESSES OF OCTADECYLDIMETHYL-
SILYL STATIONARY PHASES WITHIN PORES OF DIFFERENT DIAMETER CALCULATED
USING EQNS. 6 AND 7

Parameter	Pore diameter (nm)			
	10.8	10.0	8.0	6.0
Bonding density (groups per nm^2)	2.30	2.17	1.70	1.30
Bonded layer thickness (nm)	1.85	1.66	1.50	1.00

vide a more compact packing, in other words, to ensure the maximum bonding density for a given pore. Simultaneously, the bonded layer thickness also decreases linearly with decreasing pore diameter.

We should point out that the maximum bonding density (in pores with $D < D^*$) can be achieved through a strictly specific thickness. This also means that the bonded layer is thickened and the mobility of bonded chains is limited. This state of a bonded layer has been termed a "rigid" structure (Fig. 3b).

In contrast to stationary phases with rigid structure, the so-called "flexible" structure is realised in wide pores (with $D > D^*$). In this instance bonded molecules are not exposed to mutual steric hindrances and, depending on the external conditions, they may change their conformation over a wide range (Fig. 1).

CALCULATION AND EXPERIMENTAL DETERMINATION OF BONDING DENSITY

So far we have not taken into account the pore size distribution. To compare the results predicted by theory with experimental data and to study real stationary phases, the distribution of pore size should be taken into account.

The bonding density at $D > D^*$ corresponds to the highest possible value; for example, for trichloro-and dimethylalkylchlorosilanes it is 2.3 groups per nm^2. The bonding density for $D < D^*$ may be calculated from eqn. 4. Thus, taking into consideration the pore size distribution for the bonding density, we obtain the following relationship:

$$p = \int_{D_1}^{D^*} p(D) \, \frac{1}{\sigma\sqrt{2\pi}} \exp\left[-\frac{(D-D_0)^2}{2\sigma^2} \right] dD \left(\frac{S_1}{S_1+S_2} \right) + p_{\max}\left(\frac{S_2}{S_1+S_2} \right) \quad (8)$$

It is accepted here that pore size distribution obeys a normal law with parameters D_0 and σ. Integrating eqn. 8 with respect to diameter from the smallest diameter D_1 to D^* we obtain the bonding density p for $D < D^*$. The bonding density for $D > D^*$ is $p_{\max}$. S_1 and S_2 are the specific surface areas corresponding to definite intervals of diameter, viz., S_1 from D_1 to D^* and S_2 from D^* to the largest diameter D_2.

Using eqn. 8 we calculated the bonding densities for a number of chemically

modified silicas with different pore structures (D_0, σ) and kinds of modifier. The calculated data are given in Table III. It can be seen that the calculation agrees well with the experimental data. Unfortunately we are not in a position to treat the data in all the publications concerning the reaction of chemical modification of silica, because in order to perform calculations in conformity with eqn. 8 one needs, in addition to D_0, the value of σ, i.e., the shape of pore size distribution curve must be known.

Let us consider the determination of S_1, S_2, D_0 and σ from the experimental dV/dD curve. One can construct the curve of pore size distribution as a function of diameter from the desorption part of the sorption isotherms[6]. For calculation with eqn. 8, for instance, it is necessary to pass to a distribution dN/dD, where N is the number of pores of a fixed diameter. To pass from dV/dD to dN/dD, one can use the following relationship:

$$\frac{1}{V_0} \cdot \frac{dV}{dD} = \frac{\pi D^2 f}{4} \cdot \frac{dN}{dD} \cdot \frac{1}{N_0} \tag{9}$$

assuming that the pores are cylinders of depth f. With a normal distribution dN/dD the connection between the distribution parameters is evident. Indeed,

$$\left[\frac{d}{dD} \left(\frac{dV}{dD} \right) \right]_{D=D_m} = \frac{d}{dD} \left\{ \frac{\pi D^2 f}{4} \cdot \frac{1}{\sigma \sqrt{2\pi}} \cdot \exp \left[-\frac{(D-D_0)^2}{2\sigma^2} \right] \right\} = 0 \tag{10}$$

from which

$$D_0 = D_m - \frac{2\sigma^2}{D_m} \tag{11}$$

where D_m is coordinate of the maximum of the distribution dV/dD.

TABLE III

BONDING DENSITIES OF HEXADECYLDIMETHYLCHLOROSILANE (C_{16}) AND CYANO-DECYLTRICHLOROSILANE ($C_{10}CN$) FOR SILICAS OF DIFFERENT PORE STRUCTURE CALCULATED USING EQN. 8 AND EXPERIMENTAL DATA

Modifier	Characteristics of pore structure of original silicas				Bonding density (nm^{-2})	
	D_0 (nm)	σ (nm)	$\dfrac{S_1}{S_1+S_2}$	$\dfrac{S_2}{S_1+S_2}$	Calculated	Experimental
C_{16}	25	3	0	1	2.3	2.1 ± 0.15
C_{16}	13.0	3	0.66	0.34	1.9	2.0 ± 0.15
C_{16}	11.5	1.5	0.35	0.65	1.9	1.9 ± 0.15
C_{16}	5.3	1.0	1	0	1.3	1.4 ± 0.15
$C_{10}CN$	6.8	1.5	0.5	0.5	1.5	1.6 ± 0.15

A second ratio is obtained on equating to zero the second derivative of dV/dD at the inflection point $D = D_i$:

$$\left[\frac{d^2}{dD^2}\left(\frac{dV}{dD}\right)\right]_{D=D_i} = \frac{d^2}{dD^2}\left\{\frac{\pi D^2 f}{4} \cdot \frac{1}{\sigma\sqrt{2\pi}} \cdot \exp\left[-\frac{(D-D_0)^2}{2\sigma^2}\right]\right\} = 0 \qquad (12)$$

hence we obtain

$$\sigma^4 - 0.5\sigma^2 \left[4D_i(D_i - D_0) + D_i^2\right] + 0.5D_i^2(D_i - D_0)^2 = 0 \qquad (13)$$

From the values of D_i and D_m we can find D_0 and σ. We analysed a large number of dV/dD distributions and established that σ can be calculated as $\frac{1}{3}(D_m - D_1)$, where D_1 is the smallest value of the pore diameter. If σ is negligible compared with D_m then $D_0 = D_m$ (see eqn. 11). With a wide and/or asymmetric distribution of dV/dD, D_0 can differ significantly from D_m and should be calculated from eqn. 11.

S_1 and S_2 were calculated using the equation $S = 4V/D$. Hence

$$S_1 = \int_{D_1}^{D^*} \frac{4V}{D} \cdot N(D_0; \sigma)dD \qquad (14)$$

$$S_2 = \int_{D^*}^{D_2} \frac{4V}{D} \cdot N(D_0; \sigma)dD \qquad (15)$$

where V is the pore volume (ml/g) and $N(D_0; \sigma)$ is the normal distribution with parameters D_0 and σ:

$$N(D_0; \sigma) = \frac{1}{\sigma\sqrt{2\pi}} \cdot \exp\left[-\frac{(D-D_0)^2}{2\sigma^2}\right]$$

DETERMINATION OF BONDED LAYER THICKNESS

The bonded layer thickness is experimentally determined from the change in a pore volume after chemical modification. Assuming that the pores have a cylindrical form, one can obtain the relative change in pore volume as follows:

$$\frac{\Delta V}{V} = \frac{4f\pi[D^2 - (D-2h)^2]}{4f\pi D^2} = 1 - \frac{(D-2h)^2}{D^2} \qquad (16)$$

where D is the average pore diameter and h is the average bonded layer thickness. Solving this equation for h we obtain

$$h = D\left(0.5 - \sqrt{1 - \frac{\Delta V}{4V}}\right) \tag{17}$$

i.e., if we know the change in pore volume ΔV we can determine the average bonded layer thickness.

It is wrongly thought that the bonded layer thickness is equal to half the difference in the average pore diameters obtained from the pore volume distribution before and after modification:

$$h = 0.5(D_m - D_m^M) \tag{18}$$

Average diameters are determined from desorption curves, reconstructed into differential curves of pore volume distribution *versus* diameter. However, as was mentioned before, the average pore volume distribution is not equal to the average distribution of the number of pores, namely,

$$D_0 = D_m - \frac{2\sigma^2}{D_m}$$

Hence it is correct to write

$$h = 0.5(D_0 - D_0^M) \tag{19}$$

This equation, unfortunately, is not taken into account by many workers, which has led to discrepancies in data on bonded layer thickness and erroneous conclusions about the conformational structures of bonded molecules. For example, in one study[7] the conclusion about the "brush" structure of a bonded layer was made on the basis of the coincidence of values of the length of a molecule understood as the sum of bond lengths and h as $0.5(D_m - D_m^M)$, whereas calculation on the basis of eqn. 17 gives far smaller values for the thickness, which demonstrates a liquid-like structure as preferred. In Table IV the values of bonded layer thickness for hexadecyl- and octadecylsilyl stationary phases calculated using eqns. 17 and 18 are given, and it can be seen that they are different. With a wide and asymmetric distribution the dispersion of h values can be especially significant. Indeed, $0.5(D_m - D_m^M) = 0.5(D_0 - D_0^M)$ if σ is negligible.

Let us consider a typical example. Sample 4 (Table IV) has an asymmetric pore size distribution with a large tail in the range of small pores. This fact is likely to account for a smaller value of the bonded layer thickness than for sample 2. In fact, the bonded layer thickness in small pores is less than in large pores, but the surface area of these pores is considerable. The average value of the bonded layer thickness is reduced although one would think that a sample with $D_0 = 13$ nm should at least have a bonded layer thickness equivalent to that of sample 2 with $D_0 = 11.5$ nm (Table IV). The modified silicas studied by Roumeliotis and Unger[7] are likely to have had analogous asymmetric pore size distributions, which resulted in the excessive h values obtained using eqn. 18.

The average bonded layer thickness can be also determined from the change in the specific surface area after chemical modification:

$$\frac{\Delta S}{S} = \frac{f[\pi D - \pi(D - 2h)]}{fD\pi} = \frac{2h}{D} \tag{20}$$

However, the precision of measurement of S for modified silicas is low, because the value of the adsorption ground (*i.e.*, the average area per molecule within the BET monolayer) of an adsorbate molecule in the bonded layer is unknown.

In our opinion, the most precise and simplest approach to the determination of bonded layer thickness is to apply eqn. 17 using experimental data obtained from the change in pore volume after chemical modification. When using eqn. 17 one should replace V^M with a value that takes into account the excess weight of sorbent as a result of modification:

$$V^M_{corr} = \frac{V^M}{100 - M} \tag{21}$$

where M (%) is the excess weight due to the modifier.

Analysis of the values of bonded layer thickness given in Table IV demonstrates that, first, the bonded layer thickness, as was predicted by theory, falls as the average pore diameter decreases starting from a certain value (approximately 10 nm for C_{16} stationary phases). Second, as follows from the h value, the bonded layer does not have a "brush" structure but closer to a liquid-like structure.

The absorption methods can give values close to the actual values only for stationary phases with a rigid structure of the bonded layer, *i.e.*, when the conformational transitions of bonded alkyl chains and the penetration of absorbable molecules, for instance benzene, into the bonded layer are hindered.

CALCULATION OF BONDED LAYER THICKNESS

We have found that for the pores with a diameter D less than $D*$ the optimum

TABLE IV

BONDED LAYER THICKNESSES OF SILICAS MODIFIED WITH HEXADECYL-(C_{16}) AND OCTADECYLDIMETHYLCHLOROSILANE (C_{18}) CALCULATED USING EQNS. 17 AND 18

Modifier	D_0 (nm)	Bonded layer thickness (nm)	
		From eqn. 17	*From eqn. 18*
C_{16}	25.0	1.2	0
C_{16}	11.5	1.1	1.4
C_{16}	5.3	0.85	0.5
C_{16}	13.0	0.95	2.0
C_{16}	13.4	0.94	2.2*
C_{18}	10.0	1.1	1.5**

   * According to ref. 7.
 ** According to ref. 8.

bonded layer thickness is a strictly definite value which provides the densest attachment:

$$h = \frac{D}{6}$$

For a pore size distribution including values up to D^* the thickness of the bonded layer can be calculated by integrating eqn. 22 with respect to diameter. Unfortunately, within the framework of the suggested model we cannot evaluate the bonded layer thickness at values of D larger than D^*, *i.e.,* in wide pores. The answer to this problem can only be obtained by a direct experiment, for instance, by Fourier transform (FT) IR spectroscopy for wide-pore modified silicas. As has been shown[9], the application of this method permits the evaluation of the number of gauche defects for a bonded alkyl chain and thus gives direct information about the conformation of bonded molecules. Only in this case for the bonded layer thickness can an equation analogous to eqn. 8 be obtained, namely

$$h = h_1 \cdot \frac{S_1}{S_1 + S_2} + h_2 \cdot \frac{S_2}{S_1 + S_2} \tag{22}$$

Within the framework of the available model we can only calculate h_1 equal to $D/6$. It is interesting that values depending on the kind of molecule (for instance, the number of methylene links) are not included in equation for h_1. However, the contribution of the first term for bonded hydrocarbons of different lengths will vary as the value of D^* depends on the length of the modifier molecules.

A comparison of the h values, calculated using eqn. 22 with the bonded layer thicknesses, calculated using eqn. 17 on the basis of experimental data obtained from the change in pore volume as a result of chemical modification for pores with D less then D^* is presented in Table V.

CONCLUSIONS

The geometric structural consideration of the bonded layer of chemically modified silicas has shown that modified silicas have very complicated structures. The

TABLE V

BONDED LAYER THICKNESSES, CALCULATED USING EQN. 21, AND EXPERIMENTAL DATA FOR SILICAS MODIFIED WITH HEXADECYLDIMETHYLCHLOROSILANE (C_{16}) AND OCTADECYLDIMETHYLCHLOROSILANE (C_{18})

Modifier	D_0 (nm)	Bonded layer thickness (nm)	
		Calculated	Experimental
C_{18}	6.6	1.10	1.03*
C_{16}	5.3	0.88	0.86

* Data calculated using eqn. 17 on the basis of experimental results from ref. 7.

principal characteristics of the bonding density and thickness of the bonded layer depend on a number of parameters, *viz.*, pore structure of the support, kind of modifier and conditions of modification. Even very small changes in one of these parameters, *e.g.*, the average pore diameter, from batch to batch may cause uncontrollable changes in the state of the bonded layer and, hence, the chromatographic properties.

On the basis of this study, surface conformational structures can be divided into three groups, rigid, flexible and intermediate (mixed).

In the rigid structure the diameter of the support pores does not exceed the collision diameter D^*. The bonded molecules are exposed to steric hindrance. Conformational transformations are hampered or impossible. The bonded layer thickness is unchangeable and is equal to $h = D/6$. The bonding density is less than the maximum value, p_{max}, and the bonded layer thickness decreases linearly as the pore diameter diminishes. This layer is characterized by an adsorptive retention mechanism as the sample molecules can hardly penetrate the bonded layer.

In the flexible structure the diameter of the support pores is larger than the collision diameter D^*. The bonded molecules are virtually on a flat surface. Conformational transformations are permitted and the sample molecules can penetrate the bonded layer. The bonding density is equal to the maximum value, p_{max}, and is constant throughout the surface. The bonded layer thickness depends on the solvent and temperature.

In the intermediate (mixed) structure, if the average pore diameter is equal to the collision diameter, but if D for a number of pores is less then $D_0 = D^*$, these pores contain the rigid structure of the bonded layer and the remainder of the pores contain the flexible structure. In this instance the retention mechanism is intermediate.

Stationary phases that possess an intermediate structure are the most complicated. Indeed, even trivial alterations in the average pore diameter can substantially change the ratio of rigid structure to flexible structure, which can affect the chromatographic properties of the stationary phase.

For instance, for C_{18} stationary phases $D^* = 10.8$ nm. If a support does not contain pores with the diameter up to 10.8 nm (this is especially true of supports with an average pore diameter of 4–8 nm) the structure of the bonded layer is rigid. If the average pore diameter is close to 10.8 nm (namely 8–14 nm) the intermediate structure is realised. It should be noted that most commercial stationary phases are obtained on the basis of such supports, and therefore they differ considerably in their chromatographic properties.

When the average diameter is greater than or equal to 14 nm, the bonded layer has the flexible structure. In our opinion, these stationary phases are probably the most reproducible, as their attachment density does not depend on the pore diameter. Hence, even marked differences in the pore diameter of different batches of support can affect the capacity factor but not their selectivity.

Consideration of the geometric structural features of the bonded layer structure within the framework of the model of cylindrical pores demonstrates a good coincidence with experimental data for the average bonding density and average bonded layer thickness. However, one should not forget that in reality stationary phases are much more complicated than theoretical models. A considerable proportion of stationary phases have a globular structure, *i.e.*, they are formed in gaps
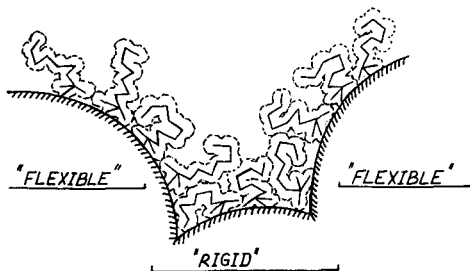
Fig. 5. Flexible and rigid structures within pores formed by primary particles of silica.

between primary globes. This structure of the pore surface should result in the formation of a rigid structure of the bonded layer in the areas close to the contact points of globes and a flexible structure on the tops of the globes. Thus, even pores of equal diameter have various bonding densities and structures of the bonded layer in different areas of the surface. The modified surface in such pores has a mozaic-like structure, each pore having sections of flexible and sections of rigid structure. An increase in the pore diameter leads to an increase in the proportion of the flexible structure and a decrease in the pore diameter leads to an increase in the proportion of the rigid structure (Fig. 5).

Geometric analysis shows that the distribution of the types of bonded layer structure in globular pores differs only insignificantly from that in cylindrical pores. For instance, C_{18} stationary phases with a pore diameter less than 7 nm actually do not contain the flexible structure at all, whereas stationary phases with a pore diameter of more than 14 nm mainly contain the flexible structure.

In recent years many papers have been devoted to the study of the bonded layer structure of reversed phases by different methods such as FT-IR spectroscopy[9], NMR spectroscopy[10,11] and luminescense spectroscopy[12].

In our opinion, when interpreting experimental data and deducing general regularities, one should have an idea of the complexity of the object being studied. Therefore, it is hardly reasonable to choose a sample with an intermediate structure as the model for studying the physico-chemical properties of the bonded layer. In our opinion, one can compare only structurally equivalent stationary phases with flexible or rigid types of structure prevailing. We mean here the analysis of the bonded layer characteristics such as the adsorptive capacity and selectivity of the bonded layer and the mobility of bonded molecules. This is the expression of the geometric structural correspondence principal.

REFERENCES

1 C. Gonnet, C. Bory and G. Lachatre, *Chromatographia,* 16 (1982) 242.
2 J. R. Chrétien, B. Walczak, L. Morin-Allory, M. Dreux and M. Lafosse, *J. Chromatogr.,* 371 (1986) 253.
3 G. E. Berendsen and L. de Galan, *J. Liq. Chromatogr.,* 3 (1980) 1437.
4 S. M. Staroverov, A. A. Serdan and G. V. Lisichkin, *J. Chromatogr.,* 364 (1986) 377.
5 G. V. Lisichkin (Editor), *Modifitsirovannye Kremnezemy v Sorbtsii, Katalize i Khromatografii (Modified Silica in Adsorption, Catalysis and Chromatography)* Khimiya, Moscow, 1986, 248 pp.
6 S. J. Gregg and K. S. W. Sing, *Adsorption, Surface Area and Porosity,* Academic Press, New York, 1967.
7 P. Roumeliotis and K. K. Unger, *J. Chromatogr.,* 149 (1978) 211.
8 H. Engelhardt, B. Dreyer and H. Shmidt, *Chromatographia,* 16 (1982) 11.
9 L. S. Sander, J. B. Callis and L. R. Field, *Anal. Chem.,* 55 (1983) 1068.
10 A. Legrand, H. Hommel and L. Facchini, *Bull. Soc. Chim. Fr.,* 6 (1985) 1103.
11 R. K. Gilpin and M. E. Gangoda, *J. Chromatogr. Sci.,* 21 (1983) 352.
12 P. G. Bogar, J. C. Thomas and J. B. Callis, *Anal. Chem.,* 56 (1984) 1080.

CHROM. 20 581

POST-CAPILLARY FLUORESCENCE DETECTION IN CAPILLARY ZONE ELECTROPHORESIS USING o-PHTHALDIALDEHYDE

DONALD J. ROSE, Jr. and JAMES W. JORGENSON*

Department of Chemistry, University of North Carolina, Chapel Hill, NC 27599-3290 (U.S.A.)

(Received March 16th, 1988)

SUMMARY

A post-capillary fluorescence detection scheme for capillary zone electrophoresis is described using o-phthaldialdehyde (OPA) as the tagging reagent. Use of a coaxial capillary reactor affords mixing of the OPA reagent with migrating zones without excessive zone broadening. The detector is linear over three orders of magnitude and shows detection limits for amino acids and proteins in the femtogram (attomol) range.

INTRODUCTION

Capillary zone electrophoresis (CZE) is a separation technique which resolves species according to their differential rate of migration through solution in the presence of an electric field. Use of a capillary provides efficient dissipation of heat which reduces the zone-broadening effects of convection. Use of a capillary, however, requires small sample sizes and thus the need for sensitive methods of detection.

Detection of zones in CZE can be done by monitoring zones either migrating within the capillary or emerging from the end of the capillary. Zone detection within the capillary has been accomplished by measuring changes in UV absorption[1], fluorescence[2,3], refractive index[4], or conductivity[5–7] as the zone migrates past the point of detection. Because the detection "cell" is a portion of the electrophoresis capillary, these techniques are relatively simple to employ and result in minimal additional broadening of the measured zones. Detection of zones after they migrate from the end of the capillary is more difficult to employ. A connection must be made with the end of the capillary permitting current to flow during electrophoresis while not significantly perturbing and broadening the zone. Examples of this type of "post-capillary" detection include interfacing to a mass spectrometer[8] and an electrochemical (amperometric) detector[9].

One area of application for CZE is the separation and characterization of amino acids, peptides and proteins. Of the detection methods previously mentioned, fluorescence detection offers the most sensitivity for this group of biological compounds and is usually accomplished by labelling the compound with a fluorescent "tag". In liquid chromatography (LC), reagents such as fluorescein isothiocyanate

(FITC)[10,11], fluorescamine[12,13], dansyl chloride[14,15], and o-phthaldialdehyde (OPA)[16-18], have been used to label amine functional groups on biological compounds before the chromatographic separation. Alternatively, fluorescamine[19,20] and OPA[21,22] have been mixed with the chromatographic effluent stream to detect sample components following the chromatographic separation.

Use of the pre-separation labelling scheme for CZE has limitations. For example, OPA-labelled amino acids decompose over time with the rate of decomposition being amino acid-dependent[23]. Another limitation arises from the fluorescent tags changing the net charge on sample molecules and thus changing the mobility of the ion during the separation. For example, each FITC molecule replaces the positive charge of the amine on the tagged molecule with a negative charge due to the carboxylate on the fluorescein. This is not critical for compounds such as amino acids with one or two reactive amine groups, but for proteins, which have many amine groups (e.g. a terminal amine plus numerous lysine epsilon amines along the peptide chain), different protein molecules can possess a different number of tags. Unless all protein molecules are tagged to the same extent (i.e. they all have the same number of tags), each compound with a different number and/or arrangement of tags will have a different electrophoretic mobility and fluorescence intensity. In this way, a single protein can yield multiple peaks.

This article reports on the successful implementation of post-capillary detection in CZE with OPA as the labelling reagent. The introduction of reagent is accomplished using a coaxial capillary reactor consisting of two concentric fused-silica capillaries. The reactor dimensions are optimized for maximum signal with minimal zone broadening. In addition, the reactor is characterized in terms of linearity and detection limits and is compared to conventional UV absorption detection. Various applications will be shown for samples of biological significance.

EXPERIMENTAL

Post-capillary reactor

Fig. 1 shows a schematic cross-section of the post-capillary reactor. The reaction capillary, held in the stainless-steel tee (Swagelok, Crawford Fitting; Ontario, Canada) by Vespel ferrules, has a 1–2 cm wide window formed by burning off the polyimide coating. The electrophoretic capillary, with an outer diameter smaller than the inner diameter of the reaction capillary, passes through the tee and inserts into the reaction capillary such that the two capillaries are concentric and form the coaxial reactor. The reagent capillary enters the short arm of the tee and is secured by a ferrule. Fused-silica capillaries (Polymicro Technologies; Phoenix, AZ, U.S.A.), were used throughout the reactor. The inner and outer diameters of electrophoretic and reaction capillaries varied according to experimental design. The reagent capillary dimensions were constant throughout the study with an inner diameter of 200 μm, an outer diameter of 325 μm, and a length of approximately 70 cm.

Fig. 2 shows the post-capillary reactor as a part of the overall CZE experimental set-up. The electrophoretic and reaction capillaries each dip into leveled buffer reservoirs, containing the operating buffer, which are connected to the high voltage power supply by platinum electrodes. The tee is not connected to ground but is left "floating" electrically. The height difference (Δh) between the OPA reservoir and the
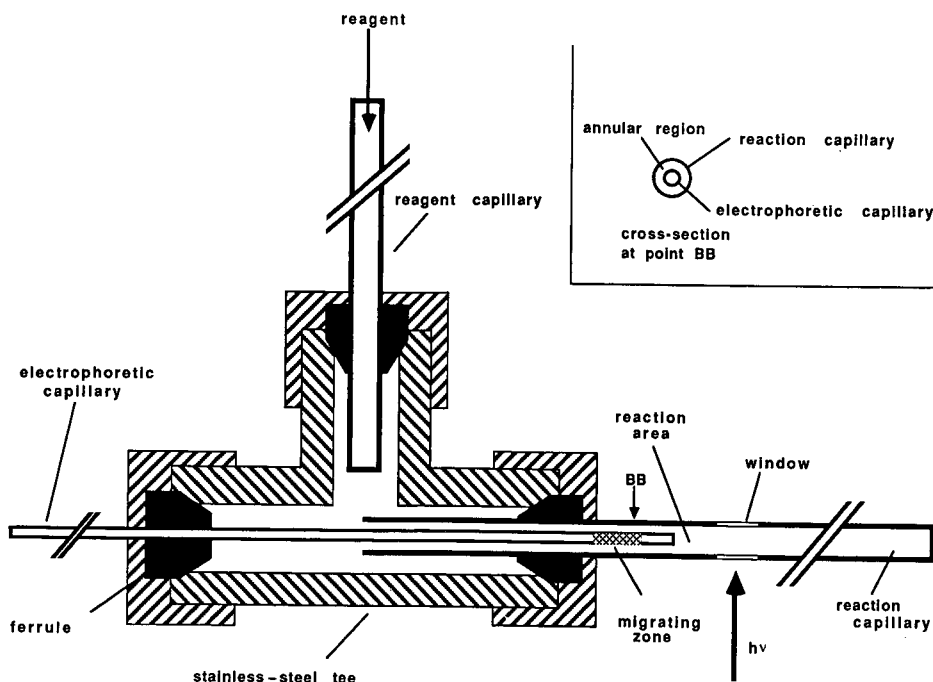
Fig. 1. Cross-sectional schematic of post-capillary reactor in stainless-steel tee.
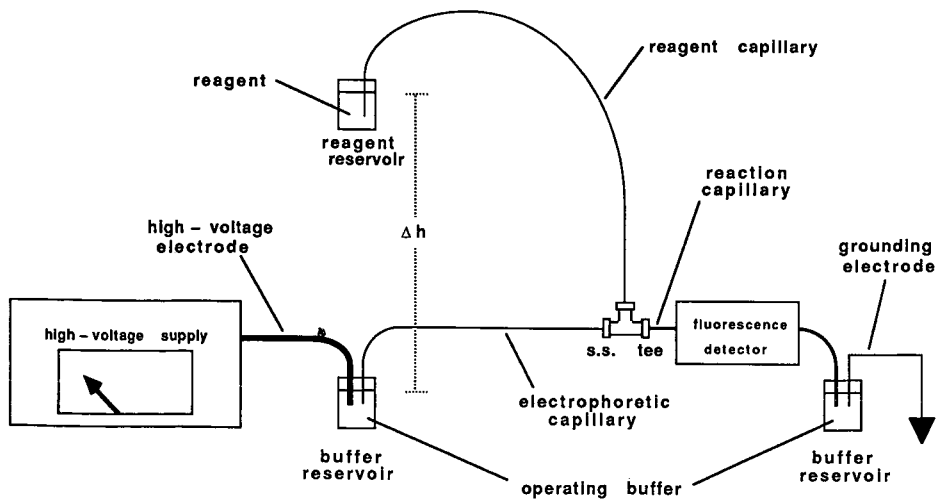
Fig. 2. Overall CZE experimental set-up for post-capillary fluorescence detection.

buffer reservoirs creates hydrostatic pressure which forces OPA reagent to flow into the tee and pass through the annular region of the coaxial reactor. A zone migrating from the tip of the electrophoretic capillary mixes with the OPA reagent in the reaction area to form a fluorescent product (see Fig. 1). Reaction products are carried a short distance (1–2 cm) "downstream" and detected by fluorescence.

Instrumentation

The apparatus for electrophoresis was similar to that previously published[5,24,25]. A ±30-kV d.c. power supply (Spellman High Voltage Electronics; Plainview, NY, U.S.A.), used in the positive voltage mode, drove the electrophoretic separations. A high-pressure mercury–xenon arc lamp source in a variable-wavelength fluorescence detector[2] was used with 312 nm as the excitation wavelength and two 400-nm cut-on filters for isolating the emission wavelength. The cell block of the detector was modified slightly to support the stainless-steel tee of the post-capillary reactor. Fluorescence intensity was measured using an R-212 photomultiplier tube (Hamamatsu; Middlesex, NJ, U.S.A.) and a photometer (Pacific Instruments; Concord, MA, U.S.A.) connected to the analog-to-digital converter of a multi-function interface board (Scientific Solutions, Solon, OH, U.S.A.) which was mounted in an IBM PC/XT microcomputer (IBM, Boca Raton, FL, U.S.A.). Analog conversions were made at a rate of 1 or 2 points per second.

Reagents and samples

High purity *o*-phthaldialdehyde, 2-mercaptoethanol, N-tris(hydroxymethyl)-methyl glycine (tricine), 3-(cyclohexylamino)-1-propanesulfonic acid (CAPS), 2-(N-cyclohexylamino)ethanesulfonic acid (CHES), amino acids, whale skeletal muscle myoglobin, bovine erythrocyte carbonic anhydrase, chicken egg ovalbumin and bovine milk β-lactoglobulin were purchased from Sigma (St. Louis, MO, U.S.A.). Bromocresol purple, boric acid, potassium hydroxide, potassium chloride, and absolute ethanol were reagent grade. Distilled water was used for all buffers.

The OPA reagent was made fresh daily by dissolving 5 mg of OPA (mol.wt. 134.1) in 50 μl of 2-mercaptoethanol plus 200 μl of absolute ethanol and then diluted up to 4 ml with buffer (see table footnotes and figure legends for specific buffers).

Procedure

The capillaries for the reactor were used as supplied except in cases where the outer diameter of the electrophoretic capillary was reduced using the following etching procedure: (i) the polyimide plastic coating was burned off over the desired length, (ii) water was forced through the capillary using helium pressure, and (iii) the capillary was dipped into a stirred bath of concentrated (48%) hydrofluoric acid for a specified time.

Insertion of the electrophoretic capillary into the reaction capillary to form the coaxial post-capillary reactor was done manually with the aid of a microscope and then the capillary combination was secured in the stainless-steel tee. The reactor was mounted in the detector with the reaction capillary secured in the detector block and the tee resting in a plexiglass holder attached to the block. A vacuum, applied to the end of the reaction capillary, filled the electrophoretic capillary with operating buffer, the reagent capillary with OPA reagent, and the reaction capillary with a mixture of operating buffer and OPA reagent. The vacuum was applied until no air bubbles passed through the reaction capillary, indicating that no leaks were present in the

reactor and OPA reagent completely filled the void volume of the tee. After returning the reaction capillary to the buffer reservoir, the OPA reservoir was raised to a specified height to begin reagent flow. The high voltage was applied until a flat baseline from background fluorescence was achieved.

Introduction of sample into the electrophoretic capillary was accomplished using the following procedure: (i) the OPA reservoir was lowered to the height of the buffer reservoirs, (ii) the high voltage was turned off, (iii) the end of the electrophoretic capillary was moved from buffer reservoir to sample vial (the high-voltage electrode dipped into both sample vial and buffer reservoir), (iv) the voltage was applied for a specific amount of time to migrate sample into the end of the electrophoretic capillary, (v) the end of the electrophoretic capillary was moved back to the buffer reservoir, (vi) the high voltage was applied to begin the run, and (vii) the OPA reservoir was raised to its original height. After the run, the fluorescence intensity was plotted as a function of time to produce an electropherogram. The peak limits were marked arbitrarily and a statistical moments calculation[26,27] was done between the marks to give peak parameters such as peak area, variance, and the number of theoretical plates (N).

To examine mixing in the coaxial reactor, the stainless-steel tee was removed from the detector and mounted next to an optical stereomicroscope such that the tip of the electrophoretic capillary in the reaction capillary window was in the microscope's field of view. A basic solution (pH 10) of bromocresol purple, a pH indicator, was migrated through the electrophoretic capillary in a continuous zone while a basic buffer (no bromocresol purple) flowed through the reagent capillary. With this configuration, the purple solution could be seen as it emerged from the tip of the electrophoretic capillary and mixed with the basic buffer flowing from the annular region of the coaxial reactor. In a second experiment, an acidic buffer was used in the reagent capillary to change the emerging purple to yellow to help reveal the extent of mixing in the reaction area.

RESULTS AND DISCUSSION

Characterization of post-capillary reactor. The coaxial capillary configuration was chosen for post-capillary detection in CZE because the OPA reagent could easily be introduced and mixed with a zone without the need for a mixing tee or reaction coil. The schematic in Fig. 3 shows a zone migrating from the tip of the electrophoretic capillary and mixing with the OPA reagent stream. Mixing of zone molecules and OPA reagent is due to diffusion, convection, and migration effects.

Radial diffusion occurs as analyte molecules emerge from the capillary tip and diffuse outward toward the walls of the reaction capillary, while OPA reagent diffuses into the zone. The time required for this radial diffusion can be estimated using the Einstein equation for diffusion,

$$x = (2Dt)^{1/2}$$

where x is the diffusion distance, D is the diffusion coefficient and t is the mean time required for a molecule to diffuse the distance x. Solving for the diffusion time, t, a small molecule ($D = 1 \cdot 10^{-5}$ cm^2 s^{-1}) would require 0.08 s to diffuse radially from the center to the edge of a 25-μm wide "cylinder" of fluid emerging from the end of an
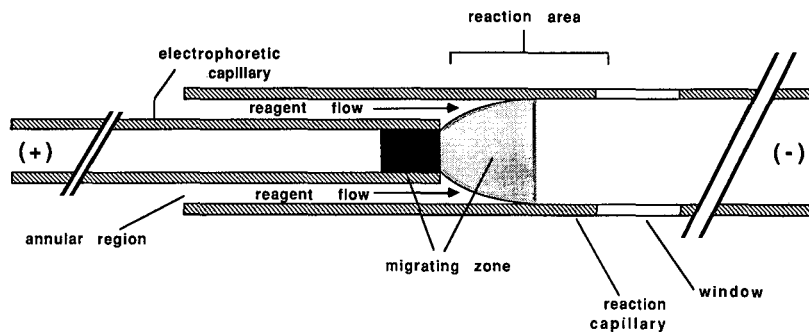
Fig. 3. Schematic of reaction area with a zone migrating from the tip of an electrophoretic capillary.

electrophoretic capillary of 25-μm I.D. (This diffusion time increases approximately ten-fold for larger molecules such as proteins). Because OPA reagent also diffuses into the cylinder of fluid emerging from the electrophoretic capillary, the time required for OPA reagent to mix with a zone will be even less than this rough calculation indicates. Turbulent convection, if it is present, will further speed this mixing process.

A final mechanism contributing to mixing of the analyte and reagent concerns the electric field. In CZE, ions are responsible for carrying current from the high-voltage electrode through the capillary to the grounded electrode. In the post-capillary reactor, the inner diameter changes in going from electrophoretic to reaction capillary. For this reason, both buffer and analyte ions will migrate radially in order to carry current over the full cross-sectional area of the reaction capillary (see Fig. 3). This phenomenon may help to carry charged analyte molecules outward and into the flowing stream of OPA reagent which facilitates mixing.

Even though thorough mixing of an emerging zone and the OPA reagent is necessary to achieve a maximum yield of fluorescent product, mixing is also a potential source of zone broadening and must be controlled to preserve high efficiency separations. To assess the effect of post-capillary reactor mixing on zone broadening, zones were monitored at two locations. A UV absorbance detector was positioned before the stainless-steel tee such that a portion of the electrophoretic capillary formed the detector cell. Also, zones were monitored after the stainless-steel tee, in the coaxial reactor, using post-capillary fluorescence labelling. Table I compares the peak efficiencies (N), a measure of zone width, at these two detection locations as a function of height difference, Δh, between the OPA reservoir and the two buffer reservoirs (see Fig. 2). An increase in the height difference causes an increase in the hydrostatic pressure resulting in an increase in the OPA reagent flow through the annular region of the capillary reactor. The data for post-capillary detection show that as the flow of OPA reagent increases, the efficiency (number of theoretical plates) increases and the peak area decreases. The inverse relationship between efficiency and peak area exists because a high flow-rate increases dilution of the zone migrating from the end of the electrophoretic capillary (thus reducing signal) but also sweeps analyte through the detection region more rapidly and thus prevents excessive residence time in the reaction area (increased efficiency). This effect was seen visually by continuously migrating a purple solution from the tip of the electrophoretic capillary (see

TABLE I

ZONE BROADENING EFFECTS OF POST-CAPILLARY REACTOR

Conditions: operating and OPA buffer 10 mM tricine + 20 mM potassium chloride, pH 8.3; sample, 1 · 10^{-4} M tyrosine; sample introduction, 5 s at 15 kV; operating current 3 μA, electrophoretic capillary, 60 cm × 150 μm O.D. × 25 μm I.D.; reaction capillary, 325-μm O.D., 200-μm I.D.

Δh (cm)*	Detection location		
	Electrophoretic capillary (absorbance): N	Reaction capillary (fluorescence)	
		N	Peak area**
2	15 200	1400	13 800
4	10 100	4400	5200
8	10 600	8700	1400
16	13 500	10 600	500

* Height difference between OPA reservoir and buffer reservoirs.
** Arbitrary units.

Experimental section for details). At low OPA reagent flow-rates, the solution would have a profile similar to that shown in Fig. 3 whereas at higher flow-rates, the profile would be confined to a narrow stream emerging from the tip of the electrophoretic capillary.

Effect of post-capillary reactor dimensions

In an effort to increase the fluorescence signal and decrease zone broadening, a series of post-capillary reactors were constructed from capillaries with varying dimensions. The 25-μm I.D. dimension of the electrophoretic capillary was kept constant throughout the study. Each capillary combination is shown in Table II and briefly described below (the combinations are represented by the notation O.D.$_{tip}$/-I.D.$_{RC}$ where O.D.$_{tip}$ is the tip outer diameter of the electrophoretic capillary and I.D.$_{RC}$ is the inner diameter of the reaction capillary).

150/200. This capillary combination was used for the data shown in Table I and represents the post-capillary reactor initially characterized in the previous section. The electrophoretic capillary was used as supplied without modification. The 150-μm O.D. electrophoretic capillary was easily inserted into the 200-μm I.D. reaction capillary to form this combination.

36/200. The tip of the electrophoretic capillary was tapered from 150-μm O.D. to 36-μm O.D. over the last 0.25 cm by etching the outside of the capillary with hydrofluoric acid. The tapered tip was an effort to reduce any turbulence due to the blunt tip of a 150-μm O.D. electrophoretic capillary. Such turbulence was observed microscopically during continuous migration of the purple indicator from the tip of the electrophoretic capillary of the 150/200 capillary combination previously described (see Experimental section for details).

110/160. By burning off the polyimide plastic coating over the last 8 cm of the

TABLE II

CAPILLARY COMBINATIONS FOR POST-CAPILLARY REACTOR

See text for explanation of each combination; reaction capillary length is 32 cm for all combinations, $O.D._{RC}$ is 350 μm for all combinations except 40/50 which was 150 μm.

Capillary combination*	Tip $O.D._{EC}$ (μm)**	Nominal $I.D._{RC}$ (μm)***	$I.D._{RC} - O.D._{tip}$ (μm)	$I.D._{RC} - I.D._{EC}$ (μm)
150/200	150	200	50	175
36/200	150 to 36	200	50 to 164	175
110/160	110	160	50	135
70/100	70	100	30	75
40/50	40	50	10	25

* Electrophoretic capillary nominal I.D. = 25 μm, O.D. = 150 μm (unmodified) for all combinations.

** Tip is terminal 8 cm of electrophoretic capillary (EC) as determined using a measuring microscope. Tip for 36/200 combination is tapered from 150 μm to 36 μm over terminal 0.25 cm.

*** Nominal inner diameter of reaction capillary as supplied by the manufacturer.

electrophoretic capillary, the outer diameter of the tip was reduced by approximately 35 μm. This electrophoretic capillary was inserted into a 160-μm I.D. reaction capillary. (Assembly of this and subsequent capillary combinations required careful
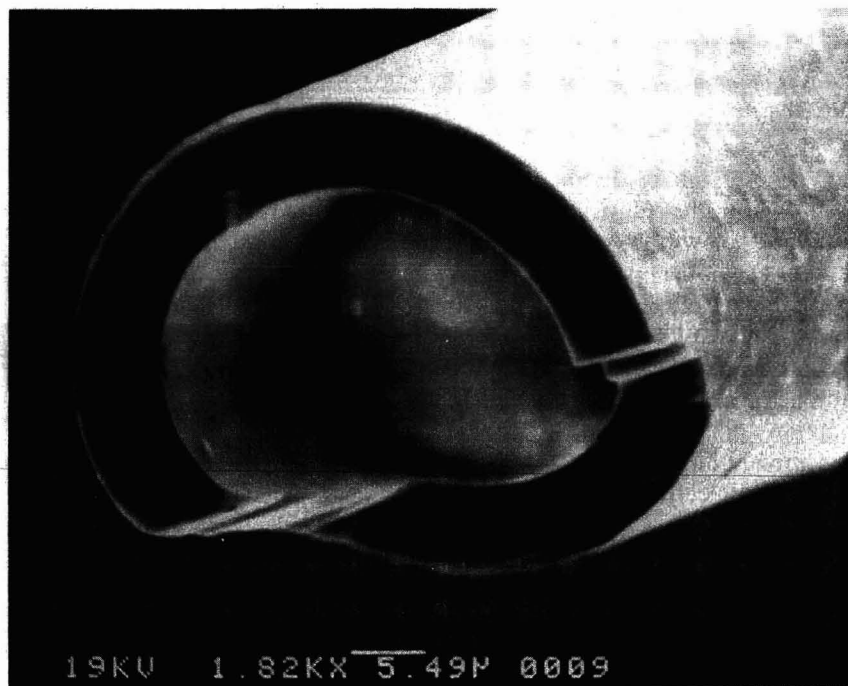
Fig. 4. Scanning electron micrograph of electrophoretic capillary tip used in 40/50 capillary combination.
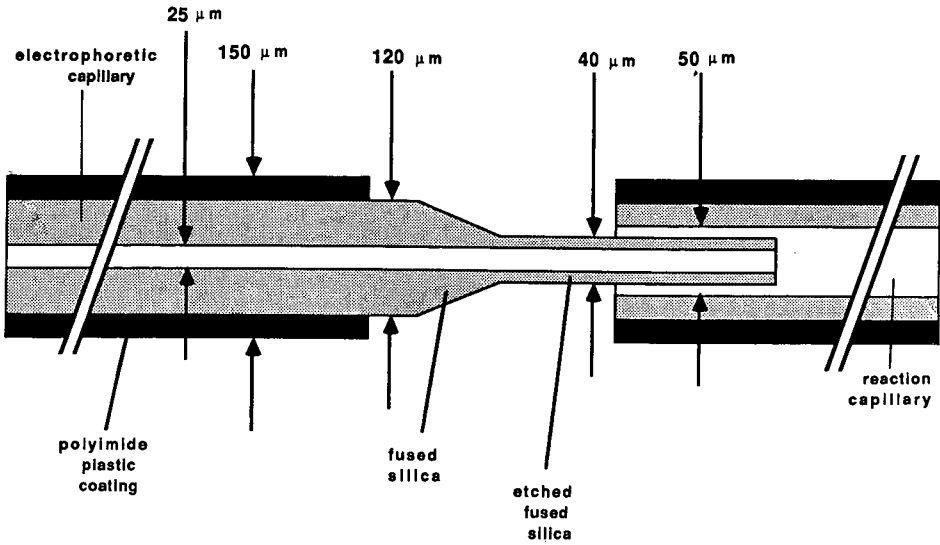
Fig. 5. Schematic of 40/50 capillary combination.

manipulation because of the fragile nature of the exposed fused silica of the electrophoretic capillary.)

70/100 and 40/50. Further reductions in the outer diameter of the electrophoretic capillary were achieved by burning off the polyimide plastic coating as with the
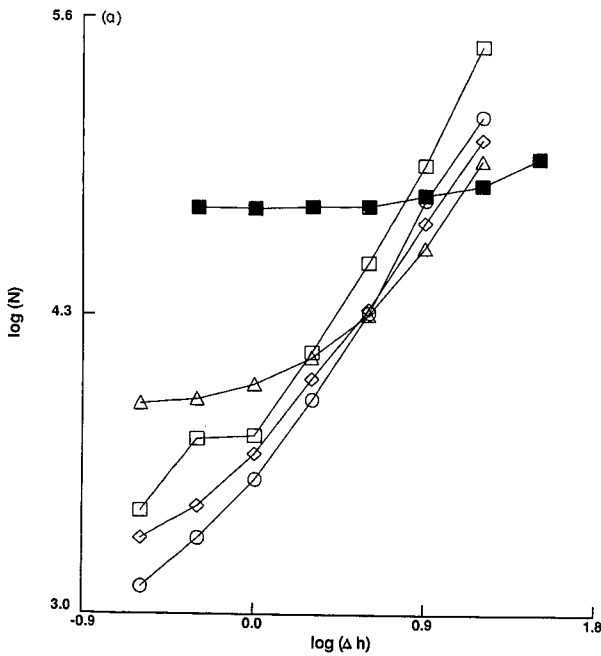
Fig. 6.
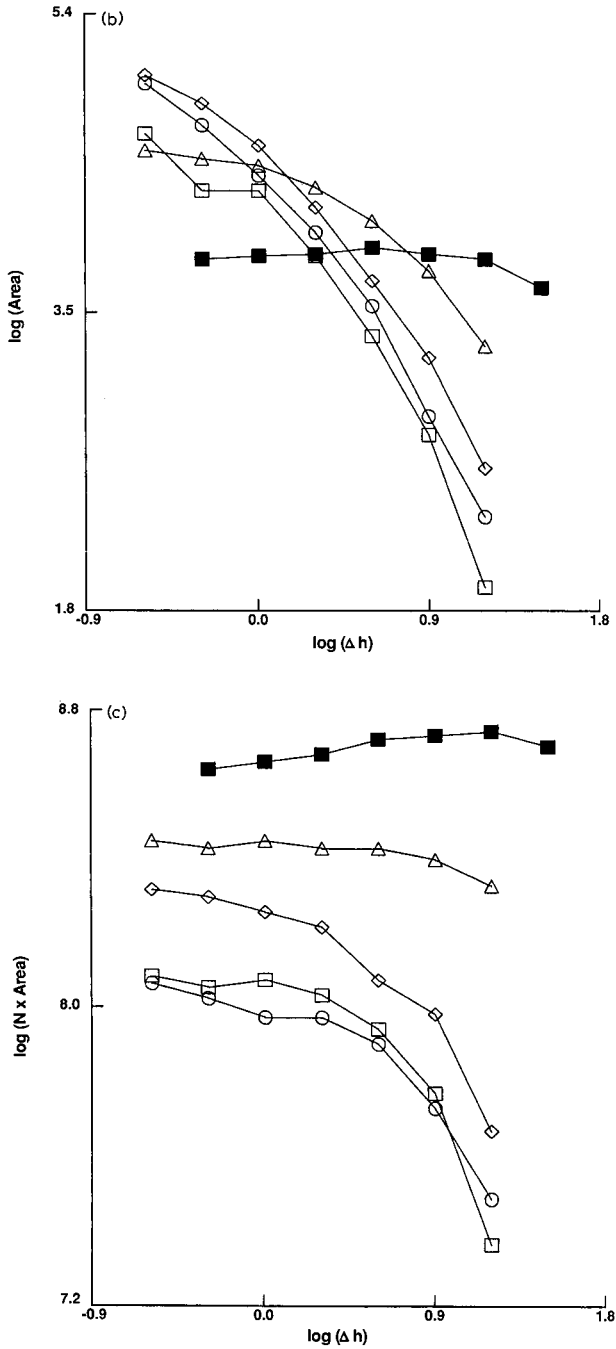
Fig. 6. Comparison of capillary combinations for a series of OPA reagent flow-rates (Δh in cm): 150/200 ($\bigcirc$), 36/200 ($\square$), 110/160 ($\diamond$), 70/100 ($\triangle$), 40/50 ($\blacksquare$).(a) log (peak efficiency, N) $vs.$ log (Δh); (b) log (peak area) $vs.$ log (Δh); (c) log(N · area) $vs.$ log(Δh); operating and OPA reagent buffers, 10 mM tricine + 20 mM potassium chloride pH 8.4; test analyte, $1 \cdot 10^{-4}$ M glycine.

110/160 combination and then etching the entire length of bare fused silica in a hydrofluoric acid bath for 15–25 min (see Experimental section for details). Fig. 4 shows an scanning electron micrograph of an etched electrophoretic capillary used in the 40/50 combination. Fig. 5 shows a schematic of the two capillaries of the 40/50 combination. In assembling this combination, care was taken to make sure that the reaction capillary was not blocked with the shoulder of the electrophoretic capillary. By reducing the outer diameter of the electrophoretic capillary to 70 μm and to 40 μm, correspondingly smaller reaction capillaries of 100 μm and 50 μm outer diameter, respectively, could be used (see Table II).

In Fig. 6, a comparison is made between these capillary combinations used for the post-capillary reactor in terms of number of theoretical plates, N, (Fig. 6a), area (Fig. 6b), and the product of N and peak area (Fig. 6c) for a series of OPA reagent flow-rates, Δh. In Fig. 6a and b, the 40/50 combination shows little OPA reagent flow-rate dependence as compared to the other combinations. As the difference between the inner diameters of the electrophoretic and reaction capillaries is reduced (see the 6th column of Table II), the efficiency–peak area product increases, as shown in Fig. 6c. The 40/50 combination, showing the largest efficiency–peak area product, differs in inner diameters by only 25 μm compared to the 150/200 combination which differs in inner diameters by 175 μm. Since a large efficiency–peak area product is desirable, the 40/50 combination was chosen as the working coaxial capillary dimension and used for the subsequent sensitivity studies and applications described below.

Linearity and limits of detection

The linearity of the post-capillary detector was evaluated from a log–log plot of peak area as a function of sample concentration. The post-capillary detector is linear over 3.5 orders of magnitude for the amino acid glycine (slope = 0.972, correlation coefficient = 0.9996). For the two proteins, whale skeletal muscle myoglobin (WSM) and carbonic anhydrase (CAH), linearity was more difficult to measure as they are more prone to exhibiting concentration dependent asymmetries in the electrophoretic process. This peak distortion made accurate measurement of peak areas difficult. This problem was further aggravated by impurities appearing as shoulders on the main protein peak. At the lower protein concentrations (less than 0.1% w/v) protein response was linear.

Fig. 7, an electropherogram of $5 \cdot 10^{-7}$ M glycine, shows a peak representing 42 fg (560 attomol) of glycine. Using the criterion of three times the RMS noise in Fig. 7, the limit of detection is 6.3 fg (83 attomol) of glycine introduced into the electrophoretic capillary. Fig. 8, an electropherogram of 0.0001% (w/v) whale skeletal muscle myoglobin or one part per million (ppm), shows a peak representing 1.6 pg (93 attomol) of protein. Using the same criteria as described for glycine, the limit of detection is 380 fg (22.1 attomol or thirteen million molecules) of myoglobin introduced into the electrophoretic capillary.

A comparison between the relative sensitivity of post-capillary fluorescence detection and on-line UV detection is shown in Fig. 9. Fig. 9a is an electropherogram of a mixture of proteins detected using post-capillary fluorescence detection. Fig. 9b is an electropherogram of the same mixture of proteins (identical amount injected) detected using a fixed-wavelength (229 nm) UV detector[1] such that the length to the
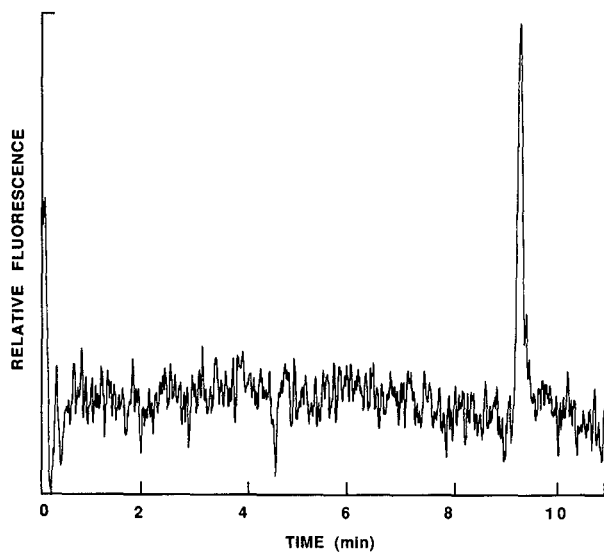
Fig. 7. Electropherogram of glycine. Peak represents 42 fg (560 attomol) glycine introduced into the capillary; data has been subjected to a nine-point Savitsky–Golay smooth[28]. Operating and OPA reagent buffer, 50 mM borate + 50 mM potassium chloride, pH 9.5. Sample introduction, 2 s at 30 kV; operating voltage, 30 kV; Δh = 16 cm.
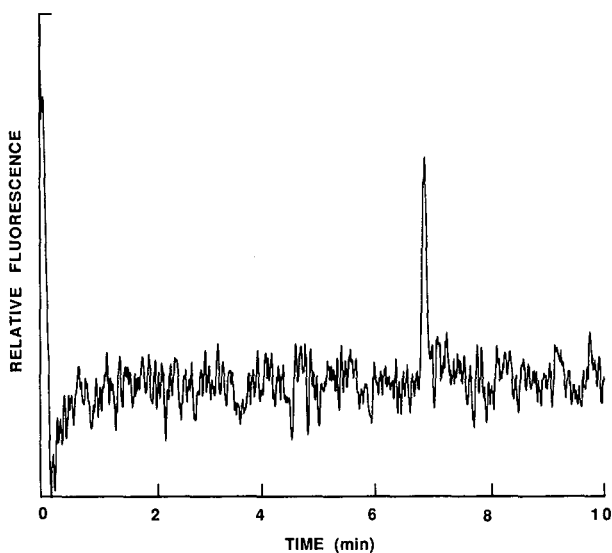
Fig. 8. Electropherogram of whale skeletal muscle myoglobin. Peak represents 1.6 pg (93 attomol) myoglobin introduced into the capillary; data has been subjected to a nine-point Savitsky–Golay smooth[28]; for operating conditions, see Fig. 7.
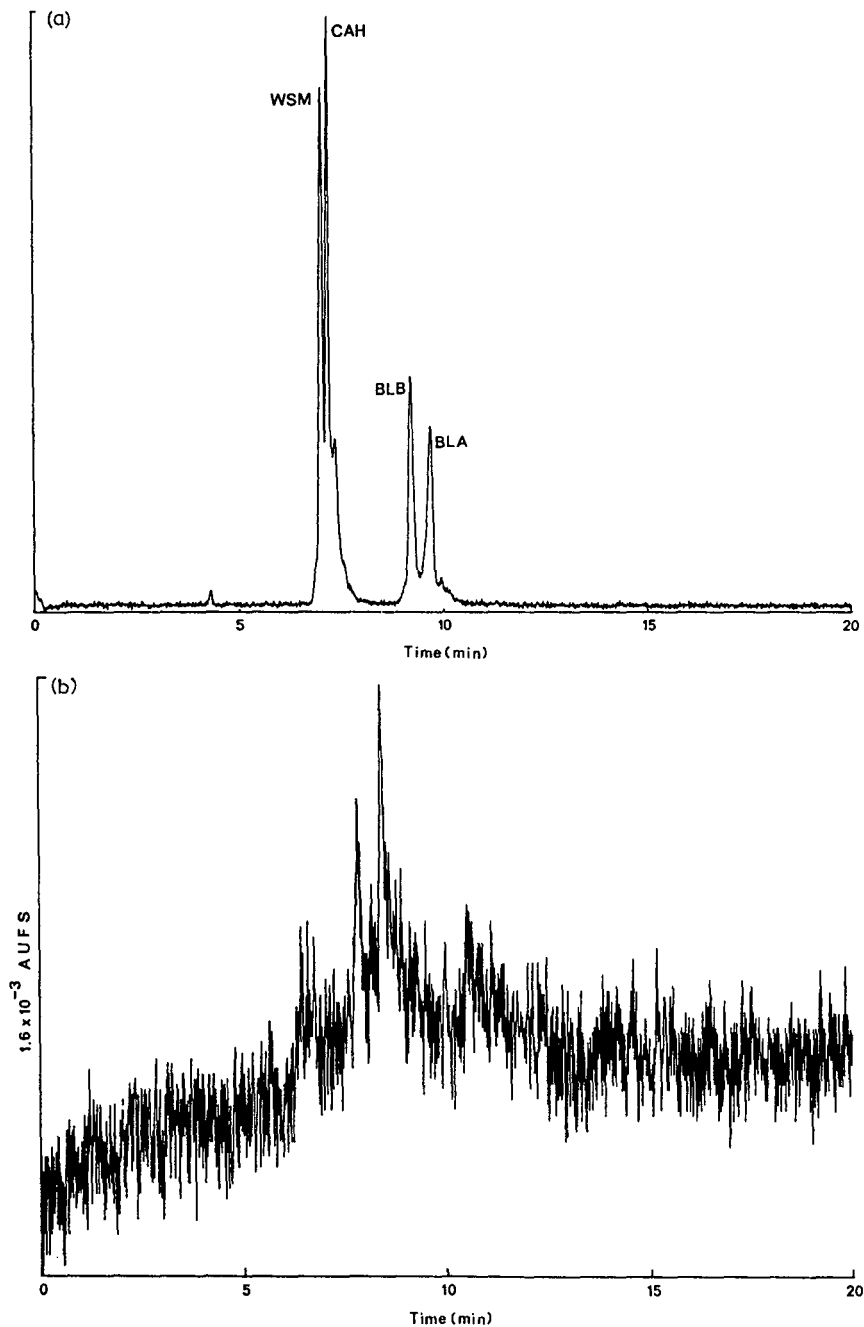
Fig. 9. Comparison of post-capillary fluorescence and UV detection of 0.01% (w/v) whale skeletal muscle myoglobin (WSM), 0.01% (w/v) carbonic anhydrase (CAH), 0.005% (w/v) β-lactoglobulin B (BLB), 0.005% (w/v) β-lactoglobulin A (BLA). (a) Post-capillary fluorescence detection; (b) UV (229 nm) detection; operating and OPA reagent buffer, 50 mM borate + 50 mM potassium chloride, pH 9.5. For operating conditions, see Fig. 7.

on-line detection window was the same as the length of the electrophoretic capillary in the post-capillary scheme (all other electrophoretic parameters such as injection/run voltage and time were the same for both runs). The improvement in signal-to-noise is approximately 100-fold using the post-capillary fluorescence detection.

Detection using post-capillary OPA derivatization affords the analysis of a variety of samples with amine-containing samples. Fig. 10 shows the separation and detection of amine-containing compounds in red wine. This figure points to the advantages of post-capillary fluorescence detection in CZE. The sample required no sample preparation other than a four-fold dilution. Also, because the detection scheme responds only to primary amines, it is more selective than UV detection, for example. This selectivity, combined with the sensitivity of fluorescence detection, enables the quantification of the minor component, histamine, in a complex sample.

A post-capillary fluorescence detection system for CZE has been described which uses no mixing tee or loops in which to react electrophoretic zones with OPA reagent. The detection limits for this system represent a major improvement over any detection scheme suitable for protein detection previously described for CZE. This detection scheme is useful for the analysis of amine-containing biomolecules in complex mixtures.

The work described herein points to several areas of improvement which would further enhance this detection system. Use of a laser as the excitation source (as opposed to the arc lamp used here) should increase the fluorescence intensity of the
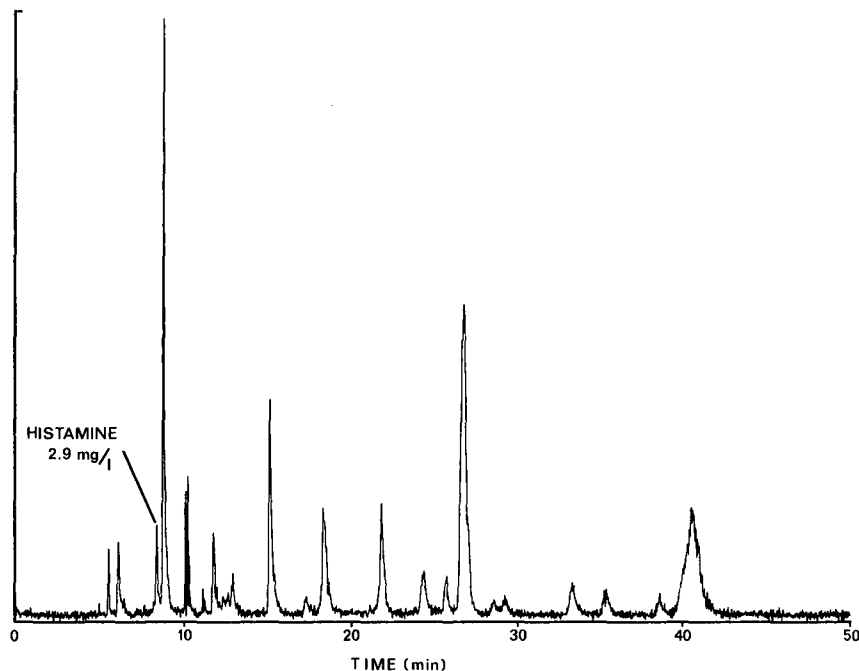
Fig. 10. Electropherogram of red wine (1984 Fonset–Lacour Bordeaux), four-fold dilution of unfiltered sample with operating buffer; operating buffer, 100 mM borate + 200 mM potassium chloride, pH 9.5; OPA reagent buffer 0.1 M CAPS, pH 11.0. $\Delta h = 32$ cm; sample introduction, 2 s at 30 kV; run voltage, 25 kV.

OPA adduct. Pumping of OPA reagent using a constant flow pump would allow precise quantitation and control of reagent flow-rate and increase the reliability of reagent flow into the reaction area. Finally, replacement of the stainless-steel tee union with a cross union would provide a more effective means of flushing out the void volume of the union with fresh OPA reagent daily.

REFERENCES

1 Y. Walbroehl and J. W. Jorgenson, *J. Chromatogr.*, 315 (1984) 135.
2 J. S. Green and J. W. Jorgenson, *J. Chromatogr.*, 352 (1986) 337.
3 P. Gozel, E. Gassman, H. Michelsen and R. N. Zare, *Anal. Chem.*, 59 (1987) 44.
4 K. D. Lukacs, *Ph.D. Dissertation*, University of North Carolina, Chapel Hill, NC, 1983.
5 X. Huang, T. J. Pang, M. J. Gordon and R. N. Zare, *Anal. Chem.*, 59 (1987) 2747.
6 F. E. P. Mikkers, F. M. Everaerts and Th. P. E. M. Verheggen, *J. Chromatogr.*, 169 (1979) 11.
7 F. Foret, M. Deml, V. Kahle and P. Boček, *Electrophoresis*, 7 (1986) 430.
8 J. A. Olivares, N. T. Nguyen, C. R. Yonker and R. D. Smith, *Anal. Chem.*, 59 (1987) 1230.
9 R. A. Wallingford and A. G. Ewing, *Anal. Chem.*, 59 (1987) 1762.
10 K. Muramoto, H. Kawauchi, Y. Yamamoto and K. Tuzimura, *Agric. Biol. Chem.*, 40 (1976) 815.
11 K. Muramoto, H. Kamiya and H. Kawauchi, *Anal. Biochem.*, 141 (1984) 446.
12 K. Samejima, *J. Chromatogr.*, 96 (1974) 250.
13 K. Imai, *J. Chromatogr.*, 105 (1975) 135.
14 V. T. Wiedmeier, S. P. Porterfield and C. E. Hendrich, *J. Chromatogr.*, 231 (1982) 410.
15 Y. Tapuhi, N. Miller and B. L. Karger, *J. Chromatogr.*, 205 (1981) 325.
16 H. Umagat, P. Kucera and L.-F. Wen, *J. Chromatogr.*, 239 (1982) 463.
17 M. J. Winspear and A. Oaks, *J. Chromatogr.*, 270 (1983) 378.
18 V. A. Fried, M. E. Ando and A. J. Bell, *Anal. Biochem.*, 146 (1985) 217.
19 R. W. Frei, L. Michel and W. Santi, *J. Chromatogr.*, 126 (1976) 665.
20 P. Bohlen, S. Stein, J. Stone and S. Udenfreind, *Anal. Biochem.*, 67 (1975) 438.
21 P. Kucera and H. Umagat, *J. Chromatogr.*, 255 (1983) 563.
22 H. P. M. van Vliet, G. J. M. Bruin, J. C. Kraak and H. Poppe, *J. Chromatogr.*, 363 (1986) 187.
23 P. Lindroth and K. Mopper, *Anal. Chem.*, 51 (1979) 1667.
24 J. W. Jorgenson and K. D. Lukacs, *Anal. Chem.*, 53 (1981) 1298.
25 J. W. Jorgenson and K. D. Lukacs, *Science (Washington, D.C.)*, 222 (1983) 266.
26 L. B. Rogers and J. E. Oberholtzer, *Anal. Chem.*, 41 (1969) 1234.
27 O. Grubner, *Anal. Chem.*, 43 (1971) 1934.
28 A. Savitsky and M. J. E. Golay, *Anal. Chem.*, 36 (1964) 1627.

CHROM. 20 519

ANALYSIS OF WATER-SOLUBLE VITAMINS BY MICELLAR ELECTRO-KINETIC CAPILLARY CHROMATOGRAPHY

SHIGERU FUJIWARA

Pharmaceuticals Research Center, Kanebo, Ltd., Miyakojima-ku, Osaka 534 (Japan)

and

SHIGEFUMI IWASE and SUSUMU HONDA*

Faculty of Pharmaceutical Sciences, Kinki University, Kowakae, Higashi-Osaka 577 (Japan)

(First received February 5th, 1988; revised manuscript received April 5th, 1988)

SUMMARY

Seven water-soluble vitamins were determined simultaneously by micellar electrokinetic capillary chromatography with UV detection. All these compounds were separated from each other within *ca.* 22 min by using a carrier containing sodium dodecyl sulphate as the surfactant. On-column detection at 254 nm with ethyl *p*-aminobenzoate as the internal standard allowed sensitive, accurate and reproducible determination of these compounds. Five principal constituents of a vitamin injection were determined with relative standard deviations of less than 2.1%.

INTRODUCTION

Capillary zone electrophoresis (CZE) is a remarkable method of separation, since it allows efficient separation of ionic substances, with large numbers of theoretical plates ranging from 10^5 to 10^6 plates/m of column length, *e.g.*, refs. 1–6. The addition of a surfactant in the carrier electrolyte solution has brought forth another mode of separation, based on differential partition of solutes between the aqueous and micellar phases in a rapid electroosmotic flow. This mode, initiated by Terabe *et al.*[7,8] and designated micellar electrokinetic capillary chromatography (MECC) by Burton *et al.*[9], is also efficient and has the advantage that it can be applied also to non-ionic substances[10,11]. Recently, several papers have demonstrated the usefulness of MECC for separation of various groups of compounds, including phenylthiohydantoin derivatives of amino acids[12], pyridoxine as well as its metabolites[9], purines[13] and nucleic acid-related compounds[14]. We also succeeded in separating antipyretic analgesics and in quantifying small amounts of these drugs[15]. Our success in this micro determination may be valuable, since it suggested the use of MECC in biomedical analysis. Therefore, we have extended the application of MECC to various drugs and biological substances. The present paper describes the results obtained for the analysis of water-soluble vitamins.

EXPERIMENTAL

Reagents

Thiamine hydrochloride (VB$_1$), nicotinamide (VB$_3$), nicotinic acid (VB$_3'$), pyridoxine hydrochloride (VB$_6$), cyanocobalamin (VB$_{12}$) and L-ascorbic acid (VC) were obtained from Wako Pure Chemicals (Dosho-machi, Higashi-ku, Osaka, Japan). The sodium salt of riboflavine phosphate (VB$_2$PNa) was obtained from Tokyo Kasei Kogyo (Nihonbashi-honcho, Chuo-ku, Tokyo, Japan). Sodium dodecyl sulphate (SDS) and ethyl *p*-aminobenzoate (EAB) used as the surfactant and the internal standard, respectively, were also from Wako Pure Chemicals. All other chemicals were of the highest grade commercially available and were used without further purification. All these vitamins were used as aqueous solutions. EAB was used as a solution in methanol–water (1:1, v/v). Phosphate solutions were made by mixing $2.0 \cdot 10^{-2}$ M disodium hydrogenphosphate with $2.0 \cdot 10^{-2}$ M potassium dihydrogenphosphate in appropriate proportions (for pH 7, 8 and 9) or by adding 1 M sodium hydroxide to the former solution (for pH 10). SDS-containing carriers were prepared by dissolving 2.5–10 mmol of SDS in 100 ml of phosphate solutions obtained as above, and were used after filtration through a membrane filter having a pore size of 0.5 μm.

Apparatus

MECC was performed in a fused-silica capillary tube (80 cm × 100 μm I.D.; Scientific Glass Engineering, Australia). An high-voltage d.c. power supplier in an IP-2A isotachophoresis apparatus (Shimadzu, Nishinokyo, Nakakyo-ku, Kyoto, Japan), capable of delivering up to 30 kV, was used to generate the electric field. On-column UV detection was carried out with a SPD-2A double-beam variable-wavelength detector (Shimadzu). The polymer coating on the capillary tube was partly removed by burning at a position 50 cm from the anodic end, and the transparent portion was set on an 100 μm × 1 mm handmade slit attached to the detector block. A Chromatopac C-R1B (Shimadzu) was used for the measurement of retention time and peak area.

Procedure for MECC

The capillary tube was filled with a carrier solution by suction. Both ends of the tube were separately dipped in the anodic and cathodic solutions having the same composition as the carrier solution, and the surfaces of these electrode solutions were adjusted to the same level. For the introduction of a sample solution into the tube, the anodic end was quickly moved into a sample solution and the level of the sample solution was raised to about 5 cm higher than that of the cathodic solution. After 5 s the end of the tube was returned to the anodic solution, and an high voltage was applied in the constant-current mode. The current applied was 100 μA in the experiments using SDS-containing carriers, whereas it was reduced to 75 μA in those using SDS-free carriers, to obtain approximately the same voltage throughout the work.

Procedure for determination of the ingredients of a vitamin injection

For the determination of VB$_1$, VB$_2$PNa, VB$_3$ and VB$_6$, 5 ml of a commercial

sample of vitamin injection were accurately taken, to which were added 5.00 ml of a $1.00 \cdot 10^{-2}$ M solution of EAB (internal standard), and the volume was adjusted to 50.0 ml with distilled water. For the determination of VC, the commercial sample was diluted 1:25 in distilled water, and a 5-ml aliquot was processed in the manner described above. Standard solutions were prepared by dissolving authentic VB_1, VB_2PNa, VB_3, VB_6 and VC in distilled water. EAB was added to give approximately the same concentration as that in the sample solution.

The sample and the standard solutions were analyzed by MECC according to the procedure described above. The sample-to-standard peak area ratio of each vitamin was measured, from which its content was calculated.

RESULTS AND DISCUSSION

Optimization of separation

Fig. 1 shows the pH dependence of the retention time of seven water-soluble vitamins in 0.02 M phosphate solutions. Since SDS was absent from the carriers under these conditions, separation was performed simply by electrophoresis. The almost neutral vitamins (VB_3 and VB_{12}) were driven from the anode (inlet) to the cathode only by the electroosmotic flow generated in the electric field by the interaction of the carrier solution with the material of the capillary inner wall. However, VB_1, which gave a positively charged species in the carrier solution in the pH range examined, was eluted more rapidly than the neutral vitamins due to a positive electrophoretic effect. In contrast, VB_2PNa, VB_3' and VC, giving negatively charged species, were eluted more slowly than the neutral vitamins, because they were pulled back electrophoretically to the anode (negative electrophoretic effect). The retention time of VB_6 was the same as that of VB_3 or VB_{12} at pH 7.0, but was greater than that of VB_3 and VB_{12} at higher pH values, due to dissociation of the phenolic hydroxyl group. Although the retention time increased almost linearly with increasing pH for all these vitamins, the extent varied depending on the ionic state and weight. As a result, VB_1, VB_2PNa, VB_3', VB_6 and VC, which gave electrically charged species,
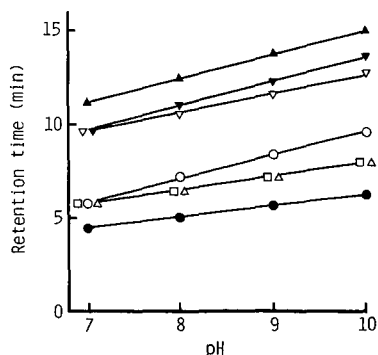
Fig. 1. Effect of the pH on the retention time in CZE of VB_1 (●), VB_2PNa (▼), VB_3 (□), VB_3' (▲), VB_6 (○), VB_{12} (△), VC (▽). Capillary tube: fused silica (80 cm × 100 μm I.D.). Carrier: 0.02 M phosphate solution. Current applied: 75 μA. Detection wavelength; 254 nm. Sample concentrations: $0.25 \cdot 10^{-3}$ (VB_2PNa and VB_{12}), $0.50 \cdot 10^{-3}$ (VB_1 and VC), $1.00 \cdot 10^{-3}$ M (VB_3, VB_3' and VB_6).
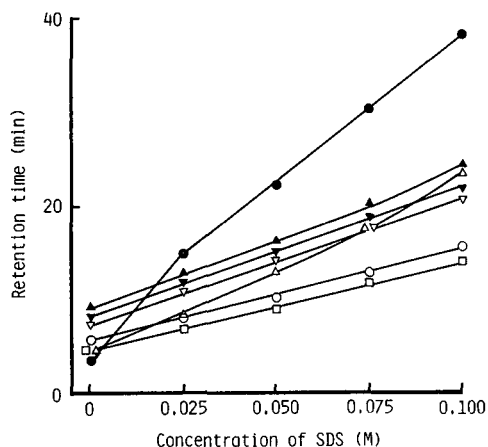
Fig. 2. Effect of the SDS concentration on the retention time in MECC. Carrier: 0.02 M phosphate solution, pH 9.0, containing 0.025–0.10 M SDS. Current applied: 100 μA. Other experimental conditions as in Fig. 1.

were all separated from each other at pH 9.0 and 10.0. However, the two neutral vitamins, VB_3 and VB_{12}, were not resolved electrophoretically at any pH value examined.

MECC gave elution profiles quite different from those in CZE. In this mode these vitamins were distributed between the aqueous and the micellar phases moving in a capillary tube, in the order of increasing hydrophobicity, resulting in good separation. Fig. 2 shows the effect of the SDS concentration on the retention time of each vitamin, obtained by adding various amounts of SDS to the phosphate solution, pH 9.0. The retention time of each vitamin increased with increasing SDS concentration. VB_3 and VB_{12}, a combination not resolvable in CZE, were readily separated from each other over the whole range of SDS concentration examined. VB_{12} gave longer retention times and a greater increase than did VB_3, because the former was more easily incorporated into SDS, presumably due to higher hydrophobicity. VB_1 was greatly retarded by the addition of SDS, being eluted last, probably due to the interaction between the positive charge of VB_1 and the negative charge of SDS. At a SDS concentration of 0.05 M all these compounds were well separated from each other. Good separation was also obtained at 0.1 M but the retention times of all these compounds were longer than those at 0.05 M.

Fig. 3 shows the effect of the pH of the phosphate solution on retention time, obtained when the SDS concentration was 0.05 M. The retention time of each compound increased almost linearly with increasing pH in this constant-current mode. At pH 7.0, the pairs VB_3–VB_6 and VC–VB_2PNa were not separated. The separations of VC from VB_2PNa at pH 8.0 and of VB_{12} from VC at pH 10.0 incomplete. The phosphate solution of pH 9.0 gave the best separation.

Based on these results, the 0.02 M phosphate solution, pH 9.0, containing 0.05 M SDS, was used for the analysis of these vitamins. EAB was chosen as the internal standard, because it was well separated from these vitamins under the separation conditions adopted. Fig. 4 shows an electropherogram of these water-soluble vit-
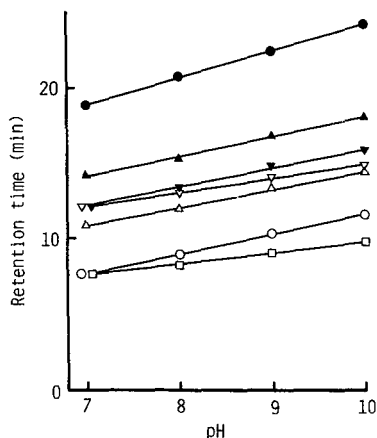
Fig. 3. Effect of the pH on the retention time in MECC. Carrier: 0.02 M phosphate solution containing 0.05 M SDS. Other experimental conditions as in Fig. 2.

amins together with the internal standard. The seven vitamins were completely resolved and eluted within *ca.* 22 min. The relative standard deviation of the relative retention time was within 0.6% for all these vitamins, indicating highly reproducible separation. The numbers of theoretical plates calculated as 5.54 $t_R^2 \, w^{-2}$, where t_R is the retention time of a compound and w is the peak width at half the peak height, for VB_1, VB_2PNa, VB_3, VB_3', VB_6, VB_{12} and VC were 40 000, 40 000, 90 000, 30 000, 60 000, 120 000 and 70 000, respectively.

Quantification
        The absorption maxima of these vitamins obtained under the aforementioned conditions ranged rather widely from 210 to 270 nm. Although individual vitamins could be monitored at the wavelength of their absorption maxima because a multi-
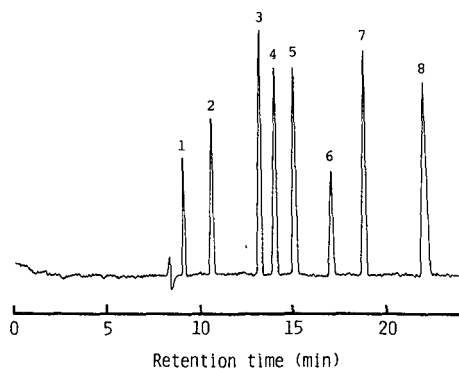
Fig. 4. Electropherogram of water-soluble vitamins. Carrier: 0.02 M phosphate solution, pH 9.0, containing 0.05 M SDS. The analytical conditions were as in Fig. 2. Peaks: 1 = VB_3; 2 = VB_6; 3 = VB_{12}; 4 = VC; 5 = VB_2PNa; 6 = VB_3'; 7 = EAB (internal standard); 8 = VB_1. The concentration of EAB was $1.00 \cdot 10^{-3} \, M$.

TABLE I

REPRODUCIBILITY OF THE DETERMINATION OF WATER-SOLUBLE VITAMINS BY THE INTERNAL STANDARD METHOD

Sample concentration: $0.25 \cdot 10^{-3}$ (VB_2PNa and VB_{12}), $0.50 \cdot 10^{-3}$ (VB_1 and VC), $1.00 \cdot 10^{-3}$ M (VB_3, VB'_3 and VB_6). Internal standard: $1.00 \cdot 10^{-3}$ M EAB.

	Sample-to-standard peak area ratio*						
	VB_1	VB_2PNa	VC	VB_3	VB'_3	VB_6	VB_{12}
$\bar{x}$**	1.18	1.02	0.81	0.36	0.55	0.64	0.82
s***	0.014	0.013	0.012	0.005	0.010	0.013	0.011
$s/\bar{x}$§	1.2	1.3	1.5	1.4	1.8	2.0	1.3

   * Ten determinations for each sample.
  ** Mean.
 *** Standard deviation.
   § Relative standard deviation.

wavelength UV detector was employed in the present work, multiple switching of wavelengths was laborious and accompanied by baseline fluctuation. Therefore, we selected 254 nm, where commercial mercury lamps emit most abundantly, as the common wavelength for the present system. Use of this single wavelength is profitable, since UV detectors employing mercury lamps are economical. At this wavelength, VB_1, VB_2PNa, VB_3, VB'_3, VB_6, VB_{12} and VC gave 62, 65, 29, 32, 25, 18 and 72%, respectively, of their maximum absorptions.

    The reproducibility of the determination of these vitamins was examined by use of the peak-area ratio mode. Table I gives the relative standard deviation for ten
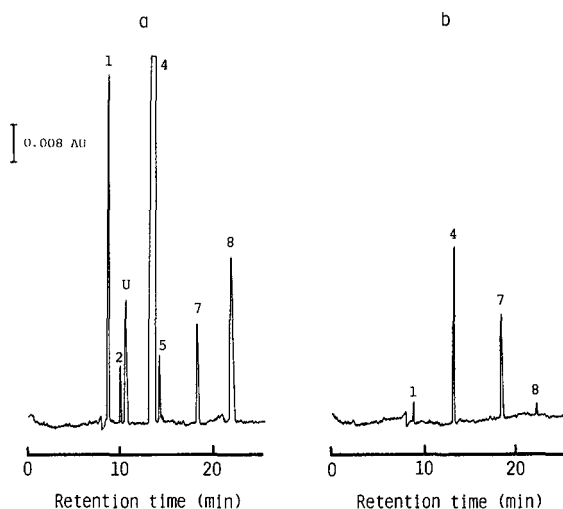
Fig. 5. Electropherograms of a commercial vitamin injection: (a) intact sample; (b) sample diluted 25-fold. The analytical conditions were as in Fig. 3. U = Unknown. Peaks as in Fig. 4.

TABLE II

ACCURACY AND REPRODUCIBILITY OF THE DETERMINATION OF THE INGREDIENTS OF A VITAMIN INJECTION

Ingredient	Amount indicated on the label (w, mg/ml)	Amount found			Found/indicated ($\bar{x}/w$, %)
		$\bar{x}$ (mg/ml)	s (mg/ml)	$s/\bar{x}$ (%)	
VB_1	5	5.07	0.062	1.2	101
VB_3	10	10.4	0.114	1.1	104
VB_6	1	1.00	0.013	1.3	100
VB_2PNa	0.5	0.52	0.011	2.1	104
VC	25	24.7	0.207	0.8	98.8

repeated determinations. In this experiment the concentration of the internal standard was fixed at $1.00 \cdot 10^{-3}$ M, and those of the vitamins were varied 0.25 · 10^{-3}, or 0.50 · 10^{-3} or 1.00 · 10^{-3} M, dependent on their molar absorptivities. The values of the relative standard deviation were in the range of 1.2–2.0%. In contrast to the peak-area ratio mode, the absolute peak-area mode gave higher values of the relative standard deviations, ranging from 5.5 to 9.7%. The calibration plots showed excellent linearity in the molar ratio ranges of 0.125–0.5 for VB_2PNa and VB_{12}, 0.25–1.0 for VB_1 and VC and 0.5–2.0 for VB_3, VB'_3 and VB_6. The detection limits were at the 0.5, 1 and 4 pmol levels for the first, second and last groups of vitamins, respectively.

Analysis of the ingredients of a vitamin injection

We applied this method to the analysis of water-soluble vitamins in a commercial injection. Since the concentration of VC was extraordinarily high, it was determined after 25-fold dilution of the sample. Fig. 5a and b show the electropherograms of the intact and diluted samples, respectively. An unknown peak presumably attributable to an additive was observed at *ca.* 11 min, but it did not interfere with the analysis.

The ingredients of this preparation were quantified by the peak-area ratio mode, based on the results mentioned above. The data on the accuracy and reproducibility of the determination are given in Table II. The $\bar{x}$ value for each ingredient was very close (98.8–104%) to the indicated value, and the relative standard deviation, $s/\bar{x}$, in its estimation was less than 2.1%, demonstrating that this method is sufficiently accurate and reproducible.

A few reports have been published on high-performance liquid chromatography of water-soluble vitamins, *e.g.*, refs. 16–20. However, these methods were disadvantageous, because they either required gradient elution[17,18], gave imperfect separation[19] or suffered from peak broadening[20] as well as tailing[16–18]. The MECC method proposed allowed complete separation of seven water-soluble vitamins with extremely high numbers of theoretical plates. The analysis time was only *ca.* 22 min. Furthermore, quantification was highly accurate and reproducible.

REFERENCES

1 F. E. P. Mikkers, F. M. Everaerts and Th. P. E. M. Verheggen, *J. Chromatogr.*, 169 (1979) 11.
2 J. W. Jorgenson and K. DeArman Lukacs, *Anal. Chem.*, 53 (1981) 1298.
3 J. W. Jorgenson and K. DeArman Lukacs, *J. Chromatogr.*, 218 (1981) 209.
4 J. W. Jorgenson and K. DeArman Lukacs, *Science (Washington, D.C)*, 222 (1983) 266.
5 T. Tsuda, K. Nomura and G. Nakagawa, *J. Chromatogr.*, 264 (1983) 385.
6 H. H. Lauer and D. McManigill, *Anal. Chem.*, 58 (1986) 166.
7 S. Terabe, K. Otsuka, K. Ichikawa and T. Ando, *Anal. Chem.*, 56 (1984) 111.
8 S. Terabe, K. Otsuka and T. Ando, *Anal. Chem.*, 57 (1985) 834.
9 D. E. Burton, M. J. Sepaniak and M. P. Maskarinec, *J. Chromatogr. Sci.*, 24 (1986) 347.
10 M. J. Sepaniak and R. O. Cole, *Anal. Chem.*, 59 (1987) 472.
11 A. T. Balchunas and M. J. Sepaniak, *Anal. Chem.*, 59 (1987) 1466.
12 K. Otsuka, S. Terabe and T. Ando, *J. Chromatogr.*, 332 (1985) 219.
13 D. E. Burton, M. J. Sepaniak and M. P. Maskarinec, *Chromatographia*, 21 (1986) 583.
14 A. S. Cohen, S. Terabe, J. A. Smith and B. L. Karger, *Anal. Chem.*, 59 (1987) 1021.
15 S. Fujiwara and S. Honda, *Anal. Chem.*, 59 (1987) 2773.
16 P. Jandera and J. Churaček, *J. Chromatogr.*, 197 (1980) 181.
17 F. L. Vandemark and G. J. Schmidt, *J. Liq. Chromatogr.*, 4 (1981) 1157.
18 R. M. Kothari and M. W. Taylor, *J. Chromatogr.*, 247 (1982) 187.
19 T. Cannella and G. Bichi, *Bull. Chim. Farm.*, 122 (1983) 205.
20 F. L. Lam, I. J. Holcomb and S. A. Fusari, *J. Assoc. Off. Anal. Chem.*, 67 (1984) 1007.

QUANTITATIVE ANALYSIS OF RESINS USED IN FIBER-REINFORCED COMPOSITES BY REVERSED-PHASE LIQUID CHROMATOGRAPHY

D. NOËL*, K. C. COLE and J.-J. HECHLER

National Research Council Canada, Industrial Materials Research Institute, 75 Boulevard de Mortagne, Boucherville, Québec J4B 6Y4 (Canada)

(First received September 17th, 1987; revised manuscript received February 18th, 1988)

SUMMARY

   An improved reversed-phase liquid chromatographic method has been developed to analyze the epoxy resin present in a typical fiber-reinforced composite system, Narmco Rigidite 5208/WC3000. After solvent extraction of the resin from the prepreg (continuous-fiber reinforcement preimpregnated with partially cured resin) using tetrahydrofuran, acetophenone is added as an internal standard in order to obtain reproducible quantitative results. The separation is achieved with a linear water–acetonitrile gradient (50% to 100% acetonitrile in 15 min). The peak area or peak height is measured and normalized with respect to the acetophenone peak and the weight of the extracted epoxy resin. A reproducibility of less than 3% relative standard deviation was obtained for quantitative measurements of the main peaks. A smaller standard deviation was obtained with peak height than with peak area measurements but the latter is recommended for definitive quantitative analysis since the results are less column-dependent and permit easier interlaboratory comparison. The main peaks in the Narmco 5208 chromatogram have been identified by comparison of their retention times with those of individual components and by infrared spectroscopy of collected fractions. Several batches of Narmco 5208 prepreg have been analyzed and their compositions estimated by comparing the results with those obtained for the individual components of the system.

INTRODUCTION

   Fiber-reinforced polymer-matrix composites are widely used in the aerospace industry to make sophisticated structural parts[1,2]. At the present time, the most common materials employed are epoxy resin as matrix and carbon or polyamide fibers as reinforcement. Variations in the chemical composition of the polymer matrix can have significant effects on the processing and on the final properties of these composites. Analytical techniques such as infrared spectroscopy or liquid chromatography must be used to obtain reliable information on the organic matrix composition of these products[3].

   High-performance liquid chromatography (HPLC) appears to be one of the

most useful techniques for characterizing such systems[4-6], and experiments involving different modes of separation have established reversed-phase liquid chromatography (RPLC) as the most widely used method. LC can be used to check the batch-to-batch reproducibility of neat epoxy resin or of prepreg (continuous-fiber reinforcement preimpregnated with partially cured resin), to determine the composition of an epoxy system, or to follow the aging of a prepreg. Epoxies have often been characterized by a "fingerprint" analysis to reveal the presence and relative amounts of different components on a chromatogram[4]. However, this technique is of limited usefulness for precise quantitative definition of such systems. Hagnauer and Setton[5] and Hagnauer[6] have calculated the weight percent of major components (epoxy or hardener) in epoxy systems by performing calibration with standard solutions of components corresponding to individual peaks. This requires the isolation of the pure compounds from the commercial products, a tedious and time-consuming procedure. An alternative is to perform calibration with the commercial resins used to formulate the prepreg system. This procedure is complicated by the fact that these resins are usually mixtures involving a number of different molecules, and the samples used for calibration may not have exactly the same composition as those used in the prepreg. The methods just described have been used to qualitatively follow the advancement of the curing reaction on a short-term basis. However, to compare batches of epoxy resin over a long time interval, accurate quantitative methods must be developed. This paper describes the optimization of the separation of an epoxy resin by RPLC and compares various methods for the quantitation of the peaks in the chromatogram. The use of an internal standard is proposed, and parameters influencing the quantitative analysis are carefully examined in order to obtain the most reproducible results and hence to facilitate quality control over a long period of time or comparison of results among different laboratories. A common commercial system, Narmco Rigidite 5208, has been chosen for this purpose.

EXPERIMENTAL

Apparatus

The chromatography system consisted of a Varian Model 5000 liquid chromatograph (Varian, Palo Alto, CA, U.S.A.) with an automatic universal injector (10 μl loop) Model 7216 (Rheodyne, Cotati, CA, U.S.A.). The detector was a Varian variable-wavelength detector Model UV-100 with a 4.5-μl flow cell. Chromatograms were recorded on a Varian Vista 401 data station and transferred to an Apple II+ computer (Apple, Cupertino, CA, U.S.A.) via an RS-232 interface to perform additional data processing. The columns used were purchased pre-packed and are as follows: MCH-5-n-CAP (Varian), 30 cm × 4.0 mm I.D., 5 μm particles; and Hypersil MOS-1 (Shandon), 25 cm × 4.6 mm I.D., 5 μm particles. Infrared spectral measurements were done on a Nicolet 170SX Fourier transform instrument equipped with a mercury cadmium telluride detector.

Chemicals

Water, acetonitrile and tetrahydrofuran (THF) were Fisher HPLC-grade (Fisher Scientific, Fair Lawn, NJ, U.S.A.). Epoxy resin Araldite MY 720 and Hardener HT 976 were obtained from Ciba-Geigy (Hawthorne, NY, U.S.A.). Epoxy resin

Epi-Rez SU-8 was from Celanese Polymer Specialities (Louisville, KY, U.S.A.). These products were stored in a refrigerator. Carbon-epoxy prepregs Rigidite 5208/WC3000 were obtained from Narmco Materials (Anaheim, CA, U.S.A.). They were stored in a freezer at all times except for sampling and performance of experiments.

Procedure

In the case of prepreg samples, the epoxy resin system was extracted at room temperature from a piece of prepreg about 5 cm × 5 cm with three consecutive extractions (about 15 min each) using 50, 30, and 20 ml of THF. This is the most effective solvent to dissolve the resin[7]. The resin concentration in the combined extract was about 6 mg/ml. The exact weight of resin extracted was determined by recovering, drying, and weighing the carbon fibers, and subtracting this weight from the initial prepreg weight. A known quantity of acetophenone (*ca.* 100 μg/ml) was added to the extract as internal standard. In the case of neat resin, solutions were prepared in THF. All solutions and extracts were filtered through a Millex-SR 0.5-μm filter unit (Millipore, Bedford, MA, U.S.A.) before injection on the column. For the resin separation, the eluent composition was changed linearly from 50% acetonitrile in water to 100% acetonitrile over 15 min, maintained at 100% acetonitrile for a further 15 min, and then returned to the initial composition over a 1-min period. The flow-rate was kept constant during the gradient run at 1.0 ml/min. The wavelength of detection was 230 nm and the column was kept at 25°C. In order to obtain infrared spectra of the major components, peaks were collected manually. They were analyzed by attenuated total reflection after depositing the solution on a KRS-5 prism and evaporating the eluent to leave a thin film.

RESULTS AND DISCUSSION

Separation and identification of peaks

Several isocratic and gradient elution methods involving various mixtures of water and organic solvents, such as acetonitrile, methanol or THF, were tested using an MCH-5-n-CAP column. Separations with isocratic eluents were always poor and gradient elution was found to be the best way to achieve an efficient separation in a reasonable time. Fig. 1 shows a typical chromatogram of the Narmco 5208 resin obtained with the linear acetonitrile–water gradient described in the Experimental section. The separation is realized in about 25 min with an excellent resolution of the main peaks.

It is very difficult to identify all the peaks in the chromatogram but the main ones must be known in order to properly characterize the system. Narmco Rigidite 5208 has been reported[8-10] to contain three main components: the principal epoxy resin, based on tetraglycidyl-4,4′-diaminodiphenylmethane (TGDDM), about 67% by weight; an amine hardener, 4,4′-diaminodiphenylsulfone (DDS), about 23% by weight; and a second epoxy resin, based on bisphenol A Novolac, about 10% by weight. Both epoxy resins are complex mixtures of monomer, higher oligomers, and by-products.

The identity of the most important peaks was established by running samples of the individual components present in the resin, by performing Fourier transform
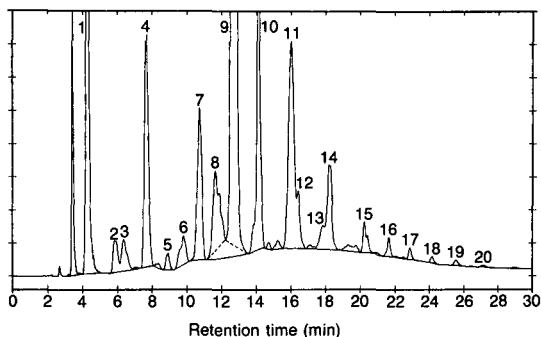
Fig. 1. Chromatogram of the extract of Narmco 5208 prepreg, batch 1103. Column: MCH-5-n-CAP, 30 cm × 4.0 mm I.D. See Experimental section for other details. Identification of major peaks: (1) DDS; (4) acetophenone; (7) reaction product; (9) TGDDM; (10) DGEBA.

infrared spectroscopy on recovered fractions, and by examining chromatograms of prepreg samples which had been partially polymerized by heating for periods up to 4 h at 100°C. In the latter case, peaks 1, 9, and 10 decreased steadily with heating time. They can be assigned respectively to DDS monomer, TGDDM monomer (from the major epoxy), and diglycidyl ether of bisphenol A (DGEBA) monomer (from the minor epoxy). Peak 7 was the only one or any importance to show an increase with heating, and its infrared spectrum showed bands characteristic of both TGDDM and DDS. It is therefore assigned to the initial reaction product of these two species. After some time, the quantity tends to stabilize because this molecule reacts further to form the polymer. Peak 4 corresponds to acetophenone added as internal standard. Peak 6, which is not found in any of the three starting materials, does not change significantly on heating, indicating that it is not a reaction product.

Fig. 2 shows the chromatogram and peak assignment obtained with the Hypersil MOS-1 column. The resolution is even better than with the MCH-5-n-CAP column, and the separation is achieved in a shorter time. The two peaks marked with an asterisk were not observed in any of the three starting materials. They could be due to an impurity in one of the particular batches used to make the prepreg or they
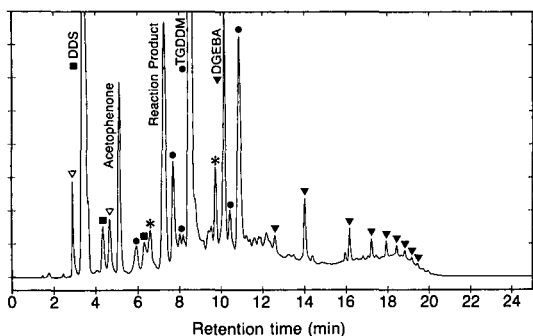
Fig. 2. Chromatogram of the extract of Narmco 5208 prepreg, batch 1103. Column: Hypersil MOS-1, 25 cm × 4.6 mm I.D. See Experimental section for other details. Symbols indicate origin of peaks: (▽) THF; (●) MY 720; (■) HT 976; (▼) SU-8; (∗) unknown.

could result from a coupling agent used to treat the surface of the carbon fiber reinforcement. They do not appear to be due to a reaction product since they do not become more intense when the prepreg is heated.

Internal standard

There are various methods for the quantitation of the peaks in the chromatogram: the ratio of the peak area with respect to the TGDDM peak, the relative area with respect to the total area, and the internal standard. The method using an internal standard is the most precise because it gives a result which is directly related to the percentage by weight of the compound in question. It could detect even foreign components which do not appear in the chromatogram, if they are present in significant amounts. However, this method is more complicated, requires more care, and is more subject to weighing errors during the preparation of solutions.

To find a suitable internal standard for use with Narmco 5208, several compounds (*p*-xylene, toluene, benzene, benzaldehyde, acetophenone) were tested using the chromatographic conditions described previously. The first three are inappropriate as regards the retention time; they are eluted in the same region as other peaks. Benzaldehyde has a suitable retention time but seems difficult to obtain commercially with sufficient purity, since injection of this product gave a chromatogram with several impurity peaks. The best internal standard was acetophenone. To account for variations in the weight of resin, after the peak areas or peak heights are divided by that of acetophenone they are normalized to a standard resin weight of 100 times the acetophenone weight:

$$\text{Normalized response} = \frac{\text{Response of peak}}{\text{Response of acetophenone}} \cdot \frac{\text{Wt. acetophenone}}{\text{Wt. resin}} \cdot 100$$

This gives normalized peak intensities in the range of 0.2 to 20.

Reproducibility

Regardless of the method of calculation, the baseline used for the evaluation of the peak area or the peak height must be clearly established to avoid quantitation differences between the chromatograms. This requirement, which is often neglected, is particularly important for comparing results obtained over a long time interval or even for comparing results obtained on different columns. Fig. 1 shows the baseline selected for this work. The ideal case consists of well-resolved peaks where baselines are drawn from valley to valley. In a complex chromatogram such as that of an epoxy resin system, it is not always possible to apply this principle unequivocally. For example, if the baseline is drawn from valley to valley for peaks 8 and 9 as shown in Fig. 1 by dotted lines, the peak area or height will be sensitive to the degree of resolution of the two peaks. Thus, it is advisable to draw a baseline closely following the base level of the chromatogram in order to minimize the variation in the measurement of peak area or peak height.

In the first experiment performed, a known quantity of acetophenone (10 μl, 10.28 mg) was added directly to the prepreg extract with a microsyringe. The reproducibility with respect to the extraction was checked by analyzing three different extracts of resin from the same sheet of prepreg. The percentages by weight of resin

extracted were respectively 40.15%, 39.23%, and 38.82%. Four injections were then performed for each extract, giving a total of twelve chromatograms for averaging. An MCH-5-n-CAP column was used. The data were analyzed by the three different methods using both peak area and peak height. Table I (columns 2 to 4) reports the results obtained for the most important peaks using peak area.

Chen and Hunter[7] have proposed the use of the strongest epoxy peak (TGDDM) as a reference. The ratio DDS–TGDDM can be used to evaluate the resin composition and the ratio of the reaction product peak against the TGDDM peak serves to follow the advancement of the resin. When the results are calculated in this way, as shown in the second column of Table I, the relative standard deviations are generally quite low. While this method may be adequate for quality control of a well-characterized prepreg system, it may not be sensitive to all variations in composition which may occur, since it uses only the ratios of a few well-defined peaks.

The results calculated in terms of relative peak areas, defined as the peak area divided by the total area of the chromatogram (sometimes called internal normalization), are given in the third column of Table I. The relative standard deviations are similar to those of the peak ratio method. However, when applied to different batches over a longer interval, this method is subject to complications. The problem is that the results are affected by all the peaks in the chromatogram, and these can have different response factors. Consequently, when changes occur in the chromatogram, their magnitude may not be truly indicative of the importance of the compositional variations.

TABLE I

QUANTITATIVE RESULTS FOR NARMCO 5208 PREPREG, BATCH 1103, BASED ON PEAK AREAS

Relative standard deviations are reported in parentheses. In experiments 1 and 2 the columns MCH-5-n-CAP (30 cm × 4.0 mm I.D.) and Hypersil MOS-1 (25 cm × 4.6 mm I.D.) were used, respectively. ACP = Acetophenone (internal standard), RP = reaction product.

Peak No.	Experiment 1			Experiment 2
	$\dfrac{Peak\ area}{TGDDM\ area}$	Relative peak area	Normalized area ACP direct addition	Normalized area ACP solution
1 (DDS)	0.3548	15.86	4.810	3.43
	(1.7%)	(1.6%)	(1.6%)	(4.7%)
7 (RP)	0.0888	3.968	1.204	1.738
	(2.5%)	(2.0%)	(3.8%)	(1.1%)
8	0.0949	4.244	1.288	0.550
	(1.4%)	(0.8%)	(1.8%)	(0.7%)
9 (TGDDM)	–	44.71	13.56	11.98
		(0.8%)	(3.1%)	(0.8%)
10 (DGEBA)	0.1385	6.194	1.879	1.042
	(0.7%)	(0.2%)	(2.5%)	(1.3%)
11	0.1470	6.573	1.994	1.335
	(1.6%)	(1.3%)	(3.6%)	(0.9%)
16	0.0083	0.369	0.112	0.064
	(9.9%)	(9.8%)	(7.7%)	(4.4%)

The use of an internal standard such as acetophenone overcomes many of the disadvantages associated with the other methods. The fourth column of Table I shows that with this method the relative standard deviation is slightly higher than for the previous two methods, but is under 4% for the main peaks. Thus, the normalization procedure with an internal standard is preferred for evaluating the chromatogram of an epoxy resin system. Its main advantage is to eliminate any effects of variation in instrumental response and loss of solvent. If pure components are available for calibration, it can be used to determine the actual percentage of these components in the resin.

Although the results just presented may be considered acceptable, direct addition of 10 μl of acetophenone with a microsyringe to the prepreg extract can produce a significant error in the amount of acetophenone. In order to improve the reproducibility of the LC method, a second experiment was subsequently performed using a different approach. A standard solution of acetophenone in THF was prepared and an aliquot of this solution was added to the prepreg extract. The standard solution consists of 0.5 ml of acetophenone in 50 ml of THF, and each component is accurately weighed to determine the percent by weight of acetophenone (about 1.1%). A 1-ml aliquot of this solution is added to an Erlenmeyer flask, with weighing before and after to allow calculation of the exact quantity of acetophenone added (about 10.2 mg). To this is added the prepreg extract, prepared as described in the Experimental section, containing a known weight of epoxy resin. This gives a solution in which the ratio of acetophenone to epoxy resin is precisely known. For this experiment, a Hypersil MOS-1 column was used.

TABLE II

QUANTITATIVE RESULTS FOR NARMCO 5208 PREPREG, BATCH 1103, BASED ON PEAK HEIGHTS

Relative standard deviations are reported in parentheses. In experiments 1 and 2 the columns MCH-5-n-CAP (30 cm × 4.0 mm I.D.) and Hypersil MOS-1 (25 cm × 4.6 mm I.D.) were used, respectively. ACP = Acetophenone (internal standard), RP = reaction product.

Peak No.	Experiment 1		Experiment 2
	Peak height / TGDDM height	Normalized height ACP direct addition	Normalized height ACP solution
1 (DDS)	0.7790 (0.8%)	10.78 (1.3%)	2.074 (3.0%)
7 (RP)	0.0777 (1.7%)	1.075 (1.2%)	1.217 (0.3%)
8	0.0441 (1.2%)	0.611 (1.6%)	0.4811 (0.3%)
9 (TGDDM)	—	13.84 (0.5%)	11.72 (0.2%)
10 (DGEBA)	0.1508 (2.0%)	2.088 (2.1%)	1.173 (2.3%)
11	0.1082 (0.2%)	1.498 (0.7%)	1.047 (1.0%)
16	0.0104 (5.2%)	0.144 (5.3%)	0.098 (2.7%)

The last column of Table I shows the results obtained using this procedure. Comparison of the relative standard deviations with those in the next-to-last column shows for the most part a significant decrease when a standard solution is employed instead of a direct addition of 10 μl of acetophenone.

In isocratic elution, it has been shown that peak height measurements are more precise than peak area measurements[11]. Peak heights are less subject to interference by adjacent, overlapping peaks. For equivalent accuracy, a lower degree of resolution is required for quantitation by peak height than by peak area.

Table II reports results calculated from the same chromatograms as Table I using the peak height instead of the peak area. A comparison with Table I shows that in general this gives lower relative standard deviations. The chromatogram of the epoxy resin system being complex, there are many overlapping peaks. Thus, accurate measurement of the area is more difficult. As in Table I, the use of an acetophenone solution gives more reproducible results than direct addition. Although in the present case height measurements give a lower standard deviation than peak area, area measurements are recommended for quantitative analysis of an epoxy resin chromatogram on a long-term basis because peak areas are less sensitive to changes in column efficiency. Comparison of results obtained with different columns or in different laboratories will be facilitated with this procedure. However, peak height measurement is recommended for characterizing an epoxy resin when the same column is used to compare several different samples over a limited time interval.

Splitting of the DDS peak

Comparison of the normalized values (area or height) obtained in the two experiments just described shows significant differences between them, especially in the case of the normalized height for the DDS peak (peak 1). A period of 2.5 years separates the two analyses and the results show that the prepreg aged somewhat during this time, probably because it had been thawed several times for sampling. The significant changes which occur over time underline the importance of good quality control of these materials. The values of the normalized height decreased for the main epoxy TGDDM peak (13.84 to 11.72), the minor epoxy DGEBA peak (2.09 to 1.17), and the DDS peak (10.78 to 2.07), while the reaction product peak increased (1.075 to 1.217). Since the amount of TGDDM in Narmco 5208 exceeds the amount required for stoichiometric reaction with the DDS, it is not surprising that the free DDS disappears relatively fast compared to the TGDDM. However, the apparent decrease in DDS is quite substantial and is much greater when peak heights are used than when areas are used. A further unusual observation was that the relative standard deviation for the DDS peak is considerably worse with the Hypersil MOS-1 column than with the MCH-5-n-CAP column.

Since the efficiency of the Hypersil MOS-1 column is better than that of the MCH-5-n-CAP column, a splitting of the DDS peak was observed in some chromatograms. This is illustrated in Fig. 3 for two different injections of the Narmco 5208 system. In one case, there is only one peak with a small shoulder, but in the other, two peaks are detected in addition to the shoulder. It is difficult to establish the origin of the different peaks; they may result from the presence of different isomers in the industrial hardener. Since the resolution with the MCH-5-n-CAP column is not good enough to separate the two peaks, this phenomenon was not observed before.
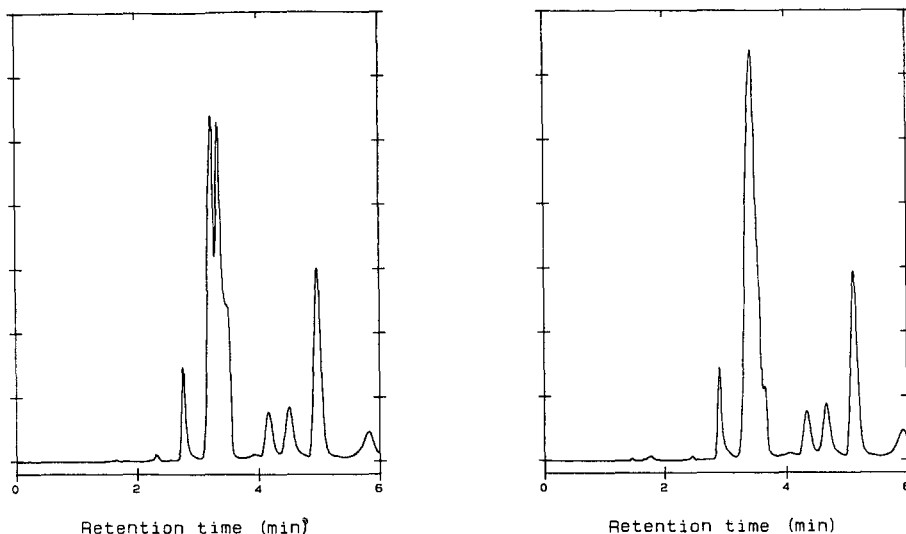
Fig. 3. Chromatograms of Narmco 5208 showing splitting of the DDS peak. Column: Hypersil MOS-1, 25 cm × 4.6 mm I.D. See Experimental section for other details.

This result underlines one of the main problems of gradient elution, namely the regeneration of the column. The splitting of the DDS peak is not always present and this is attributed to the initial conditions of the column. If, for some reason, the equilibrium between the stationary phase and the mobile phase is not always identical, certain experimental conditions can favour the separation of the DDS components whereas in other conditions, they will be completely unresolved.

The splitting of the peak obviously influences the peak height to a significant extent. The major DDS peak seems to be the first one and its height was used for the calculation. This explains the unusually low value obtained for the normalized height with the Hypersil column. Thus, a column with excellent resolution has some advantages but it must be used with circumspection in the case of the DDS peak. For quantitative measurements, it is advisable to calculate the normalized area using the combined area of these peaks, since the different compounds are included in the single peak of DDS when the separation is not complete.

Comparison of different batches of Narmco 5208 resin

Different batches of the Narmco Rigidite 5208 epoxy resin system were analyzed by RPLC on the MCH-5-n-CAP column. They included five prepreg samples (batches 1010, 1014, 1101, 1103, 1104), one sample of neat resin on a plastic backing sheet (batch 1047) and one of neat resin in bulk form (batch 1023). The results are reported in Table III as normalized areas with respect to acetophenone internal standard. In addition, ratios with respect to the TGDDM peak are reported for the main peaks of interest. These ratios are independent of the presence of acetophenone.

An estimation of the actual percentages of the two epoxy resins and the hardener in Narmco 5208 was also performed by measuring chromatograms for the individual components Hardener HT 976, Araldite MY 720, and Epi-Rez SU-8. For

each component, THF solutions were prepared containing a known concentration of acetophenone and varying known concentrations of the particular component. For each solution, the RPLC chromatogram was measured, and a normalized peak area calculated based on the main peak (DDS, TGDDM, or DGEBA, depending on the component). For a particular component, the response is effectively the same for all the solutions and the average value corresponds to a concentration of 100%. The respective values obtained for Hardener HT 976, Araldite MY 720, and Epi-Rez SU-8 are 27.7, 20.0, and 12.2. The ratio of the normalized area of the peak of interest in a sample of Narmco 5208 against that obtained for the corresponding pure component gives an estimate of the percentage of the particular component in the resin. The calculation is somewhat approximate since it is based on only the major peak of each component, and it assumes that each component in the epoxy mixture has the same composition as the product used for calibration. It should be noted that the percentages determined correspond to unreacted material, so the sum will be less than 100% if the resin is advanced. Table IV reports the values obtained for the different batches of Narmco 5208.

Examination of Tables III and IV shows that appreciable variations can be observed. For example, batch 1047 is the least advanced since it has high values for free DDS and TGDDM (peaks 1 and 9) and the lowest value for peak 7, which is the product of the reaction between TGDDM and DDS. However, the content of free DGEBA (peak 10, from the Novolac epoxy) is abnormally low compared to the other batches. The low value calculated for Novolac in Table IV underlines this fact. It appears that this batch is unbalanced with respect to the usual composition. Batch 1023 lies at the other extreme, having low values for free TGDDM, DDS and DGEBA, and the highest value for the reaction product. Although it consists of neat resin, it is more advanced than all the prepreg samples, probably the result of undue heating at some point in this history. In Table IV, the sum of the three components is only 78% and this also indicates a high degree of advancement.

TABLE III

RPLC RESULTS FOR DIFFERENT BATCHES OF THE NARMCO 5208 SYSTEM; NORMALIZED AREAS WITH RESPECT TO ACETOPHENONE, AND AREA RATIOS WITH RESPECT TO TGDDM

Column: MCH-5-n-CAP (30 cm × 4.0 mm I.D.).

Peak No.	Batch No.						
	1047	1103	1104	1014	1101	1010	1023
1 (DDS)	4.795	4.810	4.311	4.130	3.600	3.719	3.034
7 (RP)	1.110	1.204	1.336	1.623	1.742	1.785	2.406
8	0.836	1.288	0.690	0.831	0.612	0.638	0.830
9 (TGDDM)	13.54	13.56	13.19	13.37	12.72	12.70	12.33
10 (DGEBA)	0.792	1.879	1.626	1.552	1.324	1.185	0.709
11	0.898	1.994	1.899	–	1.474	0.668	0.567
16	0.136	0.112	0.101	0.127	0.082	0.107	0.026
1/9	0.354	0.355	0.327	0.309	0.283	0.293	0.246
7/9	0.082	0.089	0.101	0.121	0.137	0.141	0.195
10/9	0.058	0.139	0.123	0.116	0.104	0.093	0.057

TABLE IV

PERCENTAGE (BY WEIGHT) OF EACH COMPONENT IN DIFFERENT BATCHES OF NARM-
CO 5208 EPOXY RESIN

Batch No.	HT 976	MY 720	Novolac	Sum
1047	17.3	67.7	6.5	91.5
1103	17.4	67.7	15.5	100.6
1104	15.6	65.9	13.4	94.9
1014	14.9	66.9	12.8	94.6
1101	13.0	63.5	10.9	87.4
1010	13.5	63.4	9.7	86.6
1023	11.0	61.4	5.8	78.2
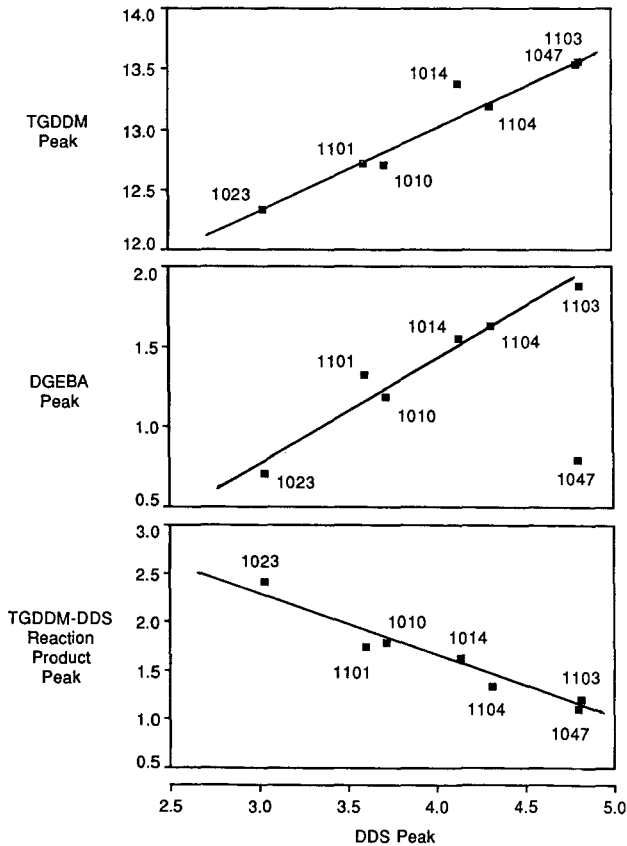
Fig. 4. Variation of the normalized peak area of the TGDDM peak, the DGEBA peak, and the reaction product peak as a function of the normalized peak area of DDS, for different batches of Narmco 5208.

Comparison of the five prepreg samples shows results which are in better agreement. Generally speaking, batches 1101 and 1010 are very similar to each other, while the other three (1103, 1104 and 1014) are also similar to each other but somewhat less advanced than the first two. In Table III, the batches are arranged approximately in order of increasing degree of advancement. The relationships between some of the main peaks are shown graphically in Fig. 4, where the normalized peak areas for the reaction product, DGEBA, and TGDDM are plotted against those of DDS. There are obvious correlations. In general, a decrease in free DDS correlates with a decrease in TGDDM and DGEBA and an increase in reaction product, as expected based on the nature of the curing reaction. These results indicate that the batches differ mainly in degree of reaction advancement and not in initial composition. One exception is batch 1047, which deviates considerably from the linear relationship in the case of the DGEBA peak. This batch appears to have a low Novolac content.

The same trends are evident whether the normalized peak intensities or the peak ratios are used as an indicator. However, the normalized peak intensities provide a more complete picture of the variations in composition.

CONCLUSION

RPLC is an excellent technique for analyzing epoxy resin systems such as Narmco 5208. The separation has been optimized by using a gradient elution method with acetonitrile–water with UV detection at 230 nm. The addition of acetophenone as an internal standard permits accurate quantitative analysis using a normalization of the peak area or peak height with respect to the weight of the extracted resin and the weight of added acetophenone. A lower relative standard deviation is obtained with a standard solution of acetophenone rather than a direct addition of acetophenone to the prepreg extract. For interlaboratory comparison and for comparison of analyses involving different columns, peak area measurements are recommended, even though the standard deviations are slightly higher than for peak height measurements. However, the baseline used for the evaluation of the peak area or the peak height must be clearly established to avoid quantitation differences between the chromatograms. A Hypersil MOS-1 column gives excellent resolution, but care must be exercised in analyzing the DDS peak because of a splitting observed in some chromatograms.

The main peaks in the chromatograms have been identified, including that of the reaction product between TGDDM and DDS. This peak is useful for following the aging of a prepreg.

ACKNOWLEDGEMENTS

REFERENCES

1 C. Y. Kam and J. Gaidulis, *Natl. SAMPE Tech. Conf.*, 15 (1983) 251.
2 M. M. Schwartz, *Composite Materials Handbook*, McGraw-Hill, New York, 1984.
3 K. C. Cole, D. Noël, J.-J. Hechler, *Natl. SAMPE Symp. Exhib. Proc.*, 30 (1985) 624.
4 S. A. Mestan and C. E. M. Morris, *J. Macromol. Sci. Rev. Macromol. Chem.*, 24 (1984) 117.
5 G. L. Hagnauer and I. Setton, *J. Liq. Chromatogr.*, 1 (1978) 55.
6 G. L. Hagnauer, *Polym. Compos.*, 1 (1980) 81.
7 J. S. Chen and A. B. Hunter, *Development of Quality Assurance Methods for Epoxy Graphite Prepregs*, Technical Report NASA-CR-3531, NTIS Document N82-22318, 1982.
8 J. F. Carpenter, *Quality Control of Structural Nonmetallics*, Report prepared for Naval Air Systems Command, Contract No N00019-76-c-0138, NTIS Document AD-A042853, Washington, July, 1977.
9 E. S. W. Kong, S. M. Lee and H. G. Nelson, *Polym. Compos.*, 3 (1982) 29.
10 H. S. Chu and J. C. Seferis, *Polym. Compos.*, 5 (1984) 124.
11 R. W. McCoy, R. L. Aiken, R. E. Pauls, E. R. Ziegel, T. Wolf, G. T. Fritz and D. M. Marmion, *J. Chromatogr. Sci.*, 22 (1984) 425.

CHROM. 20 532

STUDIES ON SAMPLE PRECONCENTRATION IN ION CHROMATO-GRAPHY

VIII. PRECONCENTRATION OF CARBOXYLIC ACIDS PRIOR TO ION-EX-CLUSION SEPARATION

P. R. HADDAD* and P. E. JACKSON

Department of Analytical Chemistry, University of New South Wales, P.O. Box 1, Kensington, N.S.W. 2033 (Australia)

SUMMARY

A procedure for the preconcentration of low-molecular-weight carboxylic acids is reported. Up to 50 ml of a sample containing trace levels of carboxylic acids was loaded onto a low-capacity anion-exchange precolumn conditioned with an eluent of methanesulphonate at pH 9.0. The carboxylate anions were found to bind quantitatively to the precolumn even when the sample contained predominantly neutral, undissociated acids. The bound ions were then transferred to an ion-exclusion analytical column using methanesulphonic acid at pH 2.7 and eluted from the analytical column with the same eluent. UV detection at 200 nm was used. The method was used for the simultaneous analysis of formic, acetic, propionic and butyric acids, giving detection limits of 5.9, 9.4, 5.6 and 9.2 ppb, respectively, for a 10-ml sample volume, and a precision of 1.85% relative standard deviation. The procedure was successfully applied to the determination of carboxylic acids in Antarctic ice.

INTRODUCTION

Ion-exclusion chromatography is widely used for the determination of carboxylic acids. This technique, first described by Wheaton and Bauman in 1953[1], utilises a cross-linked, resin-based, cation-exchange column to effect the separation of weak acids (both organic and inorganic) and even small neutral species. Strong acid anions are excluded from the resin according to the Donnan principle and elute at the void volume of the column[2]. Weaker acid anions existing largely in the molecular form are retained on the stationary phase by a combination of ion exclusion, size exclusion and hydrophobic interactions. For low-molecular-weight acids, ion exclusion is the dominant retention mechanism and the retention times are strongly correlated with the pK_a of the acid[3]. Mineral acid solutions are typically used as eluents in ion-exclusion chromatography to ensure that the organic acids are predominantly in the molecular form, resulting in increased retention times. However, water has also been used as an eluent[3].

Detection of the eluted weak acid species has conventionally been carried out by spectrophotometric methods, although recently other detection methods have also been used. Most aliphatic carboxylic acids absorb only weakly, hence the sensitivity obtained when using direct UV detection is poor. Detection limits for these solutes are typically of the order of 1 ppm or greater with spectrophotometric detection[1]. Lower detection limits have been reported for other solutes, such as 10 ppb* for dimethyl sulphoxide after separation on an ion-exclusion column using direct UV detection at 195 nm (ref. 4).

Conductimetric detection may be used with a hydrochloric acid eluent after suppression of the background conductivity with a cation-exchanger in the silver form[5], although the suppressor column ultimately becomes blocked with precipitated silver chloride. Itoh and Shinbori[6] found that non-suppressed conductimetric detection was possible in ion-exclusion chromatography when weakly conducting carbonic acid was used as the eluent. Tanaka and Fritz[7] have reported a similar approach using a benzoic acid eluent and they achieved detection limits from 60 ppb to 1.4 ppm for the C_1–C_4 aliphatic carboxylic acids. The same authors[8] have recently reported the use of post-separation "enhancement" columns for conversion of carbonic acid to the more conductive anionic form to improve detection sensitivity. A detection limit of 90 ppb was achieved using two enhancement columns in series. A similar approach has been presented by Murayama et al.,[9] who used a suppressor column which exchanged H^+ for K^+ to achieve conversion of the weak acid solute to the more conductive anionic form and the background eluent (sulphuric acid) to the less conductive potassium sulphate. Sensitivity for acetic acid was increased 33 fold using the suppressor column.

Electrochemical detection[10] has also been used in conjunction with ion-exclusion chromatography for the determination of sulphite. Sulphuric acid was used as the eluent and a detection limit of 100 ppb was obtained; however, this approach is of limited utility in ion-exclusion chromatography as most of the solutes amenable to this separation mode are not electroactive.

The above discussion illustrates that detection limits for most weak acid species, even with the aid of suppressor and enhancement columns, are generally in the order of 100 ppb or greater and these are similar to detection limits obtained for anions by conventional ion chromatography. In ion chromatography the most common way to lower detection limits is to preconcentrate the solute ions from the sample onto a small ion-exchange precolumn. The trapped solute ions are then eluted to the analytical column for separation and quantitation[11,12]. However, the analogous approach is not viable for ion-exclusion chromatography because water acts an eluent and can elute the weak acid solutes from an ion-exclusion precolumn during sample loading.

In this paper we present an ion chromatographic preconcentration method for the analysis of trace levels of carboxylic acids. The solutes are trapped as anionic species on an anion-exchange concentrator column and eluted from this column as the neutral acid species, to be separated on an ion-exclusion analytical column, with subsequent detection by direct UV absorption.

---

* Throughout this article the American billion (10^9) is meant.

EXPERIMENTAL

Instrumentation

The liquid chromatograph used consisted of a Millipore Waters (Milford, MA, U.S.A.) Model M590 programmable pump and events unit, Model M481 variable-wavelength UV detector operated at 200 nm, Model M730 data module, two pneumatically controlled high-pressure, six-port, switching-valves and two low-pressure, solvent select valves. All the valves were combined in a Waters automated valve switching (WAVS) unit. A Model U6K injector was incorporated into the liquid chromatograph when manual injection was required.

A Bio-Rad (Richmond, CA, U.S.A.) HPX-87H organic acid analysis column (300 × 7.8 mm I.D.) was used as the analytical column. A Waters IC anion concentrator (5.0 × 6.0 mm I.D.) packed with methacrylate resin to give a total ion-exchange capacity of 2.15 μequiv. was used as the concentrator column. This column was housed in a Waters Guard Pak precolumn module. A schematic diagram of the apparatus is illustrated in Fig. 1 and Fig. 2 shows details of the interconnections of the valves.

Reagents

All water was doubly distilled and passed through a Millipore (Bedford, MA, U.S.A.) Milli-Q water purification apparatus. Standard solutions (1000 ppm) of formic, acetic, propionic and n-butyric acids were prepared by dissolving the appropriate amounts of the analytical-grade acids in pure water. These solutions were diluted daily with the aid of Gilson (Villiers, France) Pipetman autopipettes to give the required trace solutions.

Methanesulphonic acid (5 mM) operated at a flow-rate of 0.8 ml/min was used as the eluent for the separation of the organic acids, and methanesulphonate (5 mM)
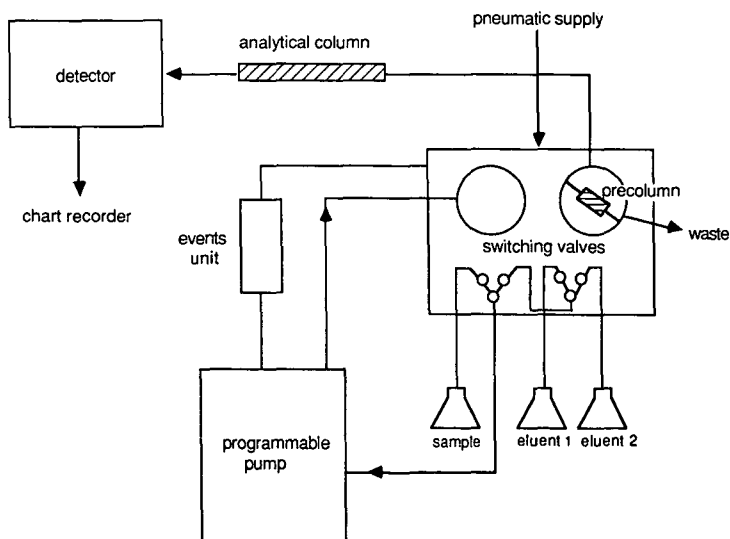
Fig. 1. Schematic diagram of the preconcentration apparatus employed in this study.
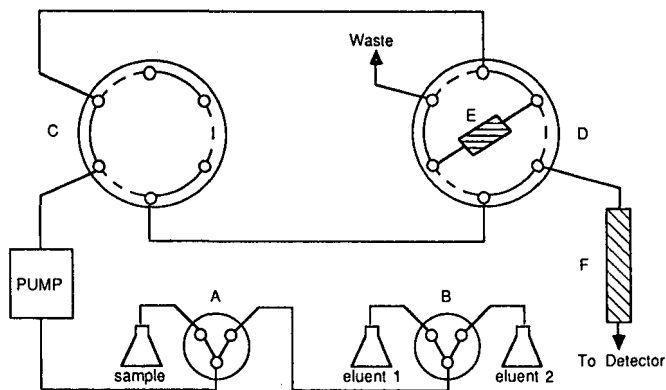
Fig. 2. Details of the interconnections of the valves. A, B = Low-pressure solvent select valves; C, D = high-pressure column switching valves; E = anion-exchange concentrator column; F = ion-exclusion column.

adjusted to a pH of 9.0 was used as the eluent to condition the concentrator column prior to sample loading. Eluents were diluted daily from stock solutions which were prepared by dissolving weighed amounts of analytical grade methanesulphonic acid in approximately 800 ml of water, after which the pH of the solution was adjusted (if required) by dropwise addition of 1.0 M lithium hydroxide and the solution diluted to 1 l. Each eluent was filtered through a 0.45-μm membrane filter and degassed in an ultrasonic bath before use.

Procedures

The preconcentration of samples was carried out by varying the flow-paths in a timed sequence, using a similar procedure to that previously reported by us for the preconcentration of anionic solutes[13]. This procedure was modified to include the use of two eluents and an outline of the basic program required for the preconcentration of organic acids is given in Table I.

RESULTS AND DISCUSSION

Selection of chromatographic approach

On-line preconcentration with ion-exchange concentrator columns is routinely used in ion chromatography for the determination of ionic solutes at the ppb level. Quantitative recovery of solute anions can be achieved for sample volumes up to 100 ml[14], provided appropriate conditions are chosen. The extension of this approach to the preconcentration of carboxylic acids using ion-exclusion concentrator and analytical columns is not practical because water acts as an eluent in ion-exclusion chromatography[3] and therefore the acids will not bind quantitatively to the concentrator column during the sample loading step.

Carboxylic acids may be preconcentrated in their anionic forms on an anion-exchange precolumn[15] but their separation by ion exchange is difficult because analytical ion exchangers exhibit very poor selectivity for carboxylate anions. In addition, it is likely that interference from inorganic anions will be encountered.

TABLE I

BASIC OUTLINE OF A TYPICAL PROGRAM FOR THE PRECONCENTRATION OF ORGANIC
ACIDS

Step No.	Solution delivered	Flow-rate (ml/min)	Volume delivered (ml)	Purpose of step
1	Eluent*	1.0	20.0	Equilibratio of ion-exchange precolumn
2	Sample	5.0	15.0	Flush pump and tubing with sample
3	Sample	1.0	10.0	Load sample onto pre-column
4	Eluent**	5.0	15.0	Flush pump and tubing with eluent 2
5	Eluent 2	0.5	1.0	Quantitatively strip acids from concentrator column
6	Eluent 2	0.8	16.0	Separate acids on analytical column***

 * 5 mM methanesulphonate, pH 9.0.
 ** 5 mM methanesulphonic acid, pH 2.7.
 *** The precolumn is removed from the flow-path for the separation step in order to minimise baseline drift. On completion of step 6, the program returns to step 1.

Alternatively, carboxylic acids could be preconcentrated in their anionic form on an ion-exchange precolumn, followed by elution of the trapped anions to an ion-exclusion analytical column, where they would be separated as the acid species. The major difficulty of this approach is to achieve reproducible, quantitative binding of the acidic solutes to the anion-exchange precolumn.

The form in which the carboxylic acid is present in the sample has an obvious influence of the degree of binding onto the concentrator column. If the ion-exchange selectivity coefficient for the carboxylate anion is sufficiently high, then this ion can be expected to be quantitatively bound provided that the sample does not contain significant concentrations of ionic species with greater selectivity coefficients. This binding will push the dissociation equilibrium of the acid towards increased ionisation, so that quantitative binding can be anticipated even for samples in which the acid is present predominantly in the neutral protonated form. Alternatively, the pH of the sample solution can be adjusted to a point where the carboxylic acids in the sample are present predominantly in their anionic forms and can therefore bind to the concentrator column.

Methanesulphonic acid, used at pH values of 2.7 or 9.0, was chosen as the eluent for two reasons. First, methanesulphonate at pH 9.0 was appropriate for conditioning of the concentrator column prior to sample loading since this eluent had been shown previously to permit quantitative binding of weakly retained anions during sample loading[16]. The pH of this eluent was high in order to encourage dissociation of the carboxylic acids. Second, methanesulphonic acid at pH 2.7 was suitable for the transfer of solutes to the ion-exclusion analytical column and for their subsequent separation since this eluent is known to give an excellent separation of car-

boxylic acids on the HPX-87H column[17]. Use of different eluents to condition the concentrator column and to separate the solutes is inadvisable because of the initial baseline disturbance created in the final chromatogram, even when direct UV detection was used. In fact, the greatest practical difficulty encountered when attempting to implement the proposed preconcentration method was the large disequilibration in the final chromatogram resulting when the ion-exchange precolumn was placed in-line with the ion-exclusion analytical column for transfer of the bound solutes. The use of the same concentration of eluent ion, *i.e.* 5 mM methanesulphonate, for the different stages of the preconcentration procedure minimised this disturbance to some extent, although a very large void peak still occurred.

Methanesulphonic acid, even at 5 mM, can also be used as an eluent with non-suppressed conductivity detection in ion-exclusion chromatography[17]. However, it was not possible to use conductivity detection with the precocentration approach described as the baseline disturbance at the start of the chromatogram was too great to allow quantitation of early eluting solutes.

Preconcentration of carboxylic acids

Fig. 3 shows the chromatogram obtained after preconcentrating a 10-ml mixture of 200–400 ppb C_1–C_4 aliphatic carboxylic acids on an anion-exchange precolumn, followed by ion-exclusion separation. Quantitative recoveries were obtained for all peaks since the peak areas agreed to within 1% with those obtained by direct injection of an equivalent amount (10 μl of 200–400 ppm) of the acids. The chromatogram also shows two additional peaks: a large solvent peak as previously dis-
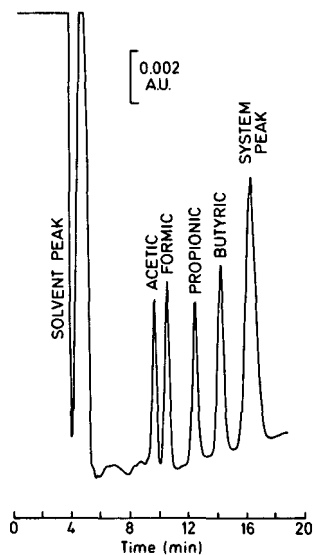
Fig. 3. Preconcentration of a standard solution of carboxylic acids. Conditions: concentrator column, Waters IC anion concentrator; analytical column, Bio-Rad HPX-87H organic acid analysis column. Eluents: 5 mM methanesulphonate at pH 9.0 (eluent 1) or pH 2.7 (eluent 2). Sample: 10 ml of 200 ppb formic, 400 ppb acetic, 200 ppb propionic and 400 ppb butyric acids loaded at a flow-rate of 1.0 ml/min. Strip volume: 700 μl. Detection: UV absorption at 200 nm, operated at 0.02 a.u.f.s.

cussed and a late eluting system peak. The system peak appeared when any preconcentration run was made and a small peak was also present when samples were injected directly without preconcentration. One possibility was that this peak was due to carbonate present in the samples, however no correlation could be found between the amount of carbonate or bicarbonate injected and the height of the system peak. The system peak may be attributable to an eluent impurity. The retention time of the system peak could be manipulated by changes in the eluent pH, so conditions could be found under which interference with carboxylate solutes was eliminated.

In the initial stages of this work, the sample solutions to be concentrated were neutralised with 0.01 M lithium hydroxide to ionise the acidic solutes and so encourage quantitative binding of the solutes on the precolumn. However, it was found that this step was unnecessary since the recoveries obtained for the preconcentration of untreated sample solutions were identical to those obtained when the acids were neutralised. It appears therefore that the carboxylate anions bind very readily to the concentrator column, and this promotes further dissociation of the acid. For very weak acids such as hydrogen cyanide, it would perhaps be necessary to neutralise the solution, although excess hydroxide in the sample should be avoided as it will compete with the acid anion for exchange sites on the precolumn and so decrease the range of linear sample loading.

Fig. 4 shows the calibration plots obtained when preconcentrating 10-ml volumes of formic, acetic and propionic acids (loaded individually). Detection limits, determined as the concentration producing a signal-to-noise ratio of 3, were 6, 9, 6 and 9 ppb for these acids and butyric acid, respectively, when using a 10-ml sample volume. Larger sample volumes also gave quantitative binding of the organic acid anions, just as in conventional ion chromatography[14]. The preconcentration of 50 ml of 50 ppb formic acid gave an identical peak to that obtained when preconcentrating 10 ml of 250 ppb formic acid. As the preconcentration apparatus used a single, high-precision pump to deliver the sample and eluents, excellent precision was obtained for the preconcentration procedure. A precision of 1.85% R.S.D. was obtained on ten preconcentration runs of 10 ml of 200 ppb formic acid.

The onset of breakthrough of formic acid (a relatively weakly retained anion) on the anion-exchange concentrator was investigated. Increasing concentrations of formic acid were loaded and the recoveries plotted against μequiv. of the solute loaded. The results (Fig. 5) show that breakthrough occurred at 0.34 μequiv., which corresponds to approximately 10 ml of 1.5 ppm formic acid. The binding affinity of formate on this type of concentrator column was similar to that found for chloride in a previous study (0.33 μequiv.)[18] and this reflects the similarity of the ion-exchange selectivity coefficients for these ions. The other carboxylic acids in the series gave slightly extended linear binding ranges.

This method has an obvious drawback in that organic acids could not be preconcentrated successfully in sample solutions containing even moderately high levels of other ionic species, particularly inorganic anions. In these cases, competition for binding sites could be expected from more strongly retained inorganic anions. However, this same limitation exists for any precolumn concentration method. A practical application of the proposed procedure is illustrated in Fig. 6, which shows the chromatogram obtained by preconcentrating 7 ml of a melted Antarctic ice sample. No sample pretreatment was used and the sample was found to contain 220 ppb
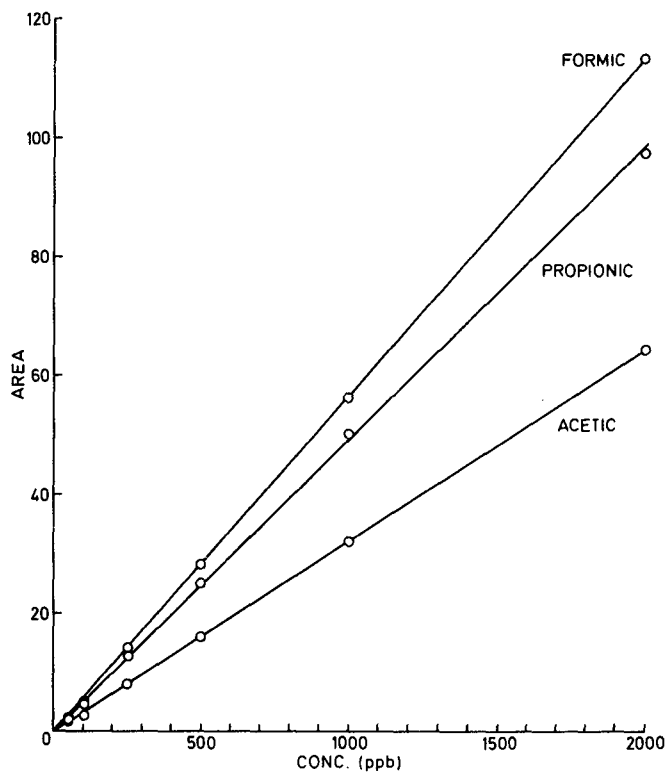
Fig. 4. Calibration plots obtained when loading 10-ml volumes of formic, acetic and propionic acids individually. Conditions as for Fig. 3, except that the sample concentrations varied as shown and a strip volume of 1.0 ml was used.
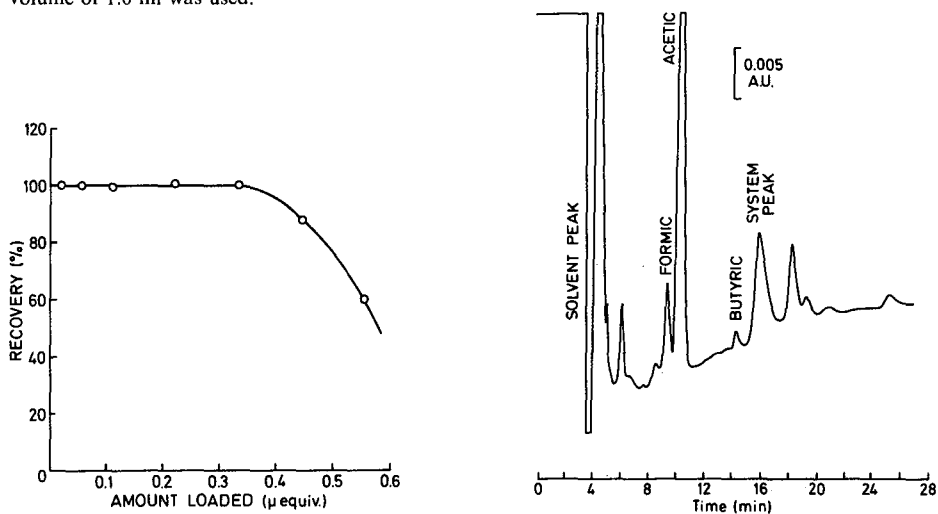
Fig. 5. Effect of the amount of sample loaded on the recovery of formic acid. Conditions as for Fig. 3, except a strip volume of 1.4 ml was used.

Fig. 6. Determination of carboxylic acids in Antarctic ice. Conditions as for Fig. 3, except that a sample volume of 7.0 ml and a strip volume of 1.0 ml were used and the detector sensitivity was 0.05 a.u.f.s.

butyric acid, 510 ppb formic acid, 6 ppm acetic (determined by direct injection) and several other unidentified species. Quantitative recoveries were obtained for all peaks as evidenced by the fact that loading different sample volumes gave linear plots for peak area *versus* sample volume.

CONCLUSIONS

This study has shown that quantitative preconcentration of carboxylic acids is possible using an ion chromatographic system employing an anion-exchange pre-column and an ion-exclusion analytical column. The preconcentration of the car-boxylic acids on the precolumn followed the same trends noted previously for the preconcentration of inorganic anions in ion chromatography[14–16,18,19]. Detection limits in the low ppb range were obtained for aliphatic carboxylic acids using direct UV detection. It is envisaged that the method will be applicable to the determination of a large number of organic acid species in sample matrices of low ionic strength, provided that the pK_a values of the acids determined are not high and suitable reso-lution of these solutes can be attained.

REFERENCES

1 R. M. Wheaton and W. C. Bauman, *Ind. Eng. Chem.*, 45 (1953) 228.
2 H. Waki and Y. Tokunaga, *J. Chromatogr.*, 201 (1980) 259.
3 K. Tanaka, T. Ishizuka and H. Sunahara, *J. Chromatogr.*, 174 (1979) 153.
4 J. P. Ivey and P. R. Haddad, *J. Chromatogr.*, 391 (1987) 309.
5 W. Rich, E. Johnson, L. Lois, P. Kabra, B. Stafford and L. Marton, *Clin. Chem.*, 26 (1980) 1492.
6 H. Itoh and Y. Shinbori, *Chem. Lett.*, (1982) 2001.
7 K. Tanaka and J S. Fritz, *J. Chromatogr.*, 361 (1986) 151.
8 K. Tanaka and J. S. Fritz, *Anal. Chem.*, 59 (1987) 708.
9 T. Murayama, T. Kubota, Y. Hanaoka, S. Rokushika, K. Kihara and H. Hatano, *J. Chromatogr.*, 435 (1988) 417.
10 H-J. Kim and Y-K. Kim, *J. Food. Sci.*, 51 (1986) 1360.
11 R. A. Wetzel, C. L. Anderson, H. Schleicher and G. D. Crook, *Anal. Chem.*, 51 (1979) 1532.
12 K. M. Roberts, D. T. Gjerde and J. S. Fritz, *Anal. Chem.*, 53 (1981) 1691.
13 A. L. Heckenberg and P. R. Haddad, *J. Chromatogr.*, 330 (1985) 95.
14 P. R. Haddad and P. E. Jackson, *J. Chromatogr.*, 367 (1986) 301.
15 P. E. Jackson and P. R. Haddad, *J. Chromatogr.*, 439 (1988) 37.
16 P. R. Haddad and A. L. Heckenberg, *J. Chromatogr.*, 318 (1985) 279.
17 R. Widiastuti, P. E. Jackson and P. R. Haddad, unpublished results.
18 P. E. Jackson and P. R. Haddad, *J. Chromatogr.*, 389 (1987) 65.
19 P. E. Jackson and P. R. Haddad, *J. Chromatogr.*, 355 (1986) 87.

CHROM. 20 545

IDENTIFICATION OF DEGRADATION PRODUCTS OF 2-CHLOROETHYL ETHYL SULFIDE BY GAS CHROMATOGRAPHY–MASS SPECTROMETRY

DENNIS K. ROHRBAUGH, YU-CHU YANG* and J. RICHARD WARD

Research Directorate, U.S. Army Chemical Research, Development and Engineering Center, Aberdeen Proving Ground, MD 21010-5423 (U.S.A.)

(First received December 14th, 1987; revised manuscript received March 15th, 1988)

SUMMARY

Gas chromatography–mass spectrometry under both electron impact and methane chemical ionization conditions has been used to detect impurities and degradation products present in the mustard simulant 2-chloroethyl ethyl sulfide, with a detection limit of 0.05 area percent. After one and two years of storage at ambient temperatures, the primary degradation product was 1,4-dithiane formed from the degradation of dimeric sulfonium ions. Oxidation and hydrolysis products were not detected.

INTRODUCTION

The vesicant, bis(2-chloroethyl) sulfide or mustard, has recently been identified on the Iran/Iraq battlefield by a United Nations team of experts[1]. The international significance of this incident points to the need for specific and sensitive means to detect such compounds. In addition, knowledge of the impurities and degradation products may help pinpoint the source and age of the contamination. Such information could also be useful to teams charged with verifying treaty compliance or for scanning manufacturers of new stores of such chemicals.

Little published research exists for the degration of mustard and 2-chloroethyl sulfides[2]. Such research was aimed at specific identification of the parent compound without regard to the nature of degradation products or the mechanism by which they form. In our laboratory we have used gas chromatography–mass spectrometry (GC–MS) under both electron impact (EI) and chemical ionization (CI) conditions to identify the degradation products of a mustard simulant, 2-chloroethyl ethyl sulfide (CEES). The simulant has a single chlorine which should simplify spectra and interpretation with respect to the degradation mechanism.

EXPERIMENTAL

The CEES samples were doubly-distilled products from Farfield Chemical Company and were stored at ambient conditions. The three samples of different ages

TABLE I

GC–MS IDENTIFICATION AND QUANTITATION OF CEES IMPURITIES (AREA %)

Retention time (s)	Structure	Fresh*	1-Year old*	2-Year old*
54	$ClCH_2CH_2Cl$	—	0.2	0.2
57	$CH_3CH_2SCH_2CH_3$	—	0.2	0.2
79	$C_5H_{12}S$**	0.5	0.6	0.4
79	$CH_3SCH_2CH_2Cl$	0.8	0.2	0.2
92	$CH_2=CHSCH_2CH_2Cl$	0.2	0.1	0.1
106	$CH_3CH_2SCH_2CH_2Cl$	97.6	94.4	94.9
121	$CH(CH_3)_2SCH_2CH_2Cl$	0.6	1.1	1.0
144	$CH_3CH_2CH_2SCH_2CH_2Cl$	—	0.3	0.8
157	MW 156 (2 Cl)	—	0.4	0.3
167		—	1.7	0.9
237	$S(CH_2CH_2Cl)_2$	—	0.06	0.05
247	$CH_3CH_2SCH_2CH_2SCH_2CH_3$	—	0.1	0.1
423	$CH_3CH_2SCH_2CH_2SCH_2CH_2Cl$	—	0.1	0.5

 * The samples were separately acquired at one-year intervals and analyzed at the same time.
 ** Perhaps $C_2H_5SC_3H_7$.

were analyzed by GC–MS techniques using both EI and CI methods to identify the impurities. The samples were analyzed on a Finnigan Model 5100 GC–MS instrument using a 15 m × 0.252 mm I.D. SE-54 capillary column with a split ratio of 50:1. The injector temperature was 200°C, the interface temperature was 230°C, the ion source temperature was 100°C and the oven was programmed from 60°C to 160°C at 10°C/min. The mass range was scanned from 60 to 450 a.m.u. for CI and from 30 to 450 a.m.u. for EI at one scan per s. Methane (0.6 Torr) was used as the chemical ionization reagent gas.

Spectral identifications were obtained by direct comparison to existing spectra or on the basis of combined EI/CI fragmentation*. Quantitation (expressed as area percent) was obtained by integration of the areas under the total ion chromatogram peaks and represents only an approximation of the relative quantities present. Sufficient quantity (0.05 μl) of neat sample was injected to observe sample components at the 0.05% concentration level.

RESULTS AND DISCUSSION

Degradation pathways

Table I lists the quantities of compounds found in freshly distilled and the one- and two-year old samples. One interesting result is the absence of oxidation products, *i.e.*, sulfone or sulfoxide in the aged samples. Second, it appears that 1,4-dithiane is

---

 * National Bureau of Standards 39000 compound mass spectral data base and a user library of mustard derivatives generated in-house.

the major degradation product and a characteristic marker for an aged sample. A number of thioethers and alkyl halides were also formed during aging.

The presence of such compounds in aged samples can be accounted for by assuming that degradation of CEES occurs through formation of dimeric sulfonium ions. The initial step in the degradation is the formation of the reactive ethylene sulfonium ion intermediate I via an S_N1 mechanism (eqn. 1). The reactive intermediate I then reacts with any available nucleophile. In water or base, the reaction would lead to the formation of 2-hydroxyethyl ethyl sulfide (HEES). Under our conditions the principal nucleophile is CEES itself which leads to the stable ethyl 2-chloroethyl thiodiethyl (ECT) sulfonium ion II (eqn. 2).

$$CH_3CH_2SCH_2CH_2Cl \rightleftharpoons CH_3CH_2S^+{\overset{CH_2}{\underset{CH_2}{|\ \ |}}} + Cl^- \tag{1}$$
$$(CEES) \qquad\qquad (I)$$

$$(I) + CEES \longrightarrow CH_3CH_2SCH_2CH_2S^+{\overset{CH_2CH_3}{\underset{CH_2CH_2Cl}{\diagdown}}} \tag{2}$$
$$(II)$$

With time II decomposes very slowly in the aged sample to form 1,4-dithiane of a six-membered ring structure, linear sulfides, and alkyl halides as shown in Table I.

The decomposition mechanism of II is proposed in eqns. 3–5 (refs. 3 and 4).

$$(3)$$

$$CH_3CH_2SCH_2CH_2SCH_2CH_3 + ClCH_2CH_2Cl \tag{4}$$

$$CH_3CH_2SCH_2CH_2S^+{\overset{CH_2CH_3}{\underset{CH_2CH_2Cl}{\diagdown}}}$$

$$CH_3CH_2SCH_2CH_2SCH_2CH_2Cl + CH_3CH_2Cl \tag{5}$$

Ethyl chloride was not detected in these samples probably because of loss due to extreme volatility. Attempts to identify sulfonium ion II directly by NMR were

not successful. However, in binary mixtures of CEES and water, direct NMR iden-
tification of ethyl 2-hydroxyethyl thiodiethyl (EHT) sulfonium ion (product of I and
HEES) has been reported[5]. We believe II can slowly hydrolyze to form EHT in the
presence of water. Presumably EHT can also cyclize to form 1,4-dithiane if sufficient
acid (H^+) is present in the aged sample to protonate the hydroxyl group as a first
step[5,6]. However, the formation of dithiane from II or EHT is a slow process at
room temperature and occurs only in aged samples. As reported previously, EHT
forms from protonated HEES[5]. A solution containing EHT and hydrochloric acid
decomposes under our GC–MS conditions (200°C injection port) to form primarily
CEES and HEES, while 1,4-dithiane is absent[7]. This also suggests that 1,4-dithiane
is not produced as an artifact of the analysis. Ethylene sulfide was not detected in
these samples*. This suggests that the preferred reaction route for I is the formation
of dimeric sulfonium ions; rather than decomposition to ethylene sulfide, as was
previously reported for 2-haloethyl sulfide derivatives[8].

Although the amount of mustard detected was small it was positively identified
by comparing the spectrum and retention time to that of a standard. We believe
mustard is a decomposition product of ethyl dichloroethyl sulfonium cation III which
is transformed from II by nucleophilic attack of CEES (eqn. 6). Similarly, II can
form other secondary sulfonium ions.

$$CH_3CH_2SCH_2CH_2S{\overset{CH_2CH_3}{\underset{CH_2CH_2Cl}{+}}} \quad + \quad CH_3CH_2SCH_2CH_2Cl \longrightarrow$$

$$CH_3CH_2S{\overset{CH_2CH_2Cl}{\underset{CH_2CH_2Cl}{+}}} \quad + \quad CH_3CH_2SCH_2CH_2SCH_2CH_3 \qquad (6)$$

$$(III)$$
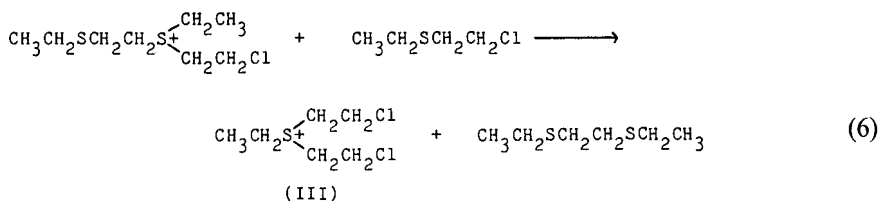
CI fragmentation pathways

Listed below are the major CI fragmentation pathways observed for CEES
and CEES dimerization products. As shown, the protonated molecular ions readily
undergo cleavage in the ionization source to form the cyclic sulfonium ion fragments.
The numbers listed in parentheses represent the percentage of base peak.

$$CH_3CH_2SCH_2CH_2Cl \overset{CH_5^+}{\longrightarrow} \underset{+}{CH_3CH_2SCH_2CH_2Cl} \overset{H}{\longrightarrow} CH_3CH_2S + {\overset{CH_2}{\underset{CH_2}{|}}} + HCl \qquad (7)$$

$$\begin{array}{cc} m/z\ 125,127 & m/z\ 89 \\ (100\%) & (96\%) \end{array}$$

---
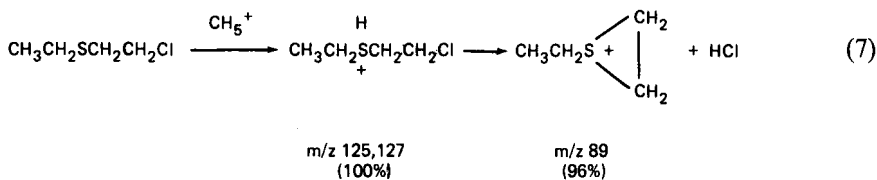
* Although ethylene sulfide is reactive and tends to polymerize, our method has been used to
identify ethylene sulfide as a degradation product from other compounds successfully.

$$CH_3CH_2SCH_2CH_2SCH_2CH_3 \xrightarrow{CH_5^+} CH_3CH_2\overset{H}{\underset{+}{S}}CH_2CH_2SCH_2CH_3 \longrightarrow CH_3CH_2\overset{CH_2}{\underset{CH_2}{S^+}} + HSCH_2CH_3 \tag{8}$$

$$\begin{array}{cc} m/z\ 151 & m/z\ 89 \\ (0\%) & (100\%) \end{array}$$

$$CH_3CH_2S\ CH_2\ CH_2\overset{H}{\underset{+}{S}}CH_2CH_2Cl \longrightarrow \overset{CH_2}{\underset{CH_2}{\diagdown}}{}^+SCH_2CH_2Cl + CH_3CH_2SH \tag{9}$$

$$\begin{array}{cc} m/z\ 185,\ 187 & m/z\ 123,125 \\ (0\%) & (38\%) \end{array}$$

$$CH_5^+ \nearrow$$

$$CH_3CH_2SCH_2CH_2SCH_2CH_2Cl$$

$$CH_5^+ \searrow$$

$$CH_3CH_2SCH_2CH_2\overset{H}{\underset{+}{S}}CH_2CH_2Cl \longrightarrow CH_3CH_2\overset{CH_2}{\underset{CH_2}{S^+}} + HSCH_2CH_2Cl \tag{10}$$

$$\begin{array}{cc} m/z\ 185,\ 187 & m/z\ 89 \\ (0\%) & (100\%) \end{array}$$
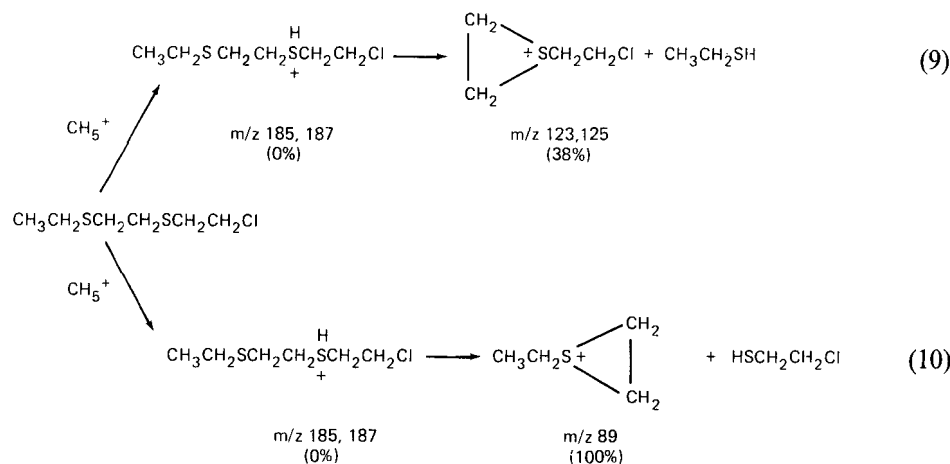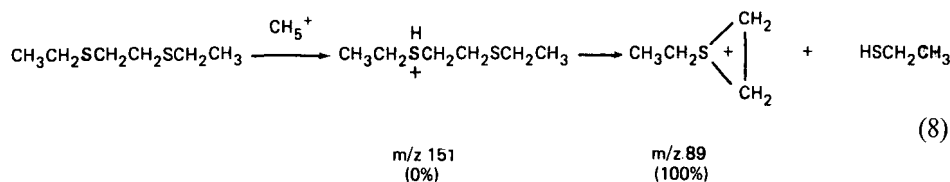
Worthy of note is the peak observed in the CI spectrum of CEES in all three samples at m/z 213 (2% of base peak), which corresponds to the dimeric sulfonium ion II.

CONCLUSION

Our results are consistent with a degradation mechanism in which dimeric sulfonium ions are formed as CEES ages. These ions transform slowly to 1,4-dithiane as a primary product. No oxidation or hydrolysis products were detected in the aged samples. The same mechanism for degradation at a slower rate is proposed for mustard, since it forms the reactive ethylene sulfonium ion less readily than CEES[9].

REFERENCES

1 *United Nations Security Council Report S/16433*, United Nations, New York, March 1986.
2 E. Ali-Mattilo, K. Sivinen, H. Kentämaa and P. Savolahti, *J. Mass Spectrom. Ion Phys.*, 47 (1983) 371–374.
3 C. G. Swain and L E. Kaiser, *J. Am. Chem. Soc.*, 80 (1958) 4089–4094.
4 E. D. Hughes, C. Ingold and Y. Pocker, *Chem. Ind. (London)*, (1959) 1282.
5 Y.-C. Yang, L. L. Szafraniec, W. T. Beaudry and J. R. Ward, *J. Org. Chem.*, 52 (1987) 1637–1638.
6 D. Welti and D. Whittaker, *J. Chem. Soc.*, 84 (1962) 3955–3960.
7 Y.-C. Yang and D.K. Rohrbaugh, unpublished results.
8 P. A. Trujilli, W. A. McMahon, Jr. and R. E. Lyle, *J. Org. Chem.*, 52 (1987) 2932–2933.
9 Y.-C. Yang, J. R. Ward and T. Lutern, *J. Org. Chem.*, 51 (1986) 2756–2759.

CHROM. 20 580

Note

Sorption of benzene on Tenax

J. VEJROSTA*, M. MIKEŠOVÁ, A. ANSORGOVÁ and J. DROZD

Institute of Analytical Chemistry, Czechoslovak Academy of Sciences, Leninova 82, 611 42 Brno (Czechoslovakia)

(First received November 27th, 1987; revised manuscript received April 11th, 1988)

The trapping of organic admixtures from gaseous mixtures on solid sorbents is mostly carried out by the method of conservation trapping[1]. Equilibration trapping was introduced[2] as an alternative and both methods were discussed in detail in earlier papers[3,4]. The wide use of the conservation method results from its relative simplicity and the possibility of easy experimental estimation of the safe sampling volumes.

The rôle played in both methods of interference (or displacement) effects arising from the competitive sorption of solutes on the sorbent surface was described in ref. 5. In the equilibration mode, the values of the resulting solute partition coefficients are necessary for the calculation of the solute concentrations in the mixture analyzed. The problems connected with the calculation or reasonable estimation of the relative changes in the partition coefficients at equilibrium and those in the absence of the interferents are probably the main reason for the rare use of the equilibration method.

Previously[6], the extent of the displacement effect on the benzene partition coefficient was investigated for three interferents, n-pentane, o-xylene and n-butanol.

The sorbent-phase concentrations of the interferents that bring about the same change in the partition coefficient of benzene do not differ much from each other. With benzene alone, the same decrease in its partition coefficient is achieved also at practically the same sorbent-phase concentration.

Under these circumstances, it is possible to assess the change in the solute partition coefficient from the known overall concentrations of the interferents in the sorbent, which is very important in view of the equilibration mode of trapping.

We suggested the following procedure: the known overall sorbent-phase concentration, easily determined from an analysis of the contents of the enrichment tube, is taken as the concentration of the model solute, for which the sorption isotherm equation is known. The change in the value of its partition coefficient relative to that at infinite dilution is calculated. The same relative changes are then supposed for the partition coefficients of solutes in the mixture analyzed.

The aim of this work is to find the form of the sorption isotherm equation, describing the sorption of non-polar and slightly polar compounds on Tenax. We chose benzene as a typically non-polar model compound and a set of its partition coefficients were measured over a wide range of concentrations and at four temperatures. An attempt was made to find the isotherm equation correlating the data obtained, which can be used in the equilibration method in the way mentioned above.

THEORETICAL

If the solute partition coefficient is defined as

$$K = c_s/c_g \qquad (1)$$

where c_s is the solute concentration in the sorbent phase in mol/g and c_g the corresponding concentration in the gaseous phase in mol/ml, the relationship between the specific retention volume of the solute, V_g, and its partition coefficient is given by

$$V_g = K \cdot \frac{273.15}{T} \qquad (2)$$

where T is the absolute temperature.

The specific retention volume, unlike the partition coefficient, is a quantity the value of which does not reflect the dependence of the volumes of the sorbent and the mobile phase on temperature.

The change in the standard Gibbs function of sorption, ΔG_s^0, is related to the specific retention volume, V_g, by

$$\Delta G_s^0 = -2.3 \, RT \log (k^0 V_g) \qquad (3)$$

where k^0 is a constant dependent on the choice of the standard states[7] and R and T are the universal gas constant and the absolute temperature of the chromatographic column at the measurement of V_g, respectively. As $\Delta G_s^0 = \Delta H_s^0 - T\Delta S_s^0$, where ΔH_s^0 and ΔS_s^0 are the changes in the standard enthalpy and entropy of sorption, eqn. 3 can be rewritten as

$$\log V_g = -\frac{\Delta H_s^0}{2.3 \, RT} + \frac{\Delta S_s^0}{2.3 \, R} - \log k^0 \qquad (4)$$

or

$$\log V_g = A + B/T \qquad (5)$$

where $A = (\Delta S_s^0/2.3 \, R) - \log k^0$ and $B = -\Delta H_s^0/2.3 \, R$. Within certain temperature limits the quantities A and B are virtually constant.

Eqns. 2–5 apply exactly to infinite dilution ($c_s \to 0, c_g \to 0$) and the relationship between the solute concentrations is given by Henry's law

$$c_s = K_0 c_g \qquad (6)$$

where K_0 is the solute partition coefficient. The interval of the solute concentrations in which eqn. 6 is valid defines the linear part of the sorption isotherm. Outside it the course of the sorption isotherm is generally non-linear and the values of the quantities K, A and B depend on the sorbent-phase concentration, c_s. The use of eqns. 2–5 is restricted to a constant value of c_s.

Since c_s and c_g are interconnected through K, the dependence of the partition coefficient on c_s is easily transformed to a dependence of c_g and *vice versa*. If the isotherm equation describing the relationship between c_s and c_g is available, the determination of the temperature dependence of its adjustable parameters will lead to the equation from which the partition coefficient can be determined at any temperature and any solute concentration (c_s or c_g). With the use of eqns. 2–5, the concentration dependence of the standard thermodynamic functions for the sorption process can be determined.

EXPERIMENTAL

The method of preparation of the model mixture, the measurements and calculation of the partition coefficients as well as the chemicals used were described earlier[3,8]. The partition coefficients of benzene were determined as a function of its concentration at four temperatures: 19.9, 27.1, 35.0 and 41.7°C. The interval of gas-phase concentrations was $6.8 \cdot 10^{-12}$–$7.0 \cdot 10^{-7}$ mol/ml.

RESULTS AND DISCUSSION

The Langmuir isotherm was successfully used for the description of benzene sorption on different sorbents[3] as follows.

Let the fraction of the active sites occupied by sorbed molecules of the solute be defined as $\alpha = c_s/c_s^*$ where c_s and c_s^* are the actual solute concentration in the sorbent and the concentration at which all available sites are occupied, respectively.

The significance of α is analogous to that of the parameter θ in Langmuir's model. The rates of desorption and sorption are defined as $r_d = k_d\alpha$ and $r_s = K_s(1 - \alpha)c_g$, respectively, where k_d and k_s are the respective rate constants. At equilibrium, $r_d = r_s$ and we can write

$$c_s = k_e c_s^* c_g/(1 + k_e c_g) \tag{7}$$

where $k_e = k_s/k_d$. Thus:

$$\frac{c_s}{c_g} = K = \frac{k_e c_s^*}{1 + k_e c_g} \tag{8}$$

Eqn. 8 can be rearranged as

$$\frac{1}{c_g} = \frac{k_e c_s^*}{c_s} - k_e \tag{9}$$

which is a linearized form of the Langmuir isotherm.

The solute partition coefficient at infinite dilution is given by:

$$\lim_{c_g \to 0} K = k_e c_s^* = K_0 \tag{10}$$
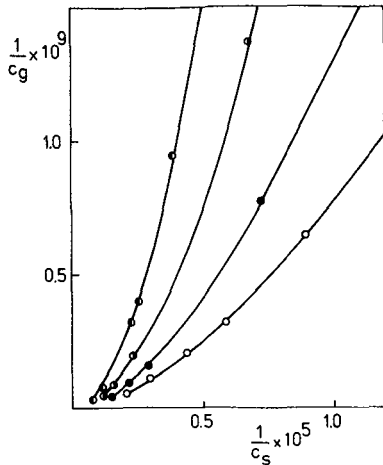
Fig. 1. The relationship $1/c_g$ vs. $1/c_s$ at high benzene concentrations: ◑, 19.9; ◐, 27.1; ●, 35.0 and ○, 41.7°C.

By plotting $1/c_g$ against $1/c_s$, a straight line having the slope

$$\frac{d\ (1/c_g)}{d\ (1/c_s)} = k_e c_s^* = K_0 \tag{11}$$

will be obtained if the Langmuir isotherm is appropriate for a given system.

We have treated our data in this way and graphical representation of the sorption isotherms in the coordinates $1/c_g$ versus $1/c_s$ is illustrated in Fig. 1. Significant deviations from linearity occur at higher benzene concentrations as already indicated elsewhere[3]. The maximum benzene gas-phase concentration up to which the Langmuir isotherm is applicable is approximately $5 \cdot 10^{-9}$ mol/ml.

The regression criterion, R_s, was defined by

$$R_s = \sum_i \frac{|K_{i,\,exp} - K_{i,\,calc}|}{K_{i,\,exp}} \tag{12}$$

and its value for the Langmuir isotherm was used to test further isotherms. About twenty isotherm equations previously described in the literature have been tested and for a surprisingly low number of equations the value of R_s was significantly lower than in the case of the Langmuir isotherm.

Even if a very good correlation was obtained, such as in the case of the Freundlich[9], Temkin[10] and especially Dubinin–Astachov[11] isotherm equations in the non-linear parts of the sorption isotherms, the condition for the transition to the Henry law in the low concentration range was not fulfilled.

Simultaneously we tested several modifications of eqns. 8 by adding one adjustable parameter. Of these

$$K = K_0/(1 + k_1 c_g)^{k_2} \tag{13}$$

where K_0 is the partition coefficient at infinite dilution and k_1, k_2 are adjustable parameters, appeared to be the most suitable. The lowest values of R_s were obtained from all the isotherm equations tested and this equation permits the transition to the Henry law if $c_g \rightarrow 0$.

The individual isotherms were correlated by eqn. 13 with the following average deviations between the calculated and experimental values of the partition coefficients: 1.2, 2.6, 1.0 and 2.2% relative in the direction of increasing temperature.

The solute sorbent-phase concentration, c_s, is of much greater importance if one keeps in mind the aim of this work. Eqn. 13 was therefore used with variable c_s

$$K = K_0/(1 + k_3 c_s)^{k_4} \tag{14}$$

and due to the interconnection of c_g and c_s through K it is not surprising that the correlation of the individual isotherms was as good as that obtained with the use of eqn. 13.

With the relationships between K and c_s which followed from the fitting of the data by eqn. 14, an attempt was made to find the dependence of the parameters A, B of eqn. 5 on the sorbent-phase concentration, c_s. The partition coefficients were calculated from the individual isotherms for a number of selected concentrations, c_s. With the use of eqns. 2 and 5, the values of A and B were calculated by linear regression of four V_g values obtained for each concentration, c_s. The resulting dependences of A and B on c_s, obviously as a consequence of the insufficient number of points for the linear regression, exhibited irregular courses with local extremes.

It was clear that the only way to proceed further was to determine the temperature dependence of the adjustable parameters, k_3 and k_4, in eqn. 14. Their values obtained from the fitting of the individual isotherms by eqn. 14, indicated that k_3 was almost independent of temperature and parameter k_4 was linearly dependent on $1/T$.

The partition coefficient, K_0, at infinite dilution is given by

$$K_0 = \lim_{c_s \to 0} V_g \frac{T}{273.15} \tag{15}$$

and its temperature dependence is that of the specific retention volume in this range (eqn. 5).

Based on these results, eqn. 16 was proposed

$$K = \frac{T}{273.15} \cdot \frac{10^{a+b/T}}{(1 + ec_s)^{-(c+d/T)}} \tag{16}$$

with five adjustable parameters a, b, c, d, e. With the use of eqn. 2, the relationship log $V_g = f(T, c_s)$ is obtained:

$$\log V_g = a + \frac{b}{T} + c \log(1 + ec_s) + \frac{d}{T} \cdot \log(1 + ec_s) \tag{17}$$
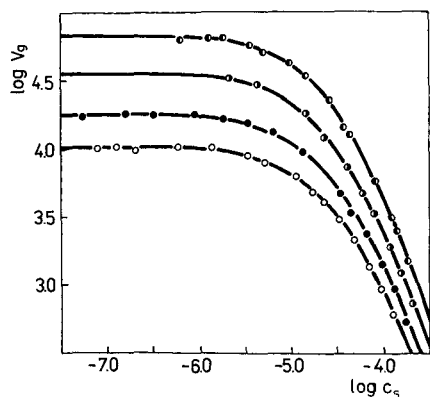
Fig. 2. The relationship log V_g vs. log c_s calculated by use of eqn. 17 (full lines) and experimental points (see Fig. 1).

From the correlation of the whole set of experimental data by eqn. 17, the following values of the adjustable parameters were obtained: $a = -7.0618$, $b = 3486.69$, $c = 1.42312$, $d = -1019.63$ and $e = 28964.9$; V_g (ml/g), c_s (mol/g).

In Fig. 2 the experimental data and the data calculated according to eqn. 17 are plotted in the coordinates log V_g vs. log c_s. An average deviation of 2.67% relative was found between the calculated and experimentally determined values of the partition coefficients.

It is evident that, at a constant temperature, eqn. 16 is reduced to eqn. 14. The values of parameters a and b are identical with the values of parameters A and B at infinite dilution, usually determined by elution gas chromatography

$$a = \lim_{c \to 0} A, \quad b = \lim_{c \to 0} B$$

Our values of a and b are in a very good agreement with parameters A and B in eqn. 5 determined previously[3] for the system nitrogen–benzene–Tenax ($A = -6.9629$, $B = 3455.25$).
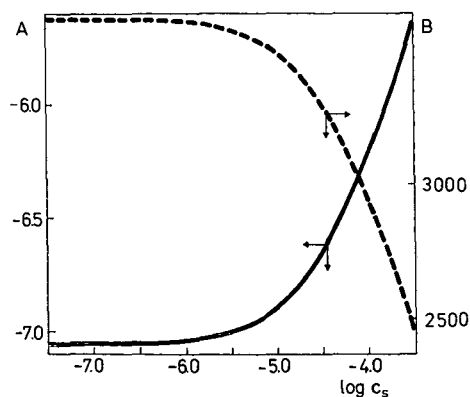
Fig. 3. Graphical illustration of eqns. 18 and 19.

The dependence of parameters A and B on the sorbent-phase solute concentration is expressed by

$$A = a + c \log (1 + ec_s) \tag{18}$$

$$B = b + d \log (1 + ec_s) \tag{19}$$

from which the standard thermodynamic functions of sorption can be calculated for any sorbent-phase solute concentration. These dependences are illustrated in Fig. 3.

CONCLUSIONS

The equation of the Langmuir isotherm modified empirically was proposed for the description of the relationship between gas-phase and sorbent-phase solute concentrations. A simple temperature dependence of the adjustable parameters was found and the resulting eqn. 17 describes well the whole set of experimental data with an average deviation of 2.67% relative, which is in agreement with the estimated experimental error ($<3\%$ relative).

Eqn. 17 can be used to calculate relative changes in the partition coefficients of the solute in the equilibration method of trapping under the above mentioned assumption.

The absolute values of the partition coefficients of benzene are of importance in the conservation method of trapping.

The surface of Tenax contains a relatively low portion of the active sites with a virtually constant value of the change in the standard Gibbs function of sorption, ΔG_s^0. The concentration necessary for a complete coverage of this part is approximately 10^{-6} mol of benzene per gram of Tenax. With increasing sorbent-phase concentration the active sites with lower values of ΔG_s^0 become available. This leads to a strong dependence of the parameters A and B of eqn. 5 on the sorbent-phase solute concentration, with consequences for both methods of trapping.

REFERENCES

1 F. R. Cropper and S. Kamiński, *Anal. Chem.*, 35 (1963) 735.
2 J. Novák, V. Vašák and J. Janák, *Anal. Chem.*, 37 (1965) 660.
3 J. Vejrosta, M. Roth and J. Novák, *J. Chromatogr.*, 217 (1981) 167.
4 J. Vejrosta, M. Roth and J. Novák, *J. Chromatogr.*, 265 (1983) 215.
5 J. Vejrosta, M. Mikešová and J. Novák, *J. Chromatogr.*, 324 (1985) 269.
6 J. Vejrosta, M. Mikešová and J. Novák, *J. Chromatogr.*, 354 (1986) 59.
7 M. R. James, J. C. Giddings and R. A. Keller, *J. Gas Chromatogr.*, 3 (1965) 57.
8 J. Vejrosta and J. Novák, *J. Chromatogr.*, 175 (1979) 261.
9 H. Freundlich, *Trans. Faraday Soc.*, 28 (1932) 195.
10 M. J. Temkin, *Zh. Fiz. Khim.*, 14 (1940) 1153.
11 M. M. Dubinin and V. A. Astachov, *Adv. Chem. Ser.*, 102 (1971) 59.

CHROM. 20 566

Note

Characterization of mobile phases for the investigation of electrokinetic phenomena in liquid chromatography

J. NEČA

Institute of Analytical Chemistry, Czechoslovak Academy of Sciences, Leninova 82, 611 42 Brno (Czechoslovakia)

F. STEHLÍK

Cooperative Farm, Práče (Czechoslovakia)

and

R. VESPALEC*

Institute of Analytical Chemistry, Czechoslovak Academy of Sciences, Leninova 82, 611 42 Brno (Czechoslovakia)

(Received April 11th, 1988)

The streaming current and the streaming potential incidental to it, which are applied in liquid chromatography for detection purposes, originate in special generating elements located after or in the chromatographic column[1]. The magnitude of the streaming current depends on, among other things, the dynamic viscosity (η) of the mobile phase, its relative permittivity (ε_r) and its conductivity (κ)[2]. Also, the dimensions of the generating elements, in which the maximum possible charge volume density in the streaming liquid is reached at the mobile phase flow-rate used, or the dimensions of earthed metal capillaries, in which the space charge carried by the liquid is completely discharged, depend on the values of ε_r and κ (ref. 3). Values of the parameters η, ε_r and κ have been tabulated for pure solvents only. In this work, these values have been measured for the binary mobile phases *n*-heptane–acetone, acetone–methanol, methanol–water and acetone–water of different compositions.

EXPERIMENTAL

Acetone and methanol of analytical-reagent grade (Lachema, Brno, Czechoslovakia) were purified and dried by rectification on a 40-plate glass bubble-cap column. Rectification, preservation of the rectified substances and all other operations with organic solvents and their mixtures were carried out in vessels dried with air cooled with solid carbon dioxide and protected against air humidity. *n*-Heptane (Laborchemie, Apolda, G.D.R.) was purified with alumina activated at 380°C. Distilled water was deionized with a mixture of cation-exchange resin (Ostion KS) and anion-exchange resin (Ostion AD) (Company for Chemical and Metallurgical Production, Ústí nad Labem, Czechoslovakia). Carbon dioxide was not removed from the water. The water content of the rectified solvents was established by Karl Fischer titration with coulometric indication. The total content of impurities in the solvents was established by measuring the conductivity (Table I).

TABLE 1

CONTENT OF WATER IN PURIFIED ORGANIC SOLVENTS AND RELATIVE PERMITTIVITIES (ε_r) AND CONDUCTIVITIES (κ) OF THE SOLVENTS PRIOR TO AND AFTER PURIFICATION

Solvent	Water content (ppm)	ε_r			κ (S m^{-1})		
		Prior to purification	After purification	Tabulated value	Prior to purification	After purification	Tabulated value***
Methanol	10	39.0	34.4	32.63*	$1.1 \cdot 10^{-4}$	$8.3 \cdot 10^{-5}$	$1.5 \cdot 10^{-7}$
Acetone	<400	23.0	20.8	20.7*	$1.9 \cdot 10^{-5}$	$9.2 \cdot 10^{-6}$	$4.9 \cdot 10^{-7}$
n-Heptane	—	1.9	1.9	1.924**	$1 \cdot 10^{-10}$	$<8 \cdot 10^{-11}$	$<10^{-14}$
Water	—	83.0	81.2	78.54*	$9.8 \cdot 10^{-4}$	$1.2 \cdot 10^{-4}$	$5.89 \cdot 10^{-6}$

* At 25°C[4].
** At 20°C[5].
*** At 25°C[5].

Polyethylene vessels for the preparation of the samples and the connecting tubes and syringes for manipulation with the solvents and samples were washed with organic solvents and dried before use.

The conductivities (κ) of the samples and their relative permittivities (ε_r) were calculated from the capacity (C) and conductance (G) of a flow condenser with the volume of 4.7 ml and an air capacity of $C_v = 6.63$ pF derived from a capacity detection cell[6]. The non-thermostated condenser was connected to a Tesla BM 484 semi-automatic compensation bridge (Tesla, Brno, Czechoslovakia) enabling the quantities C and G simultaneously to be measured. The values of ε_r and κ were calculated from the relationships

$$\varepsilon_r = C/C_v \tag{1}$$

$$\kappa = \varepsilon_0 \varepsilon_r G/C \tag{2}$$

where ε_0 is the permittivity of a vacuum. The kinetic viscosity was measured with an Ubbelohde viscosimeter thermostated in a water bath at $20 \pm 0.1°C$. The densities of the solutions were determined pycnometrically.

RESULTS AND DISCUSSION

Titration indicated that the fractional distillation completely removed water from methanol. For the determination of water in rectified acetone, a titration agent completely inert to keto groups was not available. The actual water content of rectified acetone was, therefore, lower than that calculated from the consumption of titration agent given in Table I.

According to theory[6], the relative permittivity of a binary mixture of the solvents ($\varepsilon_{r_{1,2}}$) is a linear combination of the relative permittivities of the components (ε_{r_1}, ε_{r_2}):

$$\varepsilon_{r_{1,2}} = \varepsilon_{r_1} V_1 + \varepsilon_{r_2} V_2 \tag{3}$$

where V_1 and V_2 are volume fractions of solvents 1 and 2, respectively. The results confirm the validity of this relationship for all the combinations of the solvents over the whole range of concentrations (Fig. 1). From previous work[8], it is possible to assume that the relative permittivity of a binary mobile phases can be considered, with acceptable accuracy, to be a linear function of the composition even when the original solvents contain trace amounts of foreign matter.

The viscosity of the binary mobile phases was a linear combination of the viscosities of the components only for organic solvents (n-heptane–acetone and acetone–methanol) (Fig. 2). For mixtures of water with methanol, where the viscosity reaches a marked maximum, much better agreement with Van der Wal's data[9] than with the results published by Bates and Robinson[7] was found. The measured viscosities of the mixtures of water with acetone agreed with Van der Wal's data[9] only for acetone volume concentrations up to 40%.

The dependences of the conductivities on composition were non-linear at all four combinations of the solvents (Figs. 3 and 4). For acetone–methanol, acetone–
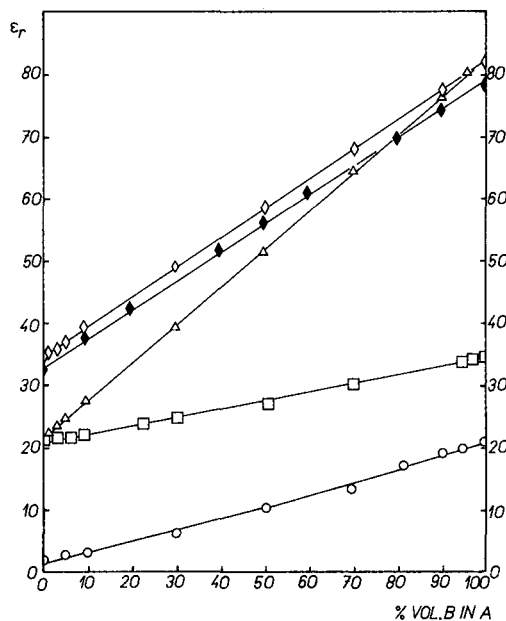
Fig. 1. Dependence of relative permittivity (ε_r) of binary mixtures of solvents on composition. $\bigcirc$, n-Heptane (A) and acetone (B); $\square$, acetone (A) and methanol (B); $\triangle$, acetone (A) and water (B); $\diamondsuit$, methanol (A) and water (B); $\blacklozenge$, methanol (A) and water (B) from ref. 7.
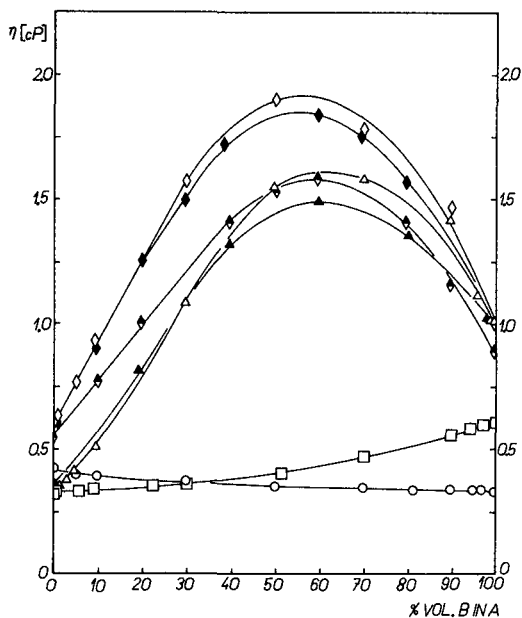

Fig. 2. Dependence of dynamic viscosity (η) of binary mixtures of solvents on composition. $\blacklozenge$, Methanol (A) and water (B)[9]; $\blacklozenge$, methanol (A) and water (B)[7]; $\blacktriangle$, acetone (A) and water (B)[9]. Other symbols as in Fig. 1.
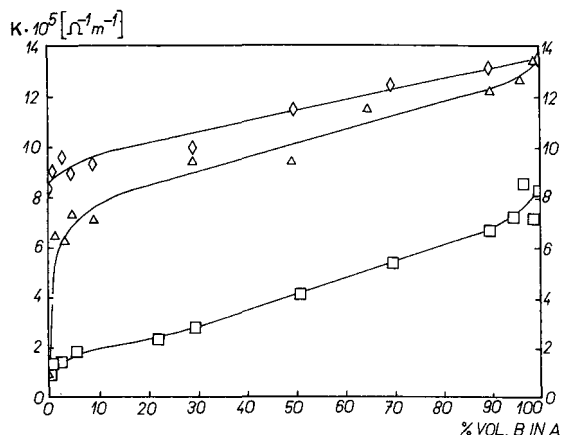
Fig. 3. Dependence of conductivity (κ) of binary mixtures of solvents on composition. Symbols as in Fig. 1.
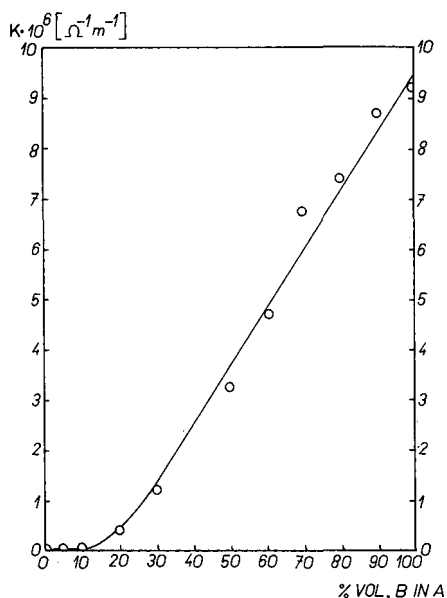
Fig. 4. Dependence of the conductivity (κ) of a mixture of n-heptane (A) and acetone (B) on composition.

water and methanol–water, the conductivity varied with composition over an order of magnitude. For mixtures of water with methanol and acetone, the conductivity is a linear function of composition at volume fractions of water $\geqslant 0.2$. For acetone–methanol, the conductivity is a linear function of composition if the volume fraction of any of the components does not fall below 0.1. The conductivity of n-heptane–acetone varied over five orders of magnitude while a linear dependence of conductivity on composition was found for the volume fractions of acetone $\geqslant 0.3$.

REFERENCES

1 J. Neča and R. Vespalec, in preparation.
2 R. J. Hunter, *Zeta Potential in Colloid Science*, Academic Press, London, 1981, pp. 64–68.
3 K. Šlais and M. Krejči, *J. Chromatogr.*, 148 (1978) 99.
4 R. C. West (Editor), *Handbook of Chemistry and Physics*, Chemical Rubber Publishing Co., Cleveland, 46th ed., 1965, pp. E-49 and E-50.
5 J. A. Riddick and W. B. Bunger, in A. Weissberger (Editor), *Organic Solvents*, Wiley-Interscience, New York, 1970, pp. 67, 87, 145 and 242.
6 O. W. Kolling, *Anal. Chem.*, 59 (1987) 674.
7 R. G. Bates and R. A. Robinson, in B. E. Conway and R. G. Barrades (Editors), *Chemical Physics of Ionic Solutions*, Wiley, New York, 1966, p. 211.
8 R. Vespalec and K. Hána, *J. Chromatogr.*, 65 (1972) 53.
9 Sj. Van der Wal, *Chromatographia*, 20 (1985) 274.

CHROM. 20 583

Note

High-performance liquid chromatography on dynamically modified silica

VIII*. Gradient elution using eluents containing cetyltrimethylammonium bromide

STEEN HONORÉ HANSEN*

Department of Organic Chemistry, The Royal Danish School of Pharmacy, 2 Universitetsparken, DK-2100 Copenhagen (Denmark)

and

PER HELBOE and MOGENS THOMSEN

National Board of Health, Drug Standardization Laboratory, 378 Frederikssundsvej, DK-2700 Brønshøj (Denmark)

Recently the dynamically modified silica approach has proved to be a valuable technique in high-performance liquid chromatography (HPLC)[1]. In this technique the surface of bare silica is modified dynamically with long-chain quaternary ammonium compounds added to the eluent, *e.g.* cetyltrimethylammonium (CTMA) ions[2–3]. The influence on the retention of various test solutes of variations in the pH (ref. 4), the nature of the quaternary ammonium ion and the CTMA concentration[2], the ionic strength and buffer components[4], and the nature and concentration of the organic modifier[5] have been thoroughly investigated. From the data obtained it is obvious that all parameters have to be controlled carefully, but if this is done, reproducible systems with respect to retention and selectivity may be obtained[6–8]. This paper describes an investigation of three ways of performing gradient elution in the dynamically modified silica mode. The gradient is formed by increasing the concentration of the organic modifier in the eluent, or by increasing the ionic strength or by increasing the CTMA concentration above the critical micellar concentration.

EXPERIMENTAL

Apparatus

Chromatographic testing of the individual systems was performed on a Waters liquid chromatograph consisting of two 6000 A pumps, a 710 A WISP autoinjector, a 440 UV absorbance detector (254 nm), a 730 data module and a 720 system controller. The column system was thermostatted in a Kratos oven at 30°C.

---

* For part VII, see *J. Chromatogr.*, 368 (1986) 39–47.

Chromatography

All experiments were performed on 120 × 4.6 mm I.D. columns from Knauer (Berlin, F.R.G.), packed with LiChrosorb Si 60 (5 μm) (E. Merck, Darmstadt, F.R.G.). The eluents in the three gradient experiments were as follows.

Elution strength gradient. Eluent A = acetonitrile–water–0.2 *M* phosphate buffer (pH 7.5) (10:85:5) with 0.25 m*M* CTMA added; eluent B = acetonitrile–water–0.2 *M* phosphate buffer (pH 7.5) (50:45:5) with 40 m*M* CTMA added. The gradient was linear from 0% to 100% B in 15 min at a flow-rate of 1 ml/min. The delay time was 10 min.

Ionic strength gradient. Eluent A = methanol–water–0.2 *M* phosphate buffer (pH 7.5) (35:63.75:1.25) with 2.5 m*M* CTMA added; eluent B = methanol–water–0.2 *M* phosphate buffer (pH 7.5) (35:40:25) with 2.5 m*M* CTMA added. The gradient was linear from 0% to 100% B in 10 min at a flow-rate of 1 ml/min.

Micellar concentration gradient. Eluent A = methanol–water–0.2 *M* phosphate buffer (pH 6.0) (30:65:5) with 5 m*M* CTMA added; eluent B = methanol–water–0.2 *M* phosphate buffer (pH 6.0) (30:65:5) with 50 m*M* CTMA added.

The buffer pH stated is that measured in the undiluted buffer and not in the final eluent. The buffer was prepared from 0.2 mol of potassium dihydrogenphosphate dissolved in 930 ml of water, titrated with 5 *M* potassium hydroxide to the appropriate pH value and finally diluted to 1000 ml. During chromatography the column was guarded by a silica saturation column (100 × 4.6 mm I.D.) situated between the pump and the injection device.

Chemicals

All chemicals were of analytical grade from E. Merck and were used as received from the manufacturer.

RESULTS AND DISCUSSION

Elution strength gradient

It is known that the elution strength of the eluent is increased in the reversed-phase mode when the concentration of the organic modifier is increased. In chromatography on dynamically modified silica this is also true, but the amount of stationary phase decreases as well since it is not chemically bonded to the surface[5].

This means that a smaller change in the concentration of the organic modifier is needed to obtain a certain effect relative to gradient elution on chemically bonded phases. It also means that the system will be totally out of equilibrium when a gradient is created by changing the concentration of the organic modifier. Following a gradient run, the next one should not be started until the initial amount of stationary phase on the silica surface in the first gradient run has been reestablished. This may require a rather long time (4–8 h), and an attempt to compensate for the loss of stationary phase during the gradient run by simultaneously increasing the amount of CTMA in the eluent was therefore made.

From data in ref. 5 it appears that in order to maintain a coverage of 0.65 mmol of CTMA per gram of silica when using a gradient from *e.g.* 40% to 70% of methanol, the CTMA concentration also has to be varied from 1 m*M* to 50 m*M* during the elution. Even then, complete equilibrium is not maintained, but repeating

the elution with a fixed delay-time between each run leads to a reproducible gradient within three or four runs[5]. It should also be noted that the saturation column in the system will contribute to the delay of the gradient.

Ionic strength gradient

From previous studies on the influence of changing the ionic strength on the retention of various solutes[4], it appears that non-ionic and cationic solutes are affected only to a minor extent by the addition of inorganic salts or buffers, whereas the retention times of the anionic compounds are markedly reduced. This is in good agreement with previous observations[4] that the amount of CTMA adsorbed on the silica surface is hardly affected by changes in the ionic strength, and thus it is possible to perform a selective gradient elution of anionic solutes (Fig. 1). Furthermore, this

Fig. 1. Isocratic (a) and ionic strength gradient (b) elution of test solutes. Column, 120 × 4.6 mm I.D. LiChrosorb Si 60, 5 μm; eluent A, methanol–water–0.2 *M* phosphate buffer (pH 7.5) (35:63.75:1.25) with 2.5 m*M* CTMA added; eluent B, methanol–water–0.2 *M* phosphate buffer (pH 7.5) (35:40:25) with 2.5 m*M* CTMA added. (a) Isocratic elution with eluent A (1 ml/min); (b) gradient elution from 100% eluent A to 100% eluent B in 10 min at a flow-rate of 1 ml/min.

technique is able to provide information about the valency of the anionic species, since divalent anions are affected more than monovalent and trivalent anions even more. The reason for this selective effect on the anionic solutes is an inhibition of the formation of ion-pairs with the CTMA ions in the liquid phase. Consecutive gradient runs may be performed without intermittent delay-times, and the repeatability of the test solute retention times is better than 0.2% between runs. However, if more lipophilic organic anions are used to increase the ionic strength the effect will be more pronounced, and ion-pairs between CTMA ions and long-chain sulphonate ions, for example, will adsorb on the lipophilic surface thus increasing the amount of stationary phase[4], and rendering the column unsuitable for gradient elution.

Micellar concentration gradient

Reversed-phase HPLC systems using micellar elution were first described by Armstrong and Henry[9], and this technique has since been utilized by several workers *e.g.* refs. 10 and 11, and also in the gradient elution mode[12,13]. In the dynamically modified silica mode, micellar gradient elution may be performed provided that the concentration of the long-chain quaternary ammonium ion (*e.g.* CTMA) in the initial eluent is above the critical micellar concentration (CMC). The CMC in the eluent
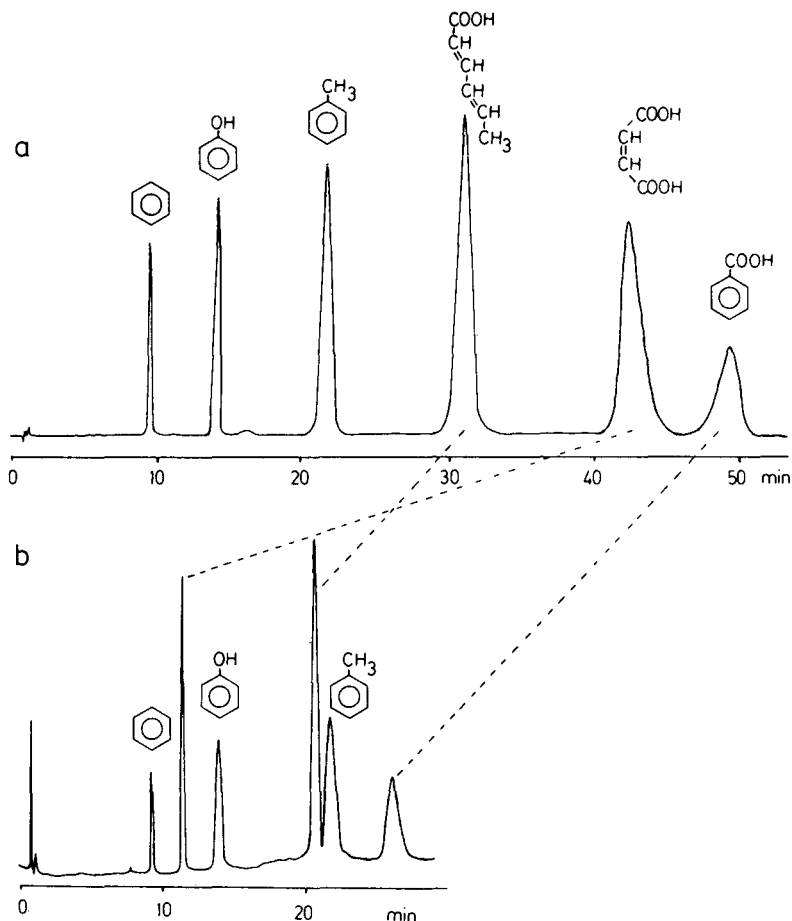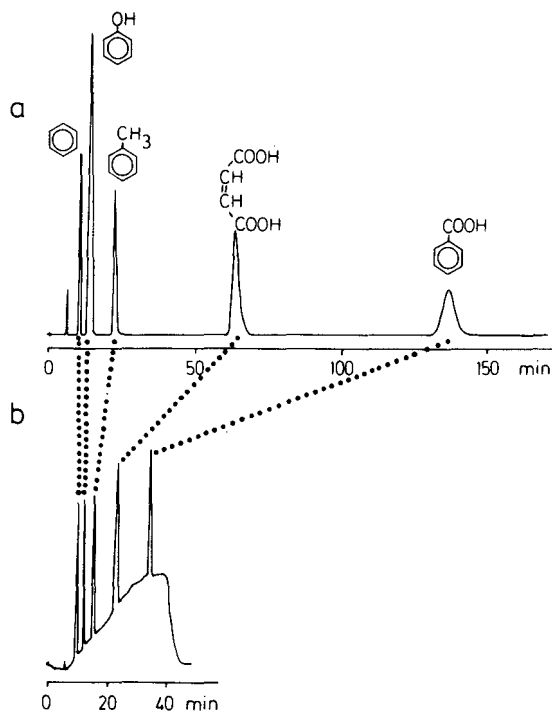

Fig. 2. Isocratic (a) and micellar gradient (b) elution of some test solutes. Column, 120 × 4.6 mm I.D. LiChrosorb Si 60, 5 μm; eluent A, methanol–water–0.2 *M* phosphate buffer (pH 6.0) (30:65:5) with 5 m*M* CTMA added; eluent B, methanol–water–0.2 *M* phosphate buffer (pH 6.0) (30:65:5) with 50 m*M* CTMA added. (a) Isocratic elution with eluent A (1 ml/min); (b) gradient elution from 100% eluent A to 100% eluent B in 30 min at a flow-rate of 1 ml/min.

may be determined as described previously[2]. When the CMC is exceeded the concentration of the free quaternary ammonium ions in the liquid phase remains constant and thereby the amount of stationary phase as well. However the number and size of the micelles in the liquid phase will increase thus causing the elution strength of the eluent to increase also. The presence of micelles in the eluent may be described as an extra lipophilic phase, migrating together with the polar eluent. Using the micellar approach, a reversed-phase gradient elution may be performed in a reproducible way without using fixed delay-times. The repeatability of retention times between runs is within 0.1–0.2%. An example of this type of gradient elution is shown in Fig. 2. The increased baseline signal is due to the increase in bromide concentration. This may be avoided by using CTMA salts with a non-UV-absorbing anion.

CONCLUSION

Three ways of performing gradient elution in the dynamically modified silica mode are presented.

When using a micellar concentration gradient it is possible to obtain results similar to those seen when using gradient elution on chemically bonded phases with increasing amounts of the organic modifier.

When increasing the ionic strength during a chromatographic run, a selective gradient elution of the anionic solutes is obtained.

Increasing the amount of organic modifier in the dynamically modified silica approach will, apart from the increase in elution strength, cause a decrease in the amount of stationary phase. Gradient elution by this technique should, therefore, only be performed under strictly controlled conditions, including fixed delay-times between runs.

ACKNOWLEDGEMENT

REFERENCES

1 P. Helboe, S. H. Hansen and M. Thomsen, *Adv. Chromatogr.*, in press.
2 S. H. Hansen, P. Helboe and U. Lund, *J. Chromatogr.*, 240 (1982) 319.
3 M. Gazdag, G. Szepesi and M. Hernyes, *J. Chromatogr.*, 316 (1984) 267.
4 S. H. Hansen, P. Helboe and U. Lund, *J. Chromatogr.*, 270 (1983) 77.
5 S. H. Hansen and P. Helboe, *J. Chromatogr.*, 285 (1984) 53.
6 S. H. Hansen, P. Helboe, M. Thomsen and U. Lund, *J. Chromatogr.*, 210 (1981) 453.
7 P. Helboe, *J. Chromatogr.*, 245 (1982) 229.
8 S. H. Hansen, P. Helboe and M. Thomsen, *J. Chromatogr.*, 409 (1987) 71.
9 D. W. Armstrong and S. J. Henry, *J. Liq. Chromatogr.*, 3 (1980) 657.
10 P. Yarmchbuk, R. Weinberger, R. F. Hirsch and L. J. Cline Love, *Anal. Chem.*, 54 (1982) 2233.
11 M. Arunyanart and L. J. Cline Love, *Anal. Chem.*, 56 (1984) 1557.
12 J. S. Landy and J. G. Dorsey, *J. Chromatogr. Sci.*, 22 (1984) 68.
13 J. G. Dorsey, M. G. Khaledi, J. S. Landy and J.-L. Lin, *J. Chromatogr.*, 316 (1984) 183.

CHROM. 20 529

Note

Behaviour of tri- and tetranuclear iron and nickel clusters in high-performance liquid chromatography

ANTONELLA CASOLI, ALESSANDRO MANGIA and GIOVANNI PREDIERI*

Istituto di Chimica Generale ed Inorganica, Università di Parma, Viale delle Scienze, I-43100 Parma (Italy)

and

ENRICO SAPPA

Istituto di Chimica Generale ed Inorganica, Università di Torino, Corso M. d'Azeglio 48, I-10125 Torino (Italy)

(Received March 29th, 1988)

High-performance liquid chromatography (HPLC) can be successfully applied to the chemistry of transition metal clusters[1] with the aim of monitoring the reaction pathways and separating the final products. Previous studies on di-, tri- and tetrametallic clusters[2–6] have shown that the nuclearity and the shape of the clusters and the nature of the metals and of the substituent ligands determine the separations of chemically and/or structurally related species.

Here we report a study on the HPLC behaviour of some tri- and tetranuclear carbonyl clusters based on iron and iron-nickel metal cores. They are listed in Table I together with their electronic absorption maxima, structures and literature references[7–14].

Most of these complexes are products of the reactions of $(cp)_2Ni_2(PPh_2C \equiv CR)$ or $(cp)_2Ni_2(RC \equiv CR')$ with $Fe_3(CO)_{12}$ or $Fe_2(CO)_9$ and belong to the same series of cluster expansion and contraction reactions[12]. Moreover, it is generally accepted that tetrahedral (6 M–M), butterfly (5 M–M), square-planar and spiked triangular (4 M–M) cluster cores are correlated by successive additions of two electrons[15]. Clusters 1–5 show triangular cores, clusters 6–9 quasi-planar square core, clusters 10 and 11 spiked triangular cores and cluster 12 butterfly geometry.

EXPERIMENTAL

The tri- and tetrametallic clusters were obtained, purified and identified according to established methods (see Table I). The chemical inertness of the products in acetonitrile, chloroform, methanol and *n*-hexane was tested by maintaining them in these solvents for several hours at room temperature and by monitoring the IR spectra (CO stretching region) of the solutions before and after the chromatographic experiments.

The chromatographic separations were performed using a Perkin-Elmer Series 3B chromatograph with a Rheodyne 7105 injection valve and an LC-75 variable-

TABLE I

FORMULAS, ELECTRONIC ABSORPTION MAXIMA AND STRUCTURES OF THE CLUSTERS

Compound*	No.	$\lambda_{max.}$ (nm)**	Structure***	Ref.
$Fe_3(CO)_9[C_2(C_2H_5)_2]$	1	270sh, 365sh		7, 8
$Fe_3(CO)_8[P(C_6H_5)_3][C_2(C_2H_5)_2]$	2	260sh, 340sh		9
$Fe_3(CO)_7(dppm)[C_2(C_2H_5)_2]$	3	270sh, 385sh		10
(cp)NiFe_2(CO)_6(tba)	4	285, 331		11
(cp)NiFe_2(CO)_5[P(C_6H_5)_3](tba)	5	270, 340		9
$(cp)_2Ni_2Fe_2(CO)_6[C_2(C_2H_5)_2]$	6	330, 560, 625		12
$(cp)_2Ni_2Fe_2(CO)_6[C_2(C_6H_5)_2]$	7	330, 580, 620		12
$(cp)_2Ni_2Fe_2(CO)_6[HC_2(t\text{-}C_4H_9)]$	8	325, 550, 655		12
$(cp)_2Ni_2Fe_2(CO)_6[HC_2(i\text{-}C_3H_7)]$	9	325, 560, 625		12
$(cp)_2Ni_2Fe_2(CO)_5[P(C_6H_5)_2][C_2(i\text{-}C_3H_7)]$	10	300sh		13
$(cp)_2Ni_2Fe_2(CO)_5[P(C_6H_5)_2](C_2C_6H_5)$	11	320sh		14
$(cp)NiFe_3(CO)_7[P(C_6H_5)_2][HC_2(i\text{-}C_3H_7)]$	12	325sh		13

* dppm = bis(diphenylphosphino)methane; cp = η^5-cyclopentadienyl; tba = tert.-buthylacetyl-ide.

** Solvent, hexane; sh = shoulder; all compounds exhibit an additional absorption maximum at $\lambda < 250$ nm.

*** Ni-bonded cyclopentadienyl and Fe-bonded σ-donor ligands (COs and phosphines) are omitted for clarity.

wavelength UV–visible detector. Stainless-steel columns (25 × 0.4 cm I.D.) filled with 10-μm LiChrosorb Si 60 or RP-8 (Merck) were used; the stability of the complexes towards stainless steel was tested as previously reported for other heterometallic clusters[4]. The flow-rate was generally 1 ml/min and the eluates were moni-
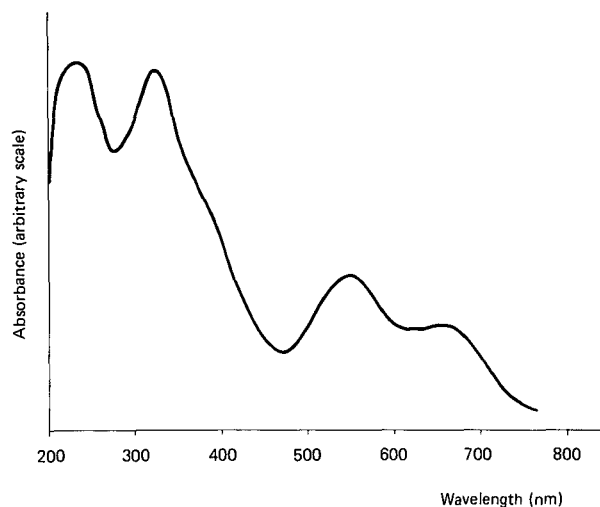
Fig. 1. Electronic spectrum of 8 in *n*-hexane.

tored at 265 or 330 nm, depending on the positions of the absorption maxima. The UV–VIS spectra of all the compounds were recorded on a Jasco 505 spectrophotometer (Table I); one of them (compound 8) is shown in Fig. 1.

Acetonitrile or *n*-hexane solutions (5 μl) of the compounds were injected; *n*-hexane–chloroform was the mobile phase for the Si 60 column and acetonitrile–methanol for the RP-8 column. Solvents were of HPLC grade (Carlo Erba).

DISCUSSION

The mixtures of clusters chromatographed on the RP-8 and Si 60 columns are listed in Table II. Fig. 2–4 show three of the separations reported in Table II.

TABLE II

RETENTION TIMES, ELUENT AND COLUMN MATERIALS

Mixtures of compounds* and retention times (min) in parentheses	Column	Eluent**	Flow-rate (ml/min)	Note
3 (4.1), 1 (4.5), 2 (5.2)	RP-8	M–A (50:50)	1.0	Fig. 2
4 (4.6), 5 (5.2)	RP-8	M–A (50:50)	1.0	—
7 (6.4), 9 (6.5), 6 (6.6), 8 (6.7)	RP-8	M–A (45:55)	1.8	—
10 (5.0), 12 (5.3), 9 (5.4)	RP-8	M–A (90:10)	1.0	—
11 (5.4), 10 (5.5)	RP-8	M–A (50:50)	1.0	—
1 (9.2), 3 (9.3), 2 (14.7)	Si 60	H–C (80:20)	1.0	—
4 (3.4), 5 (4.3)	Si 60	H–C (90:10)	1.0	Fig. 3
8 (3.2), 9 (3.3), 6 (3.4), 7 (3.8)	Si 60	H–C (95:5)	1.0	—
9 (2.9), 12 (3.0), 10 (3.2), 11 (3.3)	Si 60	H–C (70:30)	1.0	Fig. 4

* Compound numbers as in Table I.
** M = methanol; A = acetonitrile; H = *n*-hexane; C = chloroform.
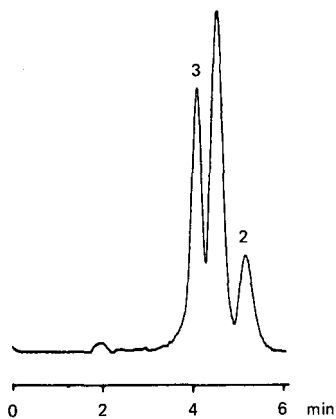
Fig. 2. Separation of 1, 2 and 3 on RP-8. Mobile phase, methanol–acetonitrile (50:50); flow-rate, 1 ml/min; detection, UV (265 nm). Resolution (R_s), 0.7 and 1.0; plate numbers (N), 1063, 895 and 896.

The separations of these clusters were slightly difficult, with close retention times. However, further information on the chromatographic behaviour of metal carbonyl clusters was achieved and in some instances valuable results in terms of effective separations were obtained.

The results concerning the two series of clusters, 1–3 and 4 and 5, confirm the

Fig. 3. Separation of 4 and 5 on Si 60. Mobile phase, n-hexane–chloroform (90:10); flow-rate, 1 ml/min; detection, UV (265 nm). Resolution (R_s), 1.6; plate numbers (N), 740 and 825.
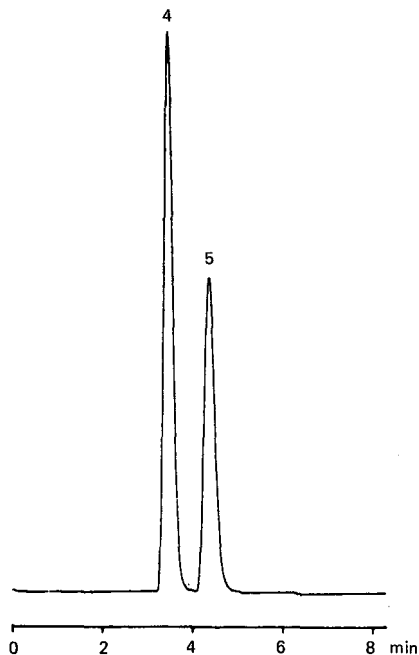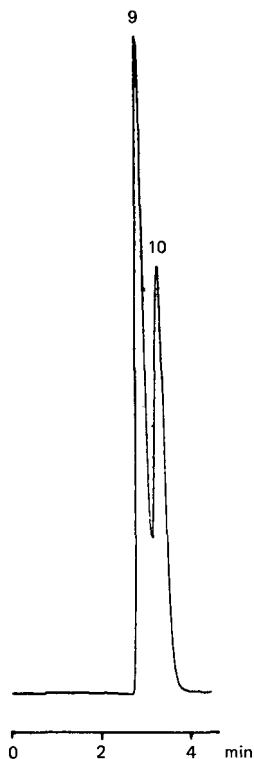
Fig. 4. Separation of 9 and 10 on Si 60. Mobile phase, *n*-hexane–chloroform (70:30); flow-rate, 1 ml/min; detection, UV (330 nm). Resolution (R_s), 0.8; plate numbers (N), 538 and 489.

general tendency observed[3,5] that triphenylphosphine monosubstituted clusters (2 and 5 in this work) give longer retention times than the parent clusters (1 and 4, respectively). In contrast, compound 3, which contains the bridging ligand 1,2-bis-(diphenylphosphino)methane, exhibits almost the same retention time as the parent compound 1 on silica and, surprisingly, is eluted before it in reversed-phase conditions. This behaviour could be related to the high solubility of 3 in all common organic solvents. It is worth noting that the tri-iron clusters 1, 2 and 3 are strongly retained on silica and hence they can be easily separated from the corresponding nickel-containing derivative (*e.g.*, cluster 6).

The chromatographic behaviour of the series of quasi-planar clusters 6–9 and of the spiked triangular clusters 10 and 11 are essentially determined by the nature of the organic radical on the alkyne ligand. On silica the phenyl derivatives are eluted after the alkyl derivatives and the order appears to be related to the Taft polar substituent constant[16,17], σ, as previously observed[2,4]: the retention time increases as σ increases ($\sigma_{C_6H_5} > \sigma_{C_2H_5} > \sigma_{i\text{-}C_3H_7} > \sigma_{t\text{-}C_4H_9}$). On the RP-8 column an opposite elution order is observed, as expected, with the exception of clusters 9 and 6, which maintain the order exhibited on silica.

The clusters 9, 12 and 10, all containing the isopropyl radical, are eluted in this

order on silica. Both 10 and 12 carry a diphenylphosphido ligand but differ in shape (spiked triangular and butterfly, respectively) and in the Ni:Fe ratio, and therefore it is difficult to rationalize the chromatographic results in terms of separate effects. However, the different retention times of 9 and 10, which have the same Ni:Fe ratio, appear to be due to the presence in 10 of the diphenylphosphido ligand, if one disregards the effects of the shape (quasi-planar and spiked triangular, respectively). In reversed-phase conditions the opposite elution order is observed and cluster 10 is eluted first.

In conclusion, it is interesting to note the different effects exerted by the PPh_3 ligand and the PPh_2 moiety: the presence of the former in a cluster always produces higher retention times in both normal and reversed-phase conditions, whereas the latter appears to be sensitive to the chromatographic conditions used.

REFERENCES

1 D. A. Roberts and G. L. Geoffroy, in G. Wilkinson, F. G. A. Stone and E. W. Abel (Editors), *Comprehensive Organometallic Chemistry*, Vol. 6, Pergamon Press, New York, 1982, p. 806.
2 A. Mangia, G. Predieri and E. Sappa, *Anal. Chim. Acta*, 149 (1983) 349.
3 A. Mangia, G. Predieri and E. Sappa, *Anal. Chim. Acta*, 152 (1984) 289.
4 A. Casoli, A. Mangia, G. Predieri and E. Sappa, *J. Chromatogr.*, 303 (1984) 404.
5 A. Casoli, A. Mangia, G. Predieri and E. Sappa, *Anal. Chim. Acta*, 176 (1985) 259.
6 A. Casoli, A. Mangia, G. Predieri and E. Sappa, *J. Chromatogr.*, 355 (1986) 285.
7 S. Aime, L. Milone, E. Sappa, A. Tiripicchio and M. Tiripicchio Camellini, *J. Chem. Soc., Dalton Trans.*, (1979) 1155.
8 G. Granozzi, E. Tondello, M. Casarin, S. Aime and D. Osella, *Organometallics*, 2 (1983) 430.
9 A. J. Carty, N. J. Taylor, E. Sappa and A. Tiripicchio, in preparation.
10 G. Predieri, A. Tiripicchio, M. Tiripicchio Camellini and E. Sappa, *Proceedings of XIX Congresso Nazionale di Chimica Inorganica, Cagliari, Italy, 1986,* University of Cagliari, Cagliari, 1986, p. 201.
11 A. Marinetti, E. Sappa, A. Tiripicchio and M. Tiripicchio Camellini, *J. Organomet. Chem.*, 197 (1980) 335.
12 E. Sappa, A. M. Manotti Lanfredi, G. Predieri, A. Tiripicchio and A. J. Carty, *J. Organomet. Chem.*, 288 (1985) 365.
13 A. J. Carty, E. Sappa, A. Tiripicchio, in preparation.
14 C. Weatherell, N. J. Taylor, A. J. Carty, E. Sappa and A. Tiripicchio, *J. Organomet. Chem.*, 291 (1985) C9.
15 E. Sappa, A. Tiripicchio and P. Braunstein, *Coord. Chem. Rev.*, 65 (1985) 219.
16 R. W. Taft, Jr., in M. S. Newman (Editor), *Steric Effects in Organic Chemistry*, Wiley, New York, 1956, Ch. 13.
17 J. Hine, *Physical Organic Chemistry*, McGraw-Hill, New York, 1962, p. 97.

CHROM. 20 530

Note

Cyclodextrins as chiral stationary phases in capillary gas chromatography

I. Pentylated α-cyclodextrin

WILFRIED A. KÖNIG*, SABINE LUTZ, PETRA MISCHNICK-LÜBBECKE and BÄRBEL BRASSAT

Institut für Organische Chemie der Universität, D-2000 Hamburg 13 (F.R.G.)

and

GERHARD WENZ

Max-Planck-Institut für Polymerforschung, D-6500 Mainz (F.R.G.)

(Received January 19th, 1988)

Carbohydrates have repeatedly been used as chiral selectors for the separation of enantiomers by liquid chromatography. A large number of racemic compounds have recently been resolved on microcrystalline triacetylcellulose[1,2], α- and β-cyclodextrins[3,4], carbohydrate derivatives covalently connected to aminopropyl silica gel[5,6] and polysaccharide derivatives adsorbed on silica gel[7,8].

Of these carbohydrate selectors, cyclodextrins are especially important. In addition to a large number of chiral centres for enantioselective interaction, these macrocyclic molecules may form diastereomeric inclusion complexes resulting in the selective retention of one enantiomer. The solubility of cyclodextrins in organic solvents also allows their application as stationary phases for gas chromatography. Koscielski *et al.*[9] have demonstrated the separation of enantiomers of terpenoid hydrocarbons on a packed column. We have increased the hydrophobicity of cyclodextrins by alkylation and used these derivatives as liquid phases for capillary gas chromatography. The fully pentylated α-cyclodextrin (Fig. 1) shows a remarkable enantioselectivity towards the enantiomers of carbohydrate derivatives and some nitrogen compounds.

EXPERIMENTAL

Gas chromatography

A Carlo Erba Model 2101 gas chromatograph with split inlet and a flame ionization detector was used.

Preparation of chiral capillary columns

Pyrex glass capillary columns were coated according to the static procedure[10] as described previously[11].
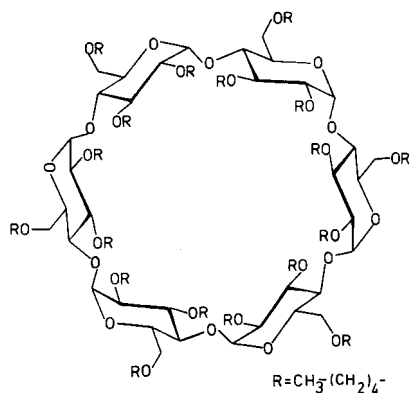
Fig. 1. Structure of per-O-pentyl-α-cyclodextrin used as chiral stationary phase.

Preparation of derivatives

Fully trifluoroacetylated sugars were prepared by heating samples of about 0.5 mg of carbohydrate in a mixture of 200 μl of dichloromethane and 50 μl of trifluoroacetic acid anhydride for 1 h at 100°C in a glass vial with a PTFE-lined screw-cap. Methylglycosides were prepared by heating sugars in 0.5 ml of dry hydrogen chloride in methanol (1.5 M) for 1 h at 100°C in glass vials. 1.5-Anhydroalditols (or 1,4-anhydroalditols) were formed according to the method described by Gray and co-workers[12,13]. For peralkylation of glucose a three-fold excess of the corresponding alkyl iodides, in the case of α-cyclodextrin pentylbromide, was added to the samples in dimethyl sulphoxide in the presence of 3 equiv. of sodium hydroxide, according to Ciucanu and Kerek[14].

RESULTS AND DISCUSSION

In most chiral stationary phases used for enantiomer separation by capillary gas chromatography, amino acids were used as optically active ligands[15]. Enantiomer resolution is mainly due to the formation of diastereomeric association complexes based on hydrogen bonding interactions. Only a few instances are known in which hydrogen bond association could definitely be ruled out but enantiomer separation is still observed[16,17]. In these instances dipole–dipole interactions may be responsible for chiral recognition.

The sepration of trifluoroacetylated hydroxy esters in capillary columns using stationary phases with optically active hydroxy acid derivatives as chiral selectors[18,19] and the separation of proline enantiomers on N-trifluoroacetyl-L-prolyl-L-proline cyclohexyl ester[16] demonstrates the beneficial effect of a close structural relationship between the chiral selector and the chiral substrate. This concept also seems to apply to the separation of carbohydrate derivatives on modified cyclodextrins. As shown in Figs. 2–6, the enantiomers of various carbohydrate derivatives can be separated on fully O-pentylated α-cyclodextrin. O-Trifluoroacetylated methylglycosides have also been separated on XE-60–L-valine-(S)-α-phenylethylamide[18,19], while pertrifluoroacetylated sugars could be separated particularly well
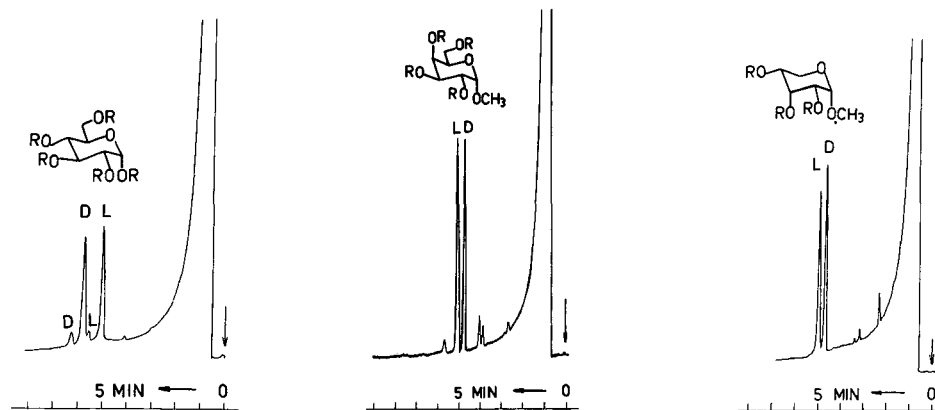
Fig. 2. Enantiomer separation of α- (large peaks) and β-glucopyranose (small peaks). R = CF₃CO. 20-m glass capillary column, coated with perpentylated α-cyclodextrin; column temperature, 100°C; carrier gas, 0.8 bar hydrogen.

Fig. 3. Enantiomer separation of α-methylgalactopyranoside. R = CF₃CO. Column as in Fig. 1; column temperature, 110°C.

Fig. 4. Enantiomer separation of α-methylribopyranoside. R = CF₃CO. Column as in Fig. 1; column temperature, 110°C.

on OV-225–L-valine-(R)-α-phenylethylamide[20]. Some polyols, including trifluoroacetylated arabinitol, were separated on XE-60–L-valine-(R)-α-phenylethylamide[21]. The 1,5-anhydroalditols (or 1,4-anhydroalditols) were formed during reductive depolymerization[22,23] in the course of structural investigations of complex polysaccharides. An example of the separation of these derivatives is shown in Fig. 6.
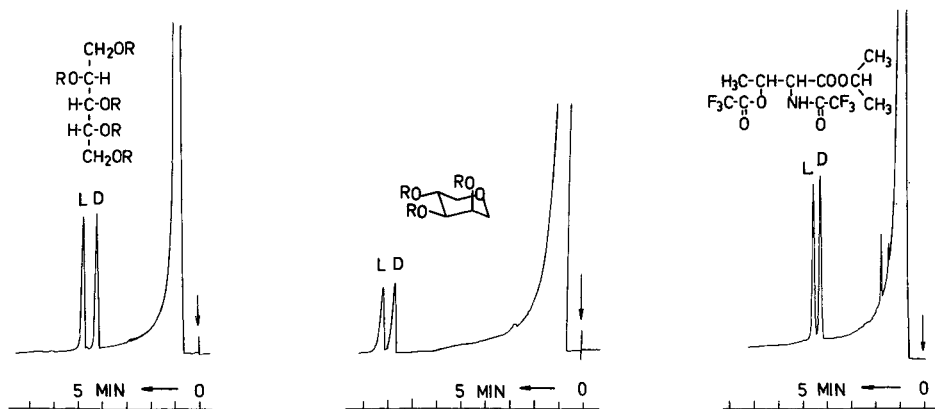
Fig. 5. Enantiomer separation of arabinitol. R = CF₃CO. Column as in Fig. 1; column temperature, 100°C.

Fig. 6. Enantiomer separation of 1,5-anhydrolyxitol. R = CF₃CO. Column as in Fig. 1; column temperature, 80°C.

Fig. 7. Enantiomer separation of N,O-trifluoroacetylthreonine isopropyl ester. Column as in Fig. 1; column temperature, 85°C.
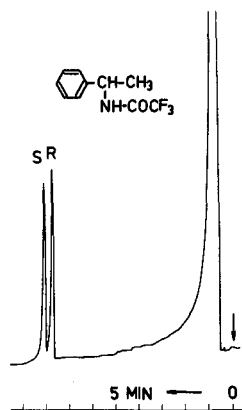
Fig. 8. Enantiomer separation of N-trifluoroacetyl-1-phenylethylamine. Column as in Fig. 1; column temperature, 100°C.

TABLE I

SEPARATION FACTORS, α, COLUMN TEMPERATURES AND ORDER OF ELUTION IN THE ENANTIOMER SEPARATION OF TRIFLUOROACETYLATED CARBOHYDRATE DERIVA- TIVES ON A 20-m GLASS CAPILLARY COLUMN, COATED WITH PER-n-PENTYL-α-CYCLO- DEXTRIN

Carbohydrate	α	Column temperature (°C)	First peak eluted
α-Glucose	1.119	100	L
β-Glucose	1.140	100	L
α-Galactose	1.070	100	L
β-Galactose	1.080	130	L
α-Allose	1.171	120	D
β-Allose	1.064	120	D
α-Mannose	1.000	100	—
β-Mannose	1.110	100	L
α-Gulose	1.000	120	—
β-Gulose	1.043	120	D
α-Talose	1.099	110	D
β-Fucose (f)*	1.039	100	L
α-Methylgalactoside	1.091	100	D
α-Methylglucoside	1.035	100	L
α-Methylmannoside	1.051	100	L
α-Methylidoside	1.040	90	D
α-Methylriboside	1.075	110	D
Sorbitol	1.042	100	D
Mannitol	1.019	90	D
Arabinitol	1.175	100	D
1,5-Anhydrofucitol	1.035	80	D
1,5-Anhydrolyxitol	1.064	80	D
1,5-Anhydroarabinitol	1.074	80	D
1,4-Anhydroribitol**	1.060	90	L
1,4-Anhydroxylitol**	1.029	80	L

   * f = Furanoside.
   ** The corresponding 1,5-anhydro derivatives are non-chiral.

Compared with previous results with chiral polysiloxane phases, it can be stated that the separation of pertrifluoroactylated aldohexoses, aldopentoses and polyols is superior on perpentylated α-cyclodextrin. The methylglycosides of aldohexoses and some aldopentoses are also well separated on the cyclodextrin phase (Figs. 3 and 4). The results in terms of separation factors (α) are given in Table I.

In addition to carbohydrate derivatives, some trifluoroacetylated amines, amino alcohols and amino acid esters could be separated on perpentylated α-cyclodextrin, although the separation factors are generally lower than on the XE-60 phases. Fig. 7 shows an example of the separation of an amino acid derivative (DL-threonine). In Fig. 8 the separation of 1-phenylethylamine is shown.

The thermal stability of perpentylated α-cyclodextrin is remarkably high. No deterioration of column performance was observed after operation of the columns at 200°C. In conclusion, it can be stated that chemically modified cyclodextrins may well serve as chiral stationary phases in capillary gas chromatography.

Attempts to separate peralkylated glucose derivatives (permethyl, -ethyl and -propyl) failed. Therefore, it seems to be questionable whether the enantiomers are really separated owing to the formation of inclusion complexes inside the cavity of the macrocyclic cyclodextrin molecule or whether a more general type of diastereomeric association applies in this system.

ACKNOWLEDGEMENT

REFERENCES

1 G. Hesse and R. Hagel, *Justus Liebigs Ann. Chem.*, (1976) 996.
2 A. Mannschreck, H. Koller and R. Wernicke, *Kontakte (Merck, Darmstadt)*, (1) (1985) 40.
3 D. W. Armstrong, T. J. Ward, R. D. Armstrong and T. E. Beesley, *Science (Washington, D.C.)*, 232 (1986) 1132.
4 D. W. Armstrong, X. Yang, S. M. Han and R. A. Menges, *Anal. Chem.*, 59 (1987) 2594.
5 J. Schulze and W. A. König, *J. Chromatogr.*, 355 (1986) 165.
6 O. Weller, J. Schulze and W. A. König, *J. Chromatogr.*, 403 (1987) 263.
7 Y. Okamoto, M. Kawashima, K. Yamamoto and K. Hatada, *Chem. Lett.*, (1984) 739.
8 Y. Okamoto, M. Kawashima and K. Hatada, *J. Am. Chem. Soc.*, 106 (1984) 5327.
9 T. Koscielski, D. Sybilska, S. Belniak and J. Jurczak, *Chromatographia*, 21 (1986) 413.
10 J. Bouche and M. Verzele, *J. Gas Chromatogr.*, 6 (1968) 501.
11 W. A. König and K. Ernst, *J. Chromatogr.*, 280 (1983) 135.
12 J. U. Bowie, P. V. Trescony and G. R. Gray, *Carbohydr. Res.*, 125 (1984) 301.
13 J. G. Jun and G. R. Gray, *Carbohydr. Res.*, 163 (1987) 247.
14 I. Ciucanu and F. Kerek, *Carbohydr. Res.*, 131 (1984) 209.
15 W. A. König, *The Practice of Enantiomer Separation by Capillary Gas Chromatography*, Hüthig, Heidelberg, 1987, and references cited therein.
16 W. A. König, K. Stölting and K. Kruse, *Chromatographia*, 10 (1977) 444.
17 W. A. König and S. Sievers, *J. Chromatogr.*, 200 (1980) 189.
18 W. A. König, I. Benecke and S. Sievers, *J. Chromatogr.*, 217 (1981) 71.
19 W. A. König, I. Benecke and H. Bretting, *Angew. Chem.*, 93 (1981) 688; *Angew. Chem., Int. Ed. Engl.*, 20 (1981) 693.
20 I. Benecke, E. Schmidt and W. A. König, *J. High Resolut. Chromatogr. Chromatogr. Commun.*, 4 (1981) 553.
21 W. A. König and I. Benecke, *J. Chromatogr.*, 269 (1983) 19.
22 D. Rolf and G. R. Gray, *J. Am. Chem. Soc.*, 104 (1982) 3539.
23 P. Mischnick-Lübbecke, M. Radeloff and W. A. König, *Stärke/Starch*, 39 (1987) 425.

CHROM. 20 578

Note

Gas chromatographic determination of calcium stearate in polyethylene food packaging sheets

SHIGERU TAN*, TAKASHI TATSUNO and TARO OKADA

Institute of Food Hygiene, Japan Food Hygiene Association, 6-1, Jingu-mae 2-chome, Shibuya-ku, Tokyo 150 (Japan)

(First received December 30th, 1987; revised manuscript received April 21st, 1988)

Calcium stearate is widely used as both a stabilizer and lubricant for synthetic rubber and resin. One very important usage is in the production of high density polyethylene which is extensively used in Japan for the fabrication of packages containing milk. For use in various synthetic resins such as poly(vinyl chloride) (PVC), polystyrene, polypropylene, etc., in polyethylene packages for milk, calcium stearate levels must not to exceed 0.25%.

We have previously reported analyses of additives[1,2] such as antioxidants in food-grade polymers using gas chromatography (GC) or high-performance liquid chromatography (HPLC). However, direct analysis by chromatography has not been achieved for calcium stearate, because it is difficult to ensure total dissolution in an appropriate organic solvent. There are, moreover, no reports in the literature of the GC analysis of calcium stearate in synthetic resins.

In this paper, a method for determining the calcium stearate in polyethylene packages using GC and HPLC is discussed. An extract from the polyethylene packaging sheet is saponified, then the resulting acid is esterified to form a methyl ester[3] for the GC analysis, and the p-bromophenacyl ester, using 18-crown-6 as the catalyst, for the HPLC analysis[4–8]. To compare the efficacy of the two methods, they were used to determine calcium stearate contents and the results were found to be in reasonable agreement. The identification of calcium stearate was confirmed by GC–mass spectrometry (MS).

EXPERIMENTAL

Materials

Polyethylene sheets containing 0.15% of calcium stearate were prepared; the sheet thickness was 200 μm (similar to polyethylene packages for retail milk samples).

Calcium stearate was obtained from Tokyo Chemical Industries (Tokyo, Japan). The p-bromophenacyl bromide and 18-crown-6 were from Dojindo Laboratories (Kumamoto City, Japan) and Aldrich Chemical Company (Milwaukee, WI, U.S.A.) respectively. Filter paper No. 5C (9 cm in diameter) was from Toyo Roshi (Tokyo, Japan). The boron trifluoride–methanol complex was from Wako Pure Chemical Industries (Osaka City, Japan). Organic solvents were of analytical reagent grade.

Preparation of standard

GC method. A stock solution of calcium stearate was prepared by dissolving 0.1 g in 10 ml of 0.5 *M* hydrochloric acid in chloroform. A 2.0-ml aliquot of this solution was transferred to an 100-ml round-bottom flask and evaporated to dryness.

HPLC method. The stock solution was prepared as above and the residue saponified with 10 ml of 0.5 *M* potassium hydroxide in methanol by refluxing for 10 min. A 2-ml aliquot of the cooled solution was transferred to an 100-ml round-bottom flask. As an internal standard, 1 ml of a margaric acid stock solution [0.01 g of margaric acid (*n*-heptadecanoic acid) dissolved in 10 ml methanol] was added to a round-bottom flask. The acids were neutralized with 0.5 *M* hydrochloric acid in methanol to the phenolphthalein endpoint[7]. The solution was evaporated to dryness and the residue was esterified (see below).

Preparation of sample

GC method. Polyethylene sheets were cut into narrow strips (*ca.* 1 cm × 0.2 cm). Samples of about 5.0 g were weighed accurately into an extraction thimble (100 mm × 28 mm) and extracted in a Soxhlet extraction apparatus with 180 ml chloroform for 4 h. The chloroform extract was discarded, and the samples (polyethylene) in the extraction thimble were transferred to a round-bottom flask and refluxed with 100 ml chloroform–10 ml hydrochloric acid (2:1) for 4 h. The extract was cooled and the chloroform layer transferred an 100-ml round-bottom flask. After the solvent had been evaporated to dryness at 35°C, the residue was esterified according to the following procedure.

HPLC method. Polyethylene sheets were extracted as above. The residue was prepared according to the preparation of the standard for HPLC.

Esterification procedure

GC method. To each residue of the standard and sample, in an 100-ml round-bottom flask, 4 ml of 0.5 *M* potassium hydroxide in methanol and 1 ml of a margaric acid stock solution (0.1 g of margaric acid dissolved in 10 ml *n*-heptane) were added. The solutions were refluxed for 10 min, through a condenser, 5 ml of the boron trifluoride–methanol complex were added and refluxed for 2 min. Moreover, to the solutions in the flask, 9 ml of *n*-heptane were added through a condenser and refluxed for 1 min.

The boiled solutions were allowed to cool to room temperature, and 30 ml of a saturated solution of sodium sulphate were added to the flasks. The flasks were capped and shaken for *ca.* 2 min. Again saturated sodium sulphate was added up to the neck of each flask. The solutions were allowed to stand until the phases had completely separated (about 30 min), and were then analyzed by GC.

HPLC method. To each residue of the standard and sample, in an 100-ml round-bottom flask, 5 ml of the alkylating reagent (0.4 g of *p*-bromophenacyl bromide and 0.2 g of 18-crown-6 dissolved in 100 ml of acetonitrile) were added. The flasks were heated at 80°C for 30 min. The solutions were filtered through filter-paper before HPLC analysis.

Gas chromatography

An Hewlett-Packard Model 5890A instrument equipped with a flame ioniza-

tion detector was used. The inlet system used was split injection. A 25 m × 0.2 mm I.D. fused-silica capillary column was coated with 0.33 μm a cross-linked methyl silicone gum phase (Hewlett-Packard Part No. 19091A-102). The nitrogen carrier gas flow-rate was 25 cm/s measured at 200°C, the nitrogen make-up gas flow-rate was 30 ml/min and the air and hydrogen flow-rates for the flame were 400 and 30 ml/min, respectively. The injection temperature was 250°C, and the detector temperature, 300°C. The column oven was held at 200°C for 0.5 min and then programmed to 270°C at 10°C/min. Integration of peaks and processing of chromatograms was carried out by the Hewlett-Packard 3392A automation system.

High-performance liquid chromatography

The chromatographic system consisted of a Model L-4000 pump (Yanagimoto Manufacturing, Kyoto, Japan), a M-315 UV detector (Yanagimoto) operated at 254 nm and a Rheodyne 7125 valve injector. A 250 mm × 4.6 mm I.D., 5 μm reversed-phase column (Nucleosil 5C$_{18}$; Macherey-Nagel, Düren, F.R.G. protected by a 50 mm × 4.6 mm I.D., 10 μm guard column (Unisil Q C$_{18}$; Gasukuro Kogyo, Tokyo, Japan) was used. Operating conditions: mobile phase, 90% acetonitrile (HPLC grade, Wako) in water; flow-rate, 1 ml/min; column temperature, 40°C; injection volume, 10 μl. Data were collected and analyzed with the Hewlett-Packard 3392A automation system.

RESULTS AND DISCUSSION

A method for the determination of calcium stearate in polyethylene sheets by GC has been developed. Separation times were less than 10 min per sample.

After extractions of the glycerine fatty acid esters and stearic acid in polyethylene by chloroform, chloroform in the presence of hydrochloric acid was chosen as the extraction solvent because calcium stearate was completely dissolved in this solvent. Zinc salts present in polyethylene were estimated by atomic absorption analysis.
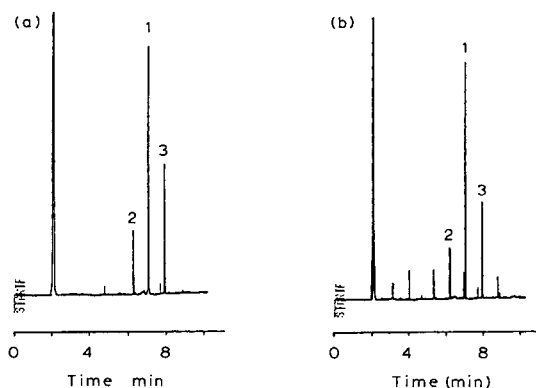

Fig. 1. Gas chromatograms of (a) standard fatty acid methyl esters from calcium stearate and (b) fatty acid methyl esters of an extract from a polyethylene food packaging sheet. Peak identification: 1 = margarate (internal standard); 2 = palmitate; 3 = stearate.
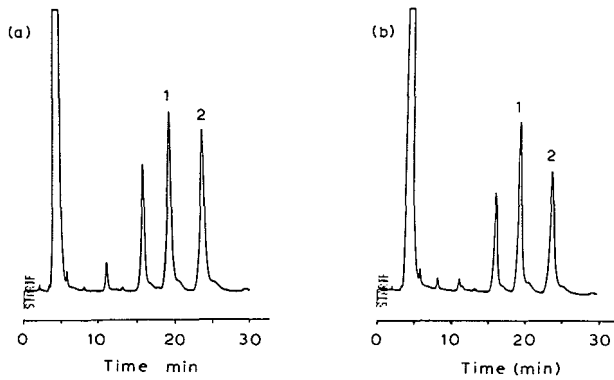
Fig. 2. HPLC chromatograms of (a) standard fatty acid *p*-bromophenacyl esters from calcium stearate and (b) fatty acid *p*-bromophenacyl esters of an extract from a polyethylene food packaging sheet. Peak identification: 1 = margarate (internal standard); 2 = stearate.

Margaric acid was used as the internal standard so that the sample esterification yields could be monitored relative to a single standard. Typical chromatograms obtained by GC and HPLC are shown in Figs. 1 and 2. For polyethylene with a known addition of 0.15% calcium stearate, the mean level (n = 10) was found by GC to be 0.16% (C.V. = 1.5%) and by HPLC was 0.15% (C.V. = 2.0%). Duplicate analyses of calcium stearate agreed reasonably well.

Finally, the practical use of the method was demonstrated. Calcium stearate from polyethylene sheets was analyzed.

REFERENCES

1 S. Tan and T. Okada, *J. Food Hyg. Soc. Jpn.*, 19 (1978) 548.
2 S. Tan, S. Tadenuma, M. Hojo, Y. Yoshida, Y. Matsuzawa, T. Tatsuno and T. Okada, *J. Food Hyg. Soc. Jpn.*, 27 (1986) 229.
3 L. Rossi, *J. Assoc. Off. Anal. Chem.*, 64 (1981) 697.
4 H. D. Durst, *Tetrahedron Lett.*, No. 28 (1974) 2421.
5 H. D. Durst, M. Milano, E. J. Kikta, Jr., S. A. Connelly and E. Grushka, *Anal. Chem.*, 47 (1975) 1797.
6 T. N. Yweeten and D. L. Wetzel, *Cereal Chem.*, 56 (1979) 398.
7 B. Jaselskis, N. L. Stemm and W. D. Johnston, *Talanta*, 29 (1982) 54.
8 Y. Yabe, S. Tan, T. Ninomiya and T. Okada, *J. Food Hyg. Soc. Jpn.*, 24 (1983) 329.

CHROM. 20 569

Note

A study of the side-reaction products of phenylhydrazine production by gas chromatography–mass spectrometry

ĽUBOR BYSTRICKÝ*, ZLATICA VESELÁ and ERVÍN SOHLER

Research Institute of Chemical Technology, 836 03 Bratislava (Czechoslovakia)

(Received February 24th, 1988)

Phenylhydrazine has been produced industrially for more than 100 years. The history of its production is closely connected with that of the origin and/or development of the production technology for organic dyes and pharmaceuticals. At present, phenylhydrazine is widely applied as an important intermediate in the industrial technology of organic compounds, *e.g.*, chloridazone (5-amino-4-chloro-2-phenyl-pyridazin-3-one), the active ingredient of the selective herbicide Burex®. Its synthesis, starting from aniline, follows the general reaction scheme:
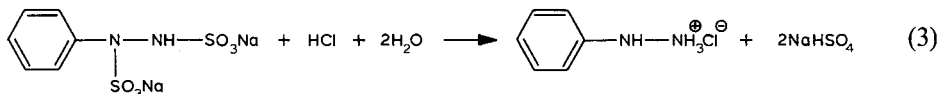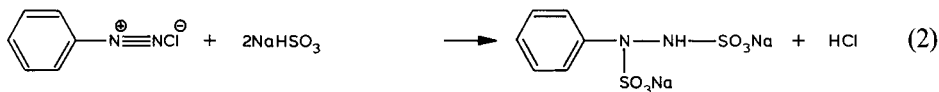
When the technological conditions of the reaction step 2 do not meet the steady-state regime, the formation of a precipitate is observed immediately after the contact of benzenediazonium chloride with sodium hydrogensulphite. This solid waste, which after isolation represented a yield of about 5%, with respect to aniline, was completely soluble in various organic solvents, *e.g.*, methanol, ethanol, diethyl ether. After subjecting the waste sample solutions to gas chromatographic–mass spectrometric (GC–MS) analysis, nine compounds, possible products of side-reactions, were identified. Extracts of the reaction mixtures from the individual reaction steps (see the above scheme) in a model synthesis of phenylhydrazine were analyzed for the compounds of interest. In addition, a sample of the collected gaseous exhaust was also subjected to analysis. Besides the nine substances mentioned, three more compounds were found and identified.

EXPERIMENTAL

The samples for GC–MS analyses were obtained as follows. A sample of solid waste was recovered by filtration of the precipitate, followed by drying in a thermostatted oven at 70°C. The homogenized sample was diluted in an appropriate solvent and 0.1-μl aliquots were injected onto a capillary column. A sample from the diazotization step (1) was obtained by addition of 277 g of analytical grade toluene, cooled to -2°C, to the reaction mixture, immediately after mixing the reagents. After a simple one-step extraction, the toluene extract was dried over sodium sulphate and 0.1-μl aliquots were subjected to GC–MS analysis. A sample from the reduction step (2) was obtained by addition of the same amount of toluene to the fresh reaction mixture as in step 1, but the toluene temperature was held at 20°C. After mixing for 10 min, the toluene layer was separated, dried over sodium sulphate and subjected to analysis. A sample from reaction step 3 was obtained by addition of 277 g of toluene at 20°C to the reaction mixture heated to 100°C. After cooling of the mixture and partitioning of the layers, the toluene layer was separated, dried over sodium sulphate and subjected to analysis. The samples of condensed gaseous exhaust collected from all three reaction steps were injected directly, without any preliminary treatment.

The GC–MS analyses were performed on an HP-5890 gas chromatograph, connected via the open-split interface to a HP-5970 mass-selective detector (Hewlett-Packard, Avondale, PA, U.S.A.). Sample solutions were injected onto a 12.5 m × 0.2 mm I.D. fused-silica column, coated with a 0.33-μm immobilized film of SE-30 (Hewlett-Packard). Helium was used as a carrier at the linear velocity, $\bar{u} = 40$ cm/s, the splitting ratio was 20:1. Samples were chromatographed under the programmed temperature conditions, starting from 40°C for 2 min, then increased to 230°C at 10°C/min. The injector port temperature was 230°C and that of the open-split interface was 250°C. Mass spectra were scanned in the mass range of $m/z = 29$–550, with a scanning ratio of 2.67/s. The photomultiplier voltage was held at 1600 V. For the toluene extracts, the detector was switched off between 2 and 4 min after the start (toluene elution region). The relative abundance of the individual components was quantified as a peak area percentage after the integration of the total ion current (TIC) signal. Benzene and phenol were quantified using the external standard technique. The calibration solution contained 0.8% benzene and 1.1% phenol in toluene respectively.

RESULTS AND DISCUSSION

Solid waste corresponding to about 5%, with respect to aniline, was recovered from the final raw reaction product of technical phenylhydrazine, obtained at elevated temperature and prolonged reaction time. After complete dissolution in the organic solvent and subsequent GC–MS analysis, this waste was found to be a mixture of benzene, phenol, thiophenol, phenylazide, 1,1'-biphenyul, azobenzene (*trans*), diphenyl sulphide, the phenyl ester of benzenesulphonic acid and the S-phenyl ester of benzenesulphinothioic acid. The main component was the S-phenyl ester of benzenesulphinothioic acid, comprising about 50% of the total peak area sum.

In a more detailed study aimed at the elucidation of the possible origins of the
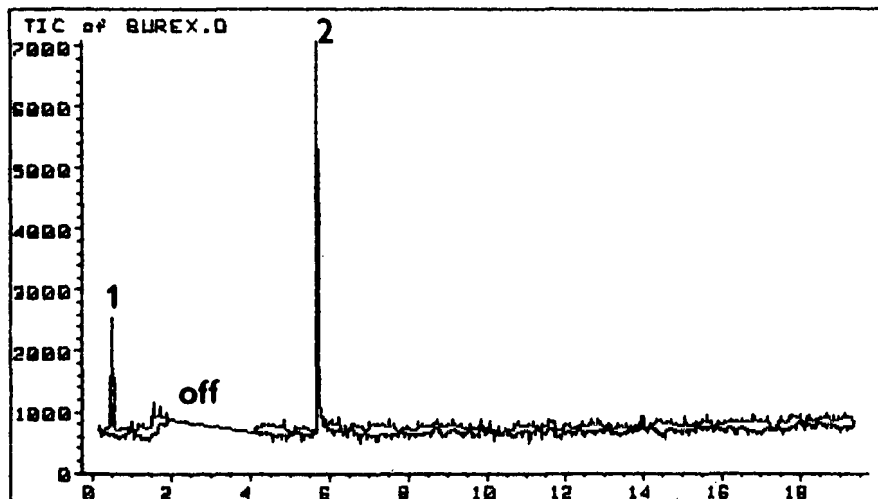
Fig. 1. Chromatogram of diazotization by-products. Peaks: 1 = benzene; 2 = phenol, "off" indicates the period when the detector was switched off. Time scale in min.

side-reaction products, the individual steps 1–3 of the reaction scheme were separately analyzed according to the procedures described in the Experimental.

Fig. 2 shows the TIC of the by-product mixture from the first reaction step (diazotization). The only by-products found were benzene and phenol, at levels of 0.08 and 0.6% respectively. The phenol could arise from decomposition of the diazonium salt in water, and a parallel homolytic decomposition of the salt could give rise to the benzene, the limiting factor being the temperature[1]. Another possible by-products, chlorobenzene, could not be found in the mixture possibly due to the fact that under the described conditions it would have been eluted in the time when detector was switched off. With regard to the amounts of the by-products, the first reaction step does not contribute substantially to their formation, though both compounds could be important from a toxicological point of view.

A chromatogram of the sample from the second reaction step is shown in Fig. 2. In addition to sulphur dioxide, the sample contains benzene, phenol (0.12 and 1.2% with respect to aniline), phenyl azide, 1,1′-biphenyl, diphenyl sulphide, diphenyl disulphide and the S-phenyl ester of benzenesulphinothioic acid. The relative sum of these compounds, without sulphur dioxide, is 2% with respect to aniline.

The chromatogram in Fig. 3 shows the sample from the third reaction step. Besides the compounds found in the samples from previous steps, this sample contains the phenyl ester of benzenesulphonic acid. The whole yield is about 10%, with respect to aniline. Fig. 4 shows a chromatogram of the sample from step 3, except that the reduction was accomplished with zinc. Compared with Fig. 3, there is a substantial decreasse in both the amount and presence of the by-products. The sample contains only phenol, thiophenol, diphenyl disulphide, cyclo-octasulphur and the S-phenyl ester of benzenesulphinothioic acid. The total content of by-products decreased to about 1%, with respect to aniline. The sample of gaseous exhaust was also analyzed. The resulting chromatogram is presented in Fig. 5. Phenyl azide and chlorobenzene were found to be the main components. The following compounds repre-
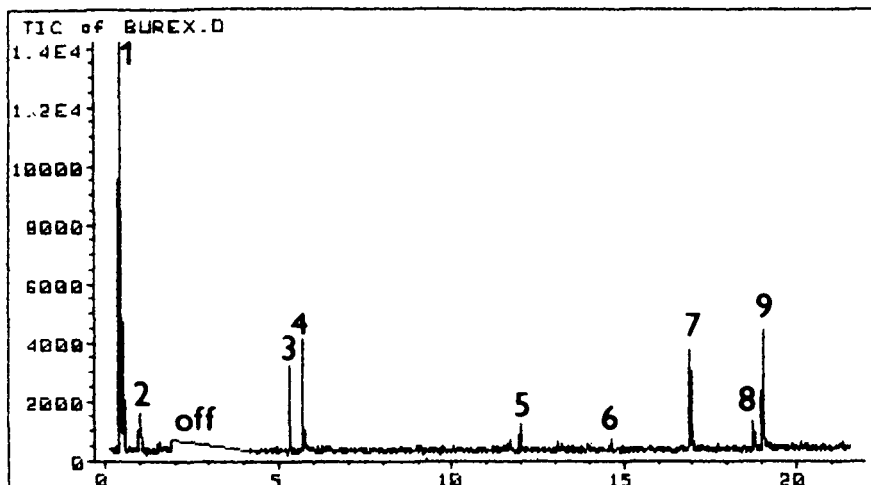
Fig. 2. Chromatogram of by-products from reaction step 2. Peaks: 1 = sulphur dioxide; 2 = benzene; 3 = phenyl azide; 4 = phenol; 5 = 1,1'-biphenyl; 6 = diphenyl sulphide; 7 = diphenyl disulphide; 8 = unknown; 9 = S-phenyl ester of benzenesulphinothioic acid.

sented the main part of the by-products: benzene, chlorobenzene, thiophenol, phenyl azide, phenol, 1,1'-biphenyl, azobenzene, diphenyl sulphide, diphenyl disulphide, cyclo–octasulphur, the phenyl ester of benzenesulphonic acid and the S-phenyl ester of benzenesulphinothioic acid. Their identities were confirmed either by chromatographing appropriate standards or by chromatographing reactions mixtures prepared according to the literature[2,3].

The origin and mechanism of formation of the by-products in the first step of phenylhydrazine synthesis, *i.e.*, diazotization was found to be rather sample and
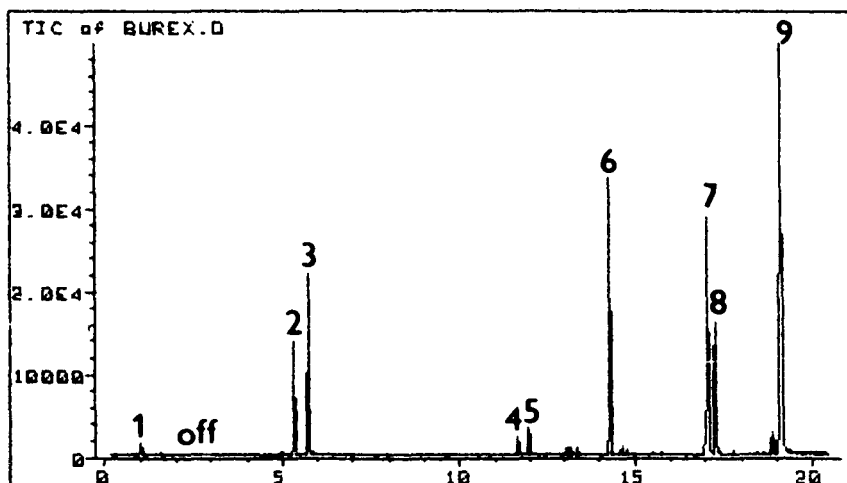

Fig. 3. Chromatogram of by-products from reaction step 3. Peaks: 1 = benzene; 2 = phenyl azide; 3 = phenol; 4 = unknown; 5 = 1,1'-diphenyl; 6 = diphenyl sulphide; 7 = diphenyl disulphide; 8 = phenyl ester of benzenesulphonic acid; 9 = S-phenyl ester of benzenesulphinothioic acid.
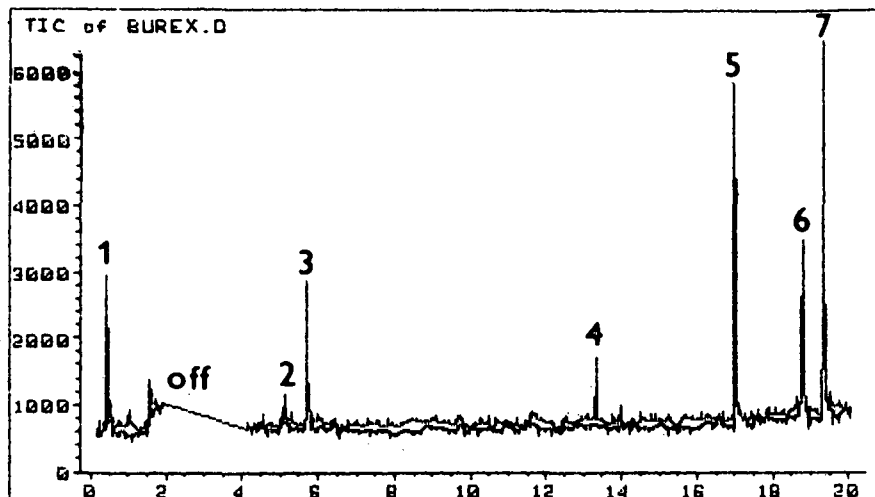
Fig. 4. Chromatogram of by-products from reaction step 3, using for the reduction. Peaks: 1 = sulphur dioxide; 2 = thiophenol; 3 = phenol; 4 = unknown; 5 = diphenyl disulphide; 6 = cyclo-octasulphur; 7 = S-phenyl ester of benzenesulphinothioic acid.

unequivocal. However, the situation is more complicated in the subsequent reaction steps. In the second step, there is a possibility of formation of by-products during the reaction, either via decomposition of the diazobenzene chloride (benzene, phenol), or via a competing reaction taking place in parallel with the formation of sodium phenylhydrazino sulphonate (phenyl azide), respectively, via decomposition of the sodium phenylhydrazino sulphonate itself. In the third step, by-products may be

Fig. 5. Chromatogram of the condensed gaseous exhaust. Peaks: 1 = sulphur dioxide; 2 = benzene; 3 = chlorobenzene; 4 = phenyl azide; 5,6 = unknown; 7 = diphenyl sulphide; 8 = azobenzene; 9 = diphenyl disulphide.

found as a result of the decomposition of phenylhydrazine. Information on the formation of most of the compounds mentioned can be found in the basic chemical manuals. The origin and preparation of benzene, thiophenol, diphenol, diphenyl sulphide, diphenyl disulphide, phenol, azobenzene and biphenyl are described in ref. 2, and the formation of phenylazide in ref. 3.
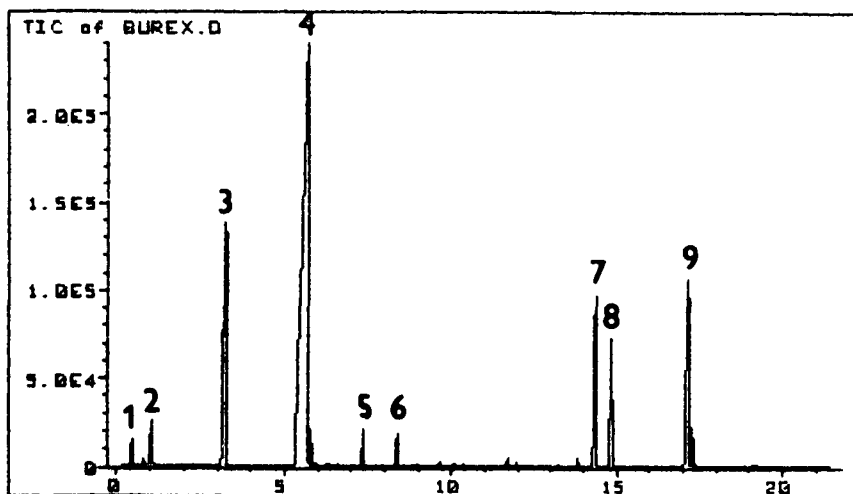
The influence of sulphur dioxide and sulphites on phenylhydrazine promoted by heat gives rise to N-sulphono acids[2]. At elevated temperature, these may rearrange, resulting in the formation of sulpho acids, which can subsequently react with phenol or thiophenol, both present in the reaction mixture. The corresponding esters of sulpho acids are the final reaction products. Ester formation represents the major competing reaction to the phenylhydrazine synthesis according to the reaction schemes 1–3.

Despite the worldwide industrial production of phenylhydrazine and the use of a general procedure, practically identical to the reaction scheme 1–3 for over 100 years, and that the conditions for the formation of the various compounds originating from benzenediazonium chloride or phenylhydrazine are well known[1-3], there is still a need for a complete analytical study of the synthesis of phenylhydrazine. The present paper was aimed at elucidating the possible risk and environmental impact of phenylhydrazine production, especially in the case of breakdown, or deviation, from the steady-state conditions. The results obtained indicate that even a simple and well known process can be a source of undesirable side-reaction by-products, some of which may present serious hazards for man and his environment (benzene, phenol, biphenyl).

ACKNOWLEDGEMENT

REFERENCES

1 I. Ernest, *Reakční Mechanismy v Organické Chemii*, SNTL, Prague, 1964, pp. 275–276.
2 *Beilsteins Handbuch der Organischen Chemie*, 4. Auflage, Springer, Berlin, 1932, Band XV, pp. 69–71.
3 *Beilsteins Handbuch der Organischen Chemie*, 4. Auflage, Springer, Berlin, 1922, Band V, p. 276.

CHROM. 20 567

Note

Resolution of enantiomeric drugs of some β-amino alcohols as their urea derivatives by high-performance liquid chromatography on a chiral stationary phase

QING YANG*, ZENG-PEI SUN and DA-KUI LING

National Institute for the Control of Pharmaceutical and Biological Products, Beijing (China)

(First received March 14th, 1988; revised manuscript received April 16th, 1988)

Compounds with a β-amino alcohol functional group are widely used as therapeutic agents. According to their pharmacological action, they may be divided into three main categories: (1) vasoconstrictors (*e.g.*, ephedrine); (2) hypertensive agents (*e.g.*, methoxamine, epinephrine); and (3) β-receptor blocking agents (*e.g.*, propranolol, alprenolol). All of them contain chiral centers. Their optical isomers may have different biological activities.

The enantiomeric separation of β-amino alcohol compounds with a commercially available (*R*)-N-(3,5-dinitrobenzoyl)phenylglycine chiral stationary phase (Pirkle-type DNBPG column) were reported by Wainer and co-workers, also condensed the amino alcohols either with β-naphthaldehyde to form oxazolidine derivatives[1,2] or with phosgene to form oxazolidone derivatives[3–5]. Both derivatization reactions require the reaction mixture to be cooled and stirred or refluxed for a long period.

We have previously reported the enantiomeric separation of derivatives of amines and alcohols with α-naphthyl isocyanate on a DNBPG column[6]. In this paper, we report the synthesis and direct resolution of a series of urea derivatives of β-amino alcohols using the same reagent.

EXPERIMENTAL

Apparatus

High-performance liquid chromatography (HPLC) was carried out with a Series 3B liquid chromatograph pump (Perkin-Elmer, Norwalk, CT, U.S.A.), an SPD-1 variable-wavelength UV–VIS detector (Shimadzu, Kyoto, Japan) set at 254 nm and sensitivity 0.04 a.u.f.s., a Perkin-Elmer 023 recorder set at a chart speed of 2.5 mm/min and a Model 7105 injector (Rheodyne, Cotati, CA, U.S.A.).

The covalently bonded Pirkle-type 1-A column (21 cm × 4 mm I.D.) was packed with 5-μm spherical particles of γ-aminopropylsilica modified with DNBPG prepared as described elsewhere[7]. The flow-rate of the mobile phase [*n*-hexane–isopropanol–acetonitrile (90:10:2)] was 2 ml/min.

TABLE I

SEPARATION OF α-NAPHTHYL ISOCYANATE DERIVATIVES OF β-AMINO ALCOHOLS ON A PIRKLE-TYPE DNBPG COLUMN
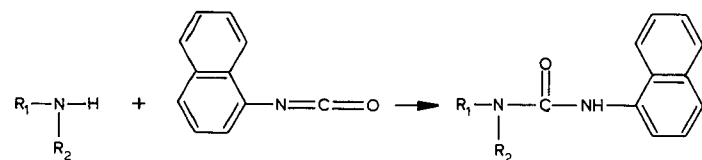
Compound	Structure	k'_1*	α	R_s	First-eluted enantiomer**
Ephedrine		23.26	1.03	0.76	d
Methoxamine		28.53	1.11	1.14	
Propranolol		19.76	1.25	1.61	
Oxprenolol		7.65	1.19	2.0	
Alprenolol		7.84	1.19	2.09	
Metroprolol***		20.64	1.14	1.54	
Timolol§		15.0	1.13	1.08	l

* Capacity factor of the first-eluted enantiomer.
** Configuration of the α-naphthyl isocyanate derivative moiety of β-amino alcohol.
*** Mobile phase, n-hexane–isopropanol–acetonitrile (90:10:1); flow-rate, 2.5 ml/min.
§ Mobile phase, n-hexane–isopropanol–acetonitrile (95:5:3.5); flow-rate, 2.5 ml/min.

Chemicals and reagents

The *l*- and *d*-ephedrine, *l*- and *d*-timolol and racemic methoxamine, propranolol, alprenolol, metroprolol and oxprenolol should be in the free base form; if not, they must be converted from the salts to the free bases by adding aqueous ammonia and then extracting with chloroform.

α-Naphthyl isocyanate (analytical-reagent grade) was purchased from BDH (Poole, U.K.). Acetonitrile (HPLC-grade; State Huang Yan Chemical Experimental Factory, China), isopropanol (analytical-reagent grade; Beijing Chemical Plant, China), which was treated with Linde type 5 Å molecular sieves and filtered, and *n*-hexane (analytical-reagent grade, Beijing 52952 Chemical Plant, China) were purchased.

Preparation of derivatives

Each β-amino alcohol was dissolved in toluene and a 10% excess of α-naphthyl isocyanate reagent was added. The mixture was shaken and kept at room temperature for 15–20 min. Finally, it was diluted with the mobile phase and chromatographed.

Order of enantiomeric elution

The *l*- and *d*-isomers were identified by comparing the chromatograms for the *l*-isomer and the racemic mixture.

RESULTS AND DISCUSSION

Björkqvist[8] has reported that phenyl isocyanate can react with amines, alcohols, water, phenols and carboxylic acids, amines showing the fastest reaction rate at room temperature. A reaction time of 5–15 min is usually sufficient for complete reaction. A single and stable derivative is obtained even with primary amines. Phenyl isocyanate has proved to be an excellent derivatizing reagent for compounds with active hydrogen atoms. These characteristics also apply to α-naphthyl isocyanate. The isocyanate group reacts rapidly and selectively with primary and secondary amines under mild conditions to form the corresponding urea derivatives[6]. As ephedrine, propranolol and related β-adrenegic antagonists are, in general, secondary amines, it appeared worthwhile examining the applicability of α-naphthyl isocyanate to the resolution of the enantiomers of these drugs. The results are given in Table I.

All of the enantiomers in Table I were well resolved when they were converted into the corresponding urea derivatives. Details of the isolation and identification of some of these derivatives have been given elsewhere[9].

The results demonstrate that the procedure has several advantages, such as simple operation, rapid derivatization, good resolution and few by-products. It is concluded that the derivatization of β-amino alcohols with α-naphthyl isocyanate is a useful technique for the separation of their enantiomers by HPLC on a Pirkle-type DNBPG column.

REFERENCES

1 I. W. Wainer, T. D. Doyle, Z. Hamidzadeh and M. Aldridge, *J. Chromatogr.*, 261 (1983) 123.
2 I. W. Wainer, T. D. Doyle, F. S. Fry, Jr. and Z. Hamidzadeh, *J. Chromatogr.*, 355 (1986) 149.

3 I. W. Wainer, T. D. Doyle, Z. Hamidzadeh and M. Aldridge, *J. Chromatogr.*, 268 (1983) 107.
4 I. W. Wainer, T. D. Doyle, K. H. Donn and K. J. Powell, *J. Chromatogr.*, 306 (1984) 405.
5 K. H. Donn, J. R. Powell and I. W. Wainer, *J. Clin. Pharmacol. Ther.*, 37 (1985) 191.
6 Q. Yang and Z. P. Sun, *Yaoxue Xuebao*, in press.
7 Q. Yang and Z. P. Sun, *Chin. J. Pharm. Anal.*, in press.
8 B. Björkqvist, *J. Chromatogr.*, 204 (1981) 109.
9 Q. Yang, Z. P. Sun and D. K. Ling, *Yaoxue Xuebao*, in press.

CHROM. 20 549

Note

Separation of oligonucleotides by high-performance ion-exchange chromatography on a non-porous ion exchanger

YOSHIO KATO*, TAKASHI KITAMURA, AKANE MITSUI, YOSUKE YAMASAKI and TSU-TOMU HASHIMOTO

Central Research Laboratory, Tosoh Corporation, Tonda, Shinnanyo, Yamaguchi 746 (Japan)

and

TOMOAKI MUROTSU, SHINICHI FUKUSHIGE and KENICHI MATSUBARA

Institute for Molecular and Cellular Biology, Osaka University, Yamadaoka, Suita, Osaka 565 (Japan)

(Received February 2nd, 1988)

Oligonucleotides are of increasing importance in the field of gene technology, and the requirement for highly pure oligonucleotides is increasing. They can be prepared rather easily in a short time by using an automated synthesizer. However, the samples synthesized usually contain many impurities together with the target oligonucleotides, and hence purifications are inevitable. Although polyacrylamide gel electrophoresis and conventional liquid chromatography are mainly employed for this purpose, high-performance liquid chromatography (HPLC), in particular reversed-phase and ion-exchange chromatography, has often been adopted[1–25]. However, the resolution or separation time in HPLC has not been fully satisfied, especially for large oligonucleotides and improvement is required.

Recently, we demonstrated that ion-exchange chromatography on non-porous ion exchangers is very effective for the rapid separation of proteins with high resolution[26]. We have now investigated the separation of oligonucleotides on a non-porous anion exchanger.

EXPERIMENTAL

Chromatographic measurements were performed with a system consisting of a double plunger pump, Model CCPM, and a variable-wavelength UV detector, Model UV-8000, operated at 260 nm (Tosoh, Tokyo, Japan). The column was TSKgel DEAE-NPR (35 mm × 4.6 mm I.D.) (Tosoh) packed with non-porous spherical hydrophilic resins of 2.5 μm in diameter whose surfaces are chemically bonded with diethylaminoethyl groups[26]. Elution was usually performed with a linear gradient of sodium chloride in 20 mM Tris–HCl buffer (pH 9.0) or 1,3-diaminopropane–HCl buffer (pH 10.5) at a flow-rate of 1.5 ml/min and 25°C. In some separations, however, the conditions were varied to study their effects.

All oligonucleotide samples were from Pharmacia (Uppsala, Sweden), except three linker oligonucleotides, d(GCGATCGC), d(CGAGCTCG) and d(GCAGCTGC), and a crude sample of a pentadecanucleotide, d(AACGCACAC-

TAAACG). The linker oligonucleotides were from Wako (Osaka, Japan). The crude sample of pentadecanucleotide was a gift from Mr. Ikari of our laboratory and the protecting groups were removed after synthesis.

RESULTS AND DISCUSSION

Fig. 1 shows a separation of a mixture of oligoadenylic acids with chain lengths of 1, 2, 3, 4, 5, 8, 10, 12, 16 and 20 nucleotides. These comparatively small oligonucleotides could be separated well in as short a time as 8 min. Oligonucleotides were eluted as very sharp peaks. However, mononucleotide was eluted as a slightly broad tailing peak. This is probably because the packing material of DEAE-NPR is resin-based and is supposed to have very small pores, although it is said to be non-porous. If small molecules like mononucleotide enter such very small pores, the diffusion rate there should be slow, which results in broad and tailing peaks.

Fig. 2. shows a separation of a hydrolysate of polyadenylic acid containing from the 17-mer through approximately the 100-mer. Baseline separations were obtained for up to the 32-mer and peaks appeared for up to about the 70-mer, and yet the separation was completed in less than 20 min. Although a similar separation to that in Fig. 2 has been reported by others, the separation time was much longer than 20 min, about 20 h[12]. As far as we know, this is the first rapid separation of large oligonucleotides with high resolution.

Fig. 3 shows a separation of four tetramers of adenylic, cytidylic, thymidylic and guanylic acids. The four components were separated well in a short time, indicating that ion-exchange chromatography on a non-porous anion exchanger is also very useful to separate oligonucleotides according to base composition. However, it was not so effective to separate sequence isomers. The separation of a mixture of

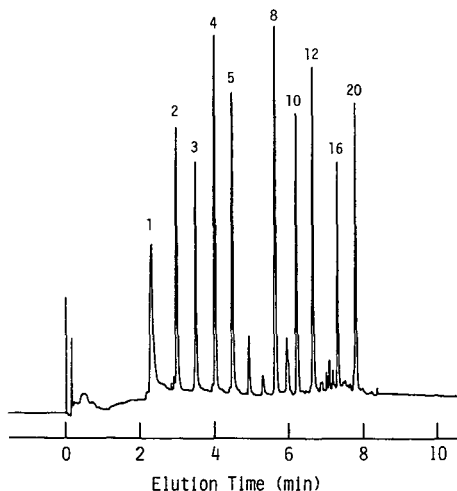

Fig. 1. Chromatogram of a mixture of oligoadenylic acids with chain lengths of 1, 2, 3, 4, 5, 8, 10, 12, 16 and 20 nucleotides (0.1 μg each). The separation was performed on a TSKgel DEAE-NPR column with a 20-min linear gradient from 0 to 1 M sodium chloride in 20 mM Tris–HCl buffer (pH 9.0) at a flow-rate of 1.5 ml/min and 25°C.
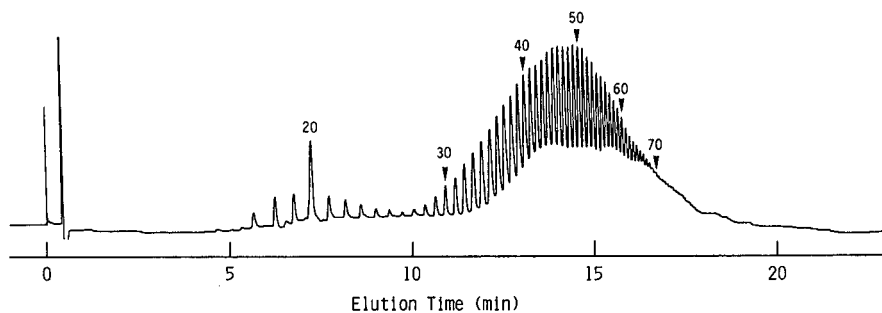
Fig. 2. Chromatogram of a hydrolysate of polyadenylic acid containing from the 17-mer through approximately the 100-mer. The separation was performed on two TSKgel DEAE-NPR columns connected in series with a 60-min linear gradient from 0.25 to 1 M sodium chloride in 20 mM Tris–HCl buffer (pH 9.0) at a flow-rate of 1.0 ml/min and 25°C.

d(GCGATCGC), d(CGAGCTCG) and d(GCAGCTGC) was examined under the same conditions as in Fig. 3. d(GCGATCGC) and d(GCAGCTGC) were eluted as a single peak although they were almost completely separated from d(CGAGCTCG).

Fig. 4 shows a separation of a crude sample of synthetic pentadecamer. The largest peak is an objective 15-mer and it was completely separated from contaminants in about 5 min. Purification and purity analysis of synthetic oligonucleotides are inevitable and very important in the syntheses of DNA or RNA. For these purposes, ion-exchange chromatography on a non-porous anion exchanger is very useful.

Fig. 5 shows the loading capacity in ion-exchange chromatography of oligonucleotides on a non-porous anion exchanger. A pure sample of the 16-mer of adenylic acid was separated using various sample loads, and the peak width was plotted
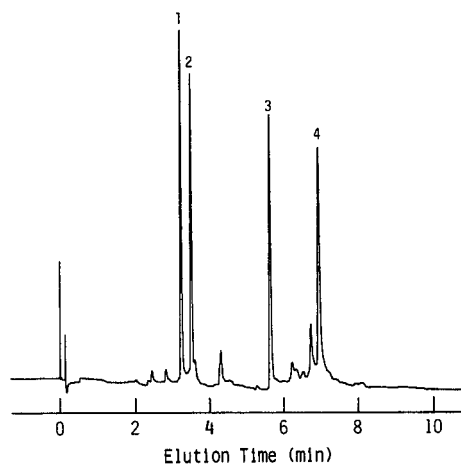

Fig. 3. Chromatogram of a mixture of tetramers of adenylic acid (1, 0.1 μg), cytidylic acid (2, 0.2 μg), thymidylic acid (3, 0.1 μg) and guanylic acid (4, 0.4 μg). The separation was performed on a TSKgel DEAE-NPR column with a 20-min linear gradient from 0 to 1 M sodium chloride in 20 mM 1,3-diaminopropane–HCl buffer (pH 10.5) at a flow-rate of 1.5 ml/min and 25°C.
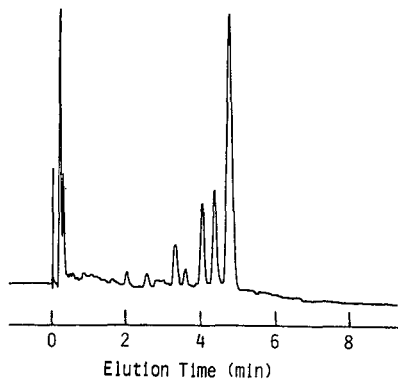
Fig. 4. Chromatogram of a crude sample of synthetic 15-mer, d(AACGCACACTAAACG). The separation was performed on a TSKgel DEAE-NPR column with a 60-min linear gradient from 0 to 1 M sodium chloride in 20 mM 1,3-diaminopropane–HCl buffer (pH 10.5) at a flow-rate of 1.5 ml/min and 25°C.

against the sample load. The peak width was constant at sample loads up to 0.2 μg, and then became broader with further increase in the sample load. Therefore, the maximum sample load in order to obtain the highest resolution is rather small, about 0.2 μg, for pure samples although it is expected to be much larger for samples containing many components, as in the separation of proteins[26]. This low loading capacity must be due to the small surface area of DEAE-NPR and it is the biggest disadvantage of non-porous packing materials.

The recovery of oligonucleotides from a TSKgel DEAE-NPR column is shown in Table I. A pure sample of the 16-mer of adenylic acid and a mixture of oligoadenylic acids with chain lengths of 12–18 nucleotides were separated at pH 9.0, and the recovery was estimated from the areas of the peaks eluted. As controls, we used peak areas observed when the column was replaced with an empty 1 mm I.D. stainless-steel tube of 1 ml total inner volume. Both samples were recovered in high yield,
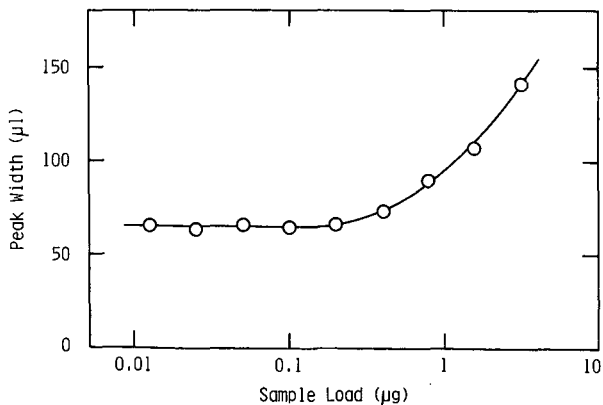

Fig. 5. Dependence of the peak width on sample load in the separation of the 16-mer of adenylic acid on TSKgel DEAE-NPR. Elution conditions as in Fig. 1.

TABLE I

RECOVERY OF OLIGONUCLEOTIDES FROM A TSKgel DEAE-NPR COLUMN

Samples were separated under the conditions in Fig. 1.

Sample	Recovery (%)
Hexadecaadenylic acid (0.1 µg)	93
A mixture of oligoadenylic acids with chain lengths of 12–18 nucleotides (0.5 µg)	96

more than 90%. Therefore, high recoveries are expected even with low sample loads such as 0.1 and 0.5 µg. However, the chromatographic conditions, especially the eluent pH, is very important to achieve high recovery, as described later.

The effects of some chromatographic conditions were studied. First, the eluent pH was examined. When oligoadenylic acids were separated at pH 8.5–10.5, similar separations as in Figs. 1 and 2 were obtained. However, the peaks were subject to tailing and the recovery decreased at pH 4.5–7.5, especially for large molecules. Therefore, the eluent pH should be $\geq$ 8.5 for the separation of oligonucleotides. Furthermore, a mixture of decamers of adenylic and thymidylic acids was eluted as a broad peak at pH 4.5–9.5, while the two components were eluted separately as sharp peaks at pH 10.5. Similar results were also obtained for a mixture of 16-mer of adenylic and thymidylic acids although the trimers were eluted separately over the whole pH range studied (4.5–10.5). Consequently, the eluent pH must be high such as 10.5 for the separation of samples containing complementary components. When a mixture of four tetramers of adenylic, cytidylic, thymidylic and guanylic acids was separated, comparatively similar results were obtained at pH 8.5–9.5, while the four components were eluted over a wider range of elution time at pH 10.5 than at lower pH; compare Fig. 6 with Fig. 3. Accordingly, the range pH 8.5–9.5 is better for a
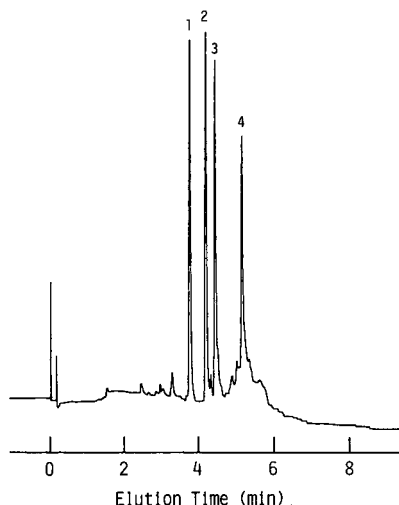

Fig. 6. Chromatogram of a mixture of four tetramers. The same mixture as in Fig. 3 was separated under the same conditions as in Fig. 3, except that the buffer was 20 mM Tris–HCl (pH 9.0).

separation based on chain length, while pH 10.5 is better for a separation based on base composition. There is no problem in operating TSKgel DEAE-NPR at high pH because it is chemically very stable. This is one of its advantages over silica-based packing materials.

Next, the effect of the type of salt was examined. Sodium chloride and sodium perchlorate were compared. Similar separations were obtained for mixtures of oligoadenylic acids except very small ones (lower than the trimer), although sodium perchlorate was approximately 2.5 times more effective than sodium chloride in the elution of oligonucleotides, compare Fig. 7 with Fig. 1. Therefore, it seems that the type of salt has little effect on the separation of homooligonucleotides provided that the gradient steepness is properly adjusted, although sodium perchlorate may be better than sodium chloride for the separation of very small oligonucleotides (lower than the trimer). However, four tetramers of adenylic, cytidylic, thymidylic and guanylic acids were eluted very closely when sodium perchlorate was used, as is seen from a comparison of Figs. 6 and 8. Consequently, sodium perchlorate seems better than sodium chloride for a separation based on chain length only. Conversely sodium chloride is better than sodium perchlorate for a separation based on base composition.

The effect of addition of organic solvent to the eluent was very small, although oligonucleotides were eluted slightly earlier and four tetramers of adenylic, cytidylic, thymidylic and guanylic acids were eluted in a slightly narrower range of elution time with the addition of 10–30% acetonitrile.

Fig. 7. Chromatogram of a mixture of oligoadenylic acids. The same mixture as in Fig. 1 was separated under the same conditions as in Fig. 1, except that the elution was performed with a 20-min linear gradient from 0 to 0.4 M sodium perchlorate in 20 mM Tris–HClO$_4$ buffer (pH 9.0).
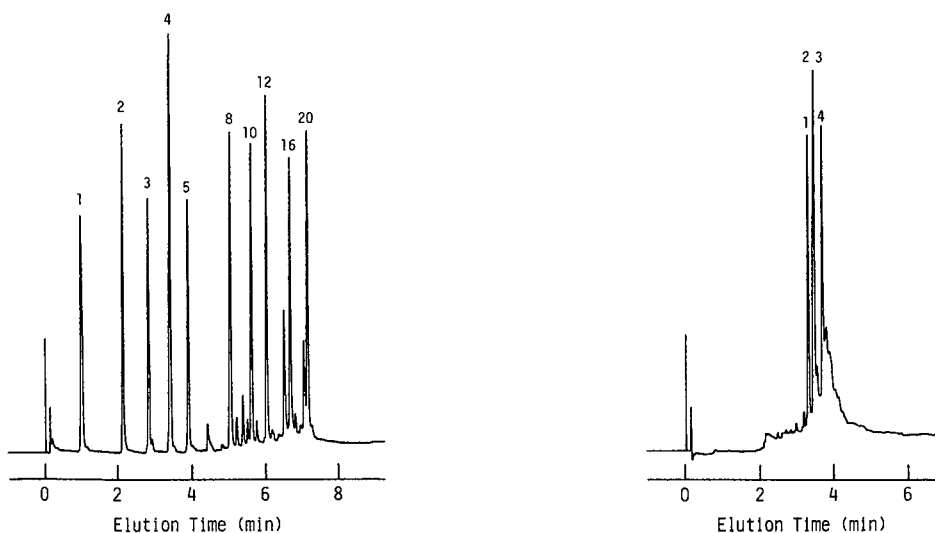
Fig. 8. Chromatogram of a mixture of four tetramers. The same mixture as in Fig. 6 was separated under the same conditions as in Fig. 6, except that the elution was performed with a 20-min linear gradient from 0 to 0.4 M sodium perchlorate in 20 mM Tris–HClO$_4$ buffer (pH 9.0).

The effect of temperature was examined by separating oligonucloetides at 25–65°C. With increasing temperature, the elution of oligonucleotides was slightly delayed and the recovery tended to decrease gradually, especially above 45°C. The resolution was almost constant in the range of 25–45°C, and gradually decreased at higher temperature. Accordingly, a temperature of around 25°C seems appropriate.

Fig. 9 shows the effect of gradient steepness on resolution. A mixture of oligoadenylic acids was separated with a linear gradient from 0 to 1 M sodium chloride at a flow-rate of 1.5 ml/min. The gradient time was varied from 5 to 80 min. The resolution increased continuously with increasing gradient time. However, the dependence of resolution on gradient time became less pronounced at times longer than about 20 min. Because longer gradient times result in longer separation times and more dilution of the sample during separation, gradient times of around 20 min, which correspond to a gradient steepness of about 50 mM sodium chloride/min, seem to be a good compromise in general. However, higher resolution can be attained by adopting a shallower salt gradient.

Fig. 9. Dependence of the resolution on gradient time in the separation of oligonucleotides on a TSKgel DEAE-NPR column. The same mixture of oligoadenylic acids as in Fig. 1 was separated under the conditions in Fig. 1 except that the gradient time was varied between 5 and 80 min. Resolutions were calculated for a pair of tetramer and pentamer (●) and a pair of 16-mer and 20-mer (○) from their peak widths and elution positions.

Fig. 10 shows the effect of flow-rate on resolution. A mixture of oligoadenylic acids was separated with a 20-min linear gradient from 0 to 1 M sodium chloride at flow-rates of 0.25–2.0 ml/min. The resolution increased with increasing flow-rate. However, the effect of flow-rate became small at rates above 1 ml/min, and especially for the pair of small oligonucleotides the resolution was almost constant at flow-rates between 1 and 2 ml/min. Because higher flow-rates result in higher column back pressure, rates of 1.0–1.5 ml/min seem to be a good compromise.

The effect of column length was also examined. Oligoadenylic acids were separated on one- and two-column systems. When the separation was performed with a gradient of 50 mM sodium chloride/min, almost identical separations were ob-
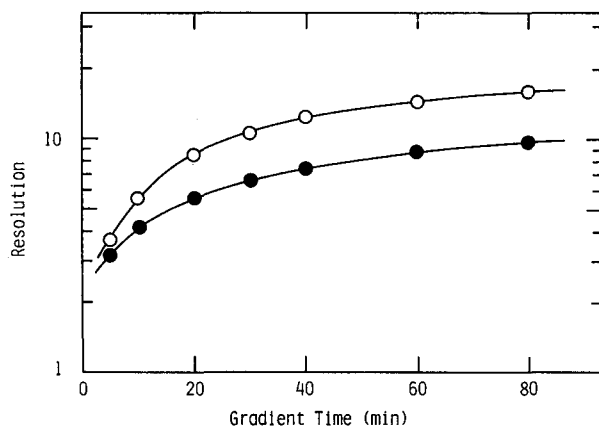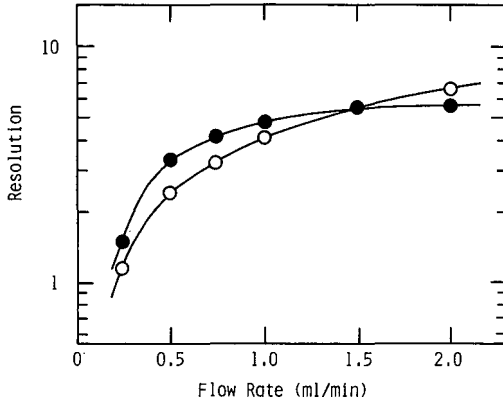
Fig. 10. Dependence of the resolution on flow-rate in the separation of oligonucleotides on a TSKgel DEAE-NPR column. The same mixture of oligoadenylic acids as in Fig. 1 was separated under the conditions in Fig. 1 except that the flow-rate was varied between 0.25 and 2.0 ml/min. Resolutions were calculated for a pair of tetramer and pentamer (●) and a pair of decamer and dodecamer (○) from their peak widths and elution positions.

tained, compare Figs. 11 and 1), suggesting that the column length has little influence on the separation when the gradient of sodium chloride is steep. With a gradient of 12.5 mM sodium chloride/min, however, a better separation was obtained on the two-column system than on the one-column system, compare Figs. 12 and 2). Therefore, it seems that higher resolution can be attained by using longer columns in the case of a shallow salt gradient.

Fig. 11. Chromatogram of a mixture of oligoadenylic acids. The same mixture as in Fig. 1 was separated under the same conditions as in Fig. 1 except that two TSKgel DEAE-NPR columns were used.

Elution Time (min)

Fig. 12. Chromatogram of an hydrolysate of polyadenylic acid. The same mixture as in Fig. 2 was separated under the same conditions as in Fig. 2 except that one TSKgel DEAE-NPR column was used.

As demonstrated above, the non-porous anion exchanger, TSKgel DEAE-NPR, is very useful to separate oligonucleotides. Oligonucle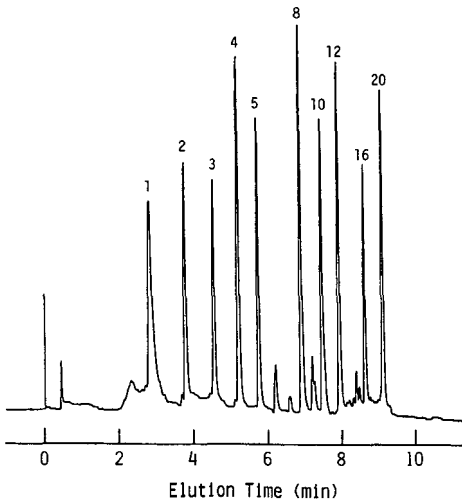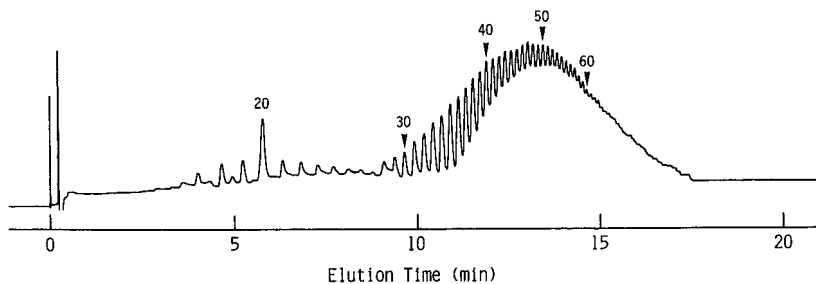otides can be separated rapidly with very high resolution and recovery, mainly based on the chain length at pH 8.5–9.5. The separation of oligonucleotides mainly according to the base composition is also possible by using an eluent of high pH around 10.5. Chromatographic conditions such as the eluent pH, type of salt, addition of organic solvent to the eluent, temperature, gradient steepness, flow-rate and column length influence the retention, selectivity, recovery, resolution, etc.

REFERENCES

1 J. F. Burd, J E. Larson and R. D. Wells, *J. Biol. Chem.,* 250 (1975) 6002.
2 G. C. Walker, O C. Uhlenbeck, E. Bedows and R. I. Gumport, *Proc. Natl. Acad. Sci. U.S.A.,* 72 (1975) 122.
3 J. B. Dodgson and R. D. Wells, *Biochemistry,* 16 (1977) 2367.
4 H.-J. Fritz, R. Belagaje, E. L. Brown, R. H. Fritz, R. A. Jones, R. G. Lees and H. G. Khorana, *Biochemistry,* 17 (1978) 1257.
5 D. Molko, R. Derbyshire, A. Guy, A. Roget, R. Teoule and A. Boucherle, *J. Chromatogr.,* 206 (1981) 493.
6 P. J. Cayley, R. E. Brown and I. M. Kerr, *J. Liq. Chromatogr.,* 5 (1982) 2027.
7 L W. McLaughlin and E. Graeser, *J. Liq. Chromatogr.,* 5 (1982) 2061.
8 L. W. McLaughlin and E. Romaniuk, *Anal. Biochem.,* 124 (1982) 37.
9 J. D. Pearson and F. E. Regnier, *J. Chromatogr.,* 255 (1983) 137.
10 W. Haupt and A. Pingoud, *J. Chromatogr.,* 260 (1983) 419.
11 R. Bischoff and L. W. McLaughlin, *J. Chromatogr.,* 270 (1983) 117.
12 R. Bischoff and L. W. McLaughlin, *J. Chromatogr.,* 296 (1984) 329.
13 C. R. Newton, A. R. Greene, G. R. Heathcliffe, T. C. Atkinson, D. Holland, A. F. Markham and M. D. Edge, *Anal. Biochem.,* 192 (1983) 22.
14 M. Colpan and D. Riesner, *J. Chromatogr.,* 296 (1984) 339.
15 H. Schott and H. Eckstein, *J. Chromatogr.,* 296 (1984) 363.
16 M. Cubellis, G. Marino, L. Mayol, G. Piccialli and G. Sannia, *J. Chromatogr.,* 329 (1985) 406.
17 D. J. Anderson, A. J. Taylor and R. J. Reischer, *J. Chromatogr.,* 350 (1985) 313.
18 T. Middleton, W. C. Herlihy, P. R. Schimmel and H N. Munro, *Anal. Biochem.,* 144 (1985) 110.
19 R. R. Drager and F. E. Regnier, *Anal. Biochem.,* 145 (1985) 47.
20 T. R. Floyd, L. W. Yu and R. A. Hartwick, *Chromatographia,* 21 (1986) 402.
21 K. Ashman, A. Bosserhoff and R. Frank, *J. Chromatogr.,* 397 (1987) 137.
22 H. Seliger and G. Schmidt, *J. Chromatogr.,* 397 (1987) 141.
23 K. Makino, H. Ozaki, T. Matsumoto, H. Imaishi, T. Takeuchi and T. Fukui, *J. Chromatogr.,* 400 (1987) 271.
24 U. Birsner, U. Gilles, P. Nielsen and G. K. McMaster, *J. Chromatogr.,* 402 (1987) 381.
25 M. W. Germann, R. T. Pon and J. H. V. D. Sande, *Anal. Biochem.,* 165 (1987) 399.
26 Y. Kato, T. Kitamura, A. Mitsui and T. Hashimoto, *J. Chromatogr.,* 398 (1987) 327.

CHROM. 20 513

Note

Indirect photometric detection of inorganic anions in micro high-performance liquid chromatography with permanently coated columns

TOYOHIDE TAKEUCHI*, EMIKO SUZUKI and DAIDO ISHII

Department of Applied Chemistry, Faculty of Engineering, Nagoya University, Chikusa-ku, Nagoya 464 (Japan)

(First received January 25th, 1988; revised manuscript received March 31st, 1988)

Ion chromatography has been widely applied to the analysis of inorganic ions as well as organic ions since it was initiated by Small *et al.*[1]. Indirect photometric detection is one of the detection methods employed in ion chromatography, in which the analyte ions displace the UV-absorbing mobile phase ions, resulting in a depression of the background signal[2].

Ion-exchange columns obtained by permanent coating of an ODS column[3], a silica gel column[4] and a polystyrene resin[5] with hydrophobic ions have been investigated for ion chromatography. The ion-exchange capacities of these columns can easily be controlled by changing the coating conditions such as the concentration of the coating solution and the composition of the matrix solution. Microcolumns facilitate examination of the preparation conditions for these permanent coatings.

The use of microcolumns in ion chromatography has been investigated by Rokushika *et al.*[6–8]. They used microcolumns packed with commercially available ion exchangers or polyallylamine-coated silica gel.

This paper describes ion chromatography using micro anion-exchange columns prepared by permanent coating of an ODS column with the hydrophobic cetyltrimethylammonium ion. The analyte anions are detected indirectly by using an UV detector.

EXPERIMENTAL

Apparatus

The liquid chromatograph comprised a Microfeeder (Azumadenki Kogyo, Tokyo, Japan) equipped with an MS-GAN 050 gas-tight syringe (0.5 ml; Ito, Fuji, Japan), an ML-422 micro valve injector (0.02 μl; Jasco, Tokyo, Japan), a micro fused-silica column, a laboratory-made water-bath and an UVIDEC-100V UV spectrophotometer (Jasco) with a modified flow cell. The separation column was immersed in the water-bath in order to decrease the effect of variations in the room temperature. The temperature of the water was not regulated.

Column preparation

Develosil ODS-3K (particle diameter 3 μm; Nomura Chemical, Seto, Japan)

was employed as the octadecylsilica packing material. This material was packed into fused-silica tubing (100 mm × 0.32 mm I.D.) by a slurry packing method. An appropriate volume of cetyltrimethylammonium bromide (cetrimide) solution was passed into the prepared ODS column, followed by washing with deionized water. The breakthrough volume of the anion-exchange column was measured by using an aqueous solution of 1 mM sodium salicylate.

Reagents

All the reagents employed were of reagent grade and were obtained from Wako (Osaka, Japan), unless otherwise noted. Deionized water was prepared by use of a MILLI-Q4 water purification system (Millipore, Bedford, MA, U.S.A.). The sample solution and the mobile phase were prepared with deionized water.

RESULTS AND DISCUSSION

The amounts of cetrimide introduced into the ODS column can be controlled by the concentration of cetimide in the coating solution and the composition of the coating matrix solution (a mixture of an organic solvent and water). The amounts increases with increasing concentration of cetrimide and/or the water content in the coating solution, and they can be estimated from the breakthrough volume of sodium salicylate and its concentration. When 0.25 ml of 1, 3 or 5 mM cetrimide dissolved in methanol–water (50:50) were passed into ODS columns of 100 mm × 0.32 mm I.D., the amounts of salicylate ions introduced onto the permanently coated columns were $1.3 \cdot 10^{-7}$, $8.9 \cdot 10^{-7}$ and $1.2 \cdot 10^{-6}$ mol, respectively. If we assume that no hydrophobic adsorption of salicylate occurs on the prepared columns, these values can be regarded as the ion-exchange capacities of the columns. Actually, the amount of sodium salicylate adsorbed on the ODS column due to the hydrophobic interaction was $1.2 \cdot 10^{-8}$ mol when a 1 mM aqueous solution of sodium salicylate was passed through it. This value was much smaller than that, for the permanently coated col-
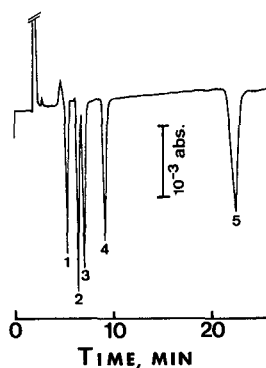
Fig. 1. Separation of inorganic anions on a permanently coated column. Column: 100 mm × 0.32 mm I.D., permanently coated with 3 mM cetrimide dissolved in methanol–water (50:50). Mobile phase: 1 mM sodium salicylate containing 5% acetonitrile. Flow-rate: 2 μl/min. Samples: 1 = chloride; 2 = bromide; 3 = nitrate; 4 = chlorate; 5 = sulphate; 0.02 μl containing 1 mM of each was injected. Wavelength of UV detection: 230 nm.
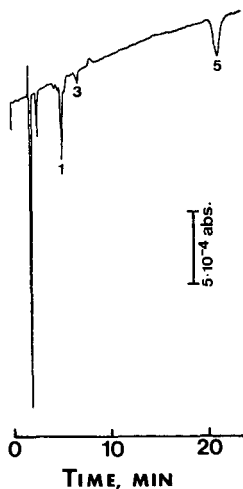
Fig. 2. Separation of anions in tap-water. Operating conditions as in Fig. 1 except for the sample: 0.02 μl of tap-water, peak numbers as in Fig. 1.

umns. However, it is reasonable to use an hydrophilic anion such as nitrate as the reagent for measurement of the ion-exchange capacity.

The retention times of anions increased with increasing amounts of salicylate introduced, as expected. The chromatographic retention behaviours of the columns prepared were the same as those commonly observed in ion chromatography[9].

Fig. 1 demonstrates the separation of an artificial mixture of inorganic anions using a 1 mM sodium salicylate aqueous solution containing 5% acetonitrile (pH 5.8) as the mobile phase. This column was prepared by using a solution of 3 mM cetrimide dissolved in methanol–water (50:50). The analyte anions appeared as negative peaks, while a non-retained system peak was observed as a positive peak. The retention times of the anions were longer than those observed when an aqueous solution of sodium salicylate was used as the mobile phase. This result may be due to the decrease in the degree of dissociation of sodium salicylate caused by the addition of acetonitrile.

The concentration of each analyte in Fig. 1 is 1 mM, which corresponds to 0.7–1.9 ng injected. The concentration detection limits at a signal-to-ratio, S/N = 2 were $ca.$ 0.02 mM (0.7–1.9 ppm), corresponding to mass detection limits of 14–38 pg. Such low mass detection limits are due to the use of microcolumns. The concentration detection limits were improved by a factor of ten by using a valve injector with an injection volume of 0.2 μl (Model 7520; Rheodyne, Cotati, CA, U.S.A.). However, the concentration detection limits were poorer than those achieved by conventional columns with electrical conductivity detection[10]. Precolumn enrichment will improve the concentration detection limits in microcolumn ion chromatography.

A good linear relationship between the peak height and the concentration of the analyte anions up to 1 mM (62 ppm) was observed.

Fig. 2 demonstrates the separation of the anions contained in tap-water in which chloride (10 ppm), nitrate (2.2 ppm) and sulphate (21 ppm) are detected.

REFERENCES

1 H. Small, T. S. Stevens and W. C. Bauman, *Anal. Chem.*, 47 (1975) 1801.
2 H. Small and T. E. Miller, Jr., *Anal. Chem.*, 54 (1982) 462.
3 R. M. Cassidy and S. Elchuk, *Anal. Chem.*, 54 (1982) 1558.
4 T. Takeuchi and E. S. Yeung, *J. Chromatogr.*, 370 (1986) 83.
5 D. L. Duval and J. S. Fritz, *J. Chromatogr.*, 295 (1984) 89.
6 S. Rokushika, Z. Y. Qiu and H. Hatano, *J. Chromatogr.*, 260 (1983) 81.
7 S. Rokushika, Z. Y. Qiu, Z. L. Sun and H. Hatano, *J. Chromatogr.*,, 280 (1983) 69.
8 S. Rokushika, D. Y. Huang, Z. Y. Qiu and H. Hatano, *J. Chromatogr.*, 332 (1985) 15.
9 T. H. Jupille and D. T. Gjerde, *J. Chromatogr. Sci.*, 24 (1986) 427.
10 J. S. Fritz, D. T. Gjerde and C. Pohlandt, *Ion Chromatography*, Hüthig, Heidelberg, 1982.

Note

Selective detection of sulphoxides and sulphimides by thin-layer chromatography using trifluoroacetic anhydride–sodium iodide as a reagent

J. DRABOWICZ*

Center of Molecular and Macromolecular Studies, Polish Academy of Sciences, Department of Organic Sulfur Compounds, Boczna 5, 90-362 Łódź (Poland)

A. KOTYŃSKI

Institute of Chemistry, Faculty of Pharmacy, Medical Academy of Łódź, Narutowicza 120A, 90-151 Łódź (Poland)

and

Z. H. KUDZIN

Institute of Chemistry, University of Łódź, Narutowicza 68, 90-136 Łódź (Poland)

(Received April 5th, 1988)

Sulphoxides and sulphimides are important intermediates in organic synthesis[1,2]. Morever, this group of organosulphur compounds also shows very interesting biological activity[3,4]. For this reason their detection and quantitation are of interest[5,6]. Their thin-layer chromatographic (TLC) detection, however, is limited to a narrow range of spray reagents. Thus, hydriodic acid[7], iodobismuthate solution[8] and 2,3-dichloro-5,6-dicyano-1,4-benzoquinone (DDQ) solution[9] were introduced as spray reagents for certain sulphoxides. Later, acetic acid–chromium trioxide solution[10] and very recently the Dragendorff reagent[11] were applied.

Recently it was shown by us[12,13] that trifluoroacetic anhydride–sodium iodide (TFAA-I) brings about the quantitative deoxygenation of sulphoxides (2) and sulphimides (3) to the corresponding sulphides (1), according to eqns. 1 and 2 and is not able to reduce sulphones (4) and sulphoximides (5).
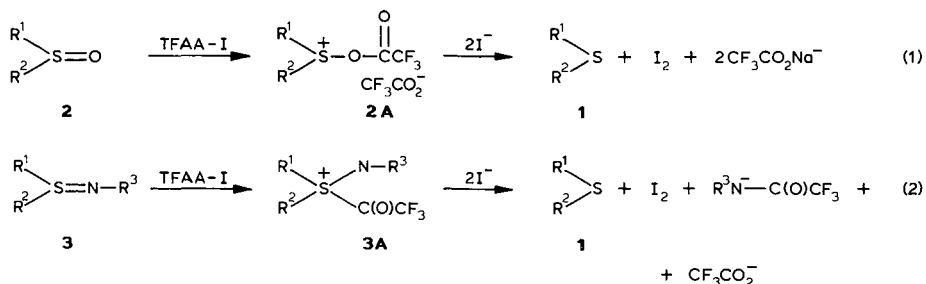
Because in the reactions 1 and 2 stoichiometric amounts of elemental iodine are formed, these procedures have been adapted for microdeterminations of sulphoxides

and sulphimides[14,15]. In this paper we present our findings on the application of TFAA-I to the detection of sulphoxides (2) and sulphimides (3) in TLC systems.

EXPERIMENTAL

Materials

Trifluoroacetic anhydride (TFAA), dimethyl sulphoxide (2a), dibutyl sulphoxide (2c) and diphenyl sulphoxide (2k) were obtained from Aldrich. The other sulphoxides were prepared by the oxidation of the corresponding sulphides either with hydrogen peroxide in methanol solution[16] or with bromine in a two-phase system[17]. The sulphimides[18], sulphones[19] and sulphoxyimides[20] were prepared by standard procedures.

Solutions

A 0.5 M solution of sodium iodide in anhydrous acetone and a 0.8 M solution of TFAA in anhydrous acetone (prepared immadiately before use) were employed. The concentration of the compounds chromatographed were approximately $5 \cdot 10^{-2}$–10^{-3} M in anhydrous acetone. The Dragendorff reagent comprised a 2% solution of potassium bismuth tetraiodide in 0.01 M hydrochloric acid[9], the DDQ reagent a 2% solution of 2,3-dichloro-5,6-dicyano-1,4-benzoquinone in benzene[10] and the chromium trioxide reagent an 1% solution of chromium trioxide in 95% acetic acid.

TABLE I

DETECTION LIMITS FOR SULPHOXIDES (2) AND SULPHIMIDES (3) USING TFAA-I AS THE DETECTION REAGENT

Me = Methyl; Et = ethyl; Pr = propyl; Bu = butyl; Ph = phenyl; Tos = tosyl.

No.	Structure	R^1	R^2	R^3	Detection limit		TLC R_F value (acetone, silica)
					μg	μmol	
2a	O	Me	Me		0.30	0.0038	0.10
2b	‖	Me	Bu		1.06	0.0088	0.20
2c	R^1–S–R^2	Bu	Bu		0.88	0.0054	0.52
2d		Me	$PhCH_2$		0.74	0.0048	0.33
2e		Pr	$PhCH_2$		1.12	0.0061	0.50
2f		$PhCH_2$	$PhCH_2$		1.08	0.0047	0.64
2g		p-$CH_3C_6H_4$	Et		1.58	0.0094	0.54
2h		p-$CH_3C_6H_4$	n-Pr		1.28	0.007	0.61
2i		Ph	$tert.$-Bu		1.1	0.006	0.59
2j		Ph	p-$CH_3C_6H_4$		1.78	0.008	0.64
2k		Ph	Ph		5.0	0.024	0.58
2l		Ph	o-$CH_3OC_6H_4$		5.0	0.022	0.62
3a	N–R^3	Ph	Me	Tos	2.8	0.0095	0.57
3b	‖	p-$CH_3C_6H_4$	Me	Tos	9.4	0.032	0.61
	R^1–S–R^2						

TABLE II

RESULTS OF THE REACTION OF TFAA-I WITH DIPHENYL SULPHIDE (1k), DIPHENYL SULPHONE (4k) AND SULPHOXIMIDE (5a) ON TLC PLATES

No.	Structure	R^1	R^2	R^3	Amount taken (μg)	Detection on alumina				Detection on silica			
						R_F	UV	I_2	TFAA-I	R_F	UV	I_2	TFAA-I
1k	R^1–S–R^2	Ph	Ph		10	0.77	–	–	–	0.70	–	–	–
					50		+	+	–		+	+	–
					100		+	+ +	–		+	+ +	–
2k	R^1–S–R^2 $\overset{O}{\underset{\parallel}{}}$	Ph	Ph		10	0.66	–	–	+ +	0.58	–	–	+ +
4k	R^1–S–R^2 $\overset{O}{\underset{\parallel}{}}\overset{}{\underset{\parallel}{O}}$	Ph	Ph		10	0.77	–	–	–	0.68	–	–	–
					50		+	+	–		+	+	+
					100		+	+	–		+	+ +	–(+)*
5a	R^1–S–R^2 $\overset{O}{\underset{\parallel}{}}$ N–R^3	Me	Ph	H	10	0.52	–	–/+	–	0.39	–	–/+	–
					50		–	+	–/+**		–	+	–
					100		–	+	–/+**		–	+	–

* A spot of iodine appeared after 1 h of exposition.
** After 2 h of exposive.

TLC

Pre-coated silica gel 60 F_{254} aluminium sheets (10 cm × 5 cm), 0.2 mm thick (Merck), were used for TLC. The plates were spotted with the appropriate amount of compound (see Tables), developed for 8 cm with acetone, air dried and sprayed with sodium iodide solution and subsequently with TFAA solution. Sulphoxides (2) and sulphimides (3) appeared almost immediately as brown spots on a white background, and are stable for more than 20 min.

RESULTS AND DISCUSSION

The results of the application of the TFAA-I reagent for visualization of sulphoxides (2) and sulphimides (3) on TLC plates are summarized in Table I. The detection of compounds 2 and 3 on TLC plates after reaction with TFAA-I is very rapid the spots of iodine being formed immediately after spraying with the reagent. The corresponding detection limits (Table I) were found to be dependent on the structures: thus dialkyl sulphoxides (2a–i) at 4–9 nmol and diaryl sulphoxides (2j–l) at 10–25 nmol. The detection limits of sulphimides 3 were in the range 10–25 nmol.

The results collected in Table II clearly indicate that this procedure allows the selective detection of sulphoxides (2) and sulphimides (3) in the presence of sulphides, sulphones and sulphoximides. Diphenyl sulphide (1k), diphenyl sulphone (3k) and phenyl methyl sulphoximide (5a) do not react with the reagent and do not interfere

TABLE III

COMPARISON OF REAGENTS FOR THE DETECTION OF SULPHOXIDES BY TLC

Sulphoxide	Amount applied (μg/spot)	Detection reagent			
		Bi(III)–KI[8]	DDQ–BH₃[9]	CrO₃–acetic acid[10]	TFAA–I*
O ‖ Me–S–Me	1	–	–	–	+
	5	–	–	–	+
	25	–	–	–	+
	74	–	+/–**	+***	+
	150	–	+	+	+
O ‖ Ph–S–Ph	1	–	–	–	+/–
	5	–	–	–	+
	25	+/–§	–	–	+
	91	+	–	+***	+
	181	+§	+**	+	+
O ‖ PhCH₂SCH₂Ph	1	–	–	–	+
	5	–	–	–	+
	25	–	–	–	+
	100	+§	+**	+***	+
	200	+	+	+	+

* This paper.

** According to ref. 9 the detection limits for dialkyl and diaryl sulphoxides are 5–10 μg.

*** According to ref. 10, dimethyl sulphoxide was detectable at 118 μg.

§ According to ref. 8 the detection limits are: dimethyl sulphoxide, no reaction, dipropyl sulphoxide, 33 μg; dibutyl sulphoxide, 110 μg. According to ref. 11. The detection limits are: phenyl ethyl sulphoxide and phenyl benzyl sulphoxide, 35–36 μg.

in the test, even at the level of 100 μg of compounds in the spot. The present reagent (see Table III) has proved to be significantly more sensitive than the previously reported sprays[8-11] for the detection of sulphoxides.

Attempts to modify the TFAA-I spray by replacement of sodium iodide with lithium bromide as well as the use of starch indicator for intensification of the iodine spots did not improve the detectability of sulphoxides and sulphanilimides.

ACKNOWLEDGEMENT

REFERENCES

1 T. Durst, in D. N. Jones (Editor), *Comprehensive Organic Chemistry*, Vol. 3, Pergamon, Oxford, 1979, p. 121.
2 T. Durst, *Specialist Periodical Reports, Organic Compounds of Sulphur, Selenium and Tellurium*, Vols. 1–9, Chemical Society, London, 1970–1986.
3 A. Kjaer, *Tetrahedron*, 30 (1974) 1551.
4 R. L. Whistler, *Carbohydr. Nucleotides, Nucleosides*, 16 (1979) 199.
5 M. R. F. Ashwroth, in *Determinations of Sulphur-containing Groups*, Vol. 1, Academic Press, London, New York, 1972, p. 30.
6 J. H. Karchmer, in *The Analytical Chemistry of Sulfur and its Compounds*, Part II, Wiley-Interscience, New York, 1972, Ch. 11.
7 J. F. Thompson, W. N. Arnold and C. J. Morris, *Nature (London)*, 197 (1963) 380.
8 L. Suchomelova, V. Horak and J. Zyka, *Microchem. J.*, 196 (1965).
9 L. Fishbein and J. Fawkes, *J. Chromatogr.*, 22 (1966) 323.
10 R. F. Langler, *J. Chromatogr.*, 104 (1975) 228.
11 D. Mal and G. Biswas, *J. Chromatogr.*, 387 (1987) 556.
12 J. Drabowicz and S. Oae, *Synthesis*, (1977) 404.
13 J. Drabowicz, P. Łyżwa and Mikołajczyk, *Synthesis*, (1981) 890.
14 W. Ciesielski, J. Drabowicz, W. Jedrzejewski, Z. H. Kudzin and R. Skowroński, *IV eme Colloque Franco-Polonais Chimie Organique, Łódź, 1987*.
15 W. Ciesielski, J. Drabowicz, W. Jedrzejewski, Z. H. Kudzin and R. Skowroński, *Talanta*, submitted for publication.
16 J. Drabowicz and M. Mikołajczyk, *Synth. Commun.*, 11 (1981) 1025.
17 J. Drabowicz, W. Midura and M. Mikołajczyk, *Synthesis*, (1979) 390.
18 M. Haake, in D. Klamann (Editor), *Methoden der Organischen Chemie (Houben-Weyl)*, Vol. Ell, Georg Thieme, Stuttgart, 5th ed., 1985, p. 887.
19 K. Schank, in D. Klamann (Editor), *Methoden der Organischen Chemie (Houben-Weyl)*, Vol. Ell Georg Thieme, Stuttgart, 5th ed., 1985, p. 1129.
20 M. Haake, in D. Klamann (Editor), *Methoden der Organischen Chemie (Houben-Weyl)*, Vol. Ell, Georg Thieme, Stuttgart, 5th ed., 1985, p. 1299.

CHROM. 20 560

Note

Determination of plasticizers in fat by gas chromatography–mass spectrometry

J. B. H. VAN LIEROP* and R. M. VAN VEEN

Food Inspection Service, Nijenoord 6, 3552 AS Utrecht (The Netherlands)

(First received January 21st, 1988; revised manuscript received March 28th, 1988)

Plasticizers, *e.g.*, phthalates, adipates and sebacates, used in food wrapping materials may migrate into the food. Limits have been placed on the presence of these compounds by the Packaging and Food Utensils Regulation of the Dutch Food Law[1]. Therefore analytical methods are required for their determination at the ppm level in foods. Capillary gas chromatography–mass spectroscopy (GC–MS) proved to be a very suitable means for quantifying the migration of plasticizers[2]. The clean-up procedure for the plasticizers in aqueous media is relatively simple. Separation of the plasticizers from fat however is rather difficult and time consuming. Techniques like thin-layer chromatography and liquid chromatography have been applied but often separation is not complete. Consequently, residual fat may damage the high-performance GC capillary columns.

The method now presented is based on the removal of the plasticizers from the fat by purging it with a flow of nitrogen at high temperature. In this way 1–10% of the plasticizers present in the fat are volatilized and subsequently trapped on the Tenax GC adsorbent. The hexane extract of the Tenax is suitable for GC–MS analysis. Fifteen plasticizers with boiling points higher than 240°C were determined in this way when added to a synthetic mixture of triglycerides (HB307). The method was also applied to a retail sample of liverwurst packed in a PVDC casing containing di-*n*-butyl sebacate and acetyl tri-*n*-butyl citrate as plasticizers.

EXPERIMENTAL

Materials

The following materials were used: Tenax GG adsorbent; antifoam solution on a silicone base; a synthetic mixture of triglycerides (HB 307); hexane and the plasticizers mentioned in Table I.

All utensils were extracted with hexane before use.

Preparation of test samples and internal standard

Suitable amounts of plasticizers were added to 10 ml of HB 307 usually in the 60 ppm range, because a global migration of 60 ppm is the limit according to Dutch Food Law. A solution of diisobutyl adipate, diisobutyl phthalate and di-2-ethylhexyl adipate in HB 307 containing such amounts was used as an internal standard.

TABLE I

Plasticizer	Formula	Molecular weight	Boiling point (°C)	Characteristic mass	Scan No.
Dimethyl phthalate	$C_{10}H_{10}O_4$	194	282	163	282
Diethyl phthalate	$C_{12}H_{14}O_4$	222	296	149	327
Diisobutyl adipate	$C_{14}H_{26}O_4$	258	282	129	356
Diisobutyl phthalate	$C_{16}H_{22}O_4$	278	295	149	425
Di-n-butyl phthalate	$C_{16}H_{22}O_4$	278	340	149	430
Di-n-butyl sebacate	$C_{18}H_{34}O_4$	314	344	241	537
Acetyl tri-n-butyl citrate	$C_{20}H_{34}O_8$	402	378	129 185	572
Diethylhexyl adipate	$C_{22}H_{42}O_4$	370	–	129	626
Di-2-ethylhexyl phthalate	$C_{24}H_{38}O_4$	390	–	149	700
Di-n-octyl azelate	$C_{25}H_{48}O_4$	412	–	171	800

Determination of plasticizers in fat

A 10-ml portion of the fat was transferred to a three-necked vessel. The internal standard solution (1–60 ppm depending on the expected migration) in HB 307 and an antifoam solution were added. The vessel was connected to a Tenax absorption column and subsequently heated at 210°C in an oil-bath. The temperature of the contents of the vessel was about 180°C. While heating the vessel, nitrogen was passed through the fat at a rate of about 170 ml/min for 30 min. The Tenax (ca. 15 mg) was extracted with 1–3 ml hexane. This extract can be concentrated if high sensitivity is required. A 1-μl volume of this hexane extract was analyzed under the following GC–MS conditions.

The analyses were carried out by means of a Finnigan 4000 GS–MS system in the electron-impact mode and with a Finnigan 6115 data system. A 1-μl volume of the hexane extract was split injected on a 30 m × 0.32 mm I.D. DB 5 fused-silica column, operated with the following temperature programme: 3 min at 60°C, then to 300°C at 40°C/min, finally held at 300°C for 15 min. Helium was used as the carrier gas. The data system was tuned to the m/z values corresponding to the plasticizer in question.

Determination of plasticizers in fatty foods

For the determination of plasticizers in food, first the fat content of the food was determined. A sample of food was taken so as to obtain at least 10 ml fat. This sample was mixed with twice its weight of dry sodium sulphate. The mixture was extracted with diethyl ether in a Soxhlet apparatus for 6–7 h. The ether was removed by evaporation. The plasticizers in a portion of 10 ml of this fat obtained from the food were determined as described above.

RESULTS

The plasticizers determined by this method are recorded in Table I. Even the high boiling di-n-octyl azelate (DOAZ) could be detected by this method. Additions
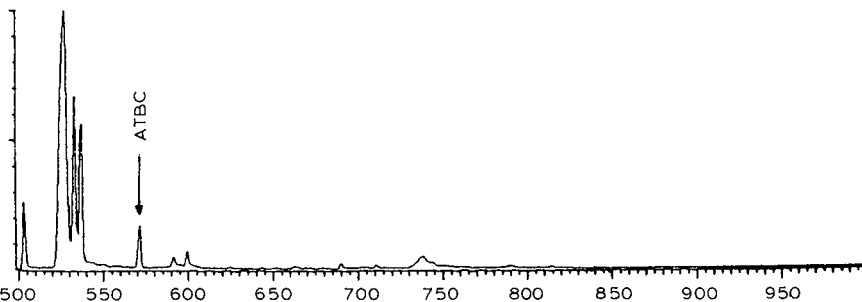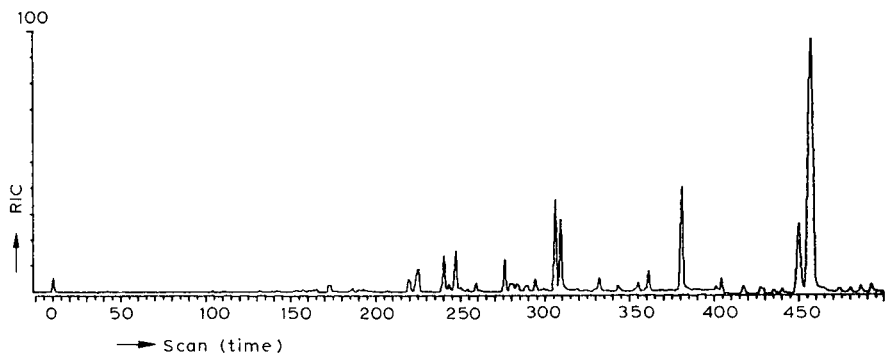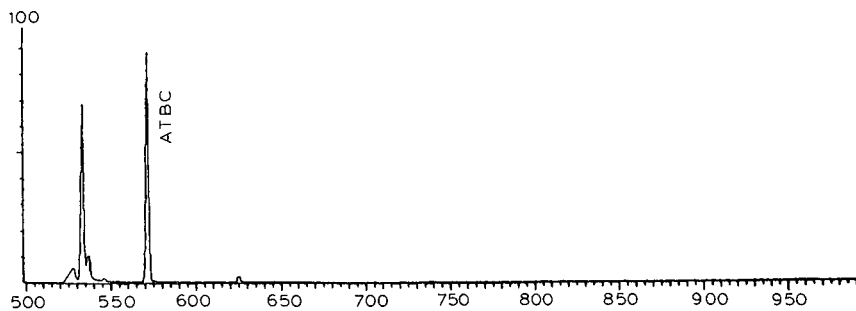
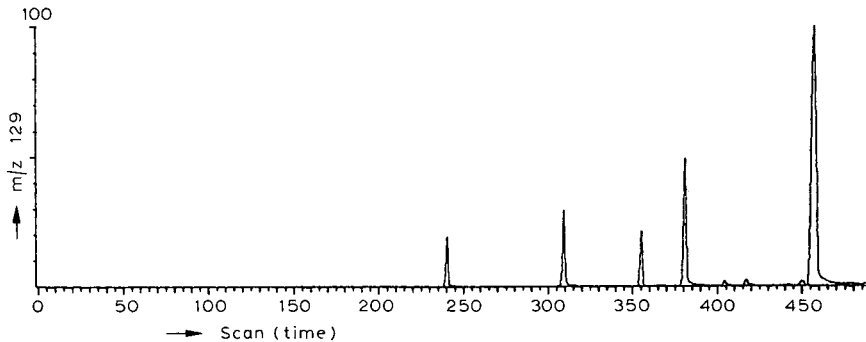Fig. 1. Reconstructed ion chromatogram of liverwurst.

Fig. 2. Mass fragmentogram at m/z 129 for liverwurst showing the plasticizer acetyltri-*n*-butyl citrate.

of 1–10 ppm of the plasticizers to the fat could be detected. Fig. 1 shows a reconstructed ion chromatogram (RIC) pertaining to a retail sample of liverwurst. Fig. 2 shows a mass fragmentogram at m/z 129 used to detect acetyl tri-*n*-butylcitrate. The difference between these two chromatograms illustrates the power of multiple-ion detection (MID). The amounts of di-*n*-butyl sebacate and acetyl tri-*n*-butyl citrate migrated were about 30 mg/kg liverwurst.

DISCUSSION

The results obtained in this preliminary investigation indicate that it is possible to determine by means of GC–MS the migration of high-boiling plasticizers like phthalates and adipates from packaging materials into fatty foods in ppm quantities.

In spite of the low recovery (1–10% of the plasticizers), a sufficient amount of the plasticizers was obtained to carry out determinations at the required ppm level. The method is applicable to a wide range of compounds because the mass fragmentographic detection is specific. The lower limit of detection depends on the volatility and the presence of characteristic peaks in the mass spectrum of each plasticizer. An estimate of the detection limit of the method can be made as follows. Starting with 10 ml fat containing 10 ppm of a plasticizer and assuming that 1% of the plasticizer is trapped on the Tenax, the total amount in the hexane extract is 1 μg. If we evaporate this extract to 10–100 μl a concentration of 10–100 ng/μl is obtained, which can easily be detected by GC–MS. A large number of plasticizers together with suitable internal standards can be investigated in one determination. Quantitations can be carried out by the use of labelled compounds. Experiments with deuterated di-2-ethylhexyl phthalate as an internal standard for di-2-ethylhexyl phthalate are in progress.

REFERENCES

1 *Packaging and Food Utensils Regulation*, Staatsuitgeverij, 's-Gravenhage, 1980.
2 J. R. Startin, I. Parker, M. Sharman and J. Gilbert, *J. Chromatogr.*, 387 (1987) 509–514.

Note

Chromatographie en phase gazeuse du dioxyde et du monoxyde de carbone

Choix d'un procédé d'étalonnage

D. PRADEAU

Laboratoire de Chimie Analytique, Faculté de Pharmacie, Université Paris XI, 3, Rue J. B. Clément, F-92290 Chatenay Malabry et Laboratoire de Contrôle de Qualité, Pharmacie Centrale des Hôpitaux de Paris, 7, Rue du Fer à Moulin, F-75005 Paris (France)

M. POSTAIRE

Laboratoire de Chimie Analytique, Faculté de Pharmacie, Université Paris XI, 3, Rue J. B. Clément, F-92290 Chatenay Malabry (France)

E. POSTAIRE*

Laboratoire de Contrôle de Qualité, Pharmacie Centrale des Hopitaux de Paris, 7, Rue du Fer à Moulin, F-75005 Paris (France)

P. PROGNON

Laboratoire de Chimie Analytique, Faculté de Pharmacie, Université Paris XI, 3, Rue J. B. Clément, F-92290 Chatenay Malabry et Laboratoire de Contrôle de Qualité, Pharmacie Centrale des Hôpitaux de Paris, 7, Rue du Fer à Moulin, F-75005 Paris (France)

et

M. HAMON

Laboratoire de Chimie Analytique, Faculté de Pharmacie, Université Paris XI, 3, Rue J. B. Clément, F-92290 Chatenay Malabry (France)

Une méthode de dosage du dioxyde de carbone, du formaldéhyde et du méthanol a récemment été mise au point, dans notre laboratoire, par chromatographie en phase gazeuse avec espace de tête. Dans le cas du méthanol ou du formaldéhyde, il est possible de faire appel à une détection classique par ionisation de flamme. En revanche, dans le cas du dioxyde de carbone nous avons eu recours à la réduction totale des composés élués en méthane par un four à méthanation avant de les détecter par ionisation de flamme[1]. Les conditions opératoires décrites dans ce travail ont été reprises en partie et adaptées au dosage du monoxyde et du dioxyde de carbone.

En ce qui concerne l'étalonnage du dioxyde de carbone, l'hydrogénocarbonate de sodium peut être utilisé comme étalon primaire. L'étalonnage du monoxyde de carbone est plus complexe. Nous avons retrouvé dans la littérature des méthodes appliquées à la recherche et au dosage de ce dernier en toxicologie[2-4]. Cependant, les techniques d'étalonnage mises en œuvre nécessitent l'emploi de monoxyde de carbone pur, ce qui alourdit la technique, ralonge la manipulation et entraîne une mauvaise reproductibilité [coefficient de variation (C.V.) $\approx$ 10%]. Nous avons donc cherché une méthode d'étalonnage plus simple. Il fallait trouver un composé organique qui,

en se décomposant, libérait de manière reproductible et stoechiométrique du monoxyde de carbone. Seuls deux produits se comportent de cette façon: l'acide formique qui se transforme en milieu acide et à chaud[5,6] en monoxyde de carbone et eau, et l'acide oxalique qui se décompose soit à sec, soit en présence d'acide sulfurique concentré à chaud en dioxyde de carbone, monoxyde de carbone et eau. Ce dernier représente l'étalon idéal dans la mesure où il donne la possibilité théorique d'un double étalonnage pour le monoxyde et le dioxyde de carbone. Il suffit alors de vérifier que la décomposition est équimolaire et de déterminer les conditions opératoires optimales.

MATÉRIEL ET MÉTHODE

Réactifs

Les réactifs suivants ont été utilisés: hydrogénocarbonate de sodium RP pour analyse; solutions d'hydrogénocarbonate de sodium à 25, 50, 100, 250; et 5000 μmol · ml^{-1}, préarées dans de l'eau fraichement bouillie; acide formique RP pour analyse; solutions d'acide formique à 25, 50, 100, 250 et 500 μmol · ml^{-1} préparées dans de l'eau distillée fraichement bouillie; acide oxalique RP pour analyse; solutions d'acide oxalique à 25, 50, 100, 250 et 500 μmol · ml^{-1} préparées dans de l'eau distillée fraichement bouillie; acide sulfurique concentré à 95% pour analyse.

Appareillage

Le chromatographe en phase gazeuse Perkin-Elmer Sigma B utilisé comporte un injecteur pour espace de tête, un four à méthanation, un détecteur à ionisation de flamme (FID), une colonne inox (4 m × 0.9 mm I.D.) remplie de Porapak Q 80–100 mesh.

Les analyses sont effectuées dans des flacons Pyrex type pénicilline de 5 ml contenant des petits tubes cylindriques à fond plat de 1 ml.

Conditions opératoires

Nous avons reproduit les conditions de dosage du dioxyde de carbone, du formaldéhyde et du méthanol[1].

Mode opératoire

Étalonnage du dosage du dioxyde de carbone par une solution d'hydrogénocarbonate de sodium. Dans des flacons type pénicilline sont introduits successivement les solutions filles d'hydrogénocarbonate de sodium (20 μl) et l'acide sulfurique (500 μl). Ce dernier est introduit dans un tube cylindrique placé dans le flacon afin d'éviter le dégazage immédiat avant fermeture de ce dernier.

Étalonnage du dosage du monoxyde de carbone par une solution d'acide formique. Dans des flacons type pénicilline sont introduites successivement les solutions filles d'acide formique (20 μl) et l'acide sulfurique (500 μl).

Étalonnage du dosage simultané du dioxyde et du monoxyde de carbone par une solution d'acide oxalique. Dans des flacons type pénicilline sont introduites successivement les solutions filles d'acide oxalique (20 μl) et l'acide sulfurique concentré (500 μl).

Les flacons sont ensuite conditionnés sous atmosphère d'azote afin d'éliminer

le dioxyde de carbone présent dans l'air. Puis ils sont recouverts d'une pastille de PTFE, d'une bague et d'une capsule d'aluminium et sertis à la pince. Ils sont enfin agités pour mettre en contact l'acide sulfurique et le produit puis portés à l'étuve à 150°C pendant 30 min.

Pour chacun des deux gaz, le dosage est réalisé sans étalon interne, par comparaison de la surface des pics à ceux obtenus avec la gamme d'étalonnage d'acide oxalique.

RÉSULTATS ET DISCUSSION

Etalonnage avec l'hydrogénocarbonate de sodium

Il ne peut être question de faire varier la température des gammes d'acide oxalique et formique. En revanche, l'étude de l'influence de la température peut être étudiée sur une gamme d'hydrogénocarbonate de sodium. Les résultats obtenus sur une gamme laissée 30 min à température ambiante ont été comparés à ceux d'une gamme portée à 100°C 30 min.

La linéarité des deux gammes est bonne. En revanche, la reproductibilité est meilleure à chaud qu'à température ambiante. Enfin, il existe une différence significative au test t de Student au seuil de 5% entre la reproductibilité sur le point 5 μmol à température ambiante et à chaud. Cette différence significative de la réponse peut être expliquée par une différence de la solubilité des gaz due à une modification de l'équilibre en faveur de la formation du dioxyde de carbonne à chaud.

Étalonnage avec l'acide formique

L'optimum de libération du monoxyde de carbone en fonction de la température et du temps a été déterminé. Les cinétiques réactionnelles font apparaître un plateau de libération du monoxyde de carbone pour un temps de 45 min à partir de 75°C. En raison des problèmes d'étanchéité des flacons qui apparaissent à partir de 150°C pour un temps de 30 min pour l'acide oxalique, nous avons choisi de travailler à 100°C pendant 45 min.

Nous avons déterminé, dans ces conditions, la linéarité et la reproductibilité d'une gamme d'acide formique. La linéarité est bonne ($r = 0.9997$) et la reproductibililé sur dix analyses satisfaisante (C.V. = 5.6%).

Etalonnage mixte avec l'acide oxalique

Dans les conditions opératoires décrites, le monoxyde de carbone et le dioxyde de carbone sont bien séparés avec des temps de rétention respectifs d'environ 1,2 et 2,1 min (Fig. 1).

L'air ambiant contient, au maximum, 50 ppm de monoxyde de carbone et 5000 ppm de dioxyde de carbone[7]. La teneur moyenne retrouvée, pour le dioxyde de carbone, est de 100 ppm[8]. Afin d'éliminer le risque d'interférence, nous avons fait barboter de l'azote dans tous les échantillons. Dans ces conditions, la quantité de monoxyde et de dioxyde de carbone résiduel devient négligeable.

L'acide sulfurique à chaud décompose, comme cela a été précisé précédemment, l'acide oxalique en monoxyde et dioxyde de carbone[9]. La cinétique de cette libération a été déterminée en utilisant comme traceur le dioxyde de carbone, en faisant varier le temps entre 5 et 30 min et la température entre 110°C et 160°C.
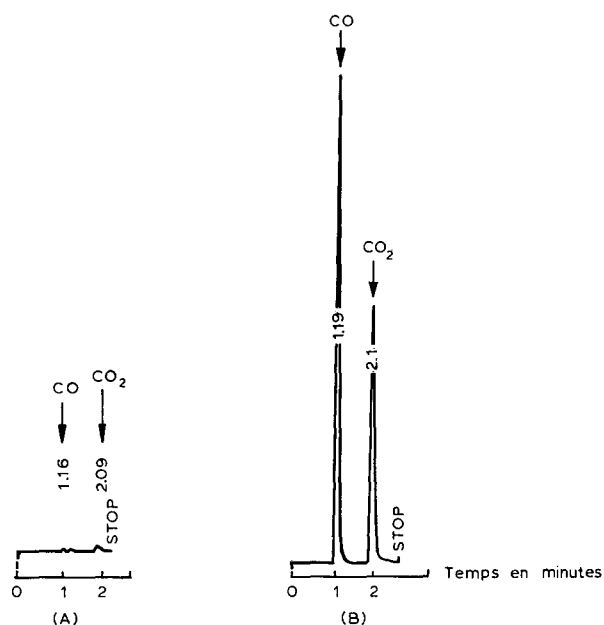
Fig. 1. Chromatogrammes obtenus à partir d'un blanc des réactifs (A) et d'une concentration (5 μmol · ml^{-1}) d'acide oxalique (B).

L'hydrogénocarbonate de sodium a été choisi comme étalon primaire, la décomposition de ce dernier en dioxyde de carbone et en eau étant total en milieu acide. L'aire du pic de dioxyde de carbone libéré par l'acide oxalique a ainsi été comparée, pour une même concentration, à celle du pic de dioxyde de carbone libéré par l'hydrogénocarbonate de sodium. Les cinétiques réactionnelles de libération du dioxyde de carbone en fonction du temps et de la température mettent en évidence un optimum pour une température de 150°C à 30 min.

Les conditions opératoires optimum pour la décomposition de l'acide oxalique étant déterminées, nous avons vérifié la linéarité et la reproductibilité de la méthode. La linéarité est satisfaisante ($r_{CO} = 0.9987$, $r_{CO_2} = 0.9995$). En ce qui concerne la reproductibilité, les coefficients de variation déterminés à partir de dix analyses sont, pour le monoxyde et le dioxyde de carboxyde voisins de 4%.

D'autre part, il a été vérifié que la libération du monoxyde de carbone, à l'intérieur du flacon, n'est pas modifiée par celle du dioxyde de carbone, et vice versa. La comparaison des aires de monoxyde de carbone entre l'acide formique et l'acide oxalique met en évidence une bonne corrélation ($p < 0.05$). Il en est de même des aires de dioxyde de carbone entre l'hydrogénocarbonate de sodium et l'acide oxalique ($p < 0.05$). Il est donc possible de conclure qu'il n'y a pas d'influence: (1) des gaz l'un sur l'autre en mélange; (2) de la différence de température de décomposition entre les étalons (100°C pour l'acide formique et le bicarbonate, et 150°C pour l'acide oxalique).

Nous avons vérifié sur 5 jours l'évolution, dans le temps, des solutions d'acides oxalique, formique et d'hydrogénocarbonate de sodium. Cette étude a été réalisée en

comparant les pourcentages de monoxyde et/ou de dioxyde de carbone d'une solution fraichement préparée et d'une solution préparée à l'avance. Il ressort de cette étude que les solutions d'étalonnage ne sont pas stables plus de 24 h. Il est donc nécessaire de les réaliser extemporanément.

CONCLUSION

La mise au point d'une méthode de dosage simultané du dioxyde et du monoxyde de carbone en solution aqueuse doit trouver un domaine d'application très large qui reste à explorer:

En analyse toxicologique: dosage du monoxyde de carbone plasmatique;

en analyse pharmaceutique: dosage du dioxyde de carbone dissous dans des solutions bicarbonatées;

en analyse organique: dosage du monoxyde et du dioxyde de carbone lors de l'étude de réactions de type oxydatif conduisant à la formation de ces composés;

en analyse biologique: dosage de ces deux gaz dans l'espace de tête de milieux de culture contenant des germes anaérobies.

BIBLIOGRAPHIE

1 E. Postaire, J. E. Hila, A. Assamoi, D. Pradeau, C. Dauphin et M. Hamon, *Analusis*, 13 (1985) 463–468.
2 A. G. Constantino, J. Park et Y. H. Caplan, *J. Anal. Toxicol.*, 10 (1986) 190–193.
3 B. R. Griffin, *J. Anal. Toxicol.*, 108 (1986) 6229–6234.
4 J. G. Guillot, J. P. Weber et J. Y. Savoie, *J. Anal. Toxicol.*, 5 (1981) 264–266.
5 R. Dolique, *Bull. Soc. Chim. Fr.*, 2 (1935) 1489–1491.
6 R. Truchet dans V. Grignard, G. Dupont et R. Locquin (Rédacteurs), *Traité de Chimie Organique*, Masson, Paris, Tome IX, 1939, p. 163.
7 N. Sax, *Dangerous Properties of Industrial Materials*, Van Nostrand Reinhold, New York, 6e éd., 1984, pp. 640 et 643.
8 Th. R. Thusse, *Atmos Environ.*, 12 (1978) 2001–2003.
9 H. J. Goudet, R. Padova et F. Salmon-Legagneur dans V. Grignard, G. Dupont et R. Locquin (Rédacteurs), *Traité de Chimie Organique*, Tome X, Masson, Paris, 1939, pp. 165–172.

CHROM. 20 548

Note

Analysis of pyrethrins in pyrethrum extracts by high-performance liquid chromatography

A. M. McELDOWNEY* and R. C. MENARY

Department of Agricultural Science, University of Tasmania, GPO Box 252 C, Hobart, Tasmania 7001 (Australia)

A rapid, reliable method of analysis, which is applicable to products containing pyrethrins, whether these are oleoresins, pale extracts or crude plant extracts, was required for screening pyrethrum lines in an extensive breeding programme.

Methods already described in the literature[1,2] for high-performance liquid chromatographic (HPLC) separation, rely on absorption readings at 254 rather than 229 nm and separation of the components can take up to 60 min[1]. The method presented here takes a step further the method of Ando *et al.*[3] in that it is possible to quantify the amount of pyrethrin present in natural pyrethrum extracts. The spectrophotometric method overestimates total pyrethrins due to the presence of extraneous UV-absorbing material in the pyrethrum extract[3,4]. HPLC techniques offer an opportunity to separate interfering substances from the six esters thus improving the reliability of estimation of pyrethrins.

EXPERIMENTAL

Materials

Pyrethrum extract (premium quality Pyrocide 175) was obtained from McLaughlin, Gormley, King Co., Minneapolis, MN, U.S.A. The *n*-hexane and tetrahydrofuran were Ajax Unichrom and Waters HPLC grade, respectively. The light petroleum (b.p. 40–60°C) was redistilled from bulk supplies.

Equipment

Total pyrethrins from flower samples were determined using a Pye Unicam SP8-200 UV–VIS spectrophotometer. The HPLC analyses were performed using a Waters HPLC system. This included a 6000A solvent delivery system, an U6K injector, an automated gradient controller, a Model 440 absorbance detector with an extended-wavelength module (229 nm) and a Waters RCM 100. Results were collected on a Hewlett-Packard Sigma 10 data station. The HPLC column used was an 8-mm, 10-μm silica Rad-Pak cartridge (Waters) with a 10-μm silica Waters RCSS Guard-Pak pre-column. For large numbers of routine samples a WISP (Waters Intelligent Sample Processor) was used.

Method

In routine analyses of pyrethrum flowers for pyrethrins content, 0.5 g of dry, finely ground pyrethrum flowers were extracted in 25-ml volumetric flasks with redistilled light petroleum (b.p. 40–60°C) for 2 h[5]. The samples were shaken three times during this period.

Automated analysis of pyrethrins in flowers necessitates that the extract of pyrethrum flowers be suitable for direct injection into the HPLC system. Hence, the dilutions of the standard were chosen to correspond to the range of concentrations usually found in pyrethrum flowers. Care was taken to ensure that no evaporation of solvent occurred from prepared samples.

For the results presented in this paper, the following parameters were used: density of standard, 0.78; density of light petroleum, 0.65; %PI in standard (as specified by the manufacturer) 11.77%; %PII in standard (as specified by the manufacturer) 8.12%, where %PI and %PII are the percentages of pyrethrins I (pyrethrin I, jasmolin I and cinerin I) and pyrethrins II (pyrethrin II, jasmolin II and cinerin II), respectively.

A 10-μl volume of each of the dilution series was chromatographed using the following HPLC conditions: flow-rate, 0.7 ml/min for 21 min, then increased to 2.3 ml/min; solvent, *n*-hexane–tetrahydrofuran (96:4). During routine analyses this solvent was recycled with no loss of resolution or accuracy. A chromatogram of a typical HPLC separation is shown in Fig. 1.

RESULTS AND DISCUSSION

Spectrophotometric analyses of the dilution series of the standard indicate that the absorbance was linear within the first half of the concentration range being studied. At concentrations of standard higher than 0.12 ml standard per 25 ml light petroleum, Beer's law did not apply.

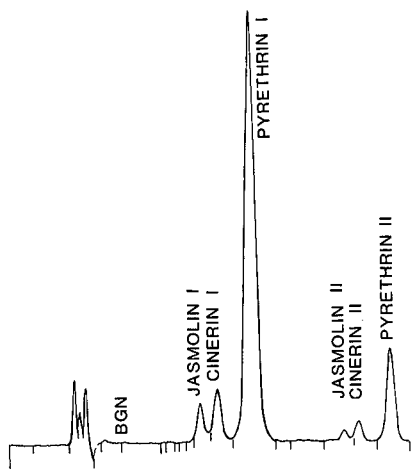In contrast, a linear relationship of total pyrethrins peak area and concentra-

Fig. 1. HPLC separation of a sample of Pyrocide 175.

tion was obtained using HPLC analysis of the same dilution series (correlation coefficient = 0.999).

Pyrethrins I and II are determined independently as it is not yet known if the response factor is identical for the two groups of esters.

Using the total peak areas of pyrethrins I (y_1) and pyrethrins II (y_2), the standard curves for each group were found to be linear, having correlation coefficients of 0.9993 and 0.9989, respectively. The regression equations are given by

$$y_1 = 197.073x_1 + 0.677$$

and

$$y_2 = 59.252x_2 + 0.03$$

where x_1 and x_2 are equivalent % of pyrethrins I and II, respectively, per 25 ml light petroleum.

From any pyrethrum sample, the total percentage of pyrethrins can be calculated from $(x_1 + x_2) \cdot$ dilution factor of actual sample.

The standard has been found to remain stable when stored, tightly sealed, at 2°C in the dark.

Identification

A preliminary identification of the six esters was obtained by collecting the six fractions and analysing them on a UV spectrophotometer. Comparison of the results with those presented by Head[6] is given in Table I. The fractions were further subjected to mass spectroscopy and confirmed as being jasmolin I, cinerin I, pyrethrin I, jasmolin II, cinerin II and pyrethrin II (in order of HPLC elution). Mass spectra were obtained from direct insertion probe samples on a VG 70/70F spectrometer at 70 eV, source temperature of 200°C and with a 4 kV accelerating voltage.

It is possible to adapt the method used for calculation of total pyrethrins for calculation of percentages of individual esters. Fig. 2 indicates a linear relationship between peak area and concentration for each ester. It is necessary to assume that the response factor is the same for each ester within either the pyrethrins I or II group. Without authentic samples of the six esters, it is impossible to quantify them

TABLE I

UV-ABSORPTION DATA FOR THE ISOLATED PYRETHRINS

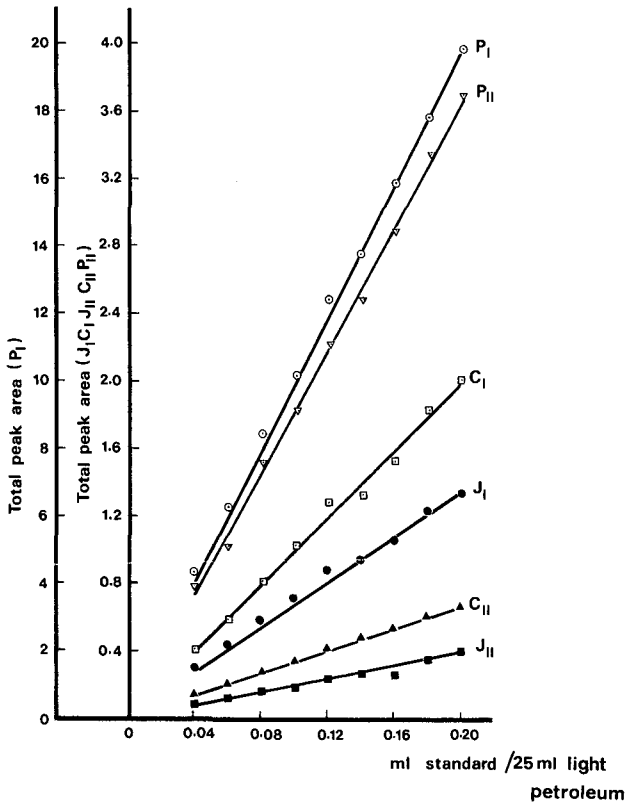| Compound	Maximum UV-absorption wavelength (nm)	
	This study	*Ref. 6.*
Jasmolin I (J_I)	220	219
Cinerin I (C_I)	221.8	220
Pyrethrin I (P_I)	224	222.5–223
Jasmolin II (J_{II})	229	229
Cinerin II (C_{II})	229.9	229
Pyrethrin II (P_{II})	225.5	227–228

Fig. 2. Area of individual esters (for abbreviations, see Table I) *vs.* concentration.

using regression equations and therefore it is necessary to determine %PI or %PII as described, then use the peak area of the ester under consideration to calculate the relative percentage of each ester.

An analytical method with the capability for determining relative proportions of the esters and pyrethrins I/pyrethrins II ratios is useful in detecting clones having pyrethrum ratios with specific commercial applications.

ACKNOWLEDGEMENTS

REFERENCES

1 D. A. Otieno, I. J. Jondiko, P. G. McDowell and F. J. Kezdy, *J. Chromatogr. Sci.*, 20 (1982) 566.
2 D. Mourot, J. Boisseau and C. Gayot, *Anal. Chim. Acta*, 97 (1978) 191.
3 T. Ando, Y. Kurotsu and M. Uchiyama, *Agric. Biol. Chem.*, 50 (1986) 491.
4 M. F. Kerslake, personal communication.
5 V. A. Beckley, *Pyrethrum Post*, 2 (1950) 23.
6 S. W. Head, in J. E. Cassida (Editor)), *Pyrethrum*, Academic Press, London, 1973, Ch. 3, p. 25.

Note

Liquid chromatographic determination of cyadox in medicated feeds and in the contents of the porcine gastrointestinal tract with fluorescence detection

G. J. DE GRAAF and Th. J. SPIERENBURG*

Central Veterinary Institute, Department of Analytical Chemistry and Toxicology, P.O. Box 65, 8200 AB Lelystad (The Netherlands)

(First received December 23rd, 1987; revised manuscript received March 24th, 1988)

Cyadox (2-formylquinoxaline-N^1,N^4-dioxide cyanoacetylhydrazone) (see Fig. 1), manufactured by SPOFA (Prague, Czechoslovakia), is used in Eastern Europe as a feed additive for pigs, calves and poultry. Like the other quinoxaline N^1,N^4-dioxides used in veterinary practice, such as carbadox and olaquindox, cyadox also has a growth-promoting effect[1,2].

For a comparative study of pharmacological and toxicological properties, weaned pigs were fed carbadox, olaquindox and cyadox by in-feed medication[3]. To evaluate the efficacy of these drugs against one of the possible causative agents of swine dysentery (*Treponema hyodysenteriae*), a high-performance liquid chromatographic (HPLC) method for the determination of cyadox in feed and gastrointestinal samples had to be developed, analogous to the previously published method for carbadox[4].

This paper describes a method for the determination of cyadox in feed and gastrointestinal samples. As cyadox exhibits native fluorescence (Fig. 2), fluorescence detection was chosen. Cyadox was extracted with acetone and the extract was filtered. An aliquot of the extract was evaporated to dryness and the residue was dissolved in the mobile phase.

EXPERIMENTAL

Apparatus and reagents

A Kratos Spectroflow 400 liquid chromatograph and a Promis autosampler, equipped with a Perkin-Elmer PE 3000 fluorescence spectrophotometer and a Spectra
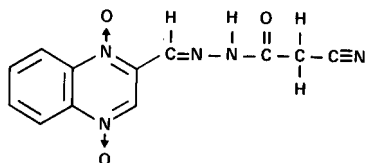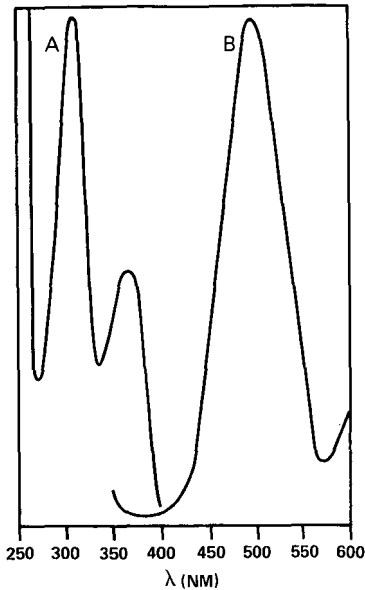

Fig. 1. Structure of cyadox.

Fig. 2. Fluorescence spectrum of cyadox, 1 μg/ml in water–acetonitrile (85:15). (A) Excitation spectrum, emission at 487 nm. (B) Emission spectrum, excitation at 310 nm. Slit width excitation and emission, 15 and 20 nm, respectively. Scan speed, 30 nm/min.

Physics SP-4290 integrator were used. The mobile phase was water–acetonitrile (85:15) at a flow-rate of 0.4 ml/min. The chromatographic column consisted of two Chromsep HPLC columns, total length 200 mm × 3 mm I.D., packed with LiChrosorb RP-18, particle size 7 μm, connected with a Chromsep guard column packed with a 30–40 μm pellicular reversed-phase material (Chrompack, Middelburg, The Netherlands). Under these conditions the retention time of cyadox was about 10.5 min. The excitation and emission wavelengths were 310 and 487 nm, respectively. The injection volume was 20 μl.

For calibration, a stock solution containing 250 μg ml/of cyadox was prepared in dimethyl sulphoxide and standard solutions containing 0.25, 0.5, 1.0 and 2.0 μg/ml of cyadox were prepared by appropriate dilution with the mobile phase. Cyadox (purity 96.4%) was generously donated by Ing. L. Huda (Chemapol, Prague, Czechoslovakia).

As cyadox is light sensitive, all manipulations were carried out in a darkened room using low actinic glassware.

Feeding of cyadox to pigs

Thirty weaned piglets, aged 7 weeks, were divided into five groups of six pigs. Each group was housed separately and treated for 6 weeks with a medicated feed containing 19, 42, 82, 185 or 335 mg/kg of cyadox. In addition, one group of six pigs received unmedicated feed. Feed and drinking water was administered *ad libitum*.

After 6 weeks the animals were fasted for 16 h and then had access to their rations; 3 h later the animals were killed and gastrointestinal samples at defined
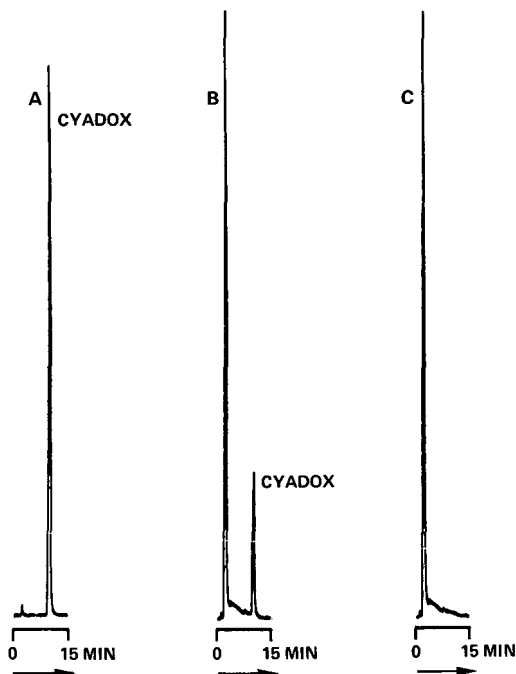
Fig. 3. (A) Cyadox standard solution, 2.0 μg/ml. (B) Sample of duodenal content of a pig fed with feed containing cyadox; the in-feed concentration was 50 mg/kg. (C) Sample of duodenal content of an untreated pig.

locations (see caption to Fig. 4) were taken at autopsy. The feed and gastrointestinal samples were stored at −20°C until analysis for cyadox.

Sample preparation

Samples of 0.1–2.0 g of freeze-dried gastrointestinal content or medicated feeds were weighed into 50-ml glass-stoppered Erlenmeyer flasks. After 20 ml of acetone had been added, the flasks were swirled on a shaking machine for 90 min. The extract was centrifuged at 300 g for 15 min and an aliquot was evaporated under a stream of nitrogen. The residue was dissolved in the mobile phase to yield solutions containing 0–2 μg/ml of cyadox. A 20-μl volume was injected for HPLC analysis.

RESULTS AND DISCUSSION

As cyadox exhibits native fluorescence, a very simple method of analysis was developed without a time-consuming clean-up and possible poor recoveries. The chromatograms showed no interference from matrix material (Fig. 3). The response for cyadox was linear in the range 0–2 μg/ml, with a correlation coefficient of $r = 0.998$ ($n = 4$). The limit of detection for a 1-g sample is *ca.* 0.1 μg of cyadox. Spiking of a control gastrointestinal sample with cyadox resulted in good recoveries (Table I).

TABLE I

RECOVERIES OF CYADOX IN SPIKED CONTROL DUODENAL SAMPLES

Cyadox added (μg/g)	Recovery (%)
250	82
100	77
50	88
25	76
12.5	75
2.5	79

During a period of 3 weeks, all gastrointestinal samples were analysed in duplicate as described. The peak areas of freshly prepared standard solutions did not change significantly during this period. On the basis of the cyadox profiles along the porcine gastrointestinal tract resulting from the feeding experiment (Fig. 4), an evaluation of the prophylactic efficacy of cyadox against enteral pathogens was made. In *Treponema hyodysenteriae*, one of the causitive agents associated with swine dysentery (dysentery Doyle), the cyadox concentrations in different parts of the gastroin-
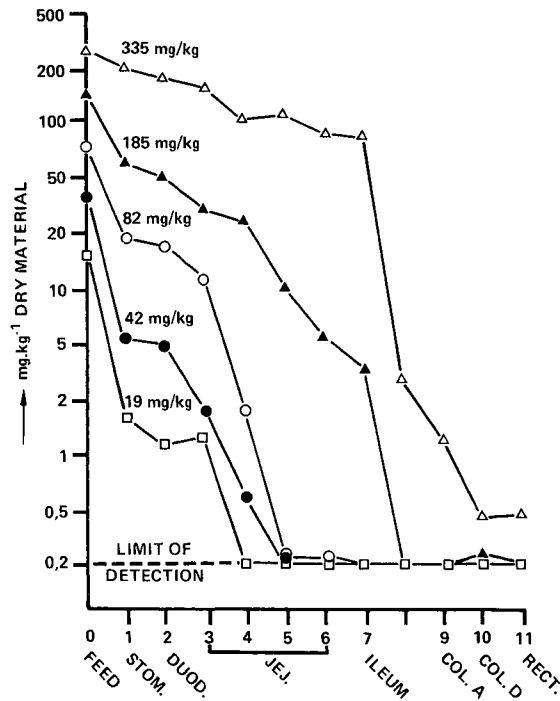

Fig. 4. Results of the determination of cyadox in feed and in gastrointestinal contents of 30 pigs fed medicated feed (mean of each treated group). Each sample was analysed in duplicate. 0 = feed sample; 1 = stomach; 2 = duodenum; 3 = jejunum, 75–125 cm from duodenum; 4 = jejunum, 50 cm around the centre; 5 = jejunum, 125–75 cm before ileum; 6 = jejunum/ileum, at junction; 7 = ileum; 8 = caecum; 9 = colomn ascendens; 10 = colon descendens; 11 = rectum.

testinal tract were interrelated with minimal inhibiting concentrations (MIC), as known from literature for this species. This showed that for cyadox in doses of 25 mg/kg or higher a prophylactic efficacy can be expected.

ACKNOWLEDGEMENT

REFERENCES

1 J. Broz, B. Sevcik and J. Hebky, *Arch. Geflügelkd.*, 44 (1980) 95.
2 J. Broz, B. Sevcik and J. Hebky, *Z. Tierphysiol. Tierernähr. Futtermittelkd.*, 41 (1979) 237.
3 E. J. van der Molen, A. J. Baars, G. J. de Graaf and L. P. Jager, *Res. Vet. Sci.*, (1987) in press.
4 G. J. De Graaf and Th. J. Spierenburg, *J. Assoc. Off. Anal. Chem.*, 68 (1985) 658.

Note

Determination of organophosphate pesticides and carbaryl on paddy rice by reversed-phase high-performance liquid chromatography

JOHN G. BRAYAN, PAUL R. HADDAD*, GERARD J. SHARP and SERGIO DILLI

School of Chemistry, University of New South Wales, P.O. Box 1, Kensington, N.S.W. 2033 (Australia)
and
JAMES M. DESMARCHELIER

CSIRO Division of Entomology, P.O. Box 1700, Canberra, A.C.T. 2601 (Australia)
(First received March 3rd, 1988; revised manuscript received May 2nd, 1988)

Carbaryl and organophosphate pesticides such as fenitrothion are frequently applied as protectants to stored grain. However, whereas the organophosphates are generally used alone, they may also be applied in conjunction with the carbamate insecticide carbaryl for the control of a specific pest showing resistance to the organophosphate. Since, in the case of stored grain, pesticides are usually applied at levels between 5 and 10 mg/kg (ref. 1) and the pesticides decay with time, there is the need to establish that, on the one hand, the grain is not consumed when residue levels are still high and, on the other, that the risk of infestation by insects is not overly increased when the levels become too low. Through loss of pesticide and its efficacy, both dependent upon the relative humidity and the temperature used for storage of the grain, the concentration where the pesticides become ineffective falls typically in the range of 1–2 mg/kg. Thus, for quality control purposes in the monitoring of pesticide levels on stored grain, the concentration range of interest is 1–10 mg/kg.

Although reversed-phase high-performance liquid chromatography (HPLC) has often been used for the analysis of carbaryl on grain[2–4], this is not the case for the organophosphate pesticides[5]. Such a situation can be attributed to the fact that carbaryl is difficult to analyse by gas chromatography because of thermal instability, and that HPLC detectors often lack the sensitivity required for organophosphate analysis. Nevertheless, the pesticide concentration in extracts of such grains is within the working sensitivity range of the UV detector so that there is no reason why the same HPLC column cannot be used for the analysis of both carbaryl and organophosphate residues to provide a simple and accurate method for monitoring the levels of these pesticides in grains.

In designing an analytical procedure, previous work[2,6,7] has suggested that methanol is the most suitable solvent for the extraction of "aged" residues* from grain. In addition, methanol extracts are suitable for direct injection onto columns employed in reversed-phase HPLC. With all of these factors in mind, this paper describes the development of a suitable method for the simultaneous determination

---

* This term is used to refer to a pesticide which has been in contact with the grain for some time.

of the carbamate pesticide carbaryl and a group of organophosphate pesticides in methanol extracts of rice, using reversed-phase HPLC. The organophosphates chosen for this study were the compounds fenitrothion, pirimiphos-methyl, chlorpyrifos-methyl, methacrifos and etrimfos and are currently in use, or under development for use, as grain protectants.

EXPERIMENTAL

Instrumentation

The liquid chromatograph consisted of Millipore Waters (Milford, MA, U.S.A.) Model 510 and 501 pumps, Model 660 solvent programmer, Model 481 variable-wavelength UV detector and Model 740 data module. The column was a Waters reversed-phase Nova-Pak C_{18} stainless-steel column (150 mm long $\times$ 3.9 mm I.D.), equipped with a Waters Guard-Pak pre-column module.

The instrument used for obtaining UV-absorption spectra was a Varian (Sunnyvale, CA, U.S.A.) Series 634 spectrophotometer. The spectra were measured over the wavelength range 200–300 nm, using a solution of the pure pesticide dissolved in methanol.

Reagents

Pure carbaryl, methacrifos, fenitrothion, chlorpyrifos-methyl, etrimfos and pirimiphos-methyl were obtained from the Curator of Standards, Australian Government Analytical Laboratories (Melbourne, Australia). The solvents used in this work were HPLC-grade methanol, Nanograde hexane and acetone (Mallinckrodt, Oakleigh, Australia) and HPLC-grade acetonitrile (Ajax, Auburn, Australia). Florisil cartridges ("Sep-Pak", from Millipore, Bedord, MA, U.S.A.) were used for the clean-up of crude extracts of the grain used in this study.

Analytical procedure

The pesticides were extracted from the grain by mixing 30 g of rice with 50 ml of methanol in a stoppered conical flask and allowing the mixture to stand for 48 h with occasional manual shaking. The following clean-up procedure was then used. An aliquot (1.0 ml) of the methanol extract was transferred to a small test-tube and evaporated to near-dryness, using a stream of nitrogen. The remaining few drops,

TABLE I

CHROMATOGRAPHIC CONDITIONS FOR PESTICIDE ANALYSIS

Pesticide	Mobile phase (% acetonitrile in water)	Retention time (min)	Detection wavelength (nm)
Carbaryl	40	6.2	225
Methacrifos	50	5.9	225
Fenitrothion	60	5.5	267
Etrimfos	60	8.9	225
Chlorpyrifos-methyl	60	11.5	225
Pirimiphos-methyl	65	8.5	247

consisting mainly of water extracted from the rice, were then shaken twice with hexane (1 ml) and, with the aid of a syringe, the combined hexane phase was carefully passed through a Florisil (Sep-Pak) cartridge, followed by 3 ml of acetone–hexane (40:60). Both eluates were collected and evaporated to dryness, using a stream of nitrogen. Finally the residue was dissolved in pure methanol (1.0 ml) for later analysis.

For HPLC analysis, 10 µl of sample were injected onto the column using a mobile phase of acetonitrile–water under isocratic or gradient conditions and a flow-rate of 1 ml/min. The percentage of acetonitrile and the detection wavelength used were varied according to the particular pesticides being analysed, and individual conditions are listed in Table I.

RESULTS AND DISCUSSION

Selection of chromatographic conditions

From UV-absorption spectra for each of the pesticides, carbaryl and methacrifos showed maximum absorption at 222 nm and 220 nm, respectively, whilst pirimiphos-methyl absorbed most strongly at 247 nm. For the remaining pesticides maximum absorption occurred at about 205 nm, with fenitrothion exhibiting a further absorption band at 267 nm. However, since methanol was found to extract a considerable amount of coloured and UV-absorbing material from rice, it was im-
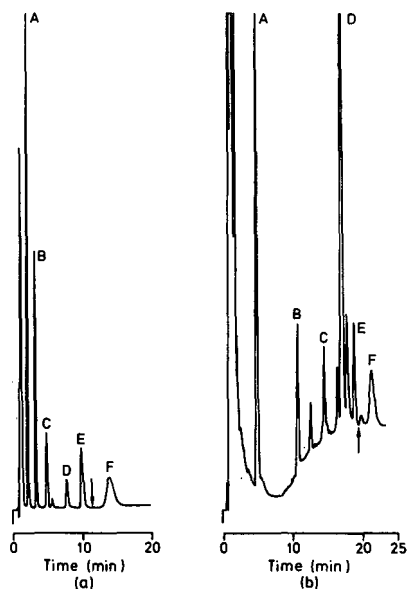

Fig. 1. Chromatograms showing the simultaneous separation of carbaryl and five organophosphates standards by isocratic elution (a) and in a methanol extract of rice by gradient elution (b). Mobile phases: (a) acetonitrile–water (60:40), and (b) gradient of acetonitrile–water (40:60) to (70:30) over 12 min. Analytical wavelength: initially 225 nm, then changed to 247 nm after 11 min (a) or 19.5 min (b), as indicated by arrows. Solute concentrations: 4 µg/ml. Peaks: A = carbaryl; B = methacrifos; C = fenitrothion; D = etrimfos; E = chlorpyrifos-methyl; F = pirimiphos-methyl.

practical to attempt detection at 205 nm. For this reason, an analytical wavelength of 225 nm was used for all pesticides, with the exception of fenitrothion and pirimiphos-methyl which were detected at 267 nm and 247 nm, respectively. Even with detection at 225 nm, direct injection of the crude extracts produced unsatisfactory chromatograms because of the number of peaks present. However, direct analysis of these extracts was possible by choosing more appropriate chromatographic conditions. Table I lists the optimal conditions which achieved resolution of each of the pesticides from the coextractives in the shortest time. It is noteworthy that even slight changes in mobile phase composition caused considerable variation to measured retention times.

Separation of all six pesticides in a single run was also possible provided the wavelength was changed to aid detection of pirimiphos-methyl (see Fig. 1a). Under the same conditions, all of the pesticides could not be fully resolved from the coextractives when using a spiked extract. However, as shown in Fig. 1b, it was possible to use gradient elution (40–70% acetonitrile over 12 min) for the determination of pesticides in untreated extracts, except in the case of etrimfos which experienced excessive interference from the co-extracted material.

Sample clean-up

Whilst manipulation of the detection wavelength was partially successful in minimising interferences from co-extracted material, it was predictable that this measure would result in some loss of sensitivity. Moreover, since the amount of coextractives from rice was dependent on both the type of rice and the area in which it was grown, a clean-up procedure became an essential part of the analytical procedure.

It is significant that most of the material extracted from the grain by methanol
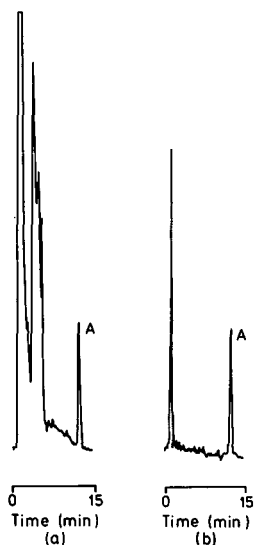

Fig. 2. Chromatograms of chlorpyrifos-methyl (A) in a methanol extract of rice before (a) and after (b) sample clean-up. Solute concentration: 6 μg/ml. Other conditions as in Table I.

TABLE II

CALIBRATION DATA AND DETECTION LIMITS FOR PESTICIDES

Pesticide	Concentration range in extracts ($\mu g/ml$)	Correlation coefficients of calibration plots	Recovery (%) ± S.D. (n = 4)	Detection limits* (mg/kg)
Carbaryl**	2–10	0.999		
	0.2–1.5	0.999	97 ± 3	0.05
Methacrifos**	2–15	0.999		
	0.2–1.5	0.999	100 ± 1	0.2
Fenitrothion	2–15	0.999	90 ± 7	
	0.3–1.5	0.999	98 ± 5	0.4
Etrimfos	2–15	0.992	97 ± 9	
	0.8–2.0	0.992	95 ± 5	1.0
Chlorpyrifos-methyl	1–10	0.998	91 ± 6	
	0.4–1.0	0.999	90 ± 8	0.6
Pirimiphos-methyl	2–15	0.999	93 ± 4	
	0.2–1.5	1.000	85 ± 3	0.3

* Calculated for the sample of rice from the detection limits of the pesticide in the methanol extract after 30 g of grain were treated with 50 ml of solvents as under *Analytical procedure* in the Experimental section.
** For this pesticide, no clean-up of the sample extract was used.

was relatively polar and was readily separated from the less polar pesticides. In fact, this separation was readily accomplished on a Florisil ("Sep-Pak") cartridge, where the pesticides were eluted with acetone–hexane but the co-extractives were retained by the adsorbent. The effect of this clean-up is shown in Fig. 2 for rice extracts treated with chlorpyrifos-methyl, before and after sample clean-up. Recoveries for this procedure, as shown in Table II, ranged from 90–100% for all pesticides except for methacrifos (70%) and carbaryl (30%), which provided quantitative recoveries without sample clean-up. The poor recoveries for these two species when the clean-up procedure was applied may be attributable to the fact that some methacrifos, being a volatile compound, may have been lost during the evaporation stage of the clean-up process, whilst the rather polar carbaryl may not be extracted quantitatively into hexane. Fortunately, since both of these pesticides absorb strongly at 225 nm, they are relatively easy to quantify without cleanup, as shown in Fig. 3.

Since the clean-up method produced superior chromatograms when compared with direct injection of grain extracts, this method is clearly preferable for the determination of low concentrations of pesticides, or for multi-residue methods where more than one pesticide may be present. However, clean-up is time-consuming and for laboratories which have a large sample throughput and require rapid results (such as those operated by grain-handling authorities), the direct injection of extracts may be adequate. Here, it may be noted that multiple injections of unclean extracts do not appear to have any adverse effects on the life-time or efficiency of the analytical column, provided that a guard column is also employed.
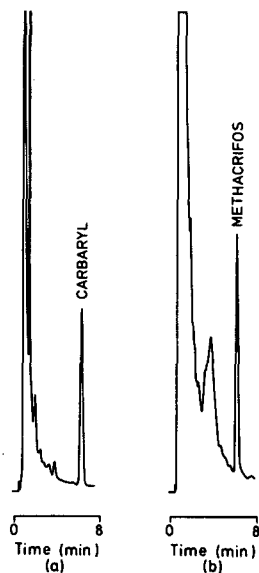
Fig. 3. Chromatograms for carbaryl (5 μg/ml) (a) and methacrifos (10 μg/ml) (b), in a methanol extract of rice, without clean-up. Mobile phases: acetonitrile–water (40:60) for carbaryl and acetonitrile–water (50:50) for methacrifos. Detection at 225 nm.

Detection limits

Table II summarizes the detection limits for each of the pesticides used in this study, as well as the correlation coefficients for the linearity of two series of standards added to rice extracts. The data shown are for samples which had been treated using the proposed clean-up procedure, except in the cases of carbaryl and methacrifos which were determined in the untreated methanol extracts, that is, without the clean-up step. The standard additions were prepared to cover the range of pesticide levels likely to be found in stored grain and where possible (depending on the individual detection limits), one order of magnitude below this. Thus the range 2–15 μg/ml in the injected solution corresponded to 3.3–25 mg/kg in the rice sample when the outlined extraction procedure was used. The detection limits quoted are defined as the concentration of pesticide in the original rice sample giving a detector response of three times the baseline noise. Since the pesticides were well separated from the peaks due to co-extractives, the detection limits for clean and unclean extracts were very similar. It is obvious from the data that good linear calibration plots were obtained for the two concentration ranges chosen.

Applications

In using the analytical procedure discussed, the conditions specified in Table I are suitable for the analysis of individual pesticides. For samples where more than one pesticide is present, separation is possible using isocratic conditions following clean-up of the sample extract, or gradient elution with the conditions discussed earlier. When analysis of extracts containing carbaryl and an organophosphate is required, clean-up is not feasible because of the poor recoveries of carbaryl. In such

cases, rather than using the gradient elution mode, it was found to be more expedient to analyse all of the samples for carbaryl using acetonitrile–water (40:60) as the mobile phase, and then to change the conditions and re-analyse for the organophosphate pesticide.

For multiresidue analysis, where the identities of the applied pesticides are unknown, sample clean-up is necessary, followed by isocratic analysis using the conditions given in Fig. 1. Although full recovery of carbaryl and methacrifos is not obtained with the clean-up procedure, the presence of these pesticides would be revealed so that the untreated extract could then be re-examined under the optimal conditions for the determination of these species.

CONCLUSION

Despite the relative lack of sensitivity for the analysis of organophosphate residues, reversed-phase HPLC does offer some advantages for the determination of grain protectants on rice. First, direct injection of grain extracts is possible without the problems of non-volatile co-extractives which can interfere with gas chromatographic analysis. Second, polar extraction solvents such as methanol can be employed, and third, both carbaryl and organophosphate insecticides can be analysed wihtout changing the column or detector. The sample clean-up procedure described is straightforward, uses minimal materials and is applicable to most of the pesticides studied. This clean-up procedure provides a method for the analysis of samples containing two pesticides, or for the screening of multiresidue samples.

ACKNOWLEDGEMENT

REFERENCES

1 J. T. Snelson, *Grain Protectants,* ACIAR Publications, Canberra, 1987.
2 P. A. Hargreaves and K. J. Melksham, *Pestic. Sci.,* 14 (1983) 347.
3 P. Bottomley and P. G. Baker, *Analyst (London),* 109 (1984) 85.
4 J. F. Lawrence and R. Leduc, *J. Assoc. Off. Anal. Chem.,* 61 (1978) 872.
5 X.-D. Ding and I. S. Krull, *J. Agric. Food Chem.,* 32 (1984) 85.
6 J. Desmarchelier, M. Bengston, M. Connell, W. Minett, B. Moore, M. Phillip, J. Snelson, R. Sticka and K. Tucker, *Pestic. Sci.,* 8 (1977) 473.
7 J. M. Desmarchelier, *J. Pestic. Sci.,* 5 (1980) 521.

Note

Determination of water-soluble vitamins using high-performance liquid chromatography and electrochemical or absorbance detection

ERKANG WANG* and WEIYING HOU

Changchun Institute of Applied Chemistry, Chinese Academy of Sciences, Changchun, Jilin 130022 (China)

(First received December 28th, 1987; revised manuscript received April 6th, 1988)

Quantitative methods available for the determination of water-soluble vitamins involve enzymatic, microbiological and chemical procedures including electrochemical and absorbance techniques[1–3]. High-performance liquid chromatography (HPLC) has been shown to be a powerful approach for the trace analysis of vitamins[4,5]. As HPLC with electrochemical detection (ED) is especially suitable for the trace determination of electroactive compounds in complex matrices, it has been applied successfully to the trace analysis of vitamins[6–11]. The main advantage of ED systems is a higher sensitivity and better selectivity than those of absorbance methods. So far, no data have been published on the determination of folic acid and *p*-aminobenzoic acid by HPLC with ED. In this work, the separation and quantitation of these compounds and the simultaneous determination of four water-soluble vitamins were studied in order to extend the scope of analysis by HPLC with ED and to improve the sensitivity and selectivity of the method.

EXPERIMENTAL

Apparatus

An amperometric analyser (made in China) was used for cyclic voltammetry. A three-electrode cell system with a glassy carbon working electrode, a silver–silver chloride (saturated potassium chloride) reference electrode and a platinum auxiliary electrode was employed.

The HPLC system consisted of a Model 510 pump, a U6K injection valve and a Model 481 variable-wavelength detector (Waters Assoc.). The injection volume was 20 μl and the wavelength was 263 nm. A Zorbax ODS (5 μm) column (15 cm × 4.6 mm I.D.) (DuPont) was used, with a Model TL-5A thin-layer electrochemical cell (Bioanalytical Systems) and a laboratory-made bipotentiostat for amperometric detection. The bipotentiostat provided certain constant potentials for both working electrodes of the electrochemical cell and detected and amplified the currents of the working electrode. It was very stable, sensitive and convenient to operate. The chromatograms were obtained at ambient temperature with a mobile phase flow-rate of 1.0 ml/min.

Reagents

All chemicals were of analytical-reagent grade, unless stated otherwise. All solutions were prepared with double distilled water. Nicotinamide was of biochemical-reagent grade and folic acid of chemical-reagent grade. The multivitamin tablets were commercially available products. A 9-vitamins-1 tablet contains vitamin A [2500 international units (i.u.)], D_2 (1000 i.u.), B_1 (2 mg), B_2 (1 mg), C (30 mg), B_6 (0.5 mg), E (1 mg), nicotinamide (10 mg) and dextro calcium pantothenate (1 mg). A 9-vitamins-2 tablet contains vitamin A (2500 i.u.), B_1 (2 mg), B_2 (1 mg), B_6 (1 mg), C (35 mg), D_2 (200 i.u.), E (1 mg), nicotinamide (10 mg) and dextro calcium pantothenate (2 mg). The vitamin contents of multivitamin–glucose power are not tabulated.

Procedures

All stock solutions were prepared at a concentration of 1 mg/ml in water and were stored at 277 K (ascorbic acid was dissolved in deoxygenated water). Just before the actual analysis, an aliquot was taken and diluted to the appropriate concentration.

The tablets were crushed to a fine powder and dissolved in water. The solution was filtered through a glass filter (porosity, 2–5 μm) and diluted to 25 ml with water. The glucose powder containing multivitamins was dissolved in water.

RESULTS AND DISCUSSION

Electrochemistry of water-soluble vitamins

The amperometric behaviour of folic acid and p-aminobenzoic acid has been reported[12]. In this study, the electrochemical behaviour of folic acid and p-aminobenzoic acid was studied using a glassy carbon working electrode. Fig. 1 shows the cyclic voltammograms of ascorbic acid, folic acid and p-aminobenzoic acid in a conventional electrochemical cell. It can be seen that ascorbic acid yields an oxidation wave at about 0.25 V and both folic acid and p-aminobenzoic acid at about 0.97 V. Nicotinamide did not yield an oxidation wave in this potential range. With an increase in pH, the E_p of ascorbic acid shifts to a more negative value but those of folic acid and p-aminobenzoic acid are hardly affected. The oxidation process of all three analytes is irreversible.

Liquid chromatographic separation and detection of water-soluble vitamins

Fig. 2 shows the change in capacity ratios (k') that occurred when the pH of the mobile phase was changed, and it can be seen that the k' values of folic acid and p-aminobenzoic acid decreased with increasing pH owing to their enhanced polarity, whereas those of ascorbic acid and nicotinamide were hardly affected. As folic acid is insoluble in solutions with a pH below 5, the pH of the mobile phase was fixed at 6 in the subsequent experiments.

Fig. 2 also shows the influence of the methanol concentration in the mobile phase on the capacity ratios. With an increase in methanol concentration, the k' values of folic acid and nicotinamide are reduced whereas those of ascorbic acid and p-aminobenzoic acid are influenced to minor extent.

A good separation of the four vitamins was achieved in with methanol–0.1 M phosphate buffer (pH 6.0) (1:4, v/v) at a flow-rate of 1 ml/min (Fig. 4A).
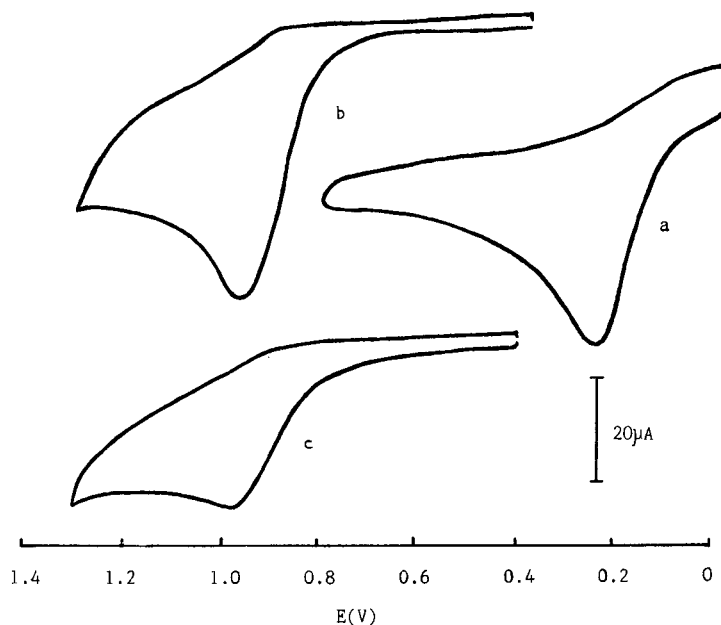
Fig. 1. Cyclic voltammograms obtained in 0.1 M phosphate buffer (pH 6.0). (a) 1 mM ascorbic acid; (b) 1 mM p-aminobenzoic acid; (c) 1 mM folic acid. Scan rate, 100 mV/s.

In order to determine the optimum potential for electrochemical detection, three hydrodynamic voltammograms were constructed (Fig. 3) by making injections of fixed volumes of the stock solutions and varying the potential between 0 and 1.3 V. It can be seen that ascorbic acid reaches its maximum current, whereas folic acid and p-aminobenzoic acid do not produce any current at $+0.70$ V but reach their
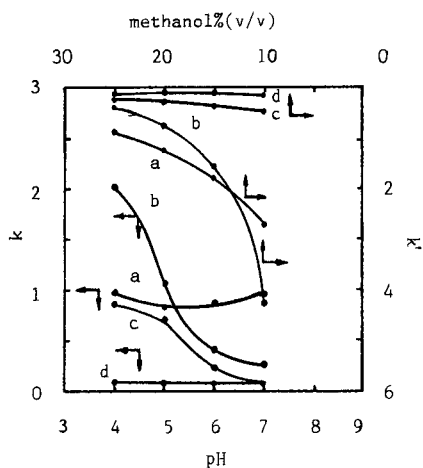
Fig. 2. Influence of mobile phase pH and methanol concentration in the mobile phase on capacity ratios. (a) Nicotinamide; (b) folic acid; (c) p-aminobenzoic acid; (d) ascorbic acid. Mobile phase: methanol–0.1 M phosphate buffer (1:3, v/v) for pH influence and methanol–0.1 M phosphate buffer (pH 6.0) for influence of methanol concentration.
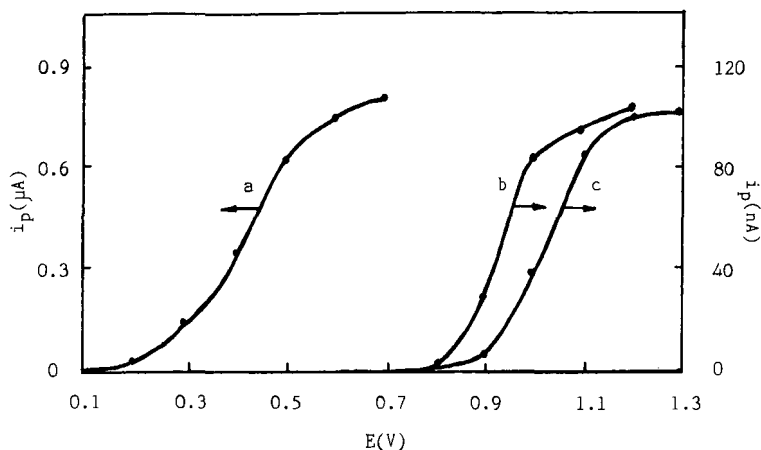
Fig. 3. Hydrodynamic voltammograms for vitamins (a) 20 ppm ascorbic acid; (b) 1 ppm p-aminobenzoic acid; (c) 15 ppm folic acid.

maximum current at + 1.20 V. Higher potentials are disadvantageous in HPLC with ED owing to the higher background current, and therefore a potential of 0.60 V was selected for the determination of ascorbic acid and 1.10 V for folic acid and p-aminobenzoic acid. A parallel dual-electrode system was applied with two different oxidative potentials, allowing the simultaneous determination of three vitamins, one at 0.60 V and the other two at 1.10 V. Fig. 4B shows the chromatograms obtained.

Fig. 4 indicates that the HPLC–ED system offers superior selectivity over absorbance detection. It was possible to detect ascorbic acid directly in multivitamin samples and the chromatographic separation process can be avoided. Most absorbable and non-electrooxidized vitamins do not interfere in the HPLC–ED determination of the vitamins studied. As almost all vitamins absorb in a certain wavelength range, the analysis of multivitamin samples with absorbance detection can only be carried out following a good chromatographic separation. The results of this study demonstrate that the HPLC method with ED for determining vitamins is convenient, sensitive and selective.

Eight replicate injections of a stock solution containing 15 ppm of nicotinamide, 20 ppm of ascorbic acid, 5 ppm of p-aminobenzoic acid and 15 ppm of folic acid were carried out to determine the precision. Nicotinamide was detected with an absorbance detector and the others with the amperometric detector. The coefficient of variation of the peak height was 1.7% for nicotinamide, 4.7% for ascorbic acid, 3.0% for fotic acid and 2.2% for p-aminobenzoic acid.

The calibration graphs were linear over the ranges 20 pg–100 ng for ascorbic acid, 40 pg–200 ng for p-aminobenzoic acid and 200 pg–100 ng for folic acid with amperometric detection and 1–500 ng for nicotinamide with absorbance detection. The correlation coefficients were better than 99.90%. The detection limit is 20 pg for ascorbic acid, 40 pg for p-aminobenzoic acid and 0.2 ng for folic acid with amperometric detection and 0.1 ng for p-aminobenzoic acid, 0.2 ng for ascorbic acid, 0.6 ng for folic acid and 1 ng for nicotinamide with absorbance detection. This also reflects

TABLE I

DETERMINATION OF VITAMINS IN TABLETS

All parameters as in Fig. 4.

Sample	Ascorbic acid				Nicotinamide			
	Label claim (mg)	Found* (mg)	C.V.** (%)	Recovery (%)	Label claim (mg)	Found* (mg)	C.V.** (%)	Recovery (%)
9-Vitamins-1	30	29.88 ± 1.13	3.80	99.60	10	9.91 ± 0.02	2.10	99.10
9-Vitamins-2	35	34.75 ± 1.08	3.10	99.29	10	9.95 ± 0.18	1.80	99.50
Multivitamin - glucose	–	0.20 ± 0.005 mg/g	2.50	99.40	–	–	–	–

* Mean ± standard deviation of six replicate sample treatments.
** C.V. = coefficient of variation.
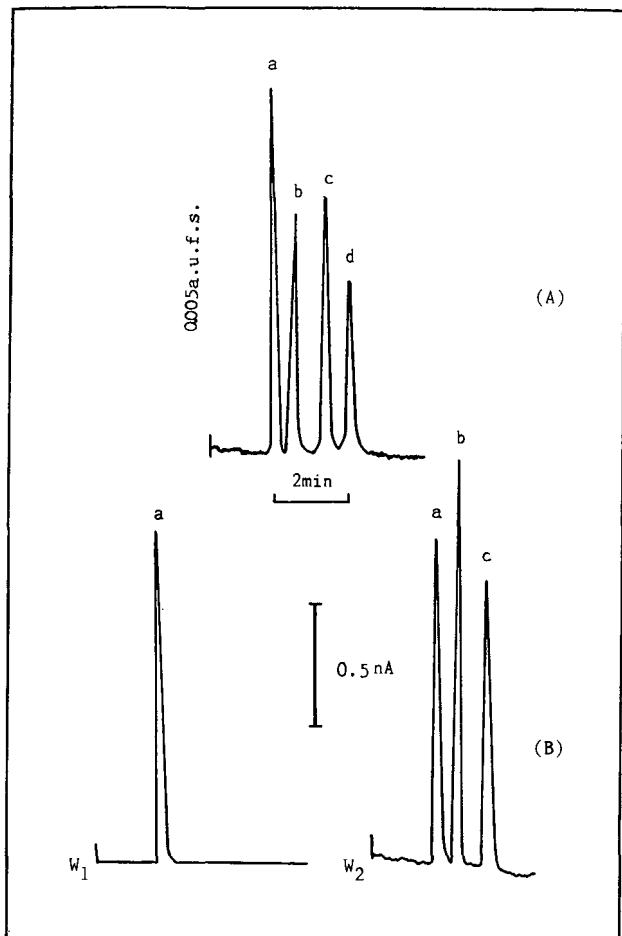
Fig. 4. Chromatograms of vitamins. (A) Absorbance detection. (a) 0.2 ppm ascorbic acid; (b) 0.1 ppm *p*-aminobenzoic acid; (c) 0.5 ppm folic acid; (d) 0.5 ppm nicotinamide. (B) Parallel dual-electrode detection. $E_1 = 0.60$ V (W_1); $E_2 = 1.10$ V (W_2). (a) 0.1 ppm ascorbic acid; (b) 0.05 ppm *p*-aminobenzoic acid; (c) 0.2 ppm folic acid; 0.5 ppm nicotinamide.

an improvement in sensitivity for determining vitamins by HPLC–ED compared with absorbance detection.

We determined ascorbic acid and nicotinamide in tablets and glucose powder containing multivitamins (Table I). Ascorbic acid was detected by amperometric detection and nicotinamide by absorbance detection. The contents found agreed well with the label claim and the reproducibility of this procedure was acceptable.

ACKNOWLEDGEMENT

REFERENCES

1 K. Okuda, S. Fujita and M. Wada, *Methods Enzymol.*, 18a (1972) 505.
2 E. E. Schrell, *Vitamins*, 2 (1968) 2.
3 K. Yosumoto, *J. Nutr. Sci. Vitaminol.*, 21 (1975) 117.
4 A. P. De Leenheer, W. E. Lambert and M. G. M. De Ruyter, *Modern Chromatographic Analysis of the Vitamins*, Vol. 30, Marcel Dekker, New York, 1985.
5 R. B. H. Wills, C. G. Shaw and W. R. Day, *J. Chromatogr. Sci.*, 15 (1977) 262.
6 C. D. B. Bridges and R. A. Alvarez, *Methods Enzymol.*, 81 (1982) 463.
7 P. P. Chou, P. K. Jaynes and J. L. Bailey, *Clin. Chem.*, 31 (1985) 880.
8 L. A. Pachla and P. T. Kissinger, *Anal. Chem.*, 48 (1976) 364.
9 J. P. Hart, M. J. Shearer and P. T. McCarthy, *Analyst (London)*, 110 (1985) 1181.
10 J. P. Hart and P. T. Kissinger, *Anal. Proc.*, 23 (1986) 439.
11 K. Kamata, T. Hayiwara, M. Takahashi, S. Uehara, K. Nakayama and K. Akiyama, *J. Chromatogr.*, 356 (1986) 326.
12 E. Jacobsen and M. W. Bjørnsen, *Anal. Chim. Acta*, 96 (1978) 345.

Note

High-performance liquid chromatographic determination of sulphur and captan in a mixture

GIANFRANCO FEDELI*, DANILO MOLTRASIO and MAURIZIO ALEOTTI

Chemical Research Laboratories, CRINOS SpA, Piazza XX Settembre 2, 22079 Villa Guardia (Italy)

and

GABRIELLA GAZZANI

Department of Pharmaceutical Chemistry, University of Pavia, Pavia (Italy)

(First received December 14th, 1987; revised manuscript received April 8th, 1988)

Captan (N-trichloromethylthio-3α,4,7,7α-tetrahydrophthalimide) and sulphur often occur together as active antimycotic agents in pharmaceutical preparations for topical use. The elaboration of the various dosage forms may make it difficult to separate the two compounds and assay them individually. Therefore, the characterization and routine quality control of pharmaceutical products of this type necessitate an analytical method that will readily separate captan and sulphur and so afford their dependable identification and accurate assay in a single operation.

Captan has already been investigated in this respect by adsorption liquid chromatography[1,2] and reversed-phase high-performance liquid chromatography (RP-HPLC) with a linear gradient of acetonitrile in water[3]. A method for determining captan by oxidoreduction with potassium tritiumcarbonate has also been reported[4]. For elemental sulphur a method based on reversed-phase liquid chromatography was published recently[5].

So far, no attempts have been made to determine the two substances in a mixture. This paper describes a solution to the problem of separating captan and sulphur from a mixture by a method of reversed-phase chromatography with simple isocratic elution.

EXPERIMENTAL

Equipment

The HPLC system consisted of a binary pump, Perkin-Elmer Series 3B liquid chromatograph equipped with a Rheodyne Model 7125 semiautomatic sampling valve with a 20-μl loop, a Perkin-Elmer 250 × 4 mm I.D. stainless-steel column packed with 10-μm reversed phase C$_8$ silica (0258-1684), a Perkin-Elmer LC 85 spectrophotometric detector with LC Autocontrol featuring a 2.4-μl cell, optical length 3 mm, and a Perkin-Elmer Sigma 15 Data Station.

For solvent and sample filtration preparatory to HPLC we used a Millipore XX10.047 filtering apparatus equipped with an HAWP 047 00 membrane, pore size 0.45 μm.

Reagents and chemicals

The solvents, methanol and carbon sulphide, were of analytical-reagent grade.

Standard captan was obtained from Elgen and Veronelli (Milan, Italy) and sulphur from Merck (Darmstadt, F.R.G.).

Chromatographic operating conditions

The mobile phase was methanol–water (90:10, v/v) at a flow-rate of 1 ml/min. The injection volume was 20 μl per sample and the detection wavelength was 254 nm. The response attenuation was 0.320 a.u.f.s., the recorder attenuation 10 mV and the chart speed 5 mm/min.

Construction of calibration graph

We prepared separate solutions of the standard chemicals in a few millilitres of methanol, starting with 26.1 mg of sulphur and 158 mg of captan, and the two solutions were mixed and diluted with methanol to a final volume of 50 ml. From the same solution we made dilutions with methanol in ratios of 7.5:10, 5:10, 2.5:10 and 1:10, to be used for constructing the concentration–response calibration graphs. For this purpose we injected 20-μl portions of these solutions and, using the operating conditions given above, assessed the peak areas as recorded and estimated by the integrator. We then plotted peak areas on the ordinate of a Cartesian coordinate system and the corresponding concentrations on the abscissa. The calculated correlation coefficients were $r = 0.998$ for captan and $r = 0.999$ for sulphur.

Sample analysis

The samples were 200-mg tablets of a preparation containing 6 mg of captan and 5 mg of sulphur, dispersed in a mixture of excipients. Each tablet was extracted by disintegration in 5 ml of carbon sulphide, the solid residue being extracted five times with 5 ml of the same solvent. The clear extracts were combined and dried to constant weight. The residue from each tablet was dissolved in 2 ml of carbon sulphide to facilitate dissolution and diluted to 10 ml with methanol. Hence the nominal concentrations in this solution were 500 μg/ml of sulphur and 600 μg/ml of captan.

Analysis was performed by injection into the chromatograph duplicate portions of the solutions obtained from four tablets and recording the peak areas of captan and sulphur.

RESULTS

Fig. 1 shows a representative chromatogram obtained by the analysis of a sample.

Table I gives the mean values, coefficients of variation and confidence limits calculated statistically from the pairs of values obtained in the analysis of four tablets.

DISCUSSION

In order to evaluate the sensitivity of an analytical method based on photometric reading and measurements, we may consider the relationship described in
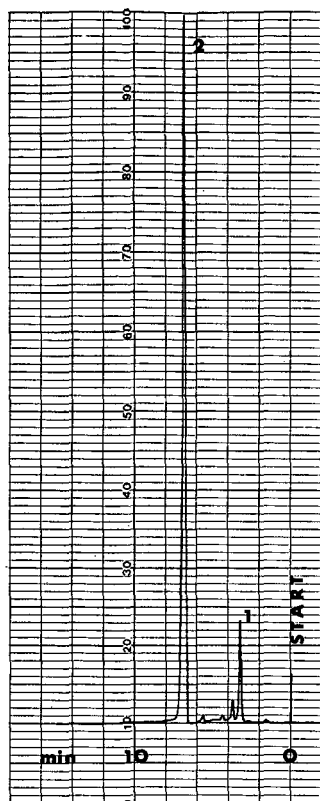
Fig. 1. RP-HPLC of a tablet sample on a C_8 reversed-phase column with methanol–water (90:10, v/v) and detection at 254 nm. The two peaks 1 and 2 (retention times 3.2 and 6.4 min) correspond to captan (600 μg/ml) and sulphur (500 μg/ml), respectively.

Vogel[6], where sensitivity is defined as the concentration of test substrate that is needed to provide a spectrophotometer response of 0.0044 absorbance units, equivalent to a 1% reduction in transmittance. Using the equation

$$\text{Sensitivity } (\mu\text{g/ml}) \ = \ C_i \cdot \frac{0.0044}{A_i}$$

TABLE I

STATISTICAL ANALYSIS OF THE RESULTS

Parameter	Captan	Sulphur
Mean concentration (mg per tablet) ($n = 8$)	6.02	4.97
Standard deviation (mg per tablet)	0.079	0.064
Coefficient of variation (%)	1.31	1.28
Confidence limits ($P < 0.05$)	±0.07	±0.05
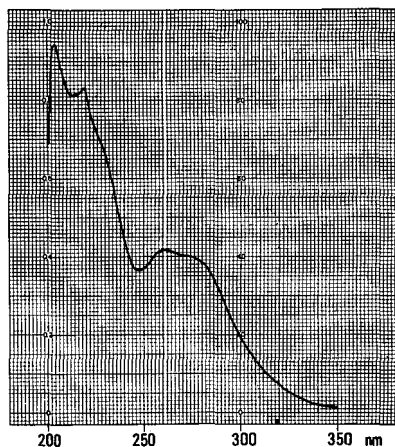
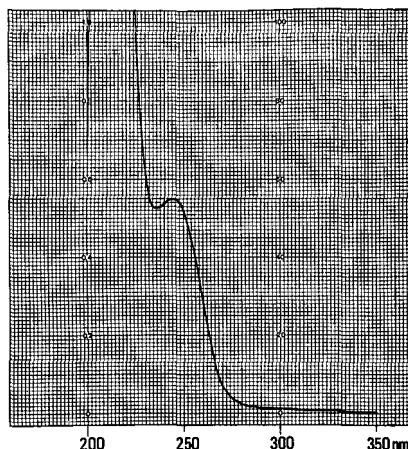Fig. 2. Absorption spectrum of sulphur in methanol, concentration 20 μg/ml.

Fig. 3. Absorption spectrum of captan in methanol, concentration 500 μg/ml.

where C_i (μg/ml) and A_i are the concentration and absorbance, respectively, of substance i, we calculated the sensitivity of the method for both captan and sulphur, based on the respective chromatographic peaks, and obtained values of 82.5 μg/ml for captan and 3.5 μg/ml for sulphur. Hence the ratio of the two masses in terms of sensitivity is 23.57:1. Confirmation of the ratio of sulphur to captan from the absorbances at 254 nm was found by spectrophotometric analysis (Figs. 2 and 3), and demonstrates the constancy of the respective parameters under the static conditions used in conventional spectrophotometry (optical pathlength 1 cm) and under the dynamic conditions used for RP-HPLC detection (optical pathlength 0.3 cm). The same ratio of captan to sulphur was obtained from calibration graphs constructed from the RP-HPLC response areas, namely approximately 23.5:1.

The closeness of the ratios measured and calculated independently indicates that the responses obtained by RP-HPLC are reliable without mutual interference when the two substances occur simultaneously. Further confirmation of the validity of these analytical conditions comes from the closeness of the coefficients of variation (see Table I), namely 1.31% for captan and 1.28% for sulphur.

The calibration graph for sulphur in RP-HPLC passes through the origin. The range of linear response and the retention time are in good agreement with that reported by Quinn and McGee[5]. For captan, as expected, the linearity of response, whilst corresponding to a calibration line passing through the origin, covers a much broader range, namely from 6000 to 60 000 ng.

Hoodless et al.[3], who studied the separation of about 20 pesticides, conducted RP-HPLC by elution with a linear gradient of acetonitrile in water and the retention time of captan was approximately 22 min. Under our operating conditions, utilizing isocratic elution with methanol–water (90:10), the retention time was much shorter (approximately 3.2 min) (Fig. 1).

CONCLUSIONS

The RP-HPLC method described here is useful for the simultaneous determination of sulphur and captan in pharmaceutical preparations. The results show that the two substances do not interfere with each other, despite their markedly different responses to the detector. The results in this study for the two components occurring together in a compound formulation agree closely with those obtained independently for the two substances in earlier studies intended for different purposes. The duration of the chromatographic run is approximately 8 min. Preliminary sample preparation is simple, a single procedure being suitable for both substances.

REFERENCES

1 B. Buettler and D. H. Wolf, *J. Agric. Food Chem.*, 29 (1981) 257.
2 A. A. Carlstrom, *J. Assoc. Off. Anal. Chem.*, 63 (1980) 1231.
3 R. A. Hoodless, J. A. Sidwell, J. C. Skinner and R. D. Treble, *J. Chromatogr.*, 166 (1978) 279.
4 B. C. Verma, N. K. Sharma, M. A. Sud, H. K. Thakur and D. K. Sharma, *Analyst (London)*, 112 (1987) 705.
5 M. E. Quinn and W. W. McGee, *J. Chromatogr.*, 393 (1987) 255.
6 J. Bassett, R. C. Denney, G. H. Jeffery and J. Mendham (Editors), *Vogel's Textbook of Quantitative Inorganic Analysis*, Longman, London, 4th ed., 1978, p. 834.

Note

Liquid chromatographic determination of carbohydrates with pulsed amperometric detection and a membrane reactor

JUN HAGINAKA*

Faculty of Pharmaceutical Sciences, Mukogawa Women's University, 11-68, Koshien Kyuban-cho, Nishinomiya, Hyogo 663 (Japan)

and

TETSUO NOMURA

Scientific Instrument Department, Abe Trading Co. Ltd., 6-32, 3-chome, Nakanoshima, Kita-ku, Osaka 530 (Japan)

(First received March 8th, 1988; revised manuscript received April 19th, 1988)

High-performance liquid chromatography (HPLC) has played an important rôle in recent advances in carbohydrate chemistry and biochemistry. The separation modes employed are based on gel permeation, borate-complex anion exchange and partition chromatography, while the detection methods are mainly based on refractivity and low-wavelength ultraviolet (UV) absorption, though a number of post-column derivatization methods have been developed[1]. However, refractive index and UV detection are insensitive and non-selective. Recently, the direct separation of carbohydrates by anion-exchange chromatography in combination with pulsed amperometric detection using a gold working electrode was developed by Rocklin and Pohl[2]. The method is highly sensitive for CHOH-bearing compounds such as carbohydrates and alcohols, but it has a disadvantage that the separation mode is limited to an anion-exchange column (OH^-) with a highly alkaline eluent. In order to extend the use of pulsed amperometry to the detection of CHOH-bearing compounds separated by various modes, we tried changing the pH of the eluent to alkaline values by using a membrane reactor. This paper deals with the determination of carbohydrates by pulsed amperometry in combination with a membrane reactor.

EXPERIMENTAL

Reagents and materials

Carbohydrates and glycerol were obtained from Nakarai Chemicals (Kyoto, Japan). Their stock solutions (1.0 mg/ml) were prepared in water and diluted in the eluent before injection onto a column. Methanol and acetonitrile of HPLC grade were obtained from Wako Pure Chemical Industries (Osaka, Japan). Water prepared by a Nanopure unit (Barnstead, Boston, MA, U.S.A.) was used for the preparation of the sample and the eluent.

A cation-exchange membrane (AMMS-1) was obtained from Dionex (Sunnyvale, CA, U.S.A.).

Chromatography

The HPLC system comprised a Model 4000i pump and a pulsed amperometric detector (both from Dionex) equipped with a gold working electrode. The columns and eluents used were as follows: method A, a Sugar SP1010 column (30 cm × 8 mm I.D.) (Showa Denko, Tokyo, Japan), which is a cation-exchange column loaded with lead, and water at a flow-rate of 1.0 ml/min; method B, an RSpak DC-613 (15 cm × 6 mm I.D.) (Showa Denko), which is a cation-exchange column loaded with sodium, and water–acetonitrile–methanol (3:6:1, v/v/v) at a flow-rate of 0.8 ml/min. The columns were maintained at 80 and 50°C, respectively, in methods A and B using a TU-310 column oven (Japan Spectroscopic, Tokyo, Japan). Sodium hydroxide solutions (0.75 M for method A and 1.5 M for method B) were used as the eluent pH modifier, and delivered into the membrane reactor (AMMS-1) at a flow-rate of 1.0 ml/min. The three potentials applied, E_1, E_2 and E_3, were 200, 600 and −800 mV at duration times of 60, 60 and 240 ms, respectively, as reported previously[2]. A 50-μl portion of the sample was loaded onto a column.

RESULTS AND DISCUSSION

Detection

Hughes and Johnson[3,4] reported an HPLC method for the determination of carbohydrates which involved their separation on a cation-exchange resin loaded with calcium using water as an eluent, modification of the eluent pH to alkaline values by delivery of sodium hydroxide solution with a pump and detection by pulsed amperometry. However, the method has a disadvantage in that the detector noise caused by flow noise and mixing inhomogeneity prevents the sensitive detection of
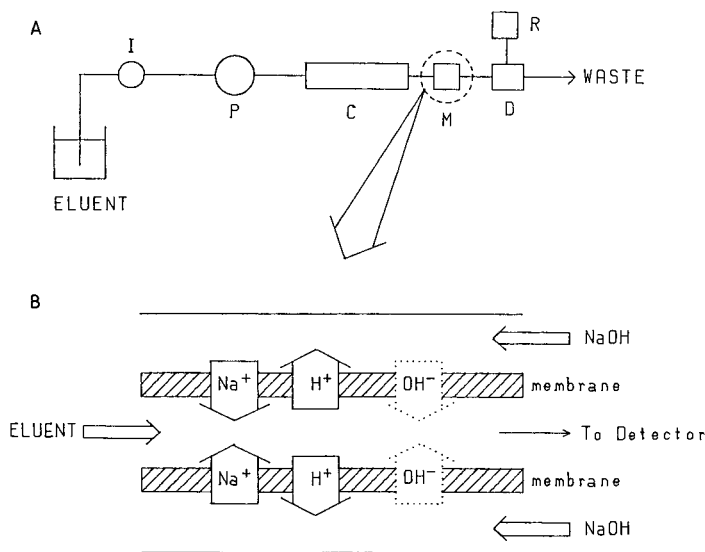

Fig. 1. Experimental set-up used (A) and the mechanism of eluent alkalization using a cation-exchange membrane and sodium hydroxide solution (B): I = injector; P = pump; C = column; M = membrane reactor; D = detector; R = recorder.
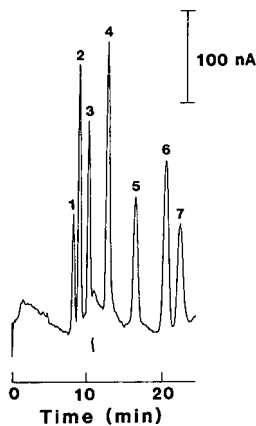
Fig. 2. Chromatogram of carbohydrates. Peaks: 1 = maltose; 2 = glucose; 3 = galactose; 4 = glycerol; 5 = mannitol; 6 = xylitol; 7 = sorbitol, each 2.0 μg/ml. HPLC conditions: column, Sugar SP1010 (30 cm $\times$ 8 mm I.D.); eluent, water; flow-rate, 1.0 ml/min; temperature, 80°C. Other conditions, see Experimental.
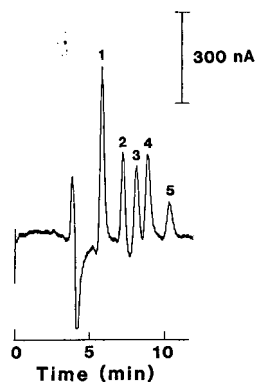
Fig. 3. Chromatogram of carbohydrates. Peaks: 1 = xylose; 2 = sucrose; 3 = maltose; 4 = lactose; 5 = maltotriose, each 5.0 μg/ml. HPLC conditions: column, RSpak DC-613 (15 cm $\times$ 6 mm I.D.); eluent, water–acetonitrile–methanol (3:6:1, v/v/v); flow-rate, 0.8 ml/min; temperature, 50°C. Other conditions, see Experimental.

carbohydrates. In previous papers, we reported that a hollow-fibre membrane can be used for postcolumn reactions (pH modification[5], degradation reaction[6,7] and derivatization[8]) with lower baseline noise and bandbroadening compared with the conventional postcolumn reaction using a pump(s) for delivering the reagent solution.

Fig. 1 illustrates the experimental set-up used in this study and the mechanism of eluent alkalization using a cation-exchange membrane and sodium hydroxide solution. As shown in Fig. 1B, the eluent is made alkaline by both exchange of sodium ion with hydrogen ion and permeation of hydroxide ion, which is a forbidden ion for a cation exchanger. Figs. 2 and 3 show chromatograms of carbohydrates separated on the cation-exchange columns using water and a mixture of water, acetonitrile and methanol, respectively, as eluents and detected by pulsed amperometry after modification of the eluent pH. These results reveal that the present method is useful for the detection of carbohydrates separated by using not only water but also a mixture of water and an organic modifier as an eluent. As shown in Fig. 3, in the presence of an organic modifier, pulsed amperometric detection is also possible. This suggests that the present method can be extended to the detection of various CHOH-bearing compounds separated by various modes.

Precision, linearity and detection limits

The precision of the present method is as follows: method A, 1.2–3.8% (n = 5) at each carbohydrate concentration of 2.0 μg/ml; method B, 3.2–5.0% (n = 5) at each carbohydrate concentration of 5.0 μg/ml. The calibration graphs of peak height *versus* concentration, over the ranges between 0.2 and 50 μg/ml (method A) and 0.5 and 25 μg/ml (method B), were linear with a correlation coefficient of $\geqslant 0.995$. The

detection limits were *ca.* 10 pmol in method A and *ca.* 50 pmol in method B at a signal-to-noise ratio of 3.

We are now investigating the application of this method to the detection of carbohydrates using gradient elution and to the detection of CHOH-bearing compounds.

REFERENCES

1 S. Honda, *Anal. Biochem.*, 140 (1984) 1; and references cited therein.
2 R. D. Rocklin and C. A. Pohl, *J. Liq. Chromatogr.*, 6 (1983) 1577.
3 S. Hughes and D. C. Johnson, *J. Agric. Food Chem.*, 30 (1982) 712.
4 S. Hughes and D. C. Johnson, *Anal. Chim. Acta*, 149 (1983) 1.
5 J. Haginaka and J. Wakai, *J. Chromatogr.*, 390 (1987) 421.
6 J. Haginaka, J. Wakai and H. Yasuda, *Anal. Chem.*, 59 (1987) 324.
7 J. Haginaka and J. Wakai, *Anal. Biochem.*, 168 (1988) 132.
8 J. Haginaka and J. Wakai, *J. Chromatogr.*, 396 (1987) 297.

Note

Determination of cinnamaldehyde, coumarin and cinnamyl alcohol in cinnamon and cassia by high-performance liquid chromatography

ALAN W. ARCHER

Division of Analytical Laboratories, New South Wales Department of Health, P.O. Box 162, Lidcombe, New South Wales 2141 (Australia)

In Europe and Australia cinnamon is defined as the dried inner bark of the coppiced tree *Cinnamomum zeylanicum* Blume (Lauraceae) and is the sole source of cinnamon oil; cassia is defined as the dried bark of *C. cassia* Blume[1]. The substitution of cassia for cinnamon is obvious when the products are not powdered but the powdered spices are not readily differentiated. Various techniques have been used to distinguish between the two products: differences in fluorescence[2], mucilage ash values[3], thin-layer chromatography (TLC) to detect eugenol in cinnamon[4], one- and two-dimensional TLC patterns[5], differences in sedimentation[6], TLC to differentiate *Cinnamomum* species[7] and TLC to detect coumarin in cassia[8]. Cinnamon and cassia may be distinguished by the presence of coumarin (2*H*-1-benzopyran-2-one) in the latter and the presence of coumarin in cinnamon is indicative of the addition of other *Cinnamomum* species. The major aromatic compound present in the *Cinnamomum* species is cinnamaldehyde (3-phenyl-2-propenal) together with smaller quantities of cinnamyl alcohol, cinnamyl acetate, eugenol and 2-methoxy-cinnamaldehyde. Cinnamaldehyde has been determined in cinnamon by colorimetry[9], polarography[10], fluorimetry[11], gas chromatography[11] and high-performance liquid chromatography (HPLC)[11] using a silica column with a mobile phase of heptane and chloroform. Cinnamaldehyde and eugenol have been determined in cinnamon and cassia oils by HPLC using a Corasil column and a mobile phase of ethyl acetate in cyclohexane[12]. This note describes the separation and determination of coumarin, cinnamyl alcohol and cinnamaldehyde in cinnamon and cassia powder using an aqueous mobile phase with a C_8 stationary phase and vanillin as an internal standard.

EXPERIMENTAL

Chromatography

The apparatus used consisted of an Altex Model 321 liquid chromatograph with a Rheodyne 7125 sample injector fitted with a 10-μl loop, and an Erma Model ERC-7210 variable-wavelength detector set at 275 nm and 0.08 absorbance units. A LiChrosorb RP-8 reversed-phase column, 250 × 7 mm O.D., 5-μm particle size with a Brownlee RP-8 5-μm, 3-cm guard column, was used with a flow-rate of 1 ml/min. The mobile phase was a mixture of 600 ml of filtered de-ionised water with 120 ml

of methanol, 200 ml of acetonitrile and 80 ml of tetrahydrofuran. All organic solvents were of HPLC grade. TLC was carried out using 10 × 5 cm silica plates, Merck 5719, with a mobile phase of dichloromethane. Coumarin was detected by spraying with 1 N potassium hydroxide and examination under long-wavelength UV light[13].

Reagents

Cinnamaldehyde and cinnamyl alcohol were both purum grade (Fluka), cinnamic acid and vanillin were Unilab grade (Ajax Chemicals, Sydney, Australia), cinnamyl acetate, coumarin, eugenol, methyl cinnamate and safrole were from Tokyo Kasei and 2-methoxycinnamaldehyde was from Aldrich. Methanol for extraction was AR grade, May and Baker.

A standard solution was prepared to contain 200 mg cinnamaldehyde, 30 mg coumarin and 25 mg cinnamyl alcohol in 100 ml of methanol. A volume of 5 ml of this solution with 5 ml internal standard solution were diluted to 100 ml with methanol to give a dilute standard solution. The internal standard solution consisted of 0.1% (w/v) vanillin in methanol.

Procedure

Inject 10 μl of the dilute standard solution and determine the ratios of the peak areas of cinnamaldehyde, cinnamyl alcohol and coumarin to vanillin. Weigh accurately about 0.5 g of powdered sample and add about 80 ml of methanol. Boil gently for 15 min, cool and add 5 ml of internal standard solution and dilute to 100 ml with methanol. Allow to stand briefly, filter the supernatant liquid through a 0.45-μm filter and inject 10 μl of the filtrate. From the peak area ratios of cinnamaldehyde, cinnamyl alcohol and coumarin to vanillin, calculate the percentage of cinnamaldehyde, cinnamyl alcohol and coumarin in the sample.

RESULTS AND DISCUSSION

Cinnamon[14] and cassia[15] contain a large number of compounds including terpenes and aromatic aldehydes and esters. The major component in both spices is cinnamaldehyde, together with cinnamyl acetate, cinnamyl alcohol and eugenol. In addition cinnamon is reported to contain safrole[14,16], absent from cassia, and 2-methoxycinnamaldehyde[8,17], although this latter compound was earlier reported to be present in cassia alone[7,18]. All these compounds have UV absorption maxima in the range 250–290 nm; a detector wavelength of 275 nm was chosen as this is one of the UV maxima of coumarin.

Methanol readily dissolves the compounds of interest and has been used to extract cinnamon and cassia for analysis by TLC[8]; it was therefore selected as the solvent for extraction. Preliminary experiments showed that an aqueous phase containing methanol, acetonitrile and tetrahydrofuran was required to give a separation of the compounds of interest. The most effective separation, *i.e.* minor components eluted before the major component, was obtained with the mobile phase composition listed under *Chromatography*. Vanillin was found to be a suitable internal standard. Methanolic solutions of vanillin have been reported[19] to produce additional peaks on standing, possibly due to acetal or hemi-acetal formation but this was not found in the present work. All standard solutions were kept at 4°C in the dark when not

in use. Methanolic extracts of cinnamon, when allowed to stand at room temperature (20–28°C) for 4 weeks, showed a loss of cinnamaldehyde, an increase in cinnamic acid and the production of an additional peak, with a retention time of 19.3 min, which was identified by co-chromatography as methyl cinnamate. Cinnamon extracts were usually analysed within 1–2 h of preparation.

The separation of reference compounds is shown in Fig. 1A. Typical retention times were (in min): cinnamic acid, 4.0–4.1; vanillin, 6.2–6.4; coumarin, 8.3–8.5; cinnamyl alcohol, 9.3–9.5; cinnamaldehyde, 11.1–11.4; eugenol, 15.5–16.1 and cinnamyl acetate, 22.5–24. The detector response for cinnamaldehyde, cinnamyl alcohol and coumarin was linear up to concentrations of 15, 2 and 3 mg/100 ml respectively, corresponding to 3% cinnamaldehyde, 0.4% cinnamyl alcohol and 0.6% coumarin in the sample. Cinnamaldehyde (10 mg), cinnamyl alcohol (1 mg) and coumarin (1.5 mg) were added to a sample of powdered cinnamon containing 0.65% cinnamaldehyde and no cinnamyl alcohol or coumarin. The means of duplicate recoveries were 95%, 110% and 103% respectively.

Chromatograms of genuine cinnamon extracts, Fig. 1B and C, showed coumarin to be absent; cinnamon was reported to contain less than 0.0008% (8 ppm) coumarin[8]. The chromatograms also showed the presence of low concentrations of cinnamyl alcohol and the presence of a peak m, identified by co-chromatography as 2-methoxycinnamaldehyde, retention time 14.0–14.4 min. These peaks, together with eugenol and cinnamyl acetate, were present in the stronger extract, Fig. 1C. The chromatogram of genuine cassia, Fig. 1D, showed the presence of coumarin and the absence of 2-methoxycinnamaldehyde. All chromatograms showed cinnamaldehyde as a major peak. Safrole, retention time 31 min, was not detected in any of the samples examined.

Samples of cinnamon, cassia, *C. burmanni* Blume and retail samples of powdered cinnamon were examined by HPLC; the results are shown in Table I. The mean cinnamaldehyde concentration found in genuine cinnamon was 1.99% and in
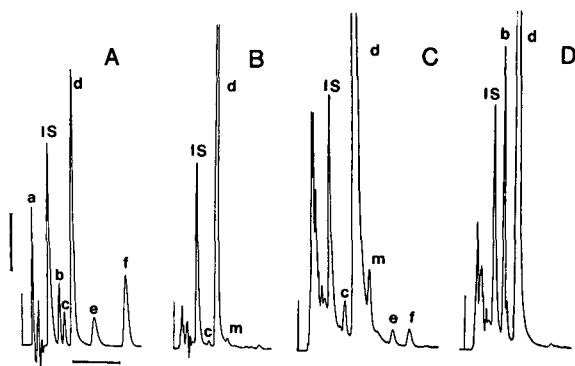

Fig. 1. HPLC chromatograms of (A) reference compounds; (B) genuine cinnamon (0.5 g/100 ml); (C) genuine cinnamon (2.5 g/100 ml); (D) genuine cassia (0.5 g/100 ml). Peaks: a = cinnamic acid, b = coumarin, c = cinnamyl alcohol, d = cinnamaldehyde, e = eugenol, f = cinnamyl acetate, m = 2-methoxy-cinnamaldehyde, IS = internal standard (vanillin). Vertical bar = 0.01 a.u.; horizontal bar = 10 min. For chromatographic conditions see text.

TABLE I

HPLC ANALYSIS OF CINNAMON AND CASSIA SAMPLES

N.D. = Not detected. Detection limits: coumarin, 0.01%; cinnamyl alcohol, 0.02%.

Sample	Cinnamaldehyde (%)	Cinnamyl alcohol (%)	Coumarin (%)
Cinnamon, quills (C. zeylanicum)			
9 Samples, mean	1.99	0.043	N.D.
Range	1.49–3.20	N.D.–0.083	
Cassia, bark (C. cassia)			
6 Samples, mean	2.56	N.D.	0.45
Range	0.76–3.37		0.14–0.70
C. burmanni, bark	0.054	0.046	0.042
Cinnamon powder retail			
1	1.10	0.031	N.D.
2	3.37	0.035	N.D.
3	0.91	ND	ND
4	1.02	0.050	ND
5	0.66	0.024	ND
6	2.57	ND	0.41
7	1.69	ND	0.20
8	3.02	ND	0.60
9	1.52	ND	0.33
10	2.39	ND	0.031
11	2.12	ND	0.046
12	1.81	ND	0.050

cassia, 2.56%. Tsai and Chen reported[11] cinnamaldehyde concentrations of 4.49% and 7.89% for cinnamon and cassia respectively, when determined by HPLC. *C. zeylanicum* is reported to contain 1–2% volatile oil[1] which contains 60–80% cinnamaldehyde[17], equivalent to 0.6–1.6% cinnamaldehyde in cinnamon. Cinnamon (Ceylon Zimt) was reported to contain 1.3–1.8% cinnamaldehyde and cassia (Chinesischer Zimt) 1.3–2.8% cinnamaldehyde[20]. The sample of *C. burmanni* contained coumarin and cinnamyl alcohol but very little cinnamaldehyde. The retail samples 1–5 appeared to be genuine cinnamon, lacking coumarin, but samples 6–9 were identified as cassia. The presence of coumarin in these samples was confirmed by TLC as described above under *Chromatography*. The remaining samples, 10–12, contained only traces of coumarin and did not appear to be either cinnamon or cassia. They may be *C. burmanni* or *C. loureirii* Nees, both of which are reported to contain coumarin[7,8].

REFERENCES

1 *The Pharmaceutical Codex*, The Pharmaceutical Press, London, 11th ed., 1979, p. 195.
2 K. Leupin and J. Steiner, *Mitt. Geb. Lebensmittelunters. Hyg.*, 30 (1939) 217.
3 A. B. Dutta, *J. Assoc. Off. Anal. Chem.*, 44 (1961) 639.
4 T. J. Betts, *J. Pharm. Pharmacol.*, 17 (1965) 520.
5 W. A. Voelker, J. N. Skarzynski and W. H. Stahl, *J. Assoc. Off. Anal. Chem.*, 50 (1967) 852.
6 W. H. Stahl, J. N. Skarzynski and W. A. Voelker, *J. Assoc. Off. Anal. Chem.*, 52 (1969) 741.
7 B. M. Lawrence, *Can. Inst. Food Technol. J.*, 2 (1969) 178.
8 .F. Karig, *Dtsch. ApothZtg.*, 115 (1975) 1781.
9 S. Collet, *Manuf. Chem.*, (1952) 411.
10 G. Dusinsky, M. Tyllova and Z. Gruntova, *Ceskosl. Farm.*, 6 (1957) 87.
11 S. Y. Tsai and S. C. Chen, *J. Nat. Prod.*, 47 (1984) 536.
12 M. S. F. Ross, *J. Chromatogr.*, 118 (1976) 273.
13 H. Wagner, S. Bladt and E. M. Zgainski, *Plant Drug Analysis*, Springer Verlag, Berlin, 1984, p. 24.
14 R. O. B. Wijesekera, A. L. Jayewardene and L. S. Rajapakse, *J. Sci. Food Agric.*, 25 (1974) 1211.
15 R. ter Heide, *J. Agr. Food Chem.*, 20 (1972) 747.
16 P. Currò, G. Micali and F. Lanuzza, *J. Chromatogr.*, 404 (1987) 273.
17 *British Pharmacopoeia 1980*, Vol. 1, Her Majesty's Stationery Office, London, 1980, p. 113.
18 M. A. Chowdhury and W. D. Williams, *J. Pharm. Pharmacol.*, 16 (1964) 347.
19 E. M. Wallace, *J. Chromatogr. Sci.*, 21 (1983) 139.
20 U. Gerhardt, *Fleischwirtschaft*, 10 (1969) 1356.

CHROM. 20 535

Note

Isolation and purification of salannin from neem seeds and its quantification in neem and chinaberry seeds and leaves

R. BRYAN YAMASAKI, THOMAS G. RITLAND, MARK A. BARNBY and JAMES A. KLOCKE*

NPI, University of Utah Research Park, 417 Wakara Way, Salt Lake City, UT 84108 (U.S.A.)

(Received April 8th, 1988)

Salannin ($C_{34}H_{44}O_9$) is a biologically active tetranortriterpenoid found in at least four species of plants in the family Meliaceae, including *Azadirachta indica* A. Juss. (neem)[1,2], *Melia azedarach* L. (chinaberry)[3], *M. dubia* Cav.[4] and *M. volkensii* Gurke[5]. The biological activities of salannin include insect feeding deterrency against *Musca domestica* L. (house fly)[6], *Acalymma vittatum* (F.) (striped cucumber beetle), *Diabrotica undecimpunctata howardi* Barber (spotted cucumber beetle)[7], *Spodoptera littoralis* (Boisd.) (Egyptian cotton leafworm), *Earias insulana* (Boisd.) (spiny bollworm)[8], *Aonidiella aurantii* (Maskell) (California red scale) and *Locusta* sp. (locust)[9]. In addition, salannin is an insect growth inhibitor against *Heliothis virescens* (F.) (tobacco budworm)[10].

Salannin has been isolated from crude plant extracts using a variety of techniques, either singly or in combination, including recrystallization[3], column chromatography[4,5,10,11], preparative normal-phase thin-layer chromatography (TLC)[12], and preparative reversed-phase high-performance liquid chromatography (HPLC)[6]. In this paper, we report on the preparative isolation of salannin of single-peak purity from high salannin-yielding neem seeds utilizing flash chromatography combined with HPLC. In addition, we report on the HPLC analysis of samples of neem and chinaberry seeds and leaves from different geographic regions in order to quantify their content of salannin.

MATERIALS AND METHODS

Extraction of salannin from neem seeds

A suspension of 29 kg of ground neem seeds (obtained from Senegal by Vikwood, Sheboygan, WI, U.S.A.) in 35 l of *n*-hexane was agitated occasionally at room temperature for 24 h. The hexane extract was decanted and the process was repeated with fresh *n*-hexane five more times. The hexane extracts were pooled and concentrated *in vacuo* to yield 8.1 kg of a brown oil.

Thin-layer chromatography

Normal-phase analytical TLC was performed on 20 × 20 cm prescored silica gel GHLF plates (0.25 mm, Analtech), using one of four solvent systems listed in Table I. Reversed-phase analytical TLC was performed on 1 × 3 in. $MKC_{18}F$ plates

TABLE I

R_F VALUES OF SALANNIN IN VARIOUS SOLVENT SYSTEMS ON SILICA GEL AND OCTA-
DECYLSILYLSILICA GEL (ODS) ANALYTICAL TLC PLATES

Solvent system (v/v)	R_F	TLC plate
Dichloromethane	0	Silica gel
Diethyl ether	0.32	Silica gel
Diethyl ether–methanol (99:1)	0.45	Silica gel
Dichloromethane–methanol (19:1)	0.57	Silica gel
Methanol–water (4:1)	0.37	ODS

(0.20 mm, Whatman) using methanol–water (4:1) (Table I). Visualization for ana-
lytical TLC was accomplished under shortwave UV light, followed by spraying with
a vanillin–sulfuric acid–ethanol (3:1.5:100, w/v/v) spray reagent and heating with a
hot air gun.

Flash column chromatography

A 2.0-l flash column (Aldrich) was packed with silica gel (40-μm particle size,
18 × 7.0 cm I.D., J. T. Baker) and equilibrated with dichloromethane. The brown oil
from the hexane extract described above was diluted with an equal volume of di-
chloromethane and applied in 1-kg batches onto the top of the column. After flushing
the column at 20 ml/min with 1.5 l of dichloromethane, salannin was eluted with
diethyl ether at 20 ml/min into fractions of 20 ml. Fractions containing salannin, as
determined by TLC (Table I), were pooled and rotary evaporated *in vacuo* yielding
127 g total of a dark brown tarry material. This material was dissolved in 500 ml of
methanol, filtered, diluted with 500 ml of methanol–water (3:2), and applied in 100-ml
batches onto the top of a second flash column (2.0 l, Aldrich) packed with octade-
cylsilylsilica gel (ODS) (40-μm particle size, 18 × 7.0 cm I.D., Regis) in methanol–
water (4:1). The column was eluted with methanol–water (4:1) at 20 ml/min into
fractions of 20 ml. Fractions containing salannin, as determined by TLC, were pooled
and rotary evaporated *in vacuo* to yield 34.3 g total of a pale yellow solid.

High-performance liquid chromatography

Preparative HPLC was carried out with a Hewlett-Packard Model 1081B
liquid chromatograph. Samples were dissolved in their respective solvents and in-
jected onto the column using a Negretti and Zambra injector. Effluents were detected
at 214 nm using a Pharmacia single-path monitor UV-1/214 optical unit and UV-1
control unit. Detected peaks and retention times (t_R) were recorded using a Hew-
lett-Packard 3388A integrator.

The first of two preparative HPLC steps was done with a Phenomenex silica
gel (5-μm particle size) stainless-steel column (25 × 2.0 cm I.D.) eluted isocratically
with isopropanol–n-hexane (1:19) at a flow-rate of 5.0 ml/min and an average pres-
sure of 630 p.s.i. The column was protected with a Whatman stainless-steel guard
column (5.0 × 0.46 cm I.D.) packed with Whatman pellicular silica gel. The second
preparative HPLC step was performed on a Phenomenex phenyl (5-μm particle size)
stainless-steel column (25 × 2.25 cm I.D.) eluted isocratically with acetonitrile–water
(2:3) at a flow-rate of 5.0 ml/min and an average pressure of 1500 p.s.i. This column

was protected with a Whatman stainless-steel guard column (5.0 × 0.46 cm I.D.) packed with Alltech pellicular phenyl.

Analytical HPLC was carried out on a reversed-phase Phenomenex phenyl (5-μm particle size) stainless-steel column (25 × 0.46 cm I.D.) using the same liquid chromatograph, corresponding guard column, detector, and injector system as described above. The solvent system consisted of acetonitrile–water (2:3) run isocratically at a flow-rate of 1.5 ml/min and an average pressure of 2100 p.s.i. Detected peaks were integrated (valley to valley) and retention times were recorded using a Hewlett-Packard 3388A integrator set at a peak width of 0.3, threshold of 0, attenuation of 2, and chart speed of 0.25 cm/min.

A second analytical HPLC method was carried out on a normal-phase Alltech silica gel (5-μm particle size) stainless-steel column (25 × 0.46 cm I.D.) eluted isocratically with isopropanol–n-hexane (1:9) at a flow-rate of 1.5 ml/min and an average pressure of 725 p.s.i.

Quantification

Between 2 and 100 g of ground neem seeds (obtained from Senegal, Benin, or Haiti by Vikwood, or from India by Tree Seeds International, Chevy Chase, MD, U.S.A.), neem leaves (obtained from plants grown in the greenhouse from Indian neem seeds), chinaberry seeds (collected in Hurricane, UT, U.S.A. in July and November, 1985), or chinaberry leaves (obtained from plants grown in the greenhouse from Utah chinaberry seeds) were exhaustively extracted in excess n-hexane at ambient temperatures. The hexane extracts were decanted and the process was repeated with fresh n-hexane three more times. The pooled hexane extracts were concentrated *in vacuo*. Following dilution with 10–100 ml of dichloromethane, 400 μl of the extracts were chromatographed on 20 × 20 cm prescored silica gel GHLF TLC plates (250 μm, Analtech) using dichloromethane–methanol (19:1) as the mobile phase. Visualization under UV light revealed the salannin standard that was run alongside the extracts. The band corresponding to the standard was cut from the plates, eluted with excess methanol, and injected onto an analytical Phenomenex phenyl (5 μm particle size) stainless-steel column (25 × 0.46 cm I.D.) using the same liquid chromatograph, corresponding guard column, detector, injector system, and solvent system as described above. Salannin was quantified by comparing its HPLC peak height with a linear standard curve generated from pure authentic salannin.

Identification of salannin

Salannin isolated from neem seeds was identified by spectral comparison (IR, ^{1}H NMR, electron impact mass spectrometry) and co-chromatography (TLC, HPLC) with an authentic sample.

RESULTS AND DISCUSSION

Similar to previously reported extraction methodologies[4,13], we used n-hexane to extract salannin from the neem and chinaberry samples (Fig. 1). Following exhaustive extraction of the samples with n-hexane, we detected only trace (<0.5%) amounts of salannin remaining in the marc. The hexane-defatted marc was utilized for the subsequent isolation of azadirachtin, another biologically active tetranortriterpenoid of academic and industrial interests[14].
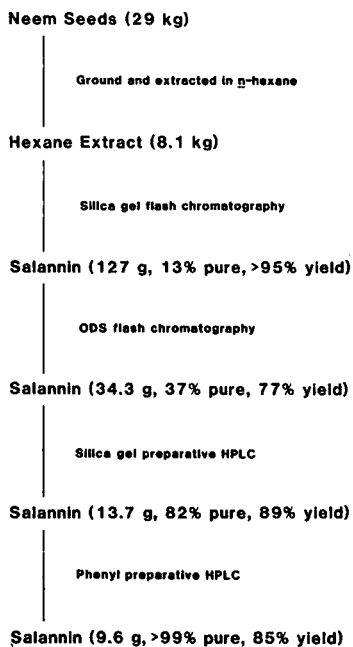
Neem Seeds (29 kg)

    Ground and extracted in n-hexane

Hexane Extract (8.1 kg)

    Silica gel flash chromatography

Salannin (127 g, 13% pure, >95% yield)

    ODS flash chromatography

Salannin (34.3 g, 37% pure, 77% yield)

    Silica gel preparative HPLC

Salannin (13.7 g, 82% pure, 89% yield)

    Phenyl preparative HPLC

Salannin (9.6 g, >99% pure, 85% yield)

Fig. 1. Flow diagram of the isolation of salannin from neem seeds.

     The majority of the components in the hexane extract consisted of fatty materials and other non-polar substances. These fatty materials may be of use in soap manufacturing[15].

     Salannin could be easily separated from the fatty materials by silica gel flash chromatography using dichloromethane as the mobile phase. Under these conditions, salannin has an R_F value of zero (Table I), whereas the fatty material is virtually unretarded. This allowed for as much as a kilogram of hexane extract to be loaded onto the 2.0-l flash column at a time. Following elution of the fatty material with dichloromethane, the column was eluted with diethyl ether and the fractions containing salannin were combined, rotary evaporated to dryness *in vacuo*, and subjected to ODS flash chromatography using methanol–water (4:1) as the mobile phase. The diethyl ether and the methanol–water (4:1) solvent systems were chosen as the mobile phases on silica gel and ODS flash chromatography, respectively, since the R_F values of salannin in these solvent systems on analytical TLC are 0.32 and 0.37, respectively. The optimum R_F for separation of a compound using flash chromatography is 0.35[16].

     Other TLC solvent systems in which the R_F of salannin approximated 0.50 were used to monitor its presence in the flash chromatography eluent. For example, the R_F values of salannin on silica gel TLC developed in 1% methanol in diethyl ether and 5% methanol in dichloromethane were 0.45 and 0.57, respectively. A vanillin spray reagent was used to visualize salannin on the TLC plates since it consistently gave a characteristic red color reaction that rapidly changed to purple.

     From a complex mixture, the two flash chromatography steps concentrated salannin to 37% purity in preparation for the final purification by HPLC (Figs. 1
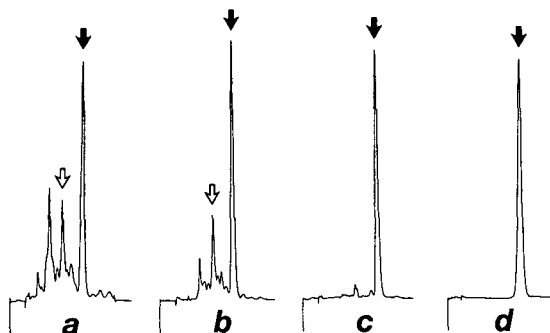
Fig. 2. Analytical HPLC of salannin (solid arrows) recovered after (a) silica gel flash chromatography; (b) ODS flash chromatography; (c) silica gel preparative HPLC; (d) phenyl preparative HPLC. Hollow arrows indicate 3-deacetylsalannin. Analytical HPLC was performed with a phenyl column (25 × 0.46 cm I.D., 5-µm particle size) eluted isocratically with acetonitrile–water (2:3) at 1.5 ml/min.

and 2). We were able to further concentrate salannin to 82% purity by silica gel preparative HPLC (Figs. 1 and 2). We found this HPLC step necessary to remove an impurity not well separated from salannin by phenyl preparative HPLC. In addition, we were able to isolate a total of 1.5 g of 3-deacetylsalannin at this step (Fig. 2). Typically, each 0.9-ml injection, containing 0.35 g of 37% pure salannin in isopropanol, yielded 0.14 g of 82% pure salannin. The appproximate t_R for salannin in this normal-phase system was 46 min.

Salannin of single peak purity could be obtained by further chromatography on phenyl preparative HPLC (Fig. 1). Typically, each 0.7-ml injection, containing 0.25 g of 82% pure salannin in acetonitrile, yielded 0.19 g of 98% pure salannin. In our hands, rechromatography by phenyl preparative HPLC was necessary to purify salannin to single-peak purity. The approximate t_R for salannin in this reversed-phase system was 80 min.

Instead of TLC, the greater resolving power of analytical HPLC was used to determine which fractions from preparative HPLC were appropriate for pooling. We used normal- and reversed-phase analytical HPLC, modifications of our previously reported isolation method for azadirachtin[14], to detect salannin, the t_R values of which were 10.9 and 10.0 min, respectively.

We chose flash chromatography for our prepurification technique, before the final purification by preparative HPLC, since it is a rapid, inexpensive, and easily performed technique with a large sample capacity[14,16]. Flash chromatography combined with phenyl preparative HPLC can generate salannin of >90% purity, adequate for certain investigations. For example, in our structure–activity relationship studies, we use salannin of 90% purity since we purify the chemically modified derivatives from their reaction mixtures.

Absolutely pure salannin was difficult to obtain in our hands, due to the complexity-in-structure of the chemicals found in neem seeds[5,10,13,17–19]. We found silica gel preparative HPLC necessary to remove some contaminants which co-chromatographed with salannin on phenyl HPLC.

In our quantification method, we prepurified the plant hexane extracts by silica

TABLE II

YIELD OF SALANNIN FROM NEEM AND CHINABERRY SEEDS AND LEAVES

Plant material (source)	Yield (g kg^{-1})
Neem seed (Benin)	1.3
Neem seed (Senegal)	1.2
Neem seed (India)	0.7
Neem seed (Haiti)	0.4
Neem leaves (India; greenhouse)	Trace
Chinaberry seed (Utah, U.S.A.; July collection)	Trace
Chinaberry seed (Utah, U.S.A.; November collection)	Trace
Chinaberry leaves (Utah, U.S.A.; greenhouse)	Trace

gel TLC in preparation for phenyl analytical HPLC. Known amounts of pure sal-annin were similarly chromatographed by TLC and the total amount was subsequently detected by phenyl HPLC. The lower limit of sensitivity of our quantification method was 0.5 μg and the linearity range was 0.5-10.0 μg.

We found that neem seeds from the African countries of Benin and Senegal were the two highest salannin-yielding sources (1.3 and 1.2 g kg^{-1}, respectively) that were available to us (Table II). Our neem seeds obtained from India and Haiti contained less salannin (0.7 and 0.4 g kg^{-1}, respectively). The leaves excised from neem plants grown in the greenhouse from our Indian neem seed yielded only trace amounts of salannin (i.e., <0.02 g kg^{-1}). Additionally, two samples of chinaberry seed collected during different times of the year in Utah, U.S.A. and leaves excised from plants grown in the greenhouse from our Utah chinaberry yielded only trace amounts of salannin. Therefore, we chose the Senegalese neem seed for our isolation scheme detailed in this paper since it was a high salannin-yielding source available to us in sufficient quantity.

We are currently preparing derivatives of our purified salannin for testing in insect bioassays. Several of our derivatives have shown significantly enhanced activity compared to salannin. The results will be published elsewhere.

REFERENCES

1 R. Henderson, R. McCrindle, K. H. Overton and A. Melera, Tetrahedron Lett., (1964) 3969.
2 R. Henderson, R. McCrindle, A. Melera and K. H. Overton, Tetrahedron, 24 (1968) 1525.
3 S. D. Srivastava, J. Nat. Prod., 49 (1986) 56.
4 L. B. de Silva, W. Stöcklin and T. A. Geissman, Phytochemistry, 8 (1969) 1817.
5 M. S. Rajab, M. D. Bentley, A. R. Alford and M. J. Mendel, J. Nat. Prod., 51 (1988) 168.

6 J. D. Warthen, Jr., E. C. Uebel, S. R. Dutky, W. R. Lusby and H. Finegold, *U.S. Dept. Agric., Sci. Educ. Admin., Agric. Res. Results*, Northeast. Ser., No. 2, Beltsville, MD, 1978, 11 p.

7 D. K. Reed, J. D. Warthen, Jr., E. C. Uebel and G. L. Reed, *J. Econ. Entomol.*, 75 (1982) 1109.

8 J. Meisner, K. R. S. Ascher, R. Aly and J. D. Warthen, Jr., *Phytoparasitica*, 9 (1981) 27.

9 J. D. Warthen, Jr., *U.S. Dept. Agric., Sci. Educ. Admin., Agric. Rev. Manuals*, Northeast. Ser., No. 4, Beltsville, MD, 1979, 21 pp.

10 I. Kubo, A. Matsumoto, T. Matsumoto and J. A. Klocke, *Tetrahedron.*, 42 (1986) 489.

11 M. Harris, R. Henderson, R. McCrindle, K. H. Overton and D. W. Turner, *Tetrahedron*, 24 (1968) 1517.

12 K. Nakanishi, *Rec. Adv. Phytochem.*, 9 (1975) 283.

13 K. K. Purushothaman, K. Duraiswamy and J. D. Connolly, *Phytochemistry*, 23 (1984) 135.

14 R. B. Yamasaki, J. A. Klocke, S. M. Lee, G. A. Stone and M. V. Darlington, *J. Chromatogr.*, 356 (1986) 220.

15 C. M. Ketkar, *Utilization of Neem (Azadirachta indica juss) and its Bye-Products*, Directorate of Nonedible Oils and Soap Industry, Khadi & Village Industries Commission, Bombay, 1976, p. 5.

16 W. C. Still, M. Kahn and A. Mitra, *J. Org. Chem.*, 43 (1978) 2923.

17 D. A. H. Taylor, *Prog. Chem. Org. Nat. Prod.*, 45 (1984) 1.

18 W. Kraus, in Atta-ur-Rahman and P. W. LeQuesne (Editors), *New Trends in Natural Products Chemistry*, Elsevier, Amsterdam, 1986, p. 237.

19 S. Siddiqui, B. S. Siddiqui, S. Faizi and T. Mahmood, *J. Nat. Prod.*, 51 (1988) 30.

CHROM. 20 628

Note

Determination of free ellagic acid by reversed-phase high-performance liquid chromatography

BHIM S. DHINGRA* and ARNOLD DAVIS

Department of Chemistry, Morgan State University, Baltimore, MD 21239 (U.S.A.)

(First received April 13th, 1988; revised manuscript received May 6th, 1988)

Ellagic acid (I), one of the polyphenol constituents of many plants, occurs widely in nature either in its free form or in the form of ellagitannins or glucosides. It is found in dicotyledonous plants in the genera of castenea, eucalyptus, eugenia, euphorbia, gerinimum, mangifera, platycarya, quercus, rhus and terminalia[1]. Its presence has also been reported in many fruits and vegatables, *e.g.* grapes, strawberries, guavas, mangoes, green tea and black walnuts[1].
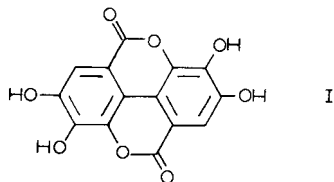
Ellagic acid has been found to be pharmacologically active as an antineoplastic, antioxidant, antimutagenic and anticarcinogenic agent[1]. These activities of ellagic acid have been ascribed to the ability of its four phenolic groups to complex readily with metals such as magnesium and calcium[2]. This ability of ellagic acid can create problems in the wood pulping process. For example, its metallic complexes can cause corrosion and scale formation and can adversely affect the wet strength of bonds of phenol-formaldehyde adhesives with wood. In view of the importance of ellagic acid, a direct and accurate method for its determination is required. Paper chromatography[3], gravimetry and gas–liquid chromatography (GLC)[4] have been used for its determination. The sensitivity and accuracy of the first two methods is limited and in GLC, derivatization of the sample is required before its determination. In this paper, we present a direct method for the determination of ellagic acid by reversed-phase high-performance liquid chromatography (HPLC). Although ellagic acid was determined qualitatively by this method in all of the above-mentioned species, quantitative determinations were carried out only in *Eucalyptus cinerea*, green grapes and black grapes (*Vitas vinifera*).

EXPERIMENTAL

Extraction

Dried, ground samples of *Eucalyptus cinerea*, green grapes or black grapes (*Vitas vinifera*) were extracted with 0.05 M triethanolamine (pH 8) in water. The extract was further washed with cyclohexane, toluene and methylene chloride to remove any non-polar impurities extracted in the amine solution. The amine extract was then concentrated for injection in the HPLC system.

HPLC

The analyses were carried out using a Perkin-Elmer Series 4 liquid chromatograph and LC-85B variable-wavelength spectrophotometric detector. A wavelength of 254 nm was used for detection. Separations were carried out using a Perkin-Elmer C_{18} reversed-phase column (125 × 4.6 mm) containing 5-μm particles. The chromatographic system was equipped with a Rheodyne 7010 injection system with a 20-μl injection loop. The mobile phase used in all the separations was 0.05 M triethanolamine in water–acetonitrile–isopropanol (85:14:1).

Reagents

Triethanolamine, acetonitrile and isopropanol were purchased from Fisher Scientific. Ellagic acid was purchased from Aldrich. All solvents were of HPLC grade.

Analysis

Calibration curves were made by injecting standard solutions of ellagic acid in the mobile phase ranging from 0.1–1 μg/ml. A 10-μl volume of the amine extract of the grapes or wood samples was injected for each analysis. The retention time of the ellagic acid at the mobile phase flow-rate of 1.0 ml/min was 1.1 min (Fig. 1). The identity of the ellagic acid peak was confirmed by running the stop-flow spectroscopy on the peak and comparing it with the spectra of the standard. Ellagic acid solutions showed evidence of photochemical reaction. Over a period of time the solution changed from a clear to a yellow and eventually to a brown solution. When the solutions were kept in the dark, they remained clear for several days. New solutions had to be made after every few days.

RESULTS AND DISCUSSION

The amount of total ellagic acid in the whole dry plant was as follows: *Eucalyptus cinerea*: 12.0 mg/g; black grapes: 7.0 mg/g; green grapes: 3.5 mg/g. The aver-
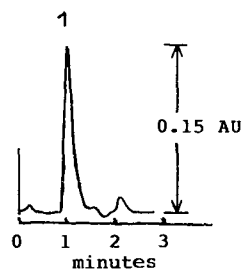
Fig. 1. Chromatogram of the extract of *Vitas vinifera*. Peak 1 = ellagic acid.

ages of five, six or seven samples showed a variation of $\pm 2\%$. The minimum quantity of the ellagic acid which could be detected with this method was 4 ng. The response of the detector was linear over a 10^6-fold range of concentration. From the results described here, our method offers a fast, simple way of determining ellagic acid. With minor modifications, this method can also be used to keep track of ellagic acid in biological fluids. Results of extraction and quantitation in such fluids will be reported in a later paper.

REFERENCES

1 R. K. Y. Zee-Chen and C. C. Chen, *Drugs Future*, 11 (1986) 1029–1031.
2 W. E. Hillis, A. N. Rozsa and L. S. Lau, *J. Chromatogr.*, 109 (1975) 172–175.
3 J. A. Klocke, B. V. Wagenen and M. F. Balandrin, *Phytochemistry*, 25 (1986) 85–91.
4 W. E. Hillis and A. Carle, *Appita*, 13 (1959) 74–76.